VOL. 677 NO. 2 AUGUST 19, 1994
THIS ISSUE COMPLETES VOL. 677

JOURNAL OF CHROMATOGRAPHY A

INCLUDING ELECTROPHORESIS AND OTHER SEPARATION METHODS

ELSEVIER

JOURNAL OF CHROMATOGRAPHY A

INCLUDING ELECTROPHORESIS AND OTHER SEPARATION METHODS

Scope. The *Journal of Chromatography A* publishes papers on all aspects of **chromatography, electrophoresis** and related methods. Contributions consist mainly of research papers dealing with chromatographic theory, instrumental developments and their applications. In the *Symposium volumes*, which are under separate editorship, proceedings of symposia on chromatography, electrophoresis and related methods are published. *Journal of Chromatography B: Biomedical Applications* —This journal, which is under separate editorship, deals with the following aspects: developments in and applications of chromatographic and electrophoretic techniques related to clinical diagnosis or alterations during medical treatment; screening and profiling of body fluids or tissues related to the analysis of active substances and to metabolic disorders; drug level monitoring and pharmacokinetic studies; clinical toxicology; forensic medicine; veterinary medicine; occupational medicine; results from basic medical research with direct consequences in clinical practice.

Submission of Papers. The preferred medium of submission is on disk with accompanying manuscript (see *Electronic manuscripts* in the Instructions to Authors, which can be obtained from the publisher, Elsevier Science B.V., P.O. Box 330, 1000 AH Amsterdam, Netherlands). Manuscripts (in English; *four* copies are required) should be submitted to: Editorial Office of *Journal of Chromatography A*, P.O. Box 681, 1000 AR Amsterdam, Netherlands, Telefax (+31-20) 5862 304, or to: The Editor of *Journal of Chromatography B: Biomedical Applications*, P.O. Box 681, 1000 AR Amsterdam, Netherlands. Review articles are invited or proposed in writing to the Editors who welcome suggestions for subjects. An outline of the proposed review should first be forwarded to the Editors for preliminary discussion prior to preparation. Submission of an article is understood to imply that the article is original and unpublished and is not being considered for publication elsewhere. For copyright regulations, see below.

Publication information. *Journal of Chromatography A* (ISSN 0021-9673): for 1994 Vols. 652–682 are scheduled for publication. *Journal of Chromatography B: Biomedical Applications* (ISSN 0378-4347): for 1994 Vols. 652–662 are scheduled for publication. Subscription prices for *Journal of Chromatography A*, *Journal of Chromatography B: Biomedical Applications* or a combined subscription are available upon request from the publisher. Subscriptions are accepted on a prepaid basis only and are entered on a calendar year basis. Issues are sent by surface mail except to the following countries where air delivery via SAL is ensured: Argentina, Australia, Brazil, Canada, China, Hong Kong, India, Israel, Japan, Malaysia, Mexico, New Zealand, Pakistan, Singapore, South Africa, South Korea, Taiwan, Thailand, USA. For all other countries airmail rates are available upon request. Claims for missing issues must be made within six months of our publication (mailing) date. Please address all your requests regarding orders and subscription queries to: Elsevier Science B.V., Journal Department, P.O. Box 211, 1000 AE Amsterdam, Netherlands. Tel.: (+31-20) 5803 642; Fax: (+31-20) 5803 598. Customers in the USA and Canada wishing information on this and other Elsevier journals, please contact Journal Information Center, Elsevier Science Inc., 655 Avenue of the Americas, New York, NY 10010, USA, Tel. (+1-212) 633 3750, Telefax (+1-212) 633 3764.

Abstracts/Contents Lists published in Analytical Abstracts, Biochemical Abstracts, Biological Abstracts, Chemical Abstracts, Chemical Titles, Chromatography Abstracts, Current Awareness in Biological Sciences (CABS), Current Contents/Life Sciences, Current Contents/Physical, Chemical & Earth Sciences, Deep-Sea Research/Part B: Oceanographic Literature Review, Excerpta Medica, Index Medicus, Mass Spectrometry Bulletin, PASCAL-CNRS, Referativnyi Zhurnal, Research Alert and Science Citation Index.

US Mailing Notice. *Journal of Chromatography A* (ISSN 0021-9673) is published weekly (total 52 issues) by Elsevier Science B.V., (Sara Burgerhartstraat 25, P.O. Box 211, 1000 AE Amsterdam, Netherlands). Annual subscription price in the USA US$ 4994.00 (US$ price valid in North, Central and South America only) including air speed delivery. Second class postage paid at Jamaica, NY 11431. **USA POSTMASTERS**: Send address changes to *Journal of Chromatography A*, Publications Expediting, Inc., 200 Meacham Avenue, Elmont, NY 11003. Airfreight and mailing in the USA by Publications Expediting.

See inside back cover for Publication Schedule, Information for Authors and information on Advertisements.

0021-9673/94/$07.00

VOL. 677, NO. 2 JOURNAL OF CHROMATOGRAPHY A AUGUST 19, 1994

CONTENTS

(Abstracts/Contents Lists published in Analytical Abstracts, Biochemical Abstracts, Biological Abstracts, Chemical Abstracts, Chemical Titles, Chromatography Abstracts, Current Awareness in Biological Sciences (CABS), Current Contents/Life Sciences, Current Contents/Physical, Chemical & Earth Sciences, Deep-Sea Research/Part B: Oceanographic Literature Review, Excerpta Medica, Index Medicus, Mass Spectrometry Bulletin, PASCAL-CNRS, Referativnyi Zhurnal, Research Alert and Science Citation Index)

REGULAR PAPERS

Column Liquid Chromatography

Gas Chromatography

(Continued overleaf)

Contents (continued)

ELSEVIER

Journal of Chromatography A, 677 (1994) 211–227

JOURNAL OF CHROMATOGRAPHY A

Evaluation of mixed-mode stationary phases in liquid chromatography for the separation of charged and uncharged oligomer-like model compounds

J.T. Eleveld[a,b], H.A. Claessens[a,*], J.L. Ammerdorffer[b], A.M. van Herk[b], C.A. Cramers[a]

[a]*Laboratory of Instrumental Analysis, Eindhoven University of Technology, P.O. Box 513, 5600 MB Eindhoven, Netherlands*
[b]*Laboratory of Polymer Chemistry, Eindhoven University of Technology, P.O. Box 513, 5600 MB Eindhoven, Netherlands*

First received 29 November 1993; revised manuscript received 26 April 1994

Abstract

The possibility to separate charged and uncharged oligomer-like test compounds by high-performance liquid chromatography was investigated, using mixed-mode (reversed-phase/anion-exchange) stationary phases. In order to examine this possibility, several columns were evaluated for their reversed-phase, anion-exchange and mixed-mode properties using neutral and charged model compounds. The OmniPac PAX-500, the PRP-X100 and the mixed-phase PLRP-S/PL-SAX columns showed promising results for the separation of real samples.

1. Introduction

A lot of kinetic–mechanistic aspects of the emulsion polymerization process are still unexplained. Oligomers play a particularly important role during the initiation of the latex particles. One of the questions unanswered concerns the length of the oligomer radicals when they enter the latex particles [1]. Besides that, it is also important to know what kind of termination takes place in the water phase. In many emulsion polymerization processes a charged initiator, like persulfate for instance, is used. Consequently, charged oligomers are formed with one or two sulfate groups. Subsequently, these sulfate groups may hydrolyse to alcohol functions.

To get more insight into the role of oligomers in emulsion polymerization processes, it is necessary to collect qualitative and quantitative information about these compounds. The separation procedures to be developed for oligomers should preferably be able to separate charged and uncharged oligomers both in one analysis procedure. In a consecutive part of this study we intend to scale-up these (analytical) separations to preparative liquid chromatography, to allow further research on the structure of the isolated compounds. This latter consideration puts specific demands on the composition of the applied eluents, with respect to removal after having finished the preparative separation. In this paper the separation of charged and neutral oligomer-like test substances is described, showing ways to analyze real oligomer samples.

* Corresponding author.

0021-9673/94/$07.00
SSDI 0021-9673(94)00408-2

Charged oligomers are especially difficult to separate through reversed-phase or anion-exchange chromatography. Therefore, in this study the use of so-called mixed-mode stationary phases for the separations of charged and neutral oligomers has been investigated. In mixed mode, stationary phases with two different retention processes on one stationary phase are intentionally prepared by the manufacturer. The columns selected for this study showed reversed-phase and anion-exchange properties by [2]: (i) interaction of the non-polar part of the sample molecules with the non-polar backbone of the stationary phase and (ii) anion-exchange interactions of the ionic part of the sample molecules with the cationic groups on the support. In this paper mixed mode reversed-phase/anion-exchange will further be indicated as mixed-mode.

In the literature a number of examples of mixed-mode stationary phases have been reported. Some early examples of mixed-mode columns are soft-gel anion-exchange resins, like DEAE-Sephadex or -cellulose [3,4]. A disadvantage of these columns is that only low pressure is allowed across these columns. Another example is the RPC-5 column. This type of column consists of a non-porous spherical polymer support (polychlorotrifluoroethylene, Plaskon 2300), which is coated with trioctylmethyl ammonium chloride [3–5]. General drawbacks of these columns are bleeding of the ammonium groups from the column, and the non-porous support which is not of a constant quality.

Several authors prepared mixed-mode columns based on silica gel supports, which already showed one of the two retention mechanisms. Two methods were used by McLaughlin and Bischoff [6–9] to prepare these mixed-mode stationary phases. The first method was by modifying an anion-exchange matrix with alkyl chains. A commercially available aminopropylsilyl bonded-phase silica (APS-Hypersil) was reacted with several organic acids that contained hydrophobic sites as well as sites for ionic interactions [6–8]. Other authors also used this first method to prepare mixed-mode silica gel supports, by reacting an anion-exchange silica support with octadecyltrichlorosilane [10]. The second method was to modify a reversed-phase matrix, by attaching anionic groups to the support. For this purpose ODS-Hypersil was coated with trioctylmethyl ammonium chloride [8,9].

Other authors used bare silica gels to prepare mixed-mode stationary phases. Crowther and coworkers [11,12] prepared mixed-mode stationary phases containing C_8 groups and quaternary ammonium groups by a two-step procedure. Kopaciewicz et al. [13] coated silica with polyethyleneimine. After cross-linking with diepoxides, the coating was derivatized with monoepoxides to control the hydrophobicity of the coating. El Rassi and Horváth [14] prepared mixed-mode phases with strong anion-exchange/weak hydrophobic and weak anion-exchange/weak hydrophobic properties on silica supports, by initially attaching dimethylpropylsilane groups to the surface and, subsequently, binding polar moieties to the carbon chains.

The columns described above were mainly used for the separation of (oligo)nucleotides, RNA, DNA and peptides.

Another group of columns also shows, beside their main retention activity, some secondary selectivity not intentionally introduced by the manufacturer (e.g. low-capacity anion-exchange columns also show some reversed-phase properties in many cases). The Hamilton PRP-X100 is an example of this kind of columns. Basically, it is a low-capacity anion-exchange column. However, it also shows reversed-phase properties, because the sample solutes may undergo interactions with its hydrophobic matrix, made up of polystyrene cross-linked with divinylbenzene. These reversed-phase properties were demonstrated by several groups [15–19].

Mixing a reversed phase with an anion-exchange stationary phase (mixed-phase), or connecting an anion-exchange and a reversed-phase column in series, are other possibilities to achieve mixed-mode properties. Comparing a mixed-mode reversed-phase/cation-exchange with a mixed-phase (reversed-phase/cation-exchange) and with a cation-exchange including a reversed-phase column in series, Issaq and Gutierrez [20] observed the best results for the mixed-mode column, using anti-depressants as the model compounds. The performance of the mixed-phase column was less compared to that

of the mixed-mode column, but the retention times were considerably shorter compared to the two columns in series. Crowther et al. [12] also observed that the mixed-phase approach showed inferior results, compared to mixed-mode stationary phases.

A number of commercial mixed-mode columns have been coming onto the market over the last few years. Examples are the ABx columns of J.T. Baker [21,22] and the mixed-mode RP C_4, C_8, C_{18}/Anion columns of Alltech [23,24]. These columns contain silica-based stationary phases. Another example is the OmniPac PAX-500 of Dionex, which is a polymer-based mixed-mode column. This column has a macroporous core of ethylvinylbenzene cross-linked with divinylbenzene showing reversed-phase properties. A latex with quaternary ammonium groups is attached to this macroporous core, giving the stationary phase its anion-exchange properties [25–27].

In this research a number of columns were investigated as to their mixed-mode properties, being in this case reversed-phase/anion exchange, and their suitability to separate charged and neutral oligomers. Polymer-based columns were mainly investigated, because of the relatively high pH of the eluent used in this study. The columns were investigated as to their hydrophobic, anion-exchange and their mixed-mode properties, respectively, by using three different test mixtures consisting of (i) alkylbenzenes, alkylpyridines and alkylhydroxybenzoates, (ii) a number of inorganic anions and (iii) a number of alkane sulfonic acids and styrene sulfates. Finally, the results obtained on the columns investigated are discussed.

2. Experimental

2.1. Instrumentation

The HPLC system consisted of a Bischoff HPLC pump (Bischoff, Leonberg, Germany), a Metrohm 690 ion chromatograph (Metrohm, Herisau, Switzerland), a Bischoff Lambda 1000 UV detector and two recorders (Kipp and Zonen, Delft, Netherlands). The ion chromatograph consisted of a Valco injector (VICI Valco-Europe, Schenkon, Switzerland) and a Metrohm conductivity detector.

2.2. Columns

A number of columns were investigated concerning their hydrophobic, anionic and mixed-mode properties. The OmniPac PAX-500 (250 × 4 mm I.D.) column was from Dionex (Sunnyvale, CA, USA). Two specially prepared mixed-phase columns were from Polymer Labs. (Shropshire, UK); the columns (150 × 4.6 mm I.D.) contained a mixture of 50% of PLRP-S, 8 μm, 1000 Å particles and 50% of PL-SAX, 8 μm, 1000 Å particles as the stationary phase. The columns were slurry packed. Column 1 (PL1) was packed as reversed-phase PLRP-S columns are usually packed, using acetonitrile–water (7:1, w/w) as the packing solvent. Column 2 (PL2) was packed as ion-exchange PL-SAX columns are usually packed, using a buffer as the solvent. Also, a number of low-capacity anion-exchange columns were tested: A Hamilton PRP-X100 (10 μm, 125 × 4 mm I.D.), (Hamilton, Reno, NV, USA); a HEMA-S 1000 Q-L, 7 and 10 μm, and a HEMA-BIO 1000 NH_2, 7 μm (150 × 3 mm I.D.) (Tessek, Prague, Czech Republic).

In addition, two non-polymer-based columns were investigated as well: a Zorbax Bioseries Oligo (5 μm, 150 Å, 80 × 6.2 mm I.D.) from Rockland Technologies (Newport, DE, USA), and an Aluspher RP-Select B (5 μm, 100 Å, 119 × 4.6 mm I.D.) from Merck (Darmstadt, Germany). The Zorbax Bioseries Oligo has a silica-based support of which the silica has a zirconia-treated surface, which is stable up to a pH of 8.5. The Aluspher RP-Select B is prepared from an alumina based material, which can be used in a pH range of 2–12.

2.3. Chemicals

Methanol and acetonitrile, HPLC grade, were purchased from Merck. Tetrahydrofuran was purchased from Westburg (Leusden, Netherlands). Water was purified using a Milli-Q water-

purification system (Millipore, Milford, MA, USA). The aqueous buffers used consisted of solutions of ammonium carbonate (Merck), pH ≈ 9. This type of buffer can be readily removed after preparative-scale separations. Before use, the eluents were filtered and degassed ultrasonically.

Benzene, toluene, ethylbenzene, propylbenzene, butylbenzene and *p*-styrene sulfate (styrene sulfate 1) were from Aldrich (Steinheim, Germany); methyl *p*-hydroxybenzoate and propyl *p*-hydroxybenzoate were from Sigma (St. Louis, MO, USA); butanesulfonic acid was from Eastman Kodak (Rochester, NY, USA); pentanesulfonic acid and octanesulfonic acid were from FSA Laboratory Supplies (Loughborough, UK); dodecanesulfonic acid, sodium fluoride, sodium chloride, sodium nitrite, sodium nitrate, sodium sulfite and sodium sulfate (analytical-reagent grade) were from Merck; *o*-pentylpyridine, *o*-hexylpyridine and 2-phenylethyl sulfate (styrene sulfate 2) were synthesised in our department.

2.4. Methods

The columns were tested in three modes: (i) reversed phase, (ii) anion exchange and (iii) mixed-mode.

The reversed-phase properties of the columns were tested using mixtures of an organic modifier (methanol, acetonitrile or tetrahydrofuran) and water as the eluents. The alkylbenzenes, the alkylhydroxybenzoates and the alkylpyridines were used as test compounds. The compounds were detected by UV detection at 254 nm. The column performance and the capacity factors of the compounds were measured at several eluent compositions. The hold-up time of the column, t_0, was determined by the injection of methanol.

The anion-exchange properties of the columns were tested, using aqueous solutions of ammonium carbonate as the eluents. For the Polymer Labs. and the OmniPac columns, 1% of organic modifier was added to the eluent, to ensure sufficient wetting of the columns. The inorganic anions were used as the test compounds. The compounds were detected using conductivity detection. The capacity factors of the compounds were measured for a range of ammonium carbonate concentrations. The t_0 was determined by the injection of water.

The mixed-mode properties of the columns were tested, using mixtures of an organic modifier and an aqueous solution of a specific concentration of ammonium carbonate as the eluents. The test compounds were the alkanesulfonic acids and the styrene sulfates. The alkanesulfonic acids were used as model compounds for butadiene oligomers and the styrene sulfates as model compounds for styrene oligomers. The detection of the alkanesulfonic acids was performed by conductivity detection, while the styrene sulfates were detected by UV detection at 254 nm. The capacity factors of the test compounds were measured for concentrations of 1 to 90% of the organic modifiers in aqueous ammonium carbonate solutions of two concentrations, $5 \cdot 10^{-3}$ and 10^{-2} *M*. The column performance under mixed-mode conditions was measured for the styrene sulfates. The t_0 was determined by the injection of water.

With exception of the HEMA columns, the flow used in the experiments described above was 1 ml/min. In the case of the HEMA columns a flow of 0.5 ml/min was used.

3. Results and discussion

Since the PRP-X100, the OmniPac PAX-500 and the Polymer Labs. columns (PL1 and PL2) were the only ones to initially show promising results for the separation of charged and uncharged oligomers, the results of the other columns used in this work will not be discussed in detail. The HEMA columns showed only few reversed-phase properties and it was impossible to obtain baseline separation for the alkylbenzenes. The plate numbers for the alkylbenzenes were ca. 2000–3000 plates/m, assuming Gaussian peak shapes, and considerable fronting of the peaks occurred. It was possible to achieve some separation between the alkanesulfonic acids, but the peaks were very broad and the reproducibility was bad. Also, the column per-

formance decreased rapidly after only a few weeks of use, probably due to the fact that these columns were not suitable for the eluents applied [28]. Due to the polarity of the Zorbax Oligo column, it was only possible to obtain separation between the alkylbenzenes at very low organic modifier concentrations. This column showed almost no separation of the inorganic ions. Using this column in reversed-phase and anion-exchange mode these results could be expected because the column consists of a normal silica-based stationary phase. In the mixed-mode test of this column the alkanesulfonic acids and the styrene sulfates also showed low capacity factors, so it was not possible to achieve a separation between these compounds. Finally, the Aluspher Select-B also showed low capacity factors only for the alkanesulfonic acids and styrene sulfates and, therefore, this column was not suitable for these separations either.

3.1. Reversed-phase mode

To test the columns in the reversed-phase mode, useful performance criteria were first defined using the retention times and the resolution of the alkylbenzenes as parameters. The criteria were to obtain a resolution as high as possible, but larger than at least 1 with a retention time below 25 min for butylbenzene. In some cases, where it was not possible to obtain a resolution higher than 1 with these restrictions, a longer retention time was accepted.

The plate number was calculated from [29]:

$$N = 5.54\left(\frac{t_R}{w_h}\right)^2 \quad (1)$$

where t_R is the retention time and w_h is the peak width at half height. In case of increased peak asymmetry values (>1.25) the accuracy of the calculated plate numbers will rapidly decrease [30]. Also from our data the asymmetry factors, *asf*, were calculated at 10% of the peak heights [30].

The resolution was calculated using the following formula [29]:

$$R_s = \frac{t_{R2} - t_{R1}}{(w_{h1} + w_{h2})/1.18} \quad (2)$$

where t_{R1} and t_{R2} are the retention times and w_{h1} and w_{h2} are the peak widths at half height for compounds 1 and 2, respectively.

Under these conditions, the plate number N, the resolution R_s and the asymmetry factor *asf* of the test compounds for the OmniPac, the PRP-X100 and the Polymer Labs. (PL1 and PL2) columns, were measured and are given in the Figs. 1, 2 and 3, respectively, for the three different organic modifiers. The highest plate numbers were observed using acetonitrile as the organic modifier (Fig. 1). The plate numbers for methanol were very low, especially for the Polymer Labs. columns. For the PL1 column it was impossible to obtain a resolution of 1 under these conditions. It is known from literature that polymer-based stationary phases show a poor performance when methanol is used as the organic modifier [31]. The plate numbers were also low for all columns using tetrahydrofuran as the organic modifier. This is in contrast with results published earlier [31]. No results are provided in this study for the OmniPac column using tetrahydrofuran because these columns are not compatible with eluent concentrations containing more than 10% tetrahydrofuran. The best resolution (Fig. 2) of the test compounds was also observed using acetonitrile as the organic modifier. Better results, in this respect, were obtained for methanol compared with tetrahydrofuran. In almost all cases peak tailing was observed on the investigated columns, *asf* > 1 (Fig. 3). Comparing the two Polymer Labs. columns, PL2 showed higher plate numbers, but the *asf* value was higher too.

As mentioned, the reversed-phase performance of the columns was determined for the alkylbenzenes. With the alkylhydroxybenzoates and the alkylpyridines as the test compounds, the behaviour of the columns for other types of compounds was investigated under the same conditions. As an example, the retention times of the alkylbenzenes, the hydroxybenzoates and the pyridines for methanol as the organic modifier in the eluent are given in Table 1 under the conditions used in Figs. 1–3. The retention times on the Polymer Labs. and the OmniPac columns were about the same as for benzene, for both the

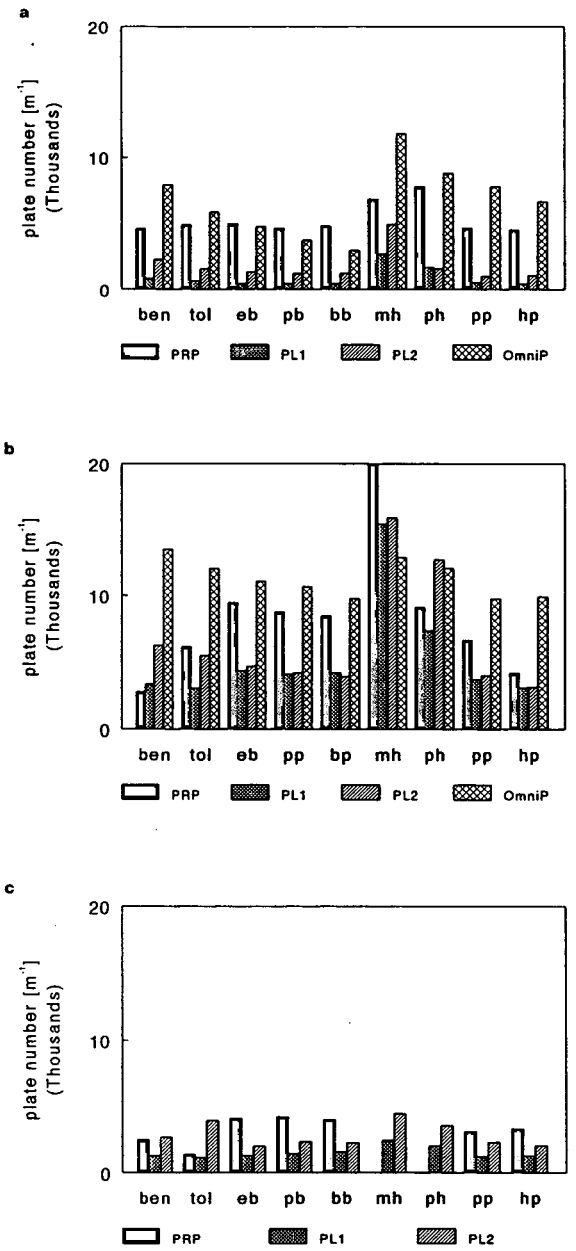

Fig. 1. Plate numbers N for benzene (ben), toluene (tol), ethylbenzene (eb), propylbenzene (pb), butylbenzene (bb), methyl p-hydroxybenzoate (mh), propyl p-hydroxybenzoate (ph), o-pentylpyridine (pp) and o-hexylpyridine (hp) in the reversed-phase mode. Eluents: (a) methanol–water; PL1, PL2: (80:20); PRP-X100: (90:10); OmniPac PAX-500: (95:5, v/v). (b) Acetonitrile–water; PL1, PL2: (45:55); PRP-X100: (73:27); OmniPac PAX-500: (77:23, v/v). (c) Tetrahydrofuran–water; PL1, PL2: (30:70); PRP-X100: (38:62, v/v).

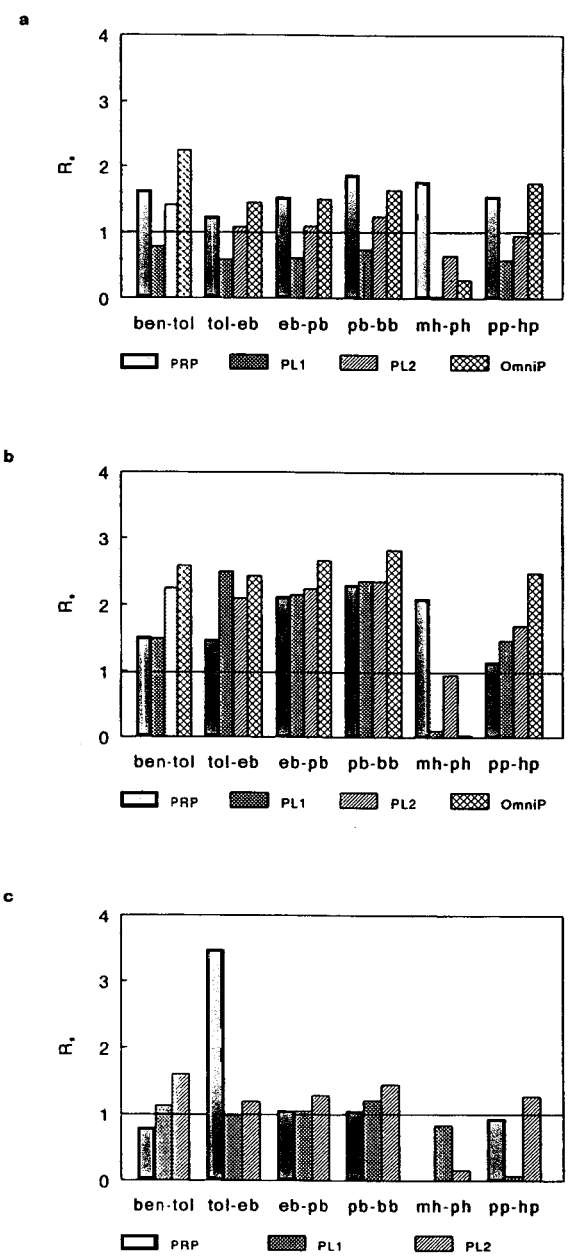

Fig. 2. Resolution R_s between the solute pairs benzene–toluene (ben-tol), toluene–ethylbenzene (tol-eb), ethylbenzene–propylbenzene (eb-pb), propylbenzene–butylbenzene (pb-bb), methyl p-hydroxybenzoate–propyl p-hydroxybenzoate (mh-ph) and o-pentylpyridine–o-hexylpyridine (pp-hp) in the reversed-phase mode. Eluents: (a) methanol–water, (b) acetonitrile–water, (c) tetrahydrofuran–water. Columns: PL1, PL2, PRP-X100 and OmniPac PAX-500. For experimental conditions see Fig. 1.

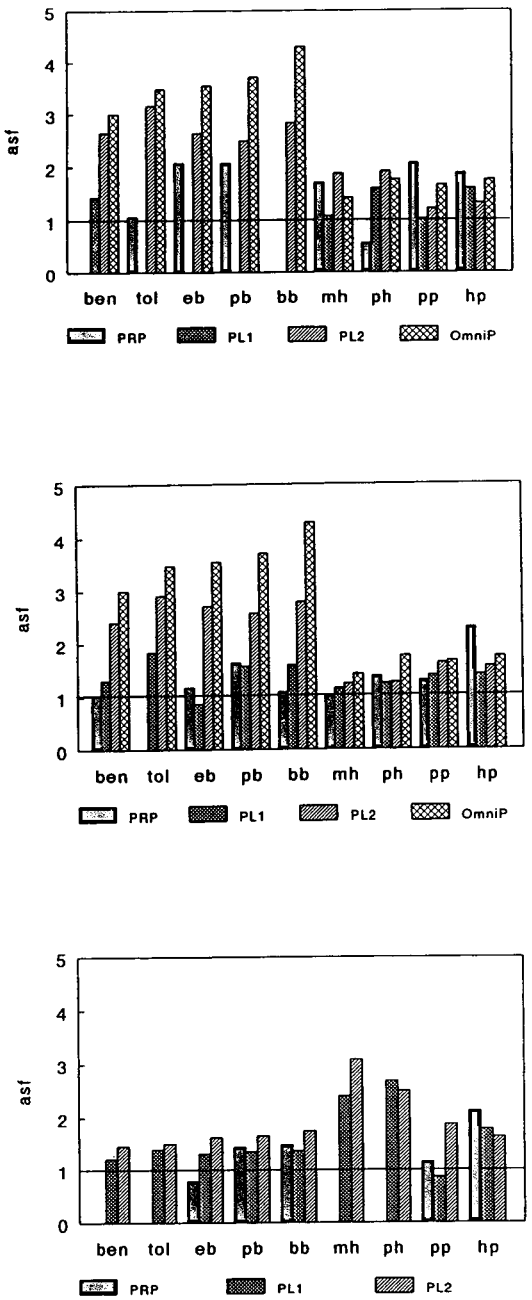

Fig. 3. Asymmetry factors *asf* for benzene, toluene, ethylbenzene, propylbenzene, butylbenzene, methyl *p*-hydroxybenzoate, propyl *p*-hydroxybenzoate, *o*-pentylpyridine and *o*-hexylpyridine in the reversed-phase mode. Eluents: (a) methanol–water, (b) acetonitrile–water, (c) tetrahydrofuran–water. Columns: PL1, PL2, PRP-X100 and OmniPac PAX-500. For experimental conditions see Fig. 1.

hydroxybenzoates and the pyridines, as could be expected considering the polarity of the compounds. However, the retention times on the PRP-X100 column were considerably larger for the alkylhydroxybenzoates than for the pyridines and were in the same range as for butylbenzene. This suggests a strong specific interaction of these esters to the PRP-X100 column.

On the PL1 column the propyl ester of the alkylhydroxybenzoates eluted before the methyl ester (Table 1). For all the columns investigated, it was observed that when the amount of organic modifier in the eluent was increased, at a certain organic modifier concentration the propyl ester eluted before the methyl ester. These observations are in contrast to the general assumption that the log k' vs. the percentage of the organic modifier of members of a specific homologous series results in more or less parallel relationships. This shows the limitations of that model, which is only valid over a limited range of organic modifier concentrations.

On these polymeric columns, the hydroxybenzoates and the pyridines showed about the same performance compared with the alkylbenzenes, as can be seen in Figs. 1–3. The columns did not show a poor performance for basic compounds, in comparison with silica-based reversed-phase columns. This is a result of the lack of interfering interactions by the basic pyridines with the free silanol groups present on silica surfaces [32]. The hydrophobicity of the columns increases in the range PL1, PL2, PRP-X100 and OmniPac PAX-500, taking the percentage of organic modifier necessary to elute the alkylbenzenes from a column into account.

As already mentioned the following formula applies for the capacity factor, as a function of the concentration of organic modifier in the eluent, for reversed-phase stationary phases (over a limited concentration range of organic modifier):

$$\log k' = a - mx \quad (3)$$

where x is the concentration of the organic modifier in the eluent, k' is the capacity factor, and a and m are constants. Bowers and Pedigo [31] showed that this formula also applies using

Table 1
Retention times t_R and capacity factor k' of the alkylbenzenes, the hydroxybenzoates and the pyridines

	PRP-X100		PL1		PL2		Omnipac PAX-500	
	t_R (min)	k'	t_R (min)	k'	t_R (min)	k'	t_R (min)	k'
Benzene	5.02	4.28	4.29	1.66	5.58	2.23	7.67	2.56
Toluene	7.29	6.67	6.53	3.04	4.19	4.19	10.42	3.84
Ethylbenzene	9.59	9.09	4.86	4.86	13.51	6.81	13.06	5.06
Propylbenzene	13.59	13.31	14.35	7.89	20.82	11.04	16.94	6.96
Butylbenzene	20.89	20.99	23.92	13.81	34.69	19.06	23.34	9.83
Methyl *p*-hydroxybenzoate	21.13	21.13	5.78	2.58	3.31	0.92	6.00	1.78
Propyl *p*-hydroxybenzoate	27.35	27.79	2.48	2.48	3.99	1.31	6.19	1.87
Pentylpyridine	4.96	4.22	4.25	1.63	5.59	2.23	7.88	2.66
Hexylpyridine	7.11	6.48	6.20	2.84	8.48	3.91	9.92	3.60

Eluent: methanol–water: PRP-X100: (90:10, v/v); PL1, PL2: (80:20, v/v); OmniPac PAX-500: (95:5, v/v).

polystyrene-based reversed-phase columns. This equation also showed to be valid for the data measured on the PL1, PL2 and the OmniPac PAX-500 columns for all three organic modifiers used, as is shown in Fig. 4.

Generally, the logarithm of the capacity factors of homologous series are linearly dependent on the length of the alkyl chain for reversed-phase columns [33]. This relationship also showed to be valid for the columns used in this study, using alkylbenzenes as the homologous series (Fig. 5).

From the data it can be concluded that the PRP-X100, the OmniPac PAX-500 and both the Polymer Labs. columns showed typical reversed-phase behaviour, when tested in the reversed-phase mode. In turn, this implicates the suitability of these columns for the separations of neutral oligomers.

3.2. Ion-exchange mode

Eq. 4 holds for ions eluting from an ion-exchange column [34].

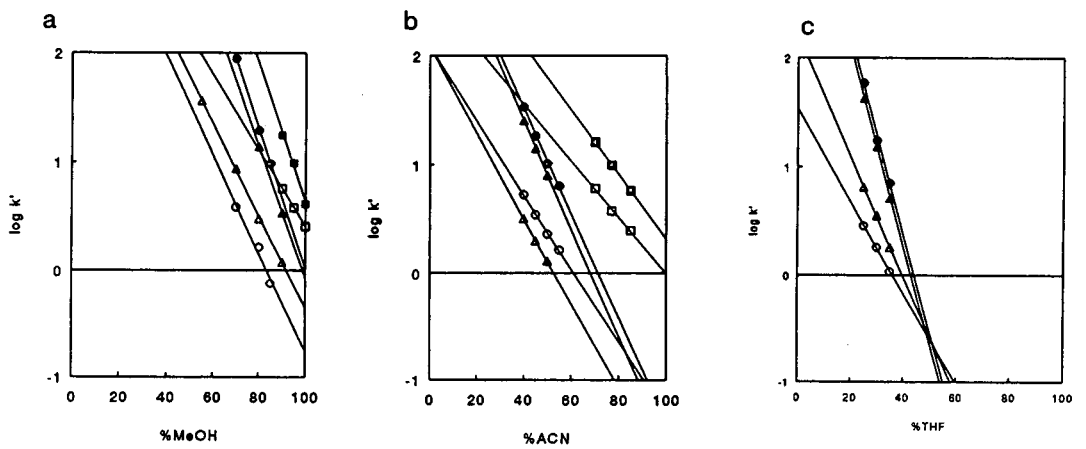

Fig. 4. Logarithm of the capacity factor k' versus the percentage organic modifier (MeOH = methanol; ACN = acetonitrile; THF = tetrahydrofuran) in the eluent. Compounds: toluene and butylbenzene. Columns: PL1, PL2 and OmniPac PAX-500. △ = toluene on PL1; ○ = toluene on PL2; □ = toluene on OmniPac; ▲ = butylbenzene on PL1; ● = butylbenzene on PL2; ■ = butylbenzene on OmniPac.

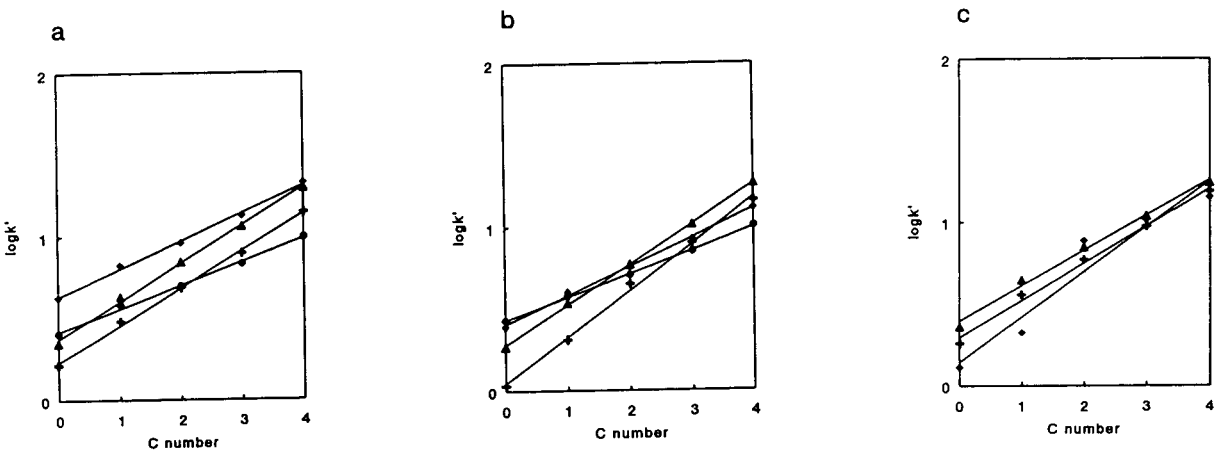

Fig. 5. Logarithm of the capacity factor k' versus the length of the alkyl chain of a homologous series of alkylbenzenes. Compounds: benzene, toluene, ethylbenzene, propylbenzene and butylbenzene. Columns: PL1, PL2, PRP-X100 and OmniPac PAX-500. Eluents: (a) methanol–water; PL1 (+), PL2 (▲): (80:20, v/v); PRP-X100 (◆): (90:10); OmniPac PAX-500 (●): (95:5, v/v). (b) Acetonitrile–water; PL1 (+), PL2 (▲): (45:55, v/v); PRP-X100 (◆): (73:27, v/v); OmniPac PAX-500 (●): (77:23, v/v). (c) Tetrahydrofuran–water; PL1 (+), PL2 (▲): (30:70, v/v); PRP-X100 (◆): (38:62, v/v).

$$\log k' = \frac{c}{b} \log C - \frac{c}{b} \log [E^-] + K \qquad (4)$$

where C is the resin capacity, $[E^-]$ the ion concentration in the eluent, c the charge of the solute ion, b the charge of the eluent ion and K a constant.

This relation also showed to be valid for the columns investigated (Fig. 6). This result could be expected for the PRP-X100 column, because it was specifically developed for anion-exchange separations. The anion-exchange behaviour of the OmniPac PAX-500 was already described previously [25]. The slopes and the correlation coefficients (R values) of the lines in Fig. 6, calculated by using linear regression, are presented in Table 2. The low value for R in the case of the fluoride ion regarding the OmniPac column is caused by the low retention times. So interaction occurs between the fluoride peak and the system peaks, yielding inaccurate results for the retention times. The slope for the OmniPac and the PRP-X100 was ca. -1, for the monovalent solute anions. For the Polymer Labs. columns the slope was higher than -1, probably due to the reversed-phase stationary phase present in these columns. Looking to Eq. 4 this means that the ammonium carbonate in the eluent is monovalent, thus in the hydrogencarbonate form, as can be expected at a pH of ca. 9. When divalent anions are used as test compounds, the slope was smaller than -1, but not -2 as was to be expected in combination with monovalent eluent ions. This implies that the divalent anions are not retained as divalent anions. To be retained as a divalent anion, it must face two adjacent anion-exchange sites on a stationary phase that are spaced appropriately [25]. This is apparently not the case.

In Table 3 capacity factors and plate numbers of the columns for nitrate are given. The poorest anion-exchange performance using these eluent mixtures was observed for the OmniPac column. However, it should be emphasized that the OmniPac column is specifically designed for hydroxide as the eluent anion [25]. Better results were observed for the Polymer Labs. columns, especially when higher buffer concentrations were used. In this case short retention times were observed, indicating that the reversed-phase stationary phase has a negative influence on the performance in the anionic mode. Similar effects of the hydrophobicity of anion-exchange columns on the performance of i.e. the nitrate ion were also observed by Weiss [35]. The results for the PRP-X100 column were constant over the

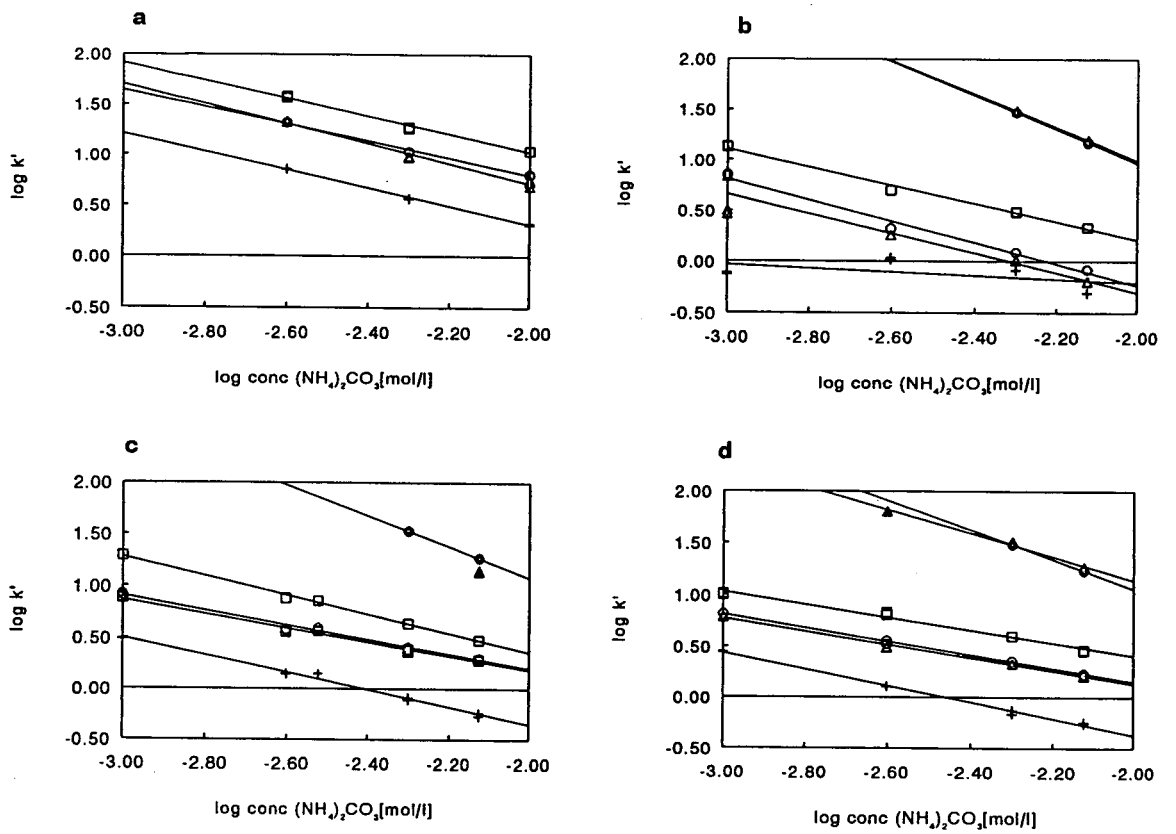

Fig. 6. Logarithm of the capacity factor versus the logarithm of the carbonate concentration in the eluent, the column is in the anion-exchange mode. Eluent: ammonium carbonate, for PL1, PL2 and OmniPac PAX-500 1% methanol was added. Compounds: fluoride (+), chloride (△), nitrite (○), nitrate (□), sulfite (▲) and sulfate (●). Columns: (a) PRP-X100, (b) OmniPac PAX-500, (c) PL1, (d) PL2.

ionic strength range and were, therefore, better at lower buffer concentrations and worse at the higher buffer concentrations.

To find out whether there is a difference between the nature of the organic modifier, used for wetting the OmniPac and the Polymer Labs.

Table 2
Slopes and R values for the lines shown in Fig. 6

	PRP-X100		OmniPac		PL1		PL2	
	Slope	R	Slope	R	Slope	R	Slope	R
F^-	−0.90	0.990	−0.17	0.485	−0.85	0.995	−0.81	0.998
Cl^-	−0.99	0.994	−0.96	0.948	−0.69	0.994	−0.64	0.998
NO_2^-	−0.85	0.998	−1.04	0.992	−0.70	0.995	−0.66	0.999
NO_3^-	−0.88	0.996	−0.89	0.995	−0.92	0.998	−0.62	0.992
SO_3^{2-}			−1.65				−1.12	0.995
SO_4^{2-}			−1.08	0.999	−1.47		−1.41	

For experimental conditions see Fig. 6.

Table 3
Plate numbers N and capacity factors k' of nitrate

$(NH_4)_2CO_3$ concentration concentration (M)	OmniPac		PL1		PL2		PRP-X100, N (plates/m)
	N (plates/m)	k'	N (plates/m)	k'	N (plates/m)	k'	
$1 \cdot 10^{-3}$	2286		–		953		–
$2.5 \cdot 10^{-3}$	1352		1347		1168		2172
$3 \cdot 10^{-3}$	–		2453		–		–
$5 \cdot 10^{-3}$	1566		5612		3845		2178
$7.5 \cdot 10^{-3}$	1621	2.17	14 959	3.01	7447	2.92	2166
$7.5 \cdot 10^{-3}$ (1% ACN)	1818	2.10	10 218	3.23	7239	2.89	

Eluent: ammonium carbonate in water; for the OmniPac PAX-500 and the Polymer Labs. columns 1% organic modifier was added to the eluent. Unless otherwise noted methanol was used as the organic modifier.

columns, the plate numbers and the retention times for nitrate were measured for 1% methanol and for 1% acetonitrile added to the eluent (see Table 3). The difference in retention time using methanol or acetonitrile was small. Somewhat higher plate numbers were observed for the OmniPac column when this column was wetted with acetonitrile. The plate numbers for the Polymer Labs. columns were higher using 1% methanol instead of 1% acetonitrile, especially for the PL1. This is in contrast with the results found for the reversed-phase behaviour of these columns found in this study and in literature [31]. This implies that the effect of the organic modifier on inorganic ions is different from the effect they have on neutral compounds [25].

3.3. Mixed-mode

As indicated above, the logarithm of the capacity factors of the test compounds versus the percentage organic modifier in the eluent provides a straight line in reversed-phase chromatography. In anion-exchange chromatography, the logarithm of the capacity factor is linearly dependent on the logarithm of the anion concentration in the eluent. These linear dependencies were not observed for the PL1 column, when it was used under mixed-mode conditions (see Fig. 7a and b). The other columns also exhibited typical mixed-mode behaviour, as is shown in Fig. 7c, d and e. At lower organic modifier concentrations the sulfonic acids and the styrene sulfates exhibit "reversed-phase" properties: the capacity factor decreases with an increasing organic modifier concentration. Here, the limiting factor for elution is the organic modifier concentration. At higher concentrations of organic modifier, the capacity factor increases rapidly for all components. In this case, the anion concentration in the eluent is the limiting factor for elution.

The same dependency of the retention mechanism with the organic modifier concentration was also observed, for instance, by Grego and Hearn [36]. On a reversed-phase column, they observed reversed-phase behaviour of the column for polypeptide hormones at low concentrations of the organic modifier, while at higher concentrations the ionogenic polypeptide hormones showed polar interactions with the column.

The fluoride ion also deviates from the usual ion-exchange behaviour, using a combination of buffer and an organic modifier as the eluent, as is shown in Fig. 7b. This is caused by the fact that the organic modifier present in the eluent will induce a decreased hydratation of the solute anion, which results in an increase in the retention time [37]. The change of the capacity factors of the alkanesulfonic acids, as a function of the shorter alkyl chains with the concentration of the organic modifier, in some cases shows similar behaviour to that of the fluoride ion. In these cases the alkyl chain is probably too short to have a substantial interaction with the hydrophobic backbone of the stationary phase.

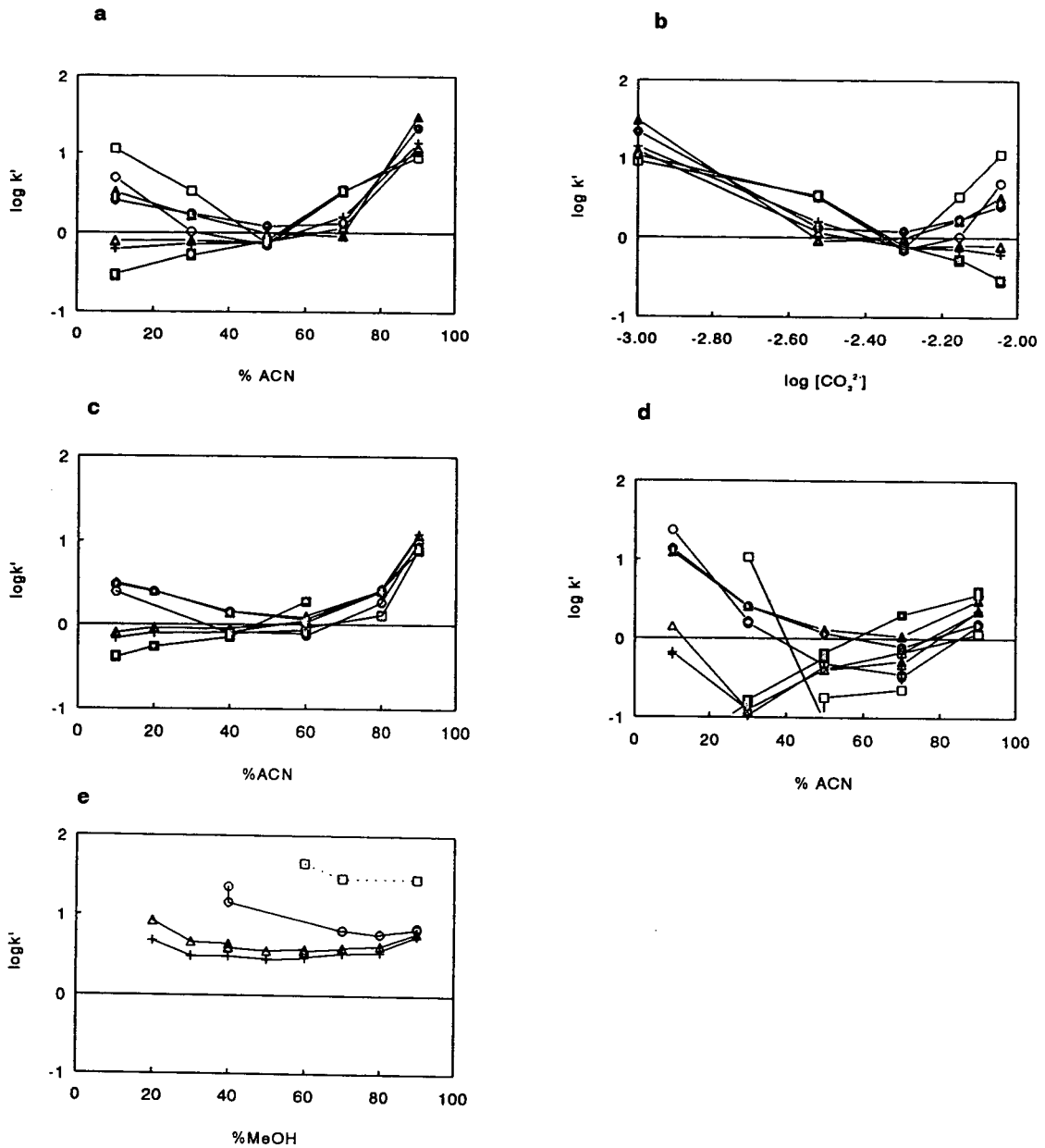

Fig. 7. Influence of the concentrations of the organic modifier and ammonium carbonate in the eluent under mixed-mode conditions. (a) PL2, percentage organic modifier versus the logarithm of the capacity factor; organic modifier: acetonitrile; concentration of $(NH_4)_2CO_3$ in water: 10^{-2} *M*; diluted with organic modifier to the concentration indicated. (b) PL2, logarithm of the concentration of $(NH_4)_2CO_3$ versus the logarithm of the capacity factor; organic modifier: acetonitrile; concentration of $(NH_4)_2CO_3$ in water: 10^{-2} *M*. (c) PL1, percentage organic modifier versus the logarithm of the capacity factor; organic modifier: acetonitrile; concentration of $(NH_4)_2CO_3$ in water: 10^{-2} *M*. (d) OmniPac PAX-500, percentage organic modifier versus the logarithm of the capacity factor; organic modifier: acetonitrile; concentration of $(NH_4)_2CO_3$ in water: 10^{-2} *M*. (e) PRP-X100, percentage organic modifier versus the logarithm of the capacity factor; organic modifier: methanol; concentration of $(NH_4)_2CO_3$ in water: 10^{-2} *M*. + = Butanesulfonic acid; △ = pentanesulfonic acid; ○ = octanesulfonic acid; □ = dodecanesulfonic acid; ▲ = styrene sulfate 1; ● = styrene sulfate 2; ■ = fluoride.

The separation factor α for the solute pairs butane-/pentanesulfonic acid and butane-/octanesulfonic acid, using as the eluents two aqueous ammonium carbonate solutions, of concentrations of respectively $5 \cdot 10^{-3}$ and 10^{-2} M, with methanol or acetonitrile as the organic modifier, is presented in Figs. 8 and 9. In all cases the separation factor was higher for methanol compared to acetonitrile. In addition, α was higher using a higher anion concentration in the eluent. This is another demonstration of the mixed-mode behaviour of the columns; no difference in α would be obtained if anion exchange as the only retention mode was active. This can be explained as follows. Combining Eqs. 4 and 5 for α, with k_1' and k_2' as the capacity factors for components 1 and 2, respectively:

$$\alpha = k_1'/k_2' \tag{5}$$

gives:

$$\alpha = e^{K_2/K_1} \tag{6}$$

where K_1 and K_2 are the constants from Eq. 4 for the compounds 1 and 2, respectively. From the resulting Eq. 6 it is obvious that α is independent of the eluent ion concentration. In addition, no difference in α would be observed if

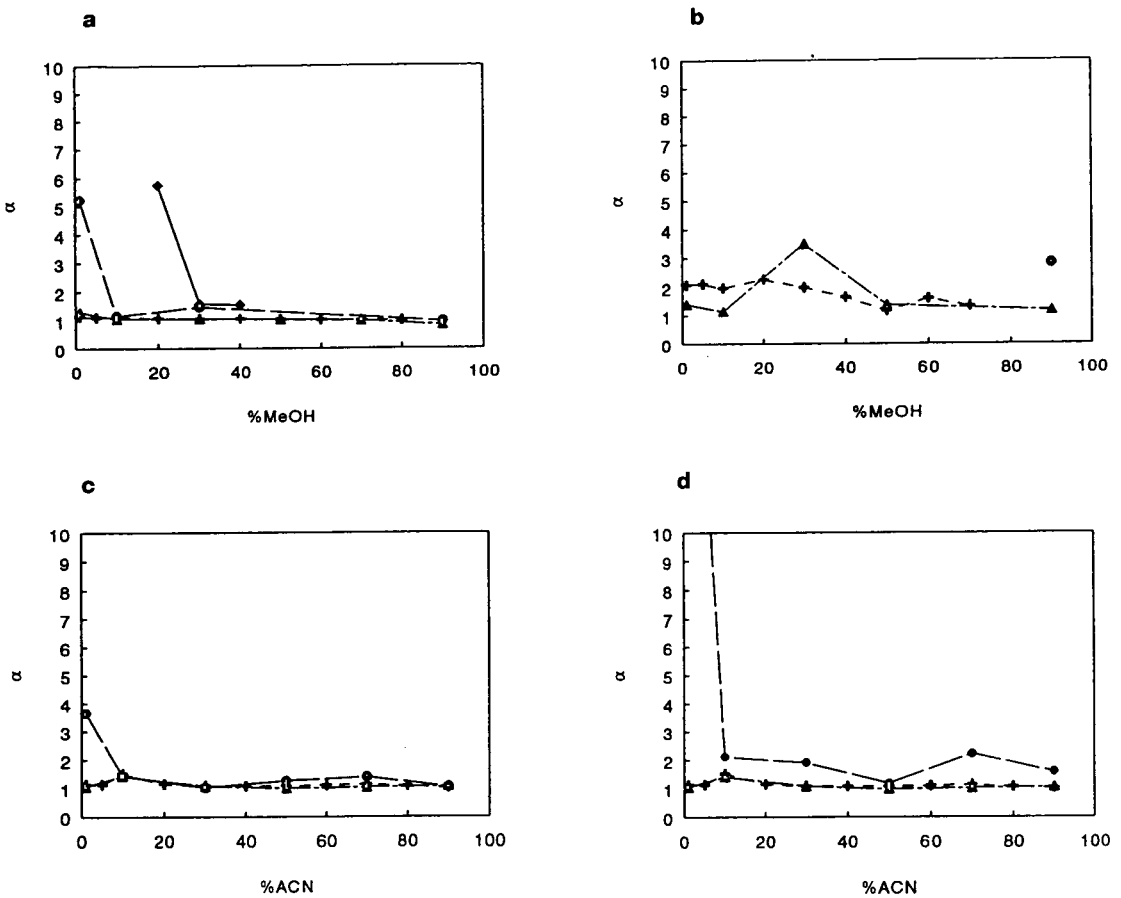

Fig. 8. Separation factor α as function of the organic modifier concentration in the eluent. Ammonium carbonate concentration in water was $5 \cdot 10^{-3}$ M. Columns: PRP-X100 (◆), PL1 (+), PL2 (▲) and OmniPac PAX-500 (○). (a) Methanol, α (butanesulfonic acid–pentanesulfonic acid); (b) methanol, α (butanesulfonic acid–octanesulfonic acid); (c) acetonitrile, α (butanesulfonic acid–pentanesulfonic acid); (d) acetonitrile, α (butanesulfonic acid–octanesulfonic acid).

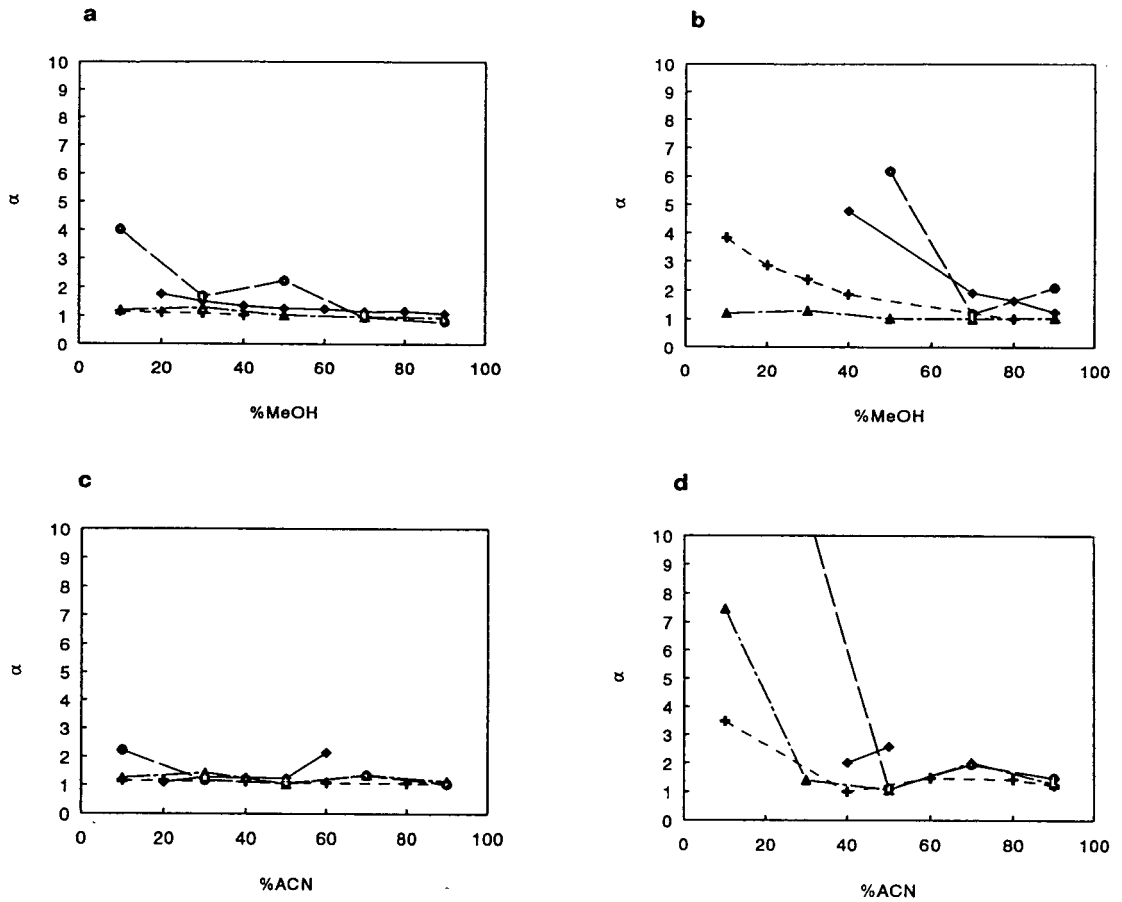

Fig. 9. Separation factor α as function of the organic modifier concentration in the eluent. Ammonium carbonate concentration in water was 10^{-2} *M*. Columns: PRP-X100 (◆), PL1 (+), PL2 (▲) and OmniPac PAX-500 (○). (a) Methanol, α (butanesulfonic acid–pentanesulfonic acid); (b) methanol, α (butanesulfonic acid–octanesulfonic acid); (c) acetonitrile, α (butanesulfonic acid–pentanesulfonic acid); (d) acetonitrile, α (butanesulfonic acid–octanesulfonic acid).

reversed-phase behaviour only took place. No difference in the capacity factors, between the two ion concentrations in the eluent, would be observed if the same concentration of organic modifier was used. The increase in α could be explained with a combination of these two retention modes. Considering the solute pair butane- and octanesulfonic acid, the octanesulfonic acid shows more reversed-phase behaviour and less anion-exchange behaviour. The influence of increasing the anion concentration in the eluent, will decrease the capacity factor less compared to the butanesulfonic acid, which shows less reversed-phase and more anion-exchange behaviour. Besides the higher α values, another advantage of higher anion concentrations in the eluent are the lower retention times of the test compounds.

Next, the efficiency of the columns for styrene sulfates 1 and 2 was investigated. The plate numbers and the asymmetry factors for the styrene sulfates are presented in Table 4 for the OmniPac PAX-500 and the PL2 columns, using methanol and acetonitrile as the organic modifiers in the eluent. A higher plate number was observed in almost all cases for styrene sulfate 1 compared to styrene sulfate 2, which is probably caused by the differences of the sulfate group's

Table 4
Plate numbers N and asymmetry factors *asf* of styrene sulfates 1 and 2 on the Omnipac PAX-500 and the PL2 columns

Organic modifier (%)	Solute	Omnipac				PL2			
		Methanol		Acetonitrile		Methanol		Acetonitrile	
		N (plates/m)	*asf*	N (plates/m)	*asf*	N (plates/m)	*asf*	N (plates/m)	*asf*
10	Styrene sulfate 1	–	–	16 824	1.38	8 964	3.16	8 466	1.76
	Styrene sulfate 2	–	–	1 873	10.70	1 043	9.45	1 887	3.73
30	Styrene sulfate 1	13 348	3.19	16 144	1.93	8 316	1.25	8 609	1.71
	Styrene sulfate 2	1 621	6.25	3 999	5.02	6 328	2.20	3 927	1.01
50	Styrene sulfate 1	2 728	2.50	10 066	2.43	7 211	1.31	8 455	1.64
	Styrene sulfate 2	2 270	5.40	4 608	0.56	6 461	1.39	1 190	0.28
70	Styrene sulfate 1	16 538	2.11	10 181	0.89	6 943	1.29	14 353	1.22
	Styrene sulfate 2	3 478	3.26	960	1.33	7 605	–	349	0.24
90	Styrene sulfate 1	13 345	1.16	18 584	0.50	7 588	1.18	21 288	0.76
	Styrene sulfate 2	998	3.63	246	–	984	3.26	455	0.18

Eluent: mixture of methanol or acetonitrile as the organic modifier and an aqueous ammonium carbonate solution; the ammonium carbonate concentration in aqueous buffer was 10^{-2} M.

location on the styrene molecule. The *asf* was also better for styrene sulfate 1, for high or low concentrations of an organic modifier. For styrene sulfate 2, high asymmetry factors were observed using low organic modifier concentrations, while at high organic modifier concentrations asymmetry factors below 1 were observed for this compound. No significant difference in performance was observed between methanol and acetonitrile when they were used as the organic modifier in the eluent. This contrasts with the reversed-phase and the anion-exchange mode. The retention times between the two styrene sulfates differed no more than 10% in most cases (see Fig. 7). The plate numbers for the alkanesulfonic acids were not measured because of the interference of system peaks which occur when a conductivity detector is used.

In conclusion, all the columns were able to separate butane- from octanesulfonic acid. A separation factor higher than 1 could be obtained using low concentrations of an organic modifier (see Figs. 8 and 9). Therefore, it is to be expected that sulfate monomers can be separated from sulfate dimers of butadiene. More general, in our opinion this approach has a potential for the separation of oligomers in real samples.

For the PRP-X100 column, the retention times for dodecanesulfonic acid and the styrene sulfates were very high for all eluent mixtures used (see Fig. 7e). For butadiene oligomers, it is known that oligomers at least up to $n = 4$, of both monosulfates and disulfates, are formed [1,38,39]. For styrene sulfate, oligomers up to $n = 2$ or 3 are formed [1,40]. This implies that with the PRP-X100 columns, the separation of these oligomers would be very time consuming. One way to decrease the retention times of these compounds is to increase the ammonium carbonate concentration in the eluent. There are two problems concerning this solution. With the increase of the ammonium carbonate concentration conductivity detection becomes difficult, as the conductivity of the eluent may exceed the range of the conductivity detector. Secondly, using a higher ammonium carbonate concentration yielded a more instable baseline, due to a

larger decrease in conductivity by the decomposition of the eluent. This also caused a decrease in the reproducibility of the retention times.

The Polymer Labs. columns showed reasonable retention times for the alkanesulfonic acids and, consequently, are more useful for this separation. However, the selectivity between the butane- and the pentanesulfonic acid is low, $\alpha \approx 1$ (see Figs. 8 and 9), so it probably is a problem to separate isomers formed during the polymerization. In this study the mixed-phase approach, using the Polymer Labs. columns, showed similar results to the mixed-mode approach. The difference in retention times between the PRP-X100 and the Polymer Labs. columns could be explained by the resin capacity of the columns. The resin capacity of the PRP-X100 is ca. 290 μequiv./ml [25]. The resin capacity of PL-SAX is >200 μequiv./ml [41], resulting in a resin capacity of >100 μequiv./ml for the Polymer Labs. columns. From Eq. 4 it is clear that increasing the resin capacity of a column increases the retention times of alkanesulfonic acids, as was shown by Pietrzyk et al., too [42].

With the OmniPac column it is possible to separate butane- from pentanesulfonic acid and to obtain reasonable retention times for the larger alkanesulfonic acids (see Fig. 7d). Here, a disadvantage is that to perform the separation of the smaller and the larger alkanesulfonic acids in one analysis, it is necessary to use a gradient.

4. Conclusions

A number of columns were investigated with respect to their ability to separate model compounds for charged and uncharged oligomers, formed during emulsion polymerization processes. The PRP-X100, the OmniPac and the Polymer Labs. columns showed promising results with respect to the separation of charged and uncharged oligomers of butadiene and styrene. The columns displayed typical reversed-phase, anion-exchange or mixed-mode behaviour when tested under reversed-phase, anion-exchange or mixed-mode conditions, respectively. As expected, the reversed-phase quality of the columns was not comparable to silica-based reversed-phase materials. Under mixed-mode conditions it was shown that manipulation of the eluent, i.e. the ionic strength and the nature and the concentration of the organic modifier therein, provides an good way to separate charged oligomers. It was possible to obtain a separation factor large enough to allow for the separation of charged oligomers. The other columns investigated, being Tessek HEMA, Aluspher RP-Select B and Zorbax Bioseries Oligo, were less useful for the separations of oligomers under the conditions applied in this study.

Acknowledgements

We would like to thank Polymer Labs., Shropshire, UK, for the gift of the two specially prepared mixed-phase columns; Dionex, Breda, Netherlands, for lending the OmniPac PAX-500 column; Tessek, Prague, Czech Republic, for providing the HEMA columns; Rockland, Nuenen, Netherlands, for providing the Zorbax Bioseries Oligo column and Merck, Amsterdam, Netherlands, for lending the Aluspher RP-Select B column.

References

[1] I.A. Maxwell, B.R. Morrison, D.H. Napper and R.G. Gilbert, *Macromolecules*, 24 (1991) 1629–1640.
[2] S. Afrashtehfar and F.F. Cantwell, *Anal. Chem.*, 54 (1982) 2422–2427.
[3] L.W. McLaughlin, *Chem. Rev.*, 89 (1989) 309–319.
[4] R. Hecker and D. Riesner, *J. Chromatogr.*, 418 (1987) 97–114.
[5] L.W. McLaughlin and R. Bischoff, *J. Chromatogr.*, 418 (1987) 51–72.
[6] L.W. McLaughlin and R. Bischoff, *J. Chromatogr.*, 270 (1983) 117–126.
[7] L.W. McLaughlin and R. Bischoff, *J. Chromatogr.*, 317 (1984) 251–261.
[8] L.W. McLaughlin and R. Bischoff, *J. Chromatogr.*, 296 (1984) 329–337.
[9] L.W. McLaughlin and R. Bischoff, *Anal. Biochem.*, 151 (1985) 526–533.
[10] J.C. Liao and C.R. Vogt, *J. Chromatogr. Sci.*, 17 (1979) 237–244.

[11] J.B. Crowther and R.A. Hartwick, *Chromatographia*, 16 (1982) 349–353.
[12] J.B. Crowther, S.D. Fazio and R.A. Hartwick, *J. Chromatogr.*, 282 (1983) 619–628.
[13] W. Kopaciewicz, M.A Rounds and F.E. Regnier, *J. Chromatogr.*, 318 (1985) 157–172.
[14] Z. El Rassi and Cs. Horváth, *Chromatographia*, 19 (1984) 9–18.
[15] D.P. Lee, *J. Chromatogr. Sci.*, 22 (1984) 9–18.
[16] P.R. Haddad and M.Y. Croft, *Chromatographia*, 11 (1986) 648–650.
[17] T.A. Walker, T.V. Ho and N. Akbari, *J. Liq. Chromatogr.*, 12 (1989) 1213–1230.
[18] T.A. Walker, T.V. Ho and N. Akbari, *J. Liq. Chromatogr.*, 14 (1991) 1351–1366.
[19] H.K. Lee and N.E. Hoffman, *J. Chromatogr. Sci.*, 30 (1992) 98–105.
[20] H.J. Issaq and J. Gutierrez, *J. Liq. Chromatogr.*, 11 (1988) 2851–2861.
[21] F.-M. Chen, G.S. Neave and A.L. Epstein, *J. Chromatogr.*, 444 (1988) 153–164.
[22] L.J. Crane and M.P. Henry, *CLB, Chem. Lab. Betr.*, 40 (1989) 2–8.
[23] R. Saari-Nordhaus and J.M. Anderson, Jr., *Anal. Chem.*, 64 (1992) 2283–2287.
[24] I.J. Weatherall, *J. Liq. Chromatogr.*, 14 (1991) 1903–1912.
[25] J.R. Stillian and C.A. Pohl, *J. Chromatogr.*, 499 (1990) 249–266.
[26] R.E. Slingsby and M. Rey, *J. Liq. Chromatogr.*, 13 (1990) 107–134.
[27] R.E. Smith and R.A. MacQuarrie, *J. Chromatogr. Sci.*, 29 (1991) 232–236.
[28] I. Vinš, personal communication.
[29] R.S. Deelder, P.H. Tommassen and J.H.M. van den Berg, *Chromatografie*, Elsevier, Amsterdam, Brussels, 1st ed., 1985.
[30] J.P. Foley and J.G. Dorsey, *Anal. Chem.*, 55 (1983) 730–737.
[31] L.D. Bowers and S. Pedigo, *J. Chromatogr.*, 371 (1986) 243–251.
[32] F. Gago, J. Alvarez-Builla and J. Elguero, *J. Chromatogr.*, 449 (1988) 95–101.
[33] P. Jandera, *Chromatographia*, 19 (1984) 101–112.
[34] D.T. Gjerde and J.S. Fritz, *Ion Chromatography*, Hüthig, Heidelberg, 2nd ed., 1987, p. 273.
[35] J. Weiss, *Handbook of Ion Chromatography*, Dionex, Sunnyvale, CA, 1986, pp. 24 and 39.
[36] B. Grego and M.T.W. Hearn, *Chromatographia*, 14 (1981) 589–592.
[37] R.W. Slingsby and C.A. Pohl, *J. Chromatogr.*, 458 (1988) 241–253.
[38] J.L. Ammerdorffer, A.A.G. Lemmens, A.L. German and F.M. Everaerts, *Polym. Comm.*, 31 (1990) 61–62.
[39] C.G.J.M. Pijls, *MS Thesis*, Eindhoven University of Technology, Eindhoven, 1989.
[40] B.R. Morrison, I.A. Maxwell, D.H. Napper, R.G. Gilbert, J.L. Ammerdorffer and A.L. German, *J. Pol. Sci., Polym. Chem. Ed.*, 31 (1993) 467–484.
[41] *High Performance Columns and Media for Today's Life Scientist*, Polymer Labs., Shropshire, 1987, p. 2.
[42] D.J. Pietrzyk, Z. Iskandarani and G.L. Schmitt, *J. Liq. Chromatogr.*, 9 (1986) 2633–2659.

ELSEVIER

Journal of Chromatography A, 677 (1994) 229–237

JOURNAL OF CHROMATOGRAPHY A

Retention and enantioselectivity of 2-arylpropionic acid derivatives on an avidin-bonded silica column Influence of base materials, spacer type and protein modification

Jun Haginaka*, Tokiko Murashima, Chikako Seyama

Faculty of Pharmaceutical Sciences, Mukogawa Women's University, 11-68, Koshien Kyuban-cho, Nishinomiya 663, Japan

First received 1 March 1994; revised manuscript received 26 April 1994

Abstract

The influences of pore sizes of base materials, spacer type and protein modification on the chiral resolution of 2-arylpropionic acid derivatives on avidin (AVD)-bonded silica materials were investigated. With regard to the pore sizes of the base silica materials, 120-Å materials gave higher enantioselectivity and resolution than 300-Å materials. With regard to spacer type, aminopropyl (AP)-silica gels activated by N,N′-disuccinimidyl carbonate (DSC) and N,N′-disuccinimidyl suberate (DSS) and glycerylpropyl (GP)-silica gels activated by 1,1′-carbonyldiimidazole (CDI) were compared. The AP-silica gels activated by DSC gave the highest protein coverage and resolution. Modified AVD-bonded materials were prepared by reaction with glutaraldehyde, glyceraldehyde and benzaldehyde. The retentive and enantioselective properties of 2-arylpropionic acid derivatives on these modified AVD columns were compared with those on an unmodified AVD column. The retentions of 2-arylpropionic acid derivatives on the modified AVD columns were shorter than those on the unmodified AVD column, whereas the modified AVD columns gave lower or approximately equal enantioselectivity compared with the unmodified AVD column. These results may be attributed to a decrease in the number of ion-exchange sites for retention and chiral recognition, and/or changes in protein conformation as a result of modification.

1. Introduction

Glycoprotein-bonded stationary phases including α_1-acid glycoprotein [1], ovomucoid (OVM) [2], avidin (AVD) [3] and cellobiohydrolase [4] have been developed for the separation of enantiomers. AVD, of molecular mass 68 300 and isoelectric point (p*I*) 10.0, is well known to biochemists because of its strong binding with biotin [5]. AVD-bonded silica materials were developed by Miwa et al. [3] and showed excellent chiral recognition for 2-arylpropionic acid derivatives. It is well known that many factors such as physical properties of base silica materials, spacer type and bonding method affect the resolution of enantiomeric pairs on protein-bonded stationary phases [6–9]. In this study, we investigated the influences of these factors on the retention, enantioselectivity and resolution of 2-

* Corresponding author.

0021-9673/94/$07.00
SSDI 0021-9673(94)00411-2

arylpropionic acid derivatives on unmodified and modified AVD-bonded silica columns.

2. Experimental

2.1. Reagents and materials

1-Butanol, 2-butanol, *tert.*-butanol, 1-propanol, 2-propanol, ethanol, methanol and acetonitrile of HPLC grade were obtained from Wako (Osaka, Japan). Ibuprofen, ketoprofen, flurbiprofen, fenoprofen calcium and pranoprofen were kindly donated by Kaken Pharmaceutical (Tokyo, Japan), Chugai Pharmaceutical (Tokyo, Japan), Yamanouchi Pharmaceutical (Tokyo, Japan) and Yoshitomi Pharmaceutical (Osaka, Japan). The structures of these compounds are shown in Fig. 1. AVD proteins from egg white were kindly donated by Eisai (Tokyo, Japan). N,N′-Disuccinimidyl carbonate (DSC) and 1,1′-carbonyldiimidazole (CDI) were purchased from Sigma Chemical (St. Louis, MO, USA) and N,N′-disuccinimidyl suberate (DSS) from Pierce (Rockford, IL, USA). Silica gels (Ultron-120, particle diameter 5 μm, pore size 120 Å, specific surface area 300 m^2/g, and Ultron-300 particle diameter 5 μm, pore size 300 Å, specific surface area 100 m^2/g) were obtained from Shinwa Chemical Industries (Kyoto, Japan). Other solvents and reagents were used as received.

Water purified with a Nanopure II unit (Barnstead, Boston, MA, USA) was used for the preparation of the eluent and sample solutions.

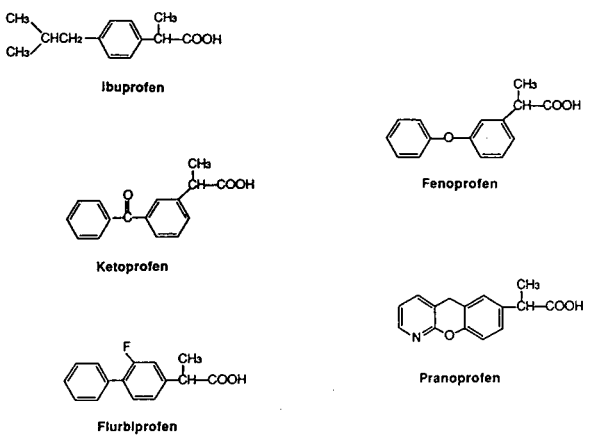

Fig. 1. Structures of the 2-arylpropionic acid derivatives.

Preparation of silica gels having different spacer types

Silica gels (5 g) were dried in vacuo over P_2O_5 at 150°C for 6 h and the dry silica gels were added to 120 ml of dry toluene. The mixture was heated to reflux until all the water had been removed as an azeotrope into a Dean–Stark-type trap. Next, 3-aminopropyltrimethoxysilane and 3-glycidoxypropyltrimethoxysilane, corresponding to 10 μmol/m^2 of the specific surface area, were added and reacted for 8 and 48 h, respectively. The reaction mixture was cooled to room temperature, filtered and washed with toluene and methanol. The isolated silica gels were dried in vacuo over P_2O_5 at 60°C for 2 h. 3-Aminopropyl (AP)-silica gel was used for the activation reaction described below. To the silica gels reacted with 3-glycidoxypropyltrimethoxysilane, 80 ml of perchloric acid (pH 3.0) were added and the mixture was refluxed for 4 h. The reaction mixture was cooled to room temperature, filtered and washed with water and methanol. The isolated 3-glycerylpropyl (GP)-silica gel was dried in vacuo over P_2O_5 at 60°C for 2 h and used for the activation reaction.

Activation of silica gels having amino or hydroxyl groups

The AP-silica gels were activated with DSC or DSS. Five grams of the gels were slurried in 70 ml of acetonitrile and reacted with 5 g of DSC or 7.2 g of DSS for 24 h at 30°C. The reaction mixture was filtered and washed with acetonitrile and methanol. The GP-silica gels were activated by CDI. Five grams of the gels were slurried in 30 ml of dioxane. To the mixture, 4 g of CDI dissolved in 20 ml of dioxane were added and reacted for 4 h at 30°C. The reaction mixture was filtered and washed with dioxane and methanol. Both activated silica gels were dried in vacuo over P_2O_5 at 60°C for 2 h.

Preparation of AVD-bonded materials

AVD-proteins were bound to the DSC or DSS-activated AP-silica gels as follows: 2 g of the DSC or DSS-activated silica gels were slurried in 20 m*M* phosphate buffer (pH 6.8). To the mixture, 1 g of AVD-proteins dissolved in 20 ml of the same buffer was added slowly and stirred for 15 h at 30°C. Similarly, AVD was bound to CDI-activated silica gels as follows: 2 g of the CDI-activated GP-silica gels were slurried in 20 m*M* phosphate buffer (pH 7.8). To the mixture, 1 g of AVD-proteins dissolved in 20 ml of the same buffer was added slowly and stirred for 15 h at 30°C. Then both the reaction mixtures were filtered, washed with water and methanol and dried in vacuo over P_2O_5 at 40°C for 6 h.

Preparation of AVD-BENZ, AVD-DIOL and AVD-GA materials

The AVD-proteins were bound to aminopropylsilica gels (120-Å base silica) activated by DSC. The materials were then further modified with benzaldehyde, glyceraldehyde and glutaraldehyde.

Three grams of the AVD materials were added to 50 ml of 20 m*M* phosphate buffer (pH 7.5), then 200 mg of sodium cyanoborohydride, 200 mg of zinc sulfate and 50 mg of benzaldehyde dissolved in 1 ml of dioxane were added. After adjusting the pH to 7.5, the mixture was slowly rotated at 30°C for 15 h. Then the mixture was filtered and washed with water and methanol. The isolated materials (AVD-BENZ) were dried in vacuo over P_2O_5 at 40°C for 6 h.

Three grams of the AVD materials were added to 50 ml of 20 m*M* phosphate buffer (pH 7.5), then 200 mg of sodium cyanoborohydride, 200 mg of zinc sulfate and 250 mg of D-glyceraldehyde were added. After adjusting the pH to 7.5, the mixture was slowly rotated at 30°C for 15 h. Then the mixture was filtered and washed with water and methanol. The isolated materials (AVD-DIOL) were dried in vacuo over P_2O_5 at 40°C for 6 h.

Three grams of the AVD materials were added to 50 ml of 100 m*M* ammonium dihydrogenphosphate buffer solution (pH 4.4) and sonicated for 5 min, then 300 μl of 5% glutaraldehyde solution were slowly added. The mixture was slowly rotated at 30°C for 15 h, filtered and washed with 100 m*M* ammonium dihydrogenphosphate buffer solution (pH 4.4), 50 m*M* sodium phosphate buffer (pH 7.0), water and methanol. The isolated materials (AVD-GA) were dried in vacuo over P_2O_5 at 40°C for 6 h.

The unmodified and modified AVD-bonded materials were packed into a 100 × 4.6 mm I.D. stainless-steel column by the slurry packing method.

2.2. Instrumentation

Chromatography

The HPLC system used was composed of an LC-9A pump, an SPD-6A spectrophotometer, an SIL-6B autoinjector, a C-R4A integrator and an SCL-6B system controller (all from Shimadzu, Kyoto, Japan). The flow-rate was maintained at 0.8 ml/min. Detection was performed at 220 or 254 nm.

Capacity factors (k'), enantioseparation factors (α), resolutions (R_s) of racemates were calculated. All separations were carried out at 25°C using a CO-1093C column oven (Uniflows, Tokyo, Japan).

The eluents are prepared by using phosphoric acid–sodium dihydrogenphosphate or sodium dihydrogenphosphate–disodium hydrogenphosphate and organic modifier, whose content was calculated to give all of the eluents equal elutropic strength, as reported by Iredale et al. [10]. The eluents used are specified in the figures and tables.

Elemental analysis

The elemental analysis of the AVD-bonded silica materials was performed using a Model NCH-12 analyser (Sumika Chemical Analysis Service, Osaka, Japan) for nitrogen or ion chromatography combined with the oxygen-flask method for sulfur.

Sample preparation

A known amount of a racemic solute was dissolved in methanol or water and the solution was diluted with the eluent to desired concen-

tration. A 20-μl aliquot of the sample solution was loaded on to a column. The amount loaded was 0.2–0.5 μg.

3. Results and discussion

3.1. Surface coverages of AVD-proteins

Table 1 shows the surface coverages of AVD-proteins on the AVD-bonded materials with different pore sizes of base silica materials and spacer type. With regard to comparison of the base silica gels having 120- and 300-Å pore sizes, the latter materials showed about 2.5-times higher surface coverages of the AVD-proteins. Only the outer surfaces of the former materials could be utilized for the binding of AVD, the molecular mass of which is 68 000. However, the amounts of AVD-proteins bound on the former materials were higher than those on the latter materials. With regard to comparison of spacer type, the AP materials activated by DSC had higher surface coverages than those activated by DSS, where C_6 carbon chains remain after cross-linking of the AP-silica and protein. The GP materials activated by CDI showed about one quarter of the surface coverages of the proteins compared with the AP materials activated by DSC. Even if one takes into account that the surface coverages of AP phases are double those of GP phases, DSC or DSS is more suitable than CDI as a cross-linking agent for binding of AVD. These results reveal that the largest amounts of AVD are bound to the 120-Å silica gels activated by DSC.

3.2. Effect of base silica materials and spacer for chiral recognition

Table 2 shows the influence of the pore sizes of base silica materials and spacer type on the retention, enantioselectivity and resolution of 2-arylpropionic acid derivatives on the AVD-bonded materials. With regard to comparison of base silica gels having 120- and 300-Å pore sizes, the former material showed slightly better enantioselectivity and resolution than the latter. This could be due to the binding of slightly larger amounts of the proteins for the former materials. The AP materials activated by DSC and DSS showed good enantioselectivity for all the 2-arylpropionic acid derivatives tested, whereas ibuprofen, ketoprofen and fenoprofen were not resolved on the GP materials activated by CDI. The AP materials activated by DSC showed better enantioselectivity and resolution than those activated by DSS. Previously, we reported [9] that ovomucoid-bonded materials using DSC and CDI as the cross-linker showed excellent enantioselectivity for a wide range of solutes, whereas the materials using DSS showed slight

Table 1
Comparison of surface coverages of AVD- and modified AVD-bonded materials

Spacer[a]	Cross-linker[b]	Pore size of base silica (Å)	AP or GP phase		Avidin phase	
			Carbon content (%)	Surface coverage[c] (μmol/m²)	Sulfur content (%)	Surface coverage[d] (μmol/g)
AP	DSC	120	3.23	3.3	0.16	3.1
AP	DSC	300	1.25	3.6	0.13	2.5
AP	DSS	120	3.23	3.3	0.13	2.5
GP	CDI	120	3.18	1.6	0.04	0.8

[a] AP and GP are aminopropyl and glycerylpropyl phases, respectively.
[b] DSC, DSS and CDI are N,N'-disuccinimidyl carbonate, N,N'-disuccinimidyl suberate and 1,1'-carbonyldiimidazole, respectively.
[c] Estimated from the nitrogen elemental analysis data.
[d] Estimated from the sulfur elemental analysis data.

Table 2
Comparison of base silica materials and spacer type with respect to retention, enantioselectivity and resolution of various solutes on an unmodified AVD-bonded material

Column	Ibuprofen			Ketoprofen			Flurbiprofen			Fenoprofen			Pranoprofen		
	k'_1	α	R_s	k'_1	α	R_s	k'_1	α	R_s	k'_1	α	R_s	k'_1	α	R_s
DSC-120	9.43	1.76	5.45	16.6	2.51	7.51	16.1	2.09	7.99	16.2	1.85	6.69	53.6	1.33	3.54
DSC-300	5.11	1.58	2.79	8.42	2.01	4.76	10.7	1.97	3.89	8.96	1.72	3.40	26.7	1.27	2.08
DSS-120	7.11	1.71	3.42	11.5	2.06	5.61	12.5	1.94	4.73	11.9	1.81	4.77	33.4	1.12	1.15
CDI-120	2.10	1.00		3.28	1.00		10.3	1.12	1.20	4.58	1.00		5.74	1.22	1.62

HPLC conditions: column, an unmodified AVD-bonded material packed into a 100 × 4.6 mm I.D. stainless-steel column; eluent, 20 m*M* phosphate buffer (pH 7.0) containing 2.14% ethanol; flow-rate, 0.8 ml/min.

enantioselectivity only for oxprenolol. It was thought that superfluous achiral interactions of a solute with the hydrophobic spacer might diminish the chiral interactions of a solute with the OVM-protein. It is interesting that the AVD-bonded materials activated by DSS gave excellent enantioselectivity for 2-arylpropionic acid derivatives. These results reveal that a suitable

Table 3
Effect of eluent pH on retention and enantioselectivity of 2-arylpropionic acid derivatives on unmodified and modified AVD-bonded materials

Column	Compound	pH 6.0[a]		pH 6.5[a]		pH 7.0[a]		pH 7.5[a]	
		k'_1	α	k'_1	α	k'_1	α	k'_1	α
AVD	Ibuprofen	9.95	1.82	6.47	1.89	4.78	1.94	3.48	2.01
	Ketoprofen	20.5	1.98	13.4	2.03	9.98	2.08	7.44	2.15
	Flurbiprofen	19.6	2.36	12.9	2.45	9.76	2.56	7.12	2.55
	Fenoprofen	18.9	1.70	12.6	1.72	9.58	1.75	7.06	1.80
	Pranoprofen	73.9	1.24	49.5	1.24	35.8	1.27	26.8	1.26
AVD-BENZ	Ibuprofen	9.68	1.68	6.25	1.73	4.54	1.79	3.32	1.86
	Ketoprofen	17.3	1.87	11.5	1.93	8.46	1.99	6.30	2.06
	Flurbiprofen	20.0	1.98	12.7	2.05	9.29	2.13	6.58	2.18
	Fenoprofen	17.0	1.61	11.1	1.65	8.29	1.69	6.15	1.75
	Pranoprofen	66.3	1.15	42.2	1.18	30.4	1.19	22.5	1.20
AVD-DIOL	Ibuprofen	9.98	1.66	6.04	1.71	3.97	1.75	2.76	1.80
	Ketoprofen	18.1	1.85	10.8	1.90	7.32	1.98	5.24	2.11
	Flurbiprofen	20.3	2.08	12.1	2.13	7.90	2.18	5.43	2.21
	Fenoprofen	17.2	1.58	10.6	1.62	7.20	1.66	5.03	1.73
	Pranoprofen	64.8	1.16	37.4	1.19	25.3	1.20	18.3	1.19
AVD-GA	Ibuprofen	8.78	1.79	5.26	1.79	3.89	1.90	2.89	1.94
	Ketoprofen	15.3	1.90	10.8	1.93	7.59	2.01	5.78	2.04
	Flurbiprofen	16.9	2.25	11.3	2.40	8.46	2.41	6.20	2.47
	Fenoprofen	14.7	1.60	9.93	1.61	7.52	1.64	5.59	1.71
	Pranoprofen	58.5	1.23	38.1	1.26	26.3	1.32	20.6	1.28

All materials were prepared by using aminopropylsilica gels (120-Å base silica) activated by DSC. HPLC conditions: column, unmodified and modified AVD-bonded materials packed into a 100 × 4.6 mm I.D. stainless-steel column; eluent, 20 m*M* phosphate buffer containing 2.07% *tert.*-butanol; flow-rate, 0.8 ml/min.
[a] Buffer pH.

spacer should be selected for binding of a protein.

On the other hand, Oda et al. [11] reported that DSS is a better spacer than DSC for direct sum injection assays for drug enantiomers on an AVD-bonded material. However, our results reveal that DSC is a better spacer than DSS for the chiral resolution of 2-arylpropionic acid derivatives on the AVD-bonded materials.

3.3. Effect of eluent pH on retention and enantioselectivity of 2-arylpropionic acid derivatives on unmodified and modified AVD-bonded materials

The AVD proteins were bound to aminopropylsilica gels (120-Å base silica) activated by DSC and used in the following experiments. The amino groups of the AVD materials were partially reacted with benzaldehyde, D-glyceraldehyde and glutaraldehyde. However, it was difficult to detect any differences before and after modification. Table 3 shows the effect of eluent pH on the retention and enantioselectivity of 2-arylpropionic acid derivatives on AVD, AVD-BENZ, AVD-DIOL and AVD-GA columns, with 20 m*M* phosphate buffer containing 2.07% *tert.*-butanol as the eluent. The capacity factors (k'_1) of the first-eluted enantiomers of 2-arylpropionic acid derivatives on the AVD-bonded columns decreased with an increase in eluent pH. Taking into account the p*I* of AVD of 10.0 and the pK_a of 2-arylpropionic acid derivatives of 4.0–4.5, the bound AVD-protein and solutes are positively and negatively charged, respectively, over the eluent pH range tested. These results reveal that hydrophobic and electrostatic interactions should play an important role in the retention properties of solutes on the AVD-bonded columns. The highest enantioselectivity (α) of these compounds was attained at an eluent pH of 7.0 or 7.5.

On the modified AVD-bonded columns, the k'_1 of 2-arylpropionic acid derivatives was slightly decreased except for flurbiprofen on the AVD-BENZ column and ibuprofen and flurbiprofen on the AVD-DIOL column at an eluent pH of 6.0 (Table 3). The α values of these compounds were almost the same or decreased except for separation of pranoprofen on the AVD-GA column. The retentive and enantioselective tendencies obtained with the modified AVD columns were similar to those with the unmodified column. Fig. 2 shows the chiral resolution of pranoprofen on the unomodified and modified AVD columns. The k'_1 value of pranoprofen decreased on the AVD-BENZ, AVD-DIOL and AVD-GA columns compared with that on the unmodified AVD column. The AVD-GA column gave a higher enantioselectivity than the unmodified AVD column under the conditions employed. These results reveal that a decrease in the number of ion-exchange sites for retention and chiral recognition, and/or changes in protein

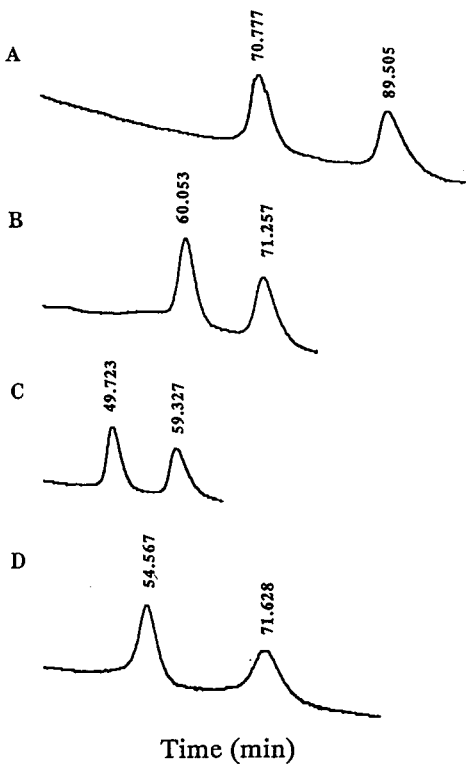

Fig. 2. Chiral resolution of pranoprofen on (A) AVD, (B), AVD-BENZ, (C) AVD-DIOL and (D) AVD-GA columns. HPLC conditions: column, unmodified and modified AVD-bonded materials packed into a 100 × 4.6 mm I.D. stainless-steel column; eluent, 20 m*M* phosphate buffer containing 2.07% *tert.*-butanol; flow-rate, 0.8 ml/min; injection volume, 20 μl (20 μg/ml).

conformation could occur as a result of modification.

3.4. Effect of organic modifier on enatioselectivity of 2-arylpropionic acid derivatives on unmodified and modified AVD-bonded materials

Table 4 shows the effects of *tert.*-butanol content on the retention and enantioselectivity of 2-arylpropionic acid derivatives on the AVD, AVD-BENZ, AVD-DIOL and AVD-GA columns, with 20 m*M* phosphate buffer (pH 7.0) containing *tert.*-butanol as the eluent. With an increase in *tert.*-butanol content, the α values of ibuprofen, ketoprofen and fenoprofen decreased on the all columns, whereas with an increase in *tert.*-butanol content, those of flurbiprofen and pranoprofen increased. It is interesting that the retentions of both flurbiprofen and pranoprofen enantiomers decreased with an increase in *tert.*-butanol content, but the enantioselectivities of flurbiprofen and pranoprofen increased. Similar results were obtained with the use of 2-propanol as an organic modifier.

Table 5 shows the effects of type of organic modifier on the retention and enantioselectivity of 2-arylpropionic acid derivatives on the AVD, AVD-BENZ, AVD-DIOL and AVD-GA columns, with 20 m*M* phosphate buffer (pH 7.0) containing various organic modifiers as the eluent. The use of *tert.*-butanol as the organic

Table 4
Effect of organic modifier content on retention and enantioselectivity of 2-arylpropionic acid derivatives on unmodified and modified AVD-bonded materials

Column	Compound	*tert.*-Butanol content (%)					
		1.04		2.07		4.14	
		k'_1	α	k'_1	α	k'_1	α
AVD	Ibuprofen	7.23	1.92	4.78	1.94	2.44	1.87
	Ketoprofen	15.6	2.26	9.98	2.08	4.68	1.82
	Flurbiprofen	13.6	2.35	9.76	2.56	5.40	2.68
	Fenoprofen	14.3	1.97	9.58	1.75	4.77	1.51
	Pranoprofen	57.5	1.16	35.8	1.27	16.0	1.44
AVD-BENZ	Ibuprofen	6.85	1.87	4.54	1.79	2.54	1.66
	Ketoprofen	13.0	2.20	8.46	1.99	4.26	1.72
	Flurbiprofen	12.8	2.09	9.29	2.13	5.72	2.13
	Fenoprofen	12.3	1.90	8.29	1.69	4.58	1.45
	Pranoprofen	48.8	1.12	30.4	1.19	13.6	1.33
AVD-DIOL	Ibuprofen	6.33	1.82	3.97	1.75	2.19	1.64
	Ketoprofen	12.1	2.23	7.32	1.98	3.78	1.17
	Flurbiprofen	11.5	2.11	7.90	2.18	4.96	2.20
	Fenoprofen	11.2	1.90	7.20	1.66	3.97	1.42
	Pranoprofen	44.0	1.10	25.3	1.20	12.1	1.33
AVD-GA	Ibuprofen	6.01	1.95	3.89	1.90	2.13	1.77
	Ketoprofen	11.9	2.17	7.59	2.01	3.81	1.73
	Flurbiprofen	12.2	2.25	8.46	2.41	5.02	2.47
	Fenoprofen	11.4	1.86	7.52	1.64	4.04	1.42
	Pranoprofen	42.0	1.21	26.3	1.32	12.6	1.44

All materials were prepared by using aminopropylsilica gels (120-Å base silica) activated by DSC. HPLC conditions: column, unmodified and modified AVD-bonded materials packed into a 100 × 4.6 mm I.D. stainless-steel column; eluent, 20 m*M* phosphate buffer (pH 7.0) containing *tert.*-butanol; flow-rate 0.8 ml/min.

Table 5
Effect of type of organic modifier on retention and enantioselectivity of 2-arylpropionic acid derivatives on unmodified and modified AVD-bonded materials

Column	Organic modifier	Ibuprofen		Ketoprofen		Flurbiprofen		Fenoprofen		Pranoprofen	
		k'_1	α	k'_1	α	k'_1	α	k'_1	α	k'_1	α
AVD	Methanol	17.5	1.65	24.6	2.25	20.1	2.26	22.3	2.03	78.9	1.14
	Ethanol	9.43	1.76	16.6	2.51	16.1	2.09	16.2	1.85	53.6	1.33
	1-Propanol	3.09	1.69	5.36	1.56	7.64	2.54	5.42	1.39	17.2	1.54
	2-Propanol	5.60	1.90	10.9	1.98	11.5	2.55	10.6	1.72	36.0	1.33
	1-Butanol	2.40	1.70	4.24	1.57	5.96	2.64	4.43	1.35	13.1	1.62
	2-Butanol	2.77	1.75	5.11	1.65	6.67	2.63	5.17	1.42	16.5	1.52
	tert.-Butanol	4.78	1.94	9.98	2.08	9.76	2.56	9.58	1.75	35.8	1.27
	Acetonitrile	10.1	1.09	9.06	1.74	14.2	1.82	9.17	1.56	30.5	1.33
AVD-BENZ	Methanol	14.3	1.59	18.6	2.22	16.5	2.05	17.7	2.05	65.8	1.08
	Ethanol	8.25	1.65	13.0	2.10	13.2	2.03	12.4	1.88	45.8	1.13
	1-Propanol	2.97	1.44	4.62	1.53	7.11	1.95	4.85	1.37	14.5	1.38
	2-Propanol	4.94	1.76	8.58	1.95	9.77	2.08	8.55	1.70	30.3	1.19
	1-Butanol	2.35	1.49	3.73	1.51	5.90	2.07	4.09	1.32	10.9	1.46
	2-Butanol	2.77	1.54	4.58	1.60	6.70	2.06	4.89	1.39	14.4	1.37
	tert.-Butanol	4.54	1.79	8.46	1.99	9.29	2.13	8.29	1.69	30.4	1.19
	Acetonitrile	8.38	1.00	7.01	1.72	11.5	1.54	7.11	1.53	24.3	1.21
AVD-DIOL	Methanol	14.9	1.54	18.5	2.26	16.7	2.07	17.2	1.99	60.2	1.08
	Ethanol	8.41	1.61	12.7	2.14	13.3	2.06	12.5	1.87	42.1	1.13
	1-Propanol	2.90	1.45	4.69	1.53	6.86	2.02	4.84	1.35	14.5	1.37
	2-Propanol	4.81	1.69	8.25	1.96	9.36	2.12	8.11	1.69	28.5	1.19
	1-Butanol	2.17	1.54	3.59	1.51	5.50	2.13	3.87	1.31	10.4	1.46
	2-Butanol	2.62	1.53	4.40	1.59	6.18	2.13	4.61	1.37	13.6	1.37
	tert.-Butanol	3.97	1.75	7.32	1.98	7.90	2.18	7.20	1.66	25.3	1.20
	Acetonitrile	8.61	1.00	6.99	1.73	11.7	1.53	7.07	1.52	22.7	1.21
AVD-GA	Methanol	13.8	1.56	18.5	2.10	16.0	2.22	16.9	1.97	61.2	1.13
	Ethanol	7.55	1.71	12.3	2.11	12.6	2.25	11.9	1.85	43.3	1.19
	1-Propanol	2.55	1.64	4.27	1.52	6.60	2.39	4.51	1.34	13.9	1.51
	2-Propanol	4.49	1.84	8.10	1.93	9.24	2.38	8.09	1.66	28.2	1.27
	1-Butanol	1.99	1.69	3.33	1.52	5.40	2.50	3.70	1.30	9.92	1.70
	2-Butanol	2.31	1.24	4.08	1.60	6.02	2.54	4.36	1.37	13.1	1.47
	tert.-Butanol	3.89	1.90	7.59	2.01	8.46	2.41	7.52	1.64	26.3	1.32
	Acetonitrile	7.66	1.07	6.77	1.73	11.1	1.71	6.86	1.52	23.2	1.27

All materials were prepared by using aminopropylsilica gels (120-Å base silica) activated by DSC. HPLC conditions: column, unmodified and modified AVD-bonded materials packed into a 100 × 4.6 mm I.D. stainless-steel column; eluent, 20 m*M* phosphate buffer (pH 7.0) containing an organic modifier, with concentrations of 2.47% for methanol, 2.14% for ethanol, 2.03% for 1-propanol and 2-butanol, 2.00% for 2-propanol and 1-butanol, 2.07% for *tert.*-butanol and 2.86% for acetonitrile; flow-rate, 0.8 ml/min.

modifier gave the highest enantioselectivity for the chiral resolution of ibuprofen on the unmodified and modified AVD-bonded columns. However, using acetonitrile the ibuprofen enantiomers were slightly resolved on the AVD-bonded columns but were not resolved on the modified AVD columns. For flurbiprofen, the enantioselectivities obtained with alkanol modifiers were better than those with acetonitrile on the unmodified and modified AVD columns. For ketoprofen and fenoprofen, the use of methanol, ethanol, 2-propanol and *tert.*-butanol gave better enantioselectivities with the unmodified and modified AVD columns. However, alkanols such as 1-propanol, 1-butanol and 2-butanol, having long alkyl chains, were not good organic modifiers for ketoprofen and fenoprofen. For pranoprofen, 1-propanol, 1-butanol and 2-butanol were better organic modifiers on the unmodified and modified AVD columns. Selection of a suitable organic modifier is an important factor in achieving good resolution.

Throughout the study, we used two columns packed with unmodified AVD materials, whereas only one column packed with modified materials was used. The results suggest that the modified AVD column is more stable than the unmodified column, as reported previously for a modified OVM column [12].

Acknowledgements

This study was partially supported by a Research Grant from Eisai (Tokyo, Japan).

References

[1] J. Hermansson, *J. Chromatogr.*, 269 (1983) 71.
[2] T. Miwa, M. Ichikawa, M. Tsuno, T. Hattori, T. Miyakawa, M. Kayano and Y. Miyake, *Chem. Pharm. Bull.*, 35 (1987) 682.
[3] T. Miwa, T. Miyakawa and Y. Miyake, *J. Chromatogr.*, 457 (1988) 227.
[4] P. Erlandsson, I. Marle, L. Hansson, R. Isaksson, C. Petterson and G. Petterson, *J. Am. Chem. Soc.*, 112 (1990) 4573.
[5] L. Stevens, *Comp. Biochem. Physiol. B*, 100 (1991) 1.
[6] R.A. Thompson, S. Anderson and S. Allenmark, *J. Chromatogr.*, 465 (1989) 263.
[7] S. Andersson, S. Allenmark, P. Erlandsson and S. Nilsson, *J. Chromatogr.*, 498 (1990) 81.
[8] S. Andersson, R.A. Thompson and S.G. Allenmark, *J. Chromatogr.*, 591 (1992) 65.
[9] J. Haginaka, Ch. Seyama, T. Murashima, H. Fujima and H. Wada, *J. Chromatogr.*, 631 (1992) 183.
[10] J. Iredale, A.-F. Aubry and I.W. Wainer, *Chromatographia*, 31 (1991) 329.
[11] Y. Oda, N. Asakawa, S. Abe, Y. Yoshida and T. Sato, *J. Chromatogr.*, 572 (1991) 133.
[12] J. Haginaka, Ch. Seyama, H. Yasuda, H. Fujima and H. Wada, *J. Chromatogr.*, 592 (1992) 301.

ELSEVIER

Journal of Chromatography A, 677 (1994) 239–253

JOURNAL OF CHROMATOGRAPHY A

Interpretive strategy for optimization of surfactant and alcohol concentration in micellar liquid chromatography

J.R. Torres-Lapasió, R.M. Villanueva-Camañas, J.M. Sanchis-Mallols, M.J. Medina-Hernández, M.C. García-Alvarez-Coque*

Departamento de Química Analítica, Facultad de Química, Universitat de Valencia, 46100 Burjassot, Valencia, Spain

First received 15 February 1994; revised manuscript received 19 April 1994

Abstract

An interpretive procedure for optimization of the retention of the solutes in a mixture, eluted with mobile phases containing a surfactant and an alcohol in micellar liquid chromatography (MLC), is proposed. Three optimization criteria were used: positional resolution, valley-to-peak ratio and overlapping. Retention data from several phenols, aromatic compounds and catecholamines were used to test the procedure. The positional criterion, together with the retention model given by an equation of the type $1/k' = c_0 + c_1\mu + c_2\varphi + c_3\mu\varphi$, led to a reliable optimum resolution using the retention data for a few mobile phases. However, the resolution criteria that take into account both the position and the peak shape are preferable in MLC, where the chromatographic peaks are asymmetric and have a low efficiency.

1. Introduction

The chromatographer is concerned with the achievement of the optimum mobile phase that permits the separation of the compounds in a mixture in the minimum time. This task may be complex when two or more variables are involved in the optimization process. The optimization may be sequential or interpretive. In a sequential strategy, the retention of the different solutes is not known a priori and each set of mobile phases is designed by taking into account the retention observed with previous eluents. In contrast, in an interpretive strategy, the experiments are designed before the optimization process. This strategy may be much more efficient and reliable, but the retention behaviour of each component in the mixture should be known, e.g., described by a mathematical equation. A sequential strategy is inadequate when several local optima exist (as occurs in chromatography), and may not give the best optimum.

In micellar liquid chromatography (MLC), the addition of a short-chain alcohol to the mobile phase, containing a surfactant above the critical micellar concentration, is usual. The alcohol improves the efficiency and increases the elution strength. In a previous paper, a model to describe the retention behaviour of solutes in any mobile phase containing a surfactant and an alcohol was proposed, which made use of the elution data in five mobile phases containing different amounts of surfactant and alcohol [1].

* Corresponding author.

0021-9673/94/$07.00
SSDI 0021-9673(94)00388-P

A function of the type

$$\frac{1}{k'} = c_0 + c_1\mu + c_2\varphi + c_3\mu\varphi \quad (1)$$

where k' is the capacity factor and μ and φ are surfactant and alcohol concentration, respectively, proved to be satisfactory for different solutes.

In this work, an interpretive procedure for optimization of the retention of the solutes in a mixture, eluted with mobile phases of surfactant and alcohol, is proposed. Three optimization criteria were used: positional resolution, valley-to-peak ratio and overlapping. The optimization process consisted of (i) achievement of the retention equations for each solute to be separated, (ii) a search of the optimum mobile phase with the aid of contour maps of the global functions of resolution, (iii) simulation of the chromatogram for the optimum mobile phase and (iv) a search of a new optimum when the selected optimum is not satisfactory.

2. Experimental

2.1. Reagents

Sodium dodecyl sulphate (SDS) (99%) was obtained from Merck (Darmstadt, Germany) and propanol (analytical-reagent grade) from Panreac (Barcelona, Spain). The mobile phases were vacuum filtered through 0.47-μ nylon membranes from Micron-Scharlau (Barcelona, Spain).

Stock standard solutions of 2×10^{-3} M catecholamines were prepared in 0.1 M acetic acid from Probus (Barcelona, Spain): L-adrenaline (biochemical), DL-noradrenaline (pure), dopamine hydrochloride (very pure) and adrenalone hydrochloride (pure) from Fluka (Buchs, Switzerland), and isoprenaline, kindly donated by Boehringer-Ingelheim (Barcelona, Spain). The pH of the mobile phases was adjusted with 0.01 M sodium dihydrogenphosphate (Probus). Nanopure deionized water (Barnstead Sybron, Boston, MA, USA) was used throughout.

2.2. Apparatus

An HP 1050 chromatograph (Hewlett-Packard, Palo Alto, CA, USA) with a UV–visible detector (absorbance was measured at 280 nm) and an HP 3396A integrator were used. Data were acquired by means of a PC and Peak-96 software from Hewlett-Packard (Avondale, PA, USA). The sample was injected through a Rheodyne (Cotati, CA, USA) valve with a 20-μl loop. A Spherisorb octadecylsilane ODS-2 (5 μm) analytical column (12 cm × 4.6 mm I.D.) and a precolumn, placed before the injector, of identical characteristics (3.5 cm × 4.6 mm I.D.) from Scharlau were used. The mobile phase flow-rate was 1 ml min^{-1}. The dead volume was determined by injection of water.

The group of programs MICHROM for data treatment, written in QuickBasic 4.5 for IBM PC or compatible computers, was developed [2]. ASCII data files generated by the Peak-96 software can be treated directly with MICHROM. MICHROM allows data smoothing, measurement of chromatographic peak properties (e.g., efficiency, N, asymmetry factor, B/A, capacity factor, k', peak area) (see Fig. 1 for the meaning of B/A), experimental design, modelling of the retention of the solutes, selection of optimization criteria, drawing of the global response surface,

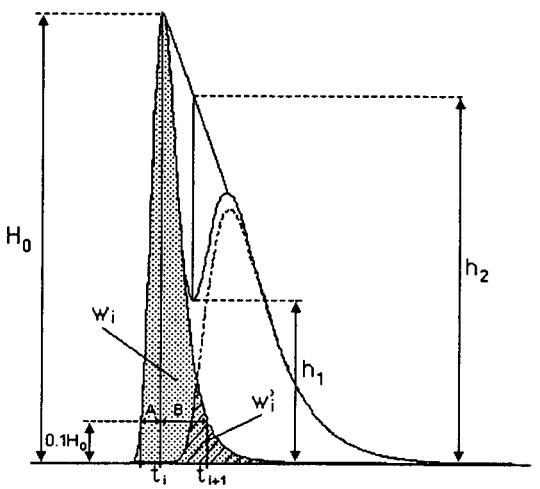

Fig. 1. Measurement of chromatographic peak properties. See text for meaning.

search and accurate definition of each resolution maximum by application of a simplex method of restricted evolution [3] and chromatogram simulation.

2.3. Optimization criteria

Three optimization criteria were used:

(i) Separation factor [4]:

$$S_{i,i+1} = \frac{t_{i+1} - t_i}{t_{i+1} + t_i} = \frac{k'_{i+1} - k'_i}{k'_{i+1} + k'_i + 2} \quad (2)$$

where t_i and t_{i+1} are the retention times of the solutes i and $i+1$.

(ii) Valley-to-peak ratio:

$$P_{i,i+1} = 1 - h_1/h_2 \quad (3)$$

where h_1 is the height of the valley and h_2 is an interpolated height between two adjacent peaks, measured at the abscissa of the valley (see Fig. 1).

(iii) Overlapping of two adjacent peaks:

$$O_{i,i+1} = 1 - W'_i/W_i \quad (4)$$

where W_i is the total area of a given peak and W'_i the area overlapped by other peaks (see Fig. 1).

The three functions may vary from 0 to 1. Proximity to unity indicates a better separation. The normalized products of these functions were used to describe the overall separation of the peaks in the chromatogram:

$$r = \prod_{i=1}^{n-1} \frac{X_{i,i+1}}{\left(\sum \frac{X_{i,i+1}}{n-1}\right)^{n-1}} \quad (5)$$

where $X_{i,i+1}$ may be $S_{i,i+1}$, $P_{i,i+1}$ or $O_{i,i+1}$. The function of resolution, r, is maximized to obtain the optimum mobile phase. Contour maps were used to find the position of the maxima and the shape of the response surface. A higher precision in the determination of the optimum mobile phase was achieved by applying the modified simplex method [3] in the final step of the optimization process, when a local optimum has been selected. This was especially useful when the optimum was located on a plateau in the contour map.

2.4. Simulation of the chromatograms

The position of the chromatographic peaks in any mobile phase was obtained from Eq. 1, fitted with the retention data of a few experimental mobile phases (usually five). To improve the accuracy in the prediction of the retention, the capacity factors used in the fitting process were calculated with the void volumes obtained for each mobile phase. However, since it was checked that the void volumes for different mobile phases were similar, the chromatograms were simulated assuming a mean value of void volume.

The efficiencies, measured as the number of theoretical plates, N, and the asymmetry factors, B/A, for the experimental mobile phases were measured. The values of N and B/A used to simulate and predict the peak profile were interpolated by fitting to a plane the values of these parameters for the three experimental mobile phases closer to the simulated mobile phase. For the examples taken from the literature [5,6], the values of N and B/A for several mobile phases were not available, and therefore a constant value of these parameters was assumed. In all instances the areas of the chromatographic peaks were normalized for the simulation.

The simulated chromatographic peaks were drawn using an asymmetric Gaussian function, where the standard deviation depended on the efficiency and the asymmetry factor:

$$h = H_0 \exp\left[-0.5\left(\frac{x - k'}{\sigma(N, B/A)}\right)^2\right] \quad (6)$$

where H_0, the height of the chromatographic peak of a given solute, is a function of $B + A$ since the areas of the peaks are normalized. The peaks were split into two parts of variable standard deviation. The width of the Gaussian curve varied asymptotically between $(B + A)/2$ and A or B, for the leading or tailing edge of the peak, respectively. The values of A and B were calculated from the efficiency and asymmetry

factor calculated from the equation of Foley and Dorsey [7]:

$$N = \frac{41.7[t_R/(A+B)]^2}{(B/A)+1.25} \quad (7)$$

2.5. Test compounds

The procedure was checked using the chromatographic data for several groups of compounds: a mixture of catecholamines (adrenaline, noradrenaline, adrenalone, dopamine and isoprenaline) at pH 6.8 (Table 1) and 3.5 (Table 2), and a mixture of aromatic compounds (anisole, benzene, naphthalene, 1-naphthalenemethanol, phenol and toluene) at pH 6.8, eluted with SDS–1-propanol micellar mobile phases as reported in Ref. [5], and a mixture of phenols (4-benzamidephenol, 4-*tert.*-butylphenol, 4-fluorophenol, 4-hydroxyacetophenone, 4-hydroxybenzaldehyde, 4-hydroxybenzyl alcohol, 4-hydroxybenzophenone, 4-hydroxybenzyl cyanide, 4-hydroxydiphenylmethane, 4-hydroxyphenemethyl alcohol, 4-hydroxypropiophenone, 4-isopropylphenol, 4-methylphenol, 4-nitrophenol and phenol) at pH 7 with cetyltrimethyl-

Table 1
Capacity factors, efficiencies and asymmetry factors in several mobile phases of SDS (μ) and propanol (φ) at pH 6.8

Catecholamine	Mobile phase composition														
	Component	Concentration													
	SDS (M)	0.035			0.035			0.035			0.052			0.052		
	Propanol (v/v)	0.000			0.050			0.100			0.015			0.085		
		k'	N	B/A	k'	N	B/A	k'	N	B/A	k'	N	B/A	k'	N	B/A
Noradrenaline		20.3	3000	1.7	11.7	280	6.7	8.5	34	9.1	10.5	950	3.4	6.2	23	12.7
Adrenaline		26.5	2010	2.1	11.9	240	7.5	8.2	31	11.5	11.6	830	3.6	6.2	20	12.9
Adrenalone		40.6	180	6.2	22.5	10	7.5	13.0	150	8.4	18.6	23	10.4	10.0	7	12.5
Dopamine		51.4	3600	1.3	20.6	1710	2.6	12.5	950	3.9	20.9	2090	1.9	9.7	400	5.2
Isoprenaline		53.1	1600	2.1	19.0	320	6.9	11.4	86	11.7	20.2	460	4.3	8.8	39	13.0
	SDS (M)	0.092			0.092			0.092			0.133			0.133		
	Propanol (v/v)	0.000			0.050			0.100			0.015			0.085		
		k'	N	B/A	k'	N	B/A	k'	N	B/A	k'	N	B/A	k'	N	B/A
Noradrenaline		6.9	2530	1.4	4.3	120	6.5	3.1	33	10.0	3.8	840	2.2	2.2	27	8.9
Adrenaline		8.4	1600	1.6	4.3	60	7.9	3.1	12	12.5	4.1	680	2.4	2.2	24	8.9
Adrenalone		12.7	110	7.2	7.4	6	10.3	5.9	3	8.0	6.4	20	8.5	4.0	1	12.5
Dopamine		15.9	2360	1.4	7.1	830	3.0	4.8	76	6.8	7.1	1700	1.6	3.4	220	4.9
Isoprenaline		16.6	1100	2.0	6.8	38	9.5	4.4	12	12.9	7.0	380	2.8	3.2	12	11.2
	SDS (M)	0.150			0.150			0.150								
	Propanol (v/v)	0.000			0.050			0.100								
		k'	N	B/A	k'	N	B/A	k'	N	B/A						
Noradrenaline		4.0	1340	1.7	2.6	380	3.2	1.9	10	11.9						
Adrenaline		5.0	1200	1.7	2.6	280	3.5	1.9	5	13.5						
Adrenalone		7.7	130	4.8	3.9	8	11.5	3.1	1	17.4						
Dopamine		9.3	1830	1.5	4.1	1180	1.9	2.9	17	9.4						
Isoprenaline		9.8	830	2.0	3.8	240	3.6	2.6	11	12.1						

Table 2
Capacity factors, efficiencies and asymmetry factors in several mobile phases of SDS (μ) and propanol (φ) at pH 3.5

Catecholamine	Mobile phase composition														
	Component	Concentration													
	SDS (M)	0.05			0.15			0.05			0.05			0.15		
	Propanol (v/v)	0.00			0.00			0.05			0.10			0.10		
		k'	N	B/A	k'	N	B/A	k'	N	B/A	k'	N	B/A	k'	N	B/A
Noradrenaline		12.1	3620	1.2	4.4	1970	1.3	5.5	3990	1.2	3.8	3780	1.0	1.6	1890	1.3
Adrenaline		15.6	3180	1.2	5.5	1680	1.2	5.9	3370	1.2	3.7	2950	1.5	1.7	1990	1.4
Adrenalone		24.3	2950	1.2	8.3	1710	1.3	9.6	2870	1.4	6.2	3260	1.3	2.5	1560	1.5
Dopamine		28.1	3460	1.3	9.5	2350	1.1	9.9	3850	1.2	6.6	4000	1.4	2.5	2240	1.2
Isoprenaline		29.0	2700	1.3	9.7	1650	1.1	9.1	2890	1.2	5.4	3100	1.2	2.6	1750	1.7

ammonium bromide (CTAB)–2-propanol mobile phases as reported in Ref. [6].

3. Results and discussion

3.1. Equations of retention

In previous work [1], several equations and about 100 experimental designs were studied to describe the retention behaviour in MLC, when hybrid mobile phases containing an alcohol are used. The models were evaluated with the retention data for several compounds (catecholamines, phenols, amino acids and different aromatic compounds). Among all the equations and designs, Eq. 1 gave the most reliable results. For an experimental design of five mobile phases (design 6 in Fig. 2), the global mean relative error in the prediction of the retention of five catecholamines and thirteen mobile phases at pH 6.8 was 3.5% [1].

However, in an attempt to reduce the error in the prediction of the retention behaviour of solutes, some modifications of Eq. 1 were checked. The retention data of the catecholamines for thirteen mobile phases at pH 6.8 were again used. Initially, linear regression was applied to fit the data, and the equation parameters were further refined using non-linear regression (Powell method [8]). More than 100 experimental designs were considered. The distribution of the experimental data for some of these designs is shown in Fig. 2 and the equations studied are indicated in Table 3, together with the global mean relative errors obtained in the prediction of the retention.

The inclusion of an interaction term in the equations was needed to obtain an adequate description of the retention behaviour of the solutes in MLC with hybrid mobile phases (see Eq. e in Table 3). The results confirmed that Eq. 1 (Eq. a in Table 3) gave the best description. The addition of a new term ($\mu\sqrt{\varphi}$ or $\varphi\sqrt{\mu}$) improved the accuracy of the prediction for some experimental designs, and Eq. g, which also contained a $\varphi\sqrt{\mu}$ term, was frequently good. Although an experimental design of four points (such as design 1) was enough to achieve the fitting parameters of the equation, design 6 is

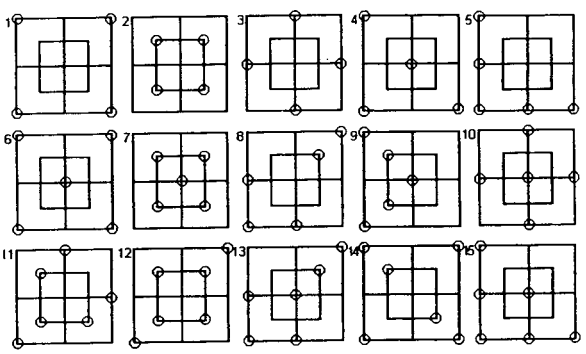

Fig. 2. Experimental designs used to check the retention equations in Table 3.

Table 3
Description of the retention behaviour and global mean errors obtained with the five catecholamines and thirteen mobile phases at pH 6.8

Equation	Relative error (%) ($n = 65$)[a]														
	1	2	3	4	5	6	7	8	9	10	11	12	13	14	15
(a) $1/k' = c_0 + c_1\mu + c_2\varphi + c_3\mu\varphi$	3.4	4.9	100	3.3	250	3.5	4.9	5.7	5.3	207	5.9	4.1	5.2	3.6	3.4
(b) $1/k' = c_0 + c_1\mu + c_2\varphi + c_3\mu\varphi + c_4\mu\sqrt{\varphi}$	–[b]	–[b]	–[b]	–[b]	111	2.8	9.8	12.8	5.5	260	7.7	7.3	3.5	2.4	4.4
(c) $1/k' = c_0 + c_1\mu + c_2\varphi + c_3\mu\varphi + c_4\varphi\sqrt{\mu}$	–[b]	–[b]	–[b]	–[b]	380	3.4	5.2	6.2	5.7	70.2	5.2	23.9	4.5	3.6	111
(d) $1/k' = c_0 + c_1\mu + c_2\varphi + c_3\mu\varphi + c_4\sqrt{\mu\varphi}$	–[b]	–[b]	–[b]	–[b]	559	2.9	8.8	42.9	4.8	153	4.8	4.2	3.7	3.4	3.8
(e) $1/k' = c_0 + c_1\mu + c_2\varphi$	727	70.2	70.9	23.1	31.6	185	44.3	90.4	15.4	69.4	17.8	27.3	121	135	21.8
(f) $1/k' = c_0 + c_1\mu + c_2\varphi + c_3\mu\sqrt{\varphi}$	7.3	117	41.7	7.2	43.2	9.2	656	10.5	17.1	66.1	16.5	26.2	10.1	9.4	7.3
(g) $1/k' = c_0 + c_1\mu + c_2\varphi + c_3\varphi\sqrt{\mu}$	4.1	7.3	52.6	4.5	1250	4.2	7.2	5.5	7.9	111	8.5	6.5	5.6	4.7	4.6
(h) $1/k' = c_0 + c_1\mu + c_2\varphi + c_3\sqrt{\mu\varphi}$	14.4	88.2	291	11.7	33.9	73.5	121	116	15.2	216	37.9	56.4	26.8	54.9	12.1

[a] Numbers correspond to the experimental designs in Fig. 2.
[b] No results could be obtained.

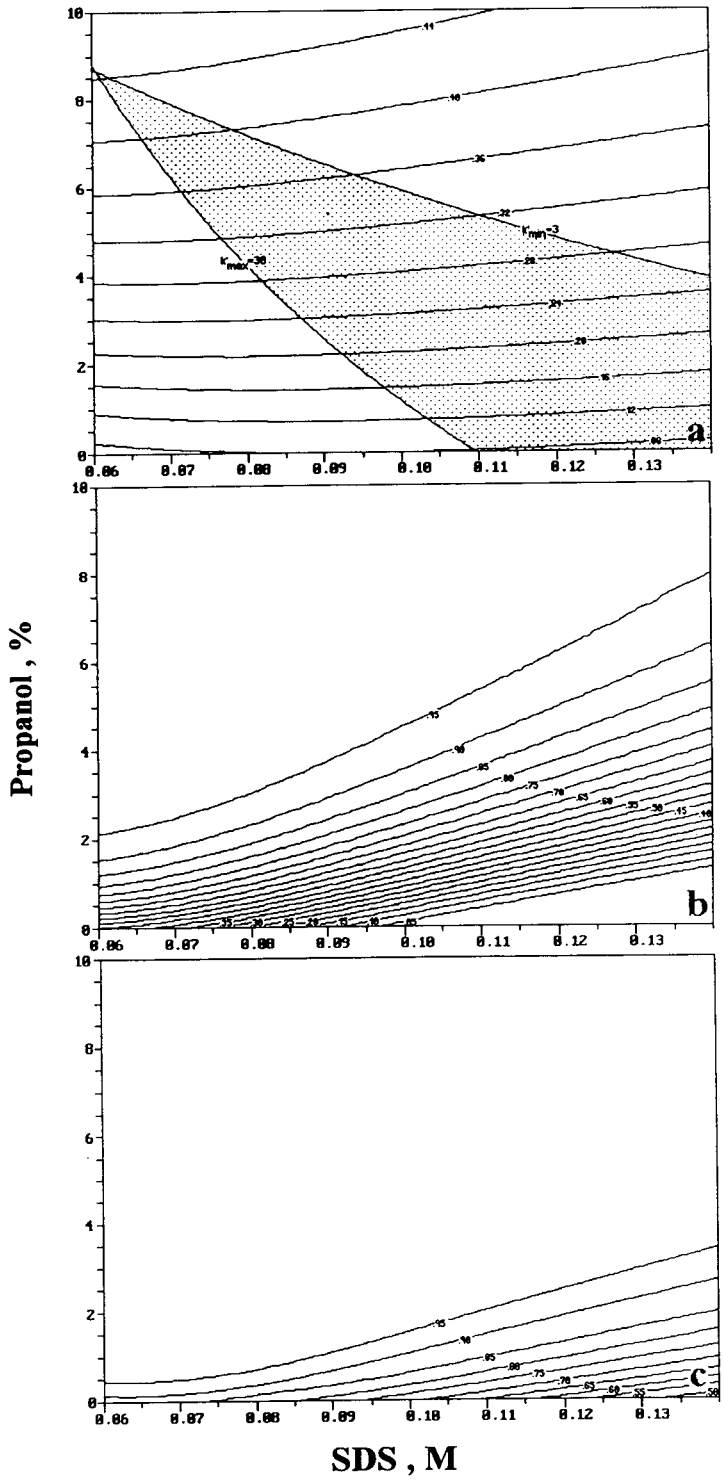

Fig. 3. Contour maps of global resolution for the mixture of six aromatic compounds, and SDS–propanol mobile phases (optima indicated): (a) positional criterion (0.06 M–10%); (b) valley-to-peak ratio criterion (0.06 M–10%); (c) overlapping criterion (0.06 M–10%).

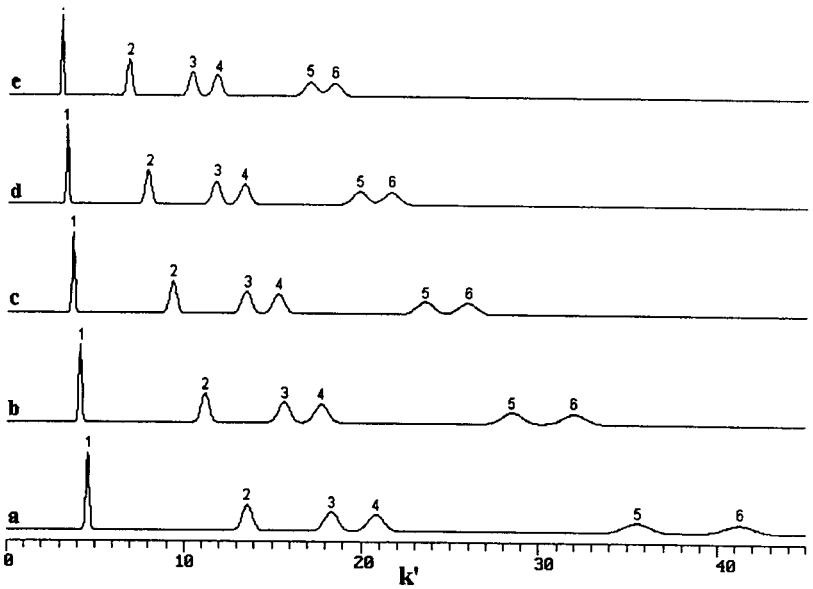

Fig. 4. Chromatograms for the mixture of aromatic compounds for mobile phases with a global positional resolution of $r(S) = 0.25$, containing the following SDS–propanol composition: (a) 0.06 M–3.23%; (b) 0.08 M–3.20%; (c) 0.10 M–3.34%; (d) 0.12 M–3.56%; (e) 0.14 M–3.83%. Peaks: 1 = phenol; 2 = 1-naphthalenemethanol; 3 = anisole; 4 = benzene; 5 = toluene; 6 = naphthalene.

recommended as it allows checking of the accuracy of the fitting. Design 2 is similar to design 1, but it considers the prediction of the retention for mobile phases with concentrations outside the concentration range used for the prediction. Designs 14 and 15, with six mobile phases, are also good. When available, design 6 was always used in this work for the optimization process. If two new phases are added in the middle of two adjacent sides of the design square, design 1 will be produced with a more restricted concentration range. Thus, with only two new phases added to design 6 in the region where the optimum appears, the precision of the predictions will be increased.

3.2. *Positional criterion vs. positional–shape criteria*

The positional criterion, together with the retention model given by Eq. (1), leads to a reliable optimum resolution using the retention data for a few mobile phases. However, as the shape and width of the chromatographic peaks are not considered, achievement of an unacceptable optimum with a high positional resolution may be possible, with peaks largely overlapped.

The positional and positional–shape criteria (valley-to-peak ratio and overlapping) give similar results when the compounds to be separated show symmetrical peaks of high efficiency. Fig. 3 shows contour maps of positional resolution, valley-to-peak ratio and overlapping for diverse aromatic compounds. Assuming an efficiency of $N = 2500$ and an asymmetry factor of $B/A = 1$ for any mobile phase, the solutes appeared well resolved along almost all the composition range studied, since the mean width of the peaks was small compared with the mean separation of adjacent peaks.

With the positional criterion (Fig. 3a), the maximum global resolution was obtained for a 0.06 M SDS–10% propanol mobile phase [$r(S) = 0.476$]. Fig. 4 shows several simulated chromatograms for the separation of the aromatic compounds for mobile phases with a global positional resolution of $r(S) = 0.25$. Although the value of global positional resolution was

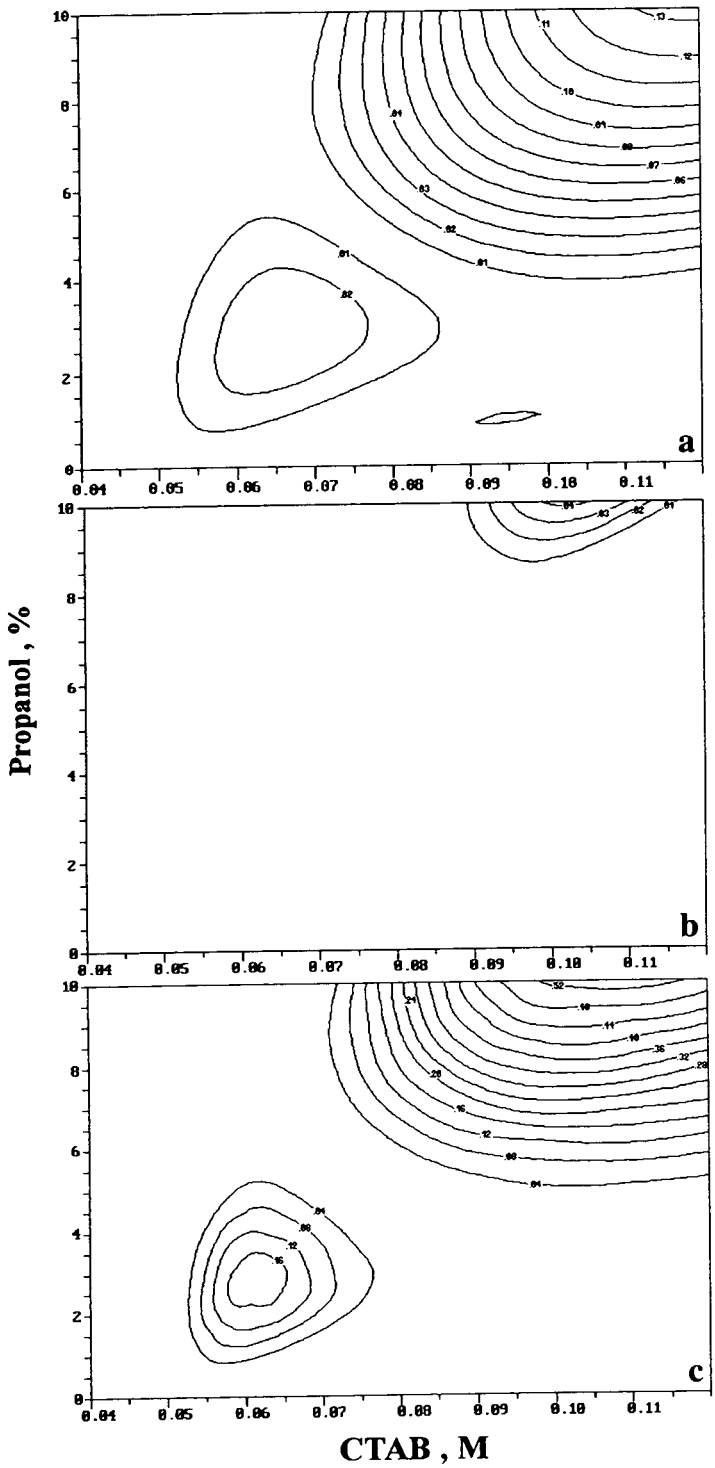

Fig. 5. Contour maps of global resolution for the mixture of fifteen phenols, and CTAB–2-propanol mobile phases (optima indicated): (a) positional criterion (0.12 M–10%); (b) valley-to-peak ratio criterion (0.102 M–10%); (c) overlapping criterion (0.107 M–10%).

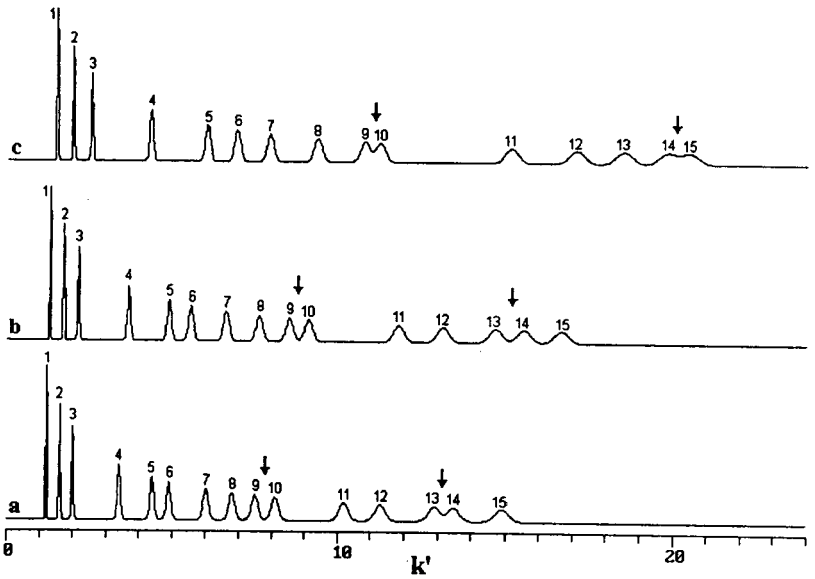

Fig. 6. Chromatograms for the mixture of phenols in mobile phases containing 10% 2-propanol and CTAB, with CTAB concentrations of (a) 0.12 *M*, (b) 0.10 *M* and (c) 0.08 *M*. Peaks: 1 = 4-benzamidephenol; 2 = 4-hydroxybenzyl alcohol; 3 = 4-hydroxyphenemethyl alcohol; 4 = 4-hydroxybenzyl cyanide; 5 = 4-hydroxyacetophenone; 6 = 4-hydroxybenzaldehyde; 7 = phenol; 8 = 4-fluorophenol; 9 = 4-hydroxypropiophenone; 10 = 4-methylphenol; 11 = 4-nitrophenol; 12 = 4-hydroxybenzophenone; 13 = 4-isopropylphenol; 14 = 4-hydroxydiphenylmethane; 15 = 4-*tert.*-butylphenol.

relatively low, a good separation was achieved for all these mobile phases, but that giving the shorter retention times is preferable. It may also be interesting to limit the parameter space by establishing maximum and minimum capacity factors. The lines corresponding to $k'_{max} = 30$ and $k'_{min} = 3$ have been drawn in Fig. 3a.

For the aromatic compounds, the application of the positional–shape criteria, valley-to-peak ratio (Fig. 3b) and overlapping (Fig. 3c) gave similar optima [0.06 *M* SDS–10% propanol, $r(P)$ and $r(O)$ being >0.999]. The contour maps for these criteria were different to that of the positional criterion. The positional resolution increased slowly. In contrast, the positional–shape resolution increased rapidly with increasing concentration of propanol for the lower concentrations and slowed above 4% propanol.

Fig. 5 shows the contour maps for the separation of fifteen phenols with mobile phases of CTAB and 2-propanol. An efficiency of $N = 2500$ was also considered. For the positional criterion, the optimum was found for a mobile phase of 0.12 *M* CTAB–10% 2-propanol (Fig. 5a), whereas for the valley-to-peak ratio criterion it was 0.102 *M* CTAB–10% 2-propanol [$r(P) = 0.047$] (Fig. 5b), and for the overlapping criterion it was 0.107 *M* CTAB–10% 2-propanol [$r(O) = 0.542$] (Fig. 5c). The simulated chromatograms for 10% 2-propanol and three concentrations of surfactant are given in Fig. 6. The disagreement between the positional and positional–shape criteria is due to the retention behaviour of peaks 13–15. As the concentration of surfactant decreased from 0.12 to 0.10 *M* (Fig. 6a and b), the overlapping of these peaks decreased, improving the valley-to-peak ratio and decreasing the overlapping to a lesser extent. However, the positional resolution became worse. A further decrease in the concentration of CTAB decreased both the positional and positional–shape resolution (see peaks 9–10 and 13–15).

The information given by the positional–shape criteria may be especially interesting when the chromatographic peaks are asymmetric, which is usual in MLC. Thus, poorly defined optima obtained with the positional criterion may be

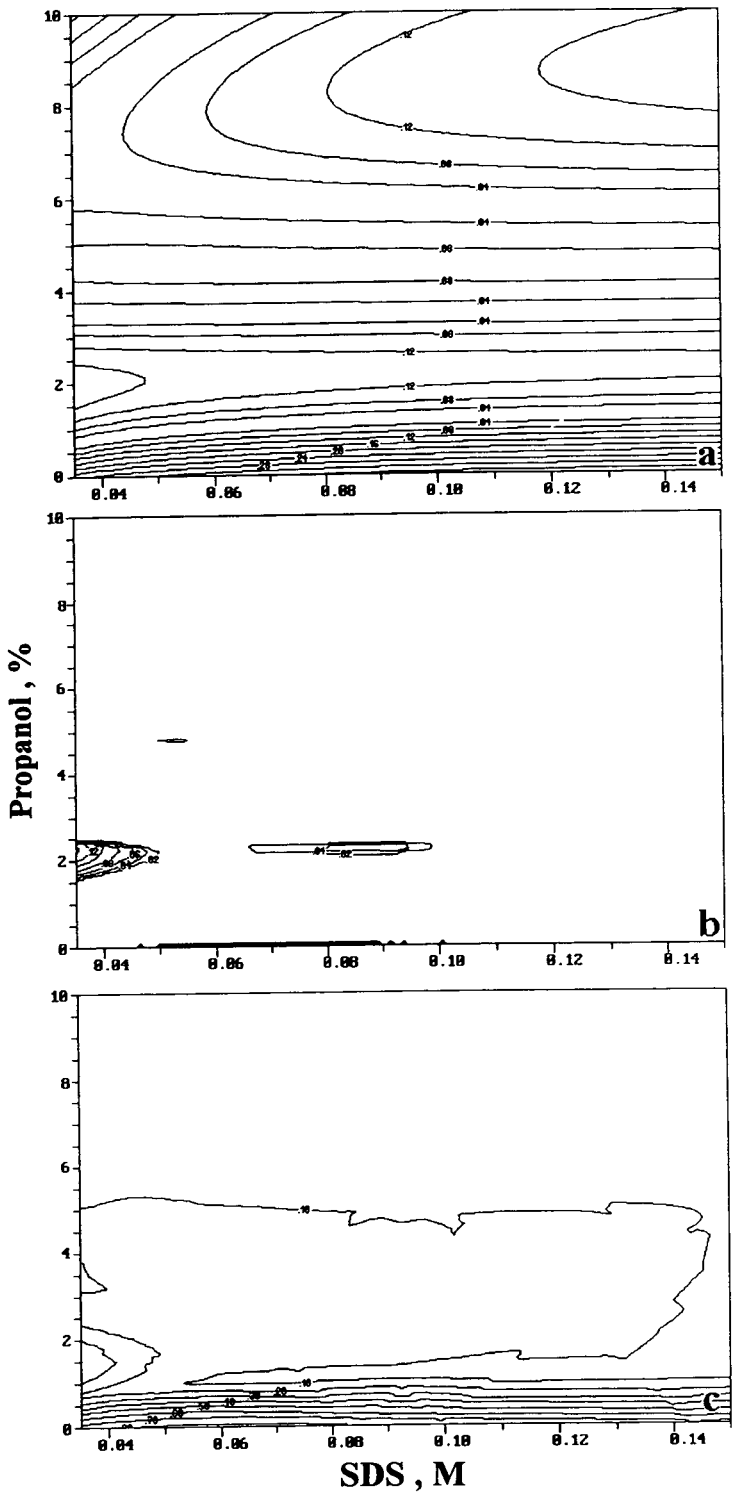

Fig. 7. Contour maps of global resolution for the mixture of five catecholamines, and SDS–propanol mobile phases at pH 6.8 (optima indicated): (a) positional criterion (0.035 to 0.15 *M*–0%); (b) valley-to-peak criterion (0.05 to 0.09 *M*–0% and 0.035 *M*–2.3%); (c) overlapping criterion (0.05 to 0.08 *M*–0%).

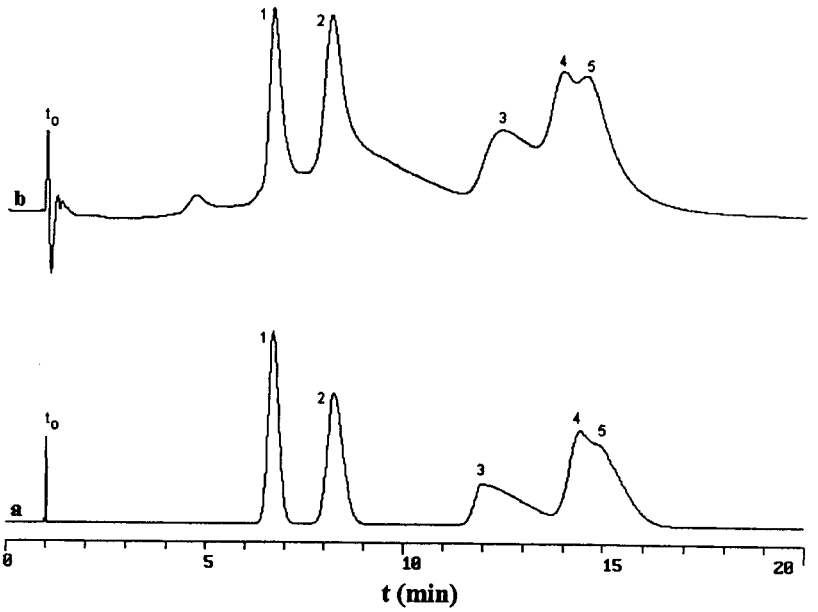

Fig. 8. (a) Simulated and (b) experimental chromatograms for the mixture of catecholamines in a mobile phase of 0.11 *M* SDS alone. Peaks: 1 = noradrenaline; 2 = adrenaline; 3 = adrenalone; 4 = dopamine; 5 = isoprenaline.

clearer when the shape of the peaks is considered. Besides, with the positional–shape criteria some characteristics of the contour maps may be magnified, such as the slope of the resolution function and the value of the maxima and minima, and some maxima may disappear. The comparison of the numerical values of the global resolution for the three criteria allows the evaluation of the quality of the optima. On the other hand, the chromatographic peaks will probably be asymmetric when marked differences are observed between the numerical values of the valley-to-peak ratio and overlapping criteria. The most satisfactory optima should be observed in the contour maps of the three criteria, and the global resolution for the valley-to-peak ratio and overlapping criteria should be both high.

The catecholamines showed very asymmetric peaks and low efficiencies when separated with a purely micellar eluent at pH 6.8. However, at pH < 4 the efficiencies increased and the asymmetry factors decreased. In contrast with the usual behaviour, the addition of short-chain alcohols (methanol, propanol and pentanol) to the micellar mobile phase at pH 6.8 resulted in extremely low efficiencies (see Table 1). The contour map of positional resolution for the five catecholamines eluted with SDS–propanol mobile phases at pH 6.8 is presented in Fig. 7a. Maximum resolution was observed for mobile phases without propanol containing 0.035–0.15 *M* SDS [$r(S) = 0.395$ for 0.15 *M* SDS]. The slope of the function at increasing concentrations of alcohol in this region was high, which is not detrimental for the preparation of the optimum mobile phase, as it does not contain an alcohol and the concentration of surfactant scarcely affected the resolution.

For the catecholamines at pH 6.8 and using the valley-to-peak ratio criterion, the optimum appeared in the 0.05–0.09 *M* SDS concentration range without alcohol [$r(P) = 0.14$], and for 0.035 *M* SDS–2.3% propanol [$r(P) = 0.144$]. Other secondary maxima disappeared (Fig. 7b). With the overlapping criterion the maximum of resolution was similar [0.05–0.08 *M* SDS without alcohol, $r(O) = 0.85$]. The maximum for 0.035 *M* SDS–1.5% propanol was less important (Fig. 7c).

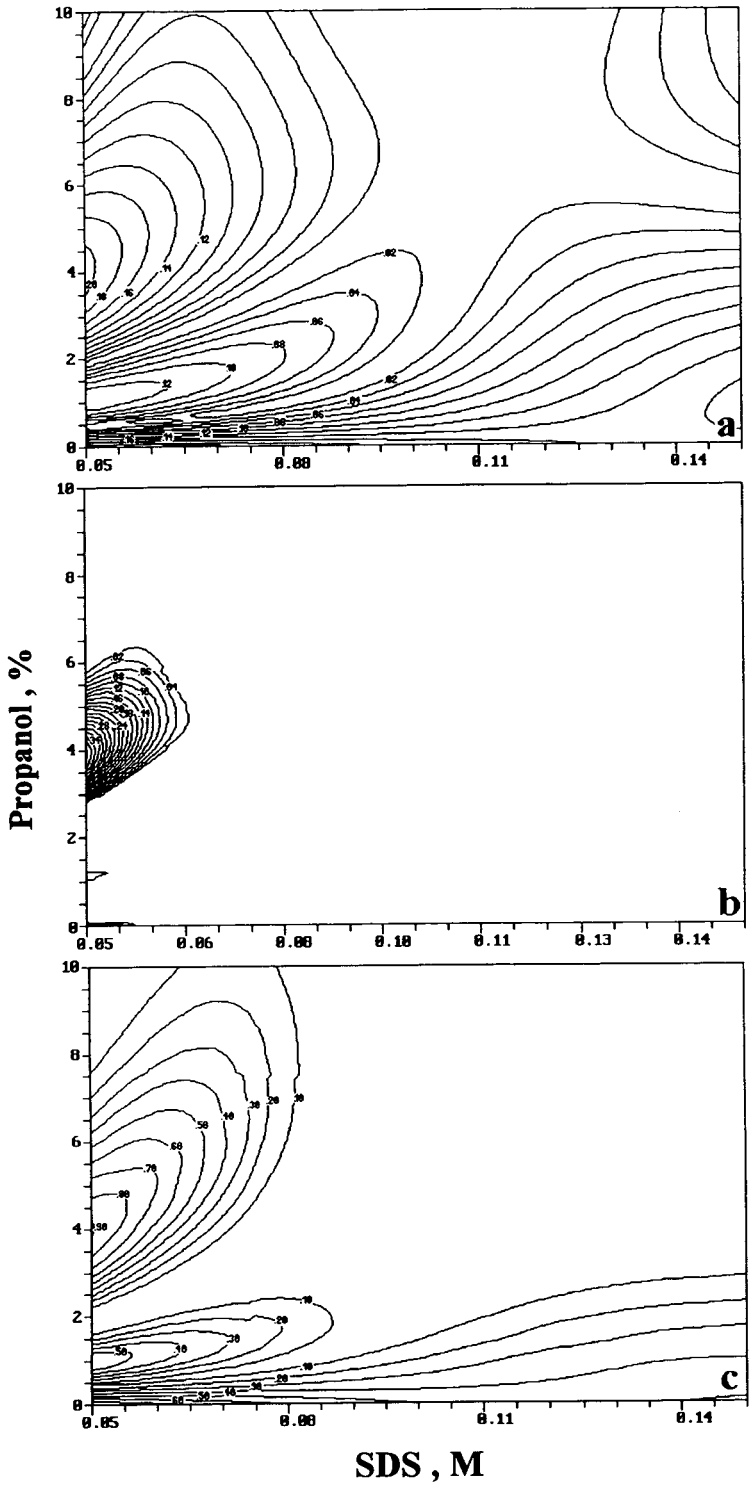

Fig. 9. Contour maps of global resolution for the mixture of five catecholamines, and SDS–propanol mobile phases at pH 3.5 (optima indicated): (a) positional criterion (0.05 *M*–0%, 0.05 *M*–1.1% and 0.05 *M*–4.2%); (b) valley-to-peak criterion (0.05 *M*–0%, 0.05 *M*–1.2% and 0.05 *M*–3.9%); (c) overlapping criterion (0.05 *M*–0%, 0.05 *M*–1.0% and 0.05 *M*–4.0%).

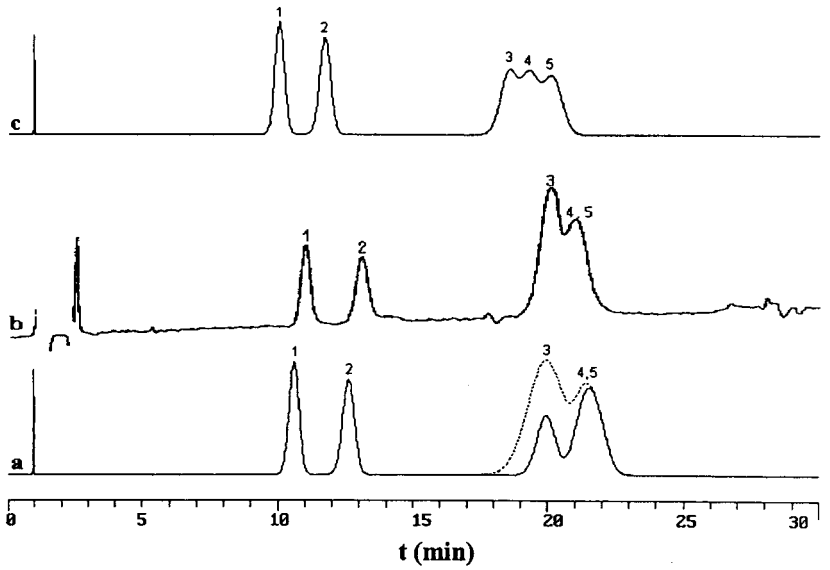

Fig. 10. (a) Simulated and (b) experimental chromatograms for the mixture of catecholamines in a 0.05 *M* SDS–0.8% propanol mobile phase at pH 3.5. (c) Simulated chromatogram for a 0.05 *M* SDS–1.1% propanol mobile phase at pH 3.5. Peaks: 1 = noradrenaline; 2 = adrenaline; 3 = adrenalone; 4 = dopamine; 5 = isoprenaline. Dashed lines in (a) correspond to a higher concentration of adrenalone.

Fig. 8 shows the simulated (a) and experimental (b) chromatograms for the separation of the five catecholamines with 0.11 *M* SDS mobile phases without alcohol at pH 6.8. Good agreement was observed between the experimental and simulated chromatograms, in spite of the low efficiencies. However, the separation of all the peaks in the chromatogram was not possible in any mobile phase at pH 6.8.

For the five catecholamines eluted with SDS–propanol at pH 3.5, several maxima of positional resolution were observed (Fig. 9a). The most interesting corresponded to 0.05 *M* SDS alone [$r(S) = 0.255$], 0.05 *M* SDS–1.1% propanol [$r(S) = 0.13$] and 0.05 *M* SDS–4.2% propanol [$r(S) = 0.21$]. These three maxima were also observed for the valley-to-peak ratio criterion for 0.05 *M* SDS alone [$r(P) = 0.168$], 0.05 *M* SDS–1.2% propanol [$r(P) = 0.04$] and 0.05 *M* SDS–3.9% propanol [$r(P) = 0.406$] (Fig. 9b) and for the overlapping criterion they were 0.05 *M* SDS alone [$r(O) = 0.80$], 0.05 *M* SDS–1.0% propanol [$r(O) = 0.55$] and 0.05 *M* SDS–4.0% propanol [$r(P) = 0.91$] (Fig. 9c). Fig. 10a and b show the simulated and experimental chromatograms for a 0.05 *M* SDS–0.8% propanol mobile phase. This mobile phase was close to a resolution maximum according to the positional and overlapping criteria, but it had a very low value of valley-to-peak resolution. A small increase in the concentration of propanol to 1.1% (Fig. 10c) led to the top of the local maximum of valley-to-peak resolution and, as observed, it gave the partial resolution of peaks 3–5.

4. Conclusions

Eq. 1 gave an adequate description of the retention behaviour of solutes in MLC with mixed mobile phases of SDS and propanol, which was useful for the determination of the optimum mobile phase in the separation of several mixtures of compounds. The use of a positional criterion of optimization may be acceptable for symmetrical peaks with high efficiencies. For asymmetric peaks, peaks with low efficiencies or mobile phases where the peaks are very close to each other, the use of positional–shape criteria may be advisable.

The combined use of the three criteria indicated in this work may give complementary information for selecting the optimum mobile phase. The positional criterion gives only a rough approximation of the region where the peaks will be separated, but it does not indicate how well separated they will be. The valley-to-peak ratio criterion gives information about the region where the peaks will be apparent. The overlapping criterion will indicate the region where the peaks will be better quantified, because a larger surface of each peak will be exposed.

As the application of the positional–shape criteria requires a good prediction of the position and shape of the chromatographic peaks (efficiency, asymmetry and retention), they are susceptible to error. However, these criteria are always preferable, even when asymmetric peaks are assumed to be symmetrical. In situations where the positional–shape criteria lead to large errors, the positional criterion also would give an unreliable prediction.

The selection of the optimum mobile phase should not only consider the value of the resolution function, but also the suitability of the preparation of the mobile phase. Thus, an optimum found in a region of large variations of the resolution function will not be adequate in practice, as the errors in the prediction of the retention and in the preparation of the mobile phase may lead to results different from those expected. For complex response surfaces showing several maxima and minima, additional experimental mobile phases should be prepared in the region where the optimum appears.

Acknowledgement

This work was supported by the DGICYT, Project PB91/629.

References

[1] J.R. Torres Lapasió, R.M. Villanueva Camañas, J.M. Sanchis Mallols, M.J. Medina Hernández and M.C. García Alvarez-Coque, *J. Chromatogr.*, 639 (1993) 87.
[2] J.R. Torres Lapasió, J.J. Baeza Baeza and M.C. García Alvarez-Coque, unpublished results.
[3] J.A. Nelder and R. Mead, *Comput. J.*, 7 (1965) 308.
[4] P. Schoenmakers, *Optimization of Chromatographic Selectivity*, Elsevier, Amsterdam, 1986.
[5] F.P. Tomasella, J. Fett and L.J. Cline-Love, *Anal. Chem.*, 63 (1991) 474.
[6] J.K. Strasters, E.D. Breyer, A.H. Rodgers and M.G. Khaledi, *J. Chromatogr.*, 511 (1990) 17.
[7] J.P. Foley and G. Dorsey, *Anal. Chem.*, 55 (1983) 730.
[8] S.S. Rao, *Optimization. Theory and Applications*, Wiley, New Delhi, 1985.

ELSEVIER

Journal of Chromatography A, 677 (1994) 255–263

JOURNAL OF CHROMATOGRAPHY A

Orthogonal array designs for the optimization of solid-phase extraction

Hai Bin Wan[a], Wei Guang Lan[a], Ming Keong Wong*[,a], Chup Yew Mok[a], Yong Heng Poh[b]

[a]*Department of Chemistry, National University of Singapore, Singapore 0511, Singapore*
[b]*Rohm and Haas Asia Inc., Supelco Singapore Technical Centre, 11 Tuas Avenue 12, Singapore 2263, Singapore*

First received 15 November 1993; revised manuscript received 29 March 1994

Abstract

A systematic approach based on orthogonal array designs for the optimization of solid-phase extraction (SPE) is described. As an example, an off-line SPE approach for extracting 30 pesticides from water was optimized based on the examination of the relevant parameters by orthogonal array designs. The advantages and the disadvantages of the method are discussed.

1. Introduction

Solid-phase extraction (SPE) is a very attractive choice for the trace enrichment of samples prior to instrumental analysis owing to its many advantages over conventional liquid–liquid extractions, such as the decreased use of hazardous solvents, extractions that are not hindered by the formation of emulsions, high extraction efficiency and convenience in automation [1,2]. In recent years there have been many studies leading to a better understanding of various effects on SPE and extended application of this technique [1–11]. This knowledge is also very helpful to those who wish to develop SPE methods for specific purposes. The process of developing an SPE method often involves the investigation of many variables which may affect the efficiency of SPE and the selection of suitable levels for each variable (optimization). The optimization can be achieved either by the trial and error method, the one factor at a time method or systematic methods. Generally, systematic methods are more efficient than trial and error and one factor at a time methods, especially when the number of variables to be tested is large and the interactions between the variables are important [12].

In recent years, some systematic methods, such as simplex optimization and factorial design, have been adopted to search efficiently for optimum conditions for an analysis [13–16]. Factorial designs have an advantage over simplex optimization that in the region preceding the optimum, a large amount of quantitative information about the significance of various effects and interactions can be obtained [17]. Also, factorial designs can deal with both continuous and discrete factors, whereas simplex optimization can only deal with continuous factors. One obvious disadvantage of the factorial de-

* Corresponding author.

0021-9673/94/$07.00
SSDI 0021-9673(94)00336-8

signs is the large number of experiments required when several variables are examined. However, the number of the experiments can be considerably reduced by the use of fractional factorial designs, such as orthogonal array designs.

Orthogonal array designs, the origin and characteristics of which have been described in detail elsewhere [18], are a sophisticated time- and cost-saving testing strategy that draws an orthogonal array to pinpoint areas where variations may be reduced [19]. Besides retaining the merit of routine fractional factorial designs, the interaction effects between variables can be considered as independent factors and estimated by orthogonal array design along with the corresponding linear graphs or triangular tables [19,20].

In this study, an off-line SPE approach for extracting 30 pesticides from water was optimized by orthogonal array designs, just as an example, to demonstrate the application and potential of this systematic optimization technique.

2. Experimental

2.1. Chemicals

HPLC-grade acetonitrile and methanol were obtained from Fisher Scientific (Fair Lawn, NJ, USA). Ascorbic acid was purchased from Merck (Darmstadt, Germany) and was dissolved in HCl-acidified water (pH 2). C_{18} cartridges (Envi-18, 3-ml tubes) and graphitized carbon black cartridges (Envi carb, 3-ml tubes) were obtained from Supelco (Bellefonte, PA, USA). A mixture of humic acid was supplied by Kasei (Tokyo, Japan). Humic acid solutions having concentrations equivalent to organic carbon contents of about 2 and 10 mg l^{-1} were prepared according to a previously reported procedure [6]. The pH of the solutions was adjusted to 8.5 or 3.5 with 0.1 *M* NaOH solution or HCl. Pesticides (listed in Table 6) were obtained from Supelco and had purities greater than 98%. Individual standard solutions were prepared by dissolving 20 mg of each pesticide in 20 ml of methanol. As it was very difficult to separate all 30 of the pesticides considered in a single chromatographic run, the pesticides were divided into two groups and studied separately. Group 1 contained nineteen and group 2 eleven pesticides.

2.2. Procedure for recovery determination

Aqueous samples (0.5 l) were fortified with know volumes of either group 1 or group 2 working standard solutions. For tap water, 0.25 g of sodium thiosulphate was added to 0.5 l of water before pesticides were added to prevent the oxidation of some pesticides. The water was forced to pass through a preconditioned cartridge by vacuum from a circulating pump. After the water had passed through the cartridge, the pump was disconnected. The cartridge was turned upside down and a 5-ml pipette tip was attached to the outlet of the cartridge as a solvent reservoir. The cartridge was washed with 10 ml of distilled water by the back-flush method. If the distilled water was unable to percolate through the cartridge, pressure was applied to the top of the solvent reservoir. The trap was air dried for 0.5 min by vacuum. The analytes were then eluted by front flushing the cartridge with 5 ml of methanol. The eluate collected in a 100-ml flask was concentrated to *ca.* 0.5 ml using a rotary evaporator set at 45°C. Isobutanol (0.2 ml) was added to the eluate as a "keeper solvent". The concentrated eluate was transferred into a 5-ml graduated cylinder using a Pasteur pipette. The flask was rinsed with 0.5 ml of methanol. The solvent was also transferred into the graduated cylinder. The volume of the liquid in the cylinder was made up to 1 ml for HPLC analysis.

2.3. Liquid chromatographic analysis

Liquid chromatographic analysis was carried out with an LC-6A liquid chromatograph (Shimadzu, Kyoto, Japan) equipped with a UV–Vis detector. The injection volume was 20 μl. The wavelength of the detector was set at 215

nm. An LC-ABZ column (25 cm × 4.6 mm I.D.) from Supelco was used for the separation. The mobile phase was acetonitrile–phosphate buffer solution (pH 2.6) (45:55).

2.4. Experimental design

The first experiment was designed to optimize the extraction using graphitized carbon black cartridges. Four variables that may affect the extraction efficiency and the possible interactions were examined by using a two-level orthogonal array design: the volume of water sample, the pesticide concentration in water, the elution method and the time for air-drying the trap. The average recovery of the pesticides in group 1 was used as the response. The selection of the variables and their levels was based on previous knowledge of SPE. For example, Di Corcia *et al.* [4] reported that back-flushing was better than the conventional front-forward elution method when a graphitized carbon black cartridge was used. A comparison between the two elution methods was made in the first experiment to see whether this statement was still true with the pesticides selected. The selection of the air-drying time as a variable was based on the consideration that the effluent air passing through the cartridge may cause evaporative losses of some volatile analytes. As the evaporation loss of the pesticides from the sorbent in the air-drying step is less likely to be affected by the other three variables, its interactions with them were neglected.

In the application of fractional factorial designs, previous knowledge of the variables is very helpful in arranging the experiment. In the first experiment, the sorbent type was not tested because each type of sorbent may have its own optimum conditions and it will be "fairer" to compare their extraction efficiencies under their own optimum conditions. Therefore, the conditions for the graphitized carbon black cartridge were optimized first. In the second experiment, it was compared with a C_{18} cartridge under conditions favouring the graphitized carbon black cartridges. If a C_{18} cartridge is better than a graphitized carbon black cartridge, C_{18} will be selected for the analysis. Otherwise, another comparison may be conducted after the optimum conditions for C_{18} have been found.

It has been reported that pre-eluting graphitized carbon black cartridges with ascorbic acid solution after conditioning with methanol can prevent partial irreversible adsorption of some compounds, and that the addition of sodium thiosulphate to tap water can prevent the oxidation of some compounds [4]. In addition to the comparison between the graphitized carbon black and C_{18} cartridges, the effects of these two treatments were also tested in the second experiment. Consideration was also given to the interaction effects between the variables.

In the analysis of real samples, a large amount of humic substances may decrease the extraction efficiency [2,4,6]. The pH and salinity may also affect the extraction [2,7]. Liska *et al.* [2] observed that the adverse effect of humic acid was more serious at lower pH. There is a possibility of decreasing this adverse effect by adjusting the pH and increasing the salinity. The third experiment was accordingly designed to test this possibility by examining the effects of humic substances, pH and salinity and their interactions. In the first experiment, the two elution methods (back-flush and front-forward) were compared with a graphitized carbon black cartridge. The result may differ if a C_{18} cartridge is used. Therefore, in the third experiment, the two methods were compared again with a C_{18} cartridge. The assignment of the factors and the levels is shown in Table 1. Details on the assignment of factors in the orthogonal array designs have been given elsewhere [19,20].

3. Results and discussion

The results of the three experiments are given in Table 2. The level means of the average recoveries for each factor were calculated according to the assignment of the experiments. For example, to obtain the level mean of factor *B* at level 2 in the first experiment, the average recovery data of the four trials in which the level of *B* was set at 2 (trials 3, 4, 7 and 8; see Table

Table 1
Assignment of factors and levels of the OA_7 (2^7) matrix for investigating the effects of the factors on the recoveries of pesticides from water

Experiment	Level	Column No.						
		1	2	3	4	5	6	7
		Factor[a]						
		A	*B*	*A* × *B*	*C*	*A* × *C*	*B* × *C*	*E*
First	1	0.5	60		Back-flush			5
	2	1.0	10		Front-flush			30
Second	1	C_{18}	200		0.5			
	2	GCB	0		0			
Third	1	2	3.5		0			Front-flush
	2	10	8.5		10			Back-flush

[a] For the first experiment: *A* = volume of the sample (l); *B* = concentration of the pesticides in water ($\mu g\ l^{-1}$); *C* = elution method; *E* = air-drying time (min). For the second experiment: *A* = type of cartridge (GCB = graphitized carbon black); *B* = amount of ascorbic acid used for cartridge conditioning (mg); *C* = concentration of sodium thiosulphate in water ($g\ l^{-1}$); *E* = unassigned column. For the third experiment: *A* = concentration of dissolved organic substances ($mg\ l^{-1}$); *B* = pH of water; *C* = concentration of sodium chloride in water (%); *E* = elution method. *A* × *B*, *A* × *C* and *B* × *C* mean the interactions between the factors.

2) were pooled and divided by the number of the trials: $B_2 = (69.5 + 75.0 + 85.9 + 57.9)/4 = 72.1$. The means at the two levels of a variable reveal how the response will change when the level of the variable is changed. When significant interactions exist between two variables, say *A* and *B*, the level means for *B* were calculated according to the level of *A*. Thus, to obtain the mean for variable *B* at level 1 when *A* was set at level 2, the average recovery data of the two trials in which *A* was set at level 2 and *B* was set at level 1 (trials 5 and 6) were pooled and divided by 2.

Fig. 1 shows the relationship between the level means of average recovery and the variable levels of significant variables. The analysis of variance tables were constructed for testing the significance of the effects (Tables 3–5). The sum of squares for an effect was calculated by using

Table 2
An OA_8 (2^7) matrix along with the results of the three experiments

Trial No.	Column No.							Average recovery (%)[a]		
	1	2	3	4	5	6	7	I	II	III
1	1	1	1	1	1	1	1	87.8	83.8	95.3
2	1	1	1	2	2	2	2	59.3	91.9	84.1
3	1	2	2	1	1	2	2	69.5	89.5	72.2
4	1	2	2	2	2	1	1	75.0	87.3	72.3
5	2	1	2	1	2	1	2	84.5	78.1	69.1
6	2	1	2	2	1	2	1	80.9	86.1	60.6
7	2	2	1	1	2	2	1	85.9	79.6	51.4
8	2	2	1	2	1	1	2	57.9	75.5	63.1

[a] Average recovery of the pesticides studied; I = the firsts experiment; II = the second experiment; III = the third experiment.

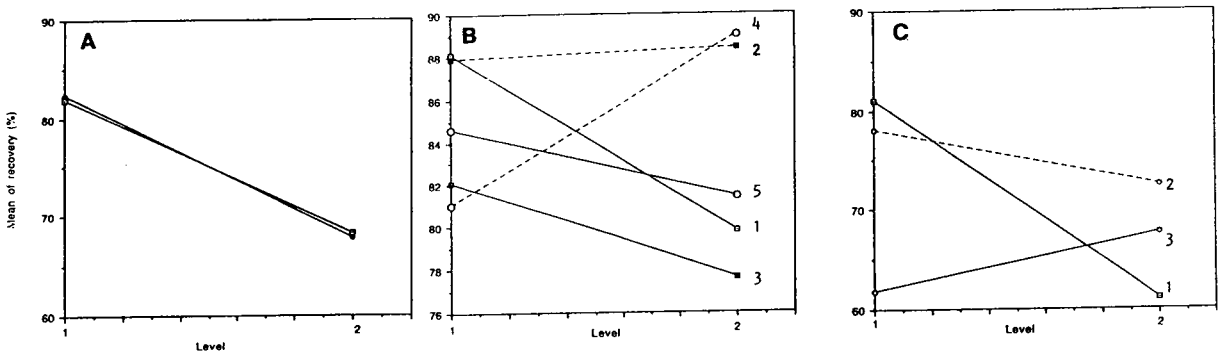

Fig. 1. Relationship between the level mean of average recoveries and the factor level. (A) The first experiment; □ = elution method (back-flush and front forward elution), ◆ = air-drying time (5 and 30 min). (B) The second experiment; 1 = cartridge type (C_{18} and GCB), 2 = use of ascorbic acid with C_{18} cartridge (used and not used), 3 = use of ascorbic acid with GCB cartridge (used and not used), 4 = addition of sodium thiosulphate with ascorbic acid (added and not added), 5 = addition of sodium thiosulphate without ascorbic acid (added and not added). (C) The third experiment; 1 = concentration of humic acid (2 and 10 mg l^{-1}), 2 = concentration of sodium chloride at pH 3.5 (0 and 10%), 3 = concentration of sodium chloride at pH 8.5 (0 and 10%).

Table 3
An ANOVA table for the first experiment

Source of variance	Sum of squares	Degrees of freedom	Mean square	*F* value	Significance[a]
Volume of sample (*A*)	38.7	1	38.7	3.72	
Concentration (*B*)	73.2	1	73.2	7.04	
Elution method (*C*)	372.6	1	372.6	35.8	$P < 0.05$
Air-drying time (*E*)	426.3	1	426.3	41.0	$P < 0.05$
$A \times B$	49.0	1	49.0	4.71	
Pooled error[b]	20.8	2	10.4		
Total	980.6	7			

[a] The critical *F* value is 8.53 at 90% confidence and 18.5 at 95% confidence.
[b] Pooled error result from pooling negligible effects ($A \times C$, $B \times C$).

Table 4
An ANOVA table for the second experiment

Source of variance	Sum of squares	Degrees of freedom	Mean square	*F* value	Significance[a]
Type of cartridge (*A*)	137.8	1	137.8	285	$P < 0.01$
Ascorbic acid (*B*)	8.0	1	8.0	16.7	$P < 0.1$
Sodium thiosulphate (*C*)	13.0	1	13.0	23.7	$P < 0.05$
$A \times B$	12.0	1	12.0	25.0	$P < 0.05$
$B \times C$	62.7	1	62.7	131	$P < 0.01$
Pooled error[b]	0.95	2	0.48		
Total	233.9	7			

[a] The critical *F* value is 8.53 at 90% confidence, 18.5 at 95% confidence and 98.5 at 99.0% confidence.
[b] Pooled error result from pooling negligible effect ($A \times C$) and unassigned column effect.

Table 5
An ANOVA table for the third experiment

Source of variance	Sum of squares	Degrees of freedom	Mean square	F value	Significance[a]
Humic acid (A)	792.0	1	792.0	29.2	$P<0.05$
Water pH (B)	312.5	1	312.5	11.5	$P<0.05$
NaCl (C)	8.0	1	8.0	0.3	
$B \times C$	128.8	1	128.8	4.8	
Pooled error[b]	81.4	3	27.1		
Total	1322.7	7			

[a] The critical F value is 5.54 at 90% confidence, 10.1 at 95% confidence and 34.1 at 99.0% confidence.
[b] Pooled error result from pooling negligible effects ($A \times B$, $A \times C$ and E).

the equation $SS_i = [(M_2 - M_1) \cdot 4]^2/8$, where M_2 and M_1 are the means for effect i at levels 2 and 1, 4 is the number of data used to calculate the mean and 8 is the number of data produced by the experiment. The importance of each effect was calculated using the relative contribution (RC), which was calculated by using the equation $RC_i = SS_i/\Sigma SS$. As the trials in the experiments were not repeated, the error was estimated by combining the mean squares of negligible effects. The negligible effects were selected by using the method described by Montgomery [16].

The ANOVA results of the first experiment (Table 3) indicate that the air-drying time and the elution method have significant effects on the average recovery ($RC = 38.0\%$ for elution method and 43.5% for air-drying time), whereas the effects of the sample volume and the concentration of the pesticide are not significant. Fig. 1 suggests that back-flush elution is better than front-forward elution and a shorter air-drying time is better. The results with the elution method confirmed Di Corcia *et al.*'s results [4], although the effect of the air-drying time had not been expected to be so important before. The flow-rate of air passing through the cartridge was 3 l min^{-1}. Such a high flow-rate can possibly cause considerable evaporative losses of pesticides from the cartridge. Even 5 min may still be too long for air-drying. In subsequent experiments, the air-drying time was decreased to 0.5 min and the back-flush method was adopted for elution.

The ANOVA results of the second experiment (Table 4) suggest that the cartridge type (A), ascorbic acid (B) and sodium thiosulphate (C) have significant effects on the average recovery, among which the cartridge type is the most important ($RC = 58.9\%$). Significant interactions also exist between the cartridge type and ascorbic acid treatment ($A \times B$) and between ascorbic acid treatment and the addition of sodium thiosulphate ($B \times C$). Fig. 1 suggests that a C_{18} cartridge is better than a graphitized carbon black cartridge and that ascorbic acid treatment can improve the extraction efficiency when graphitized carbon black cartridges are used, but has no effect when C_{18} cartridges are used. Fig. 1 also suggests that the addition of sodium thiosulphate to tap water can increase the recovery if the cartridge is not pre-eluted with ascorbic acid solution, but can decrease the recovery if the cartridge is pre-eluted with ascorbic acid solution. Therefore, the two treatments should not be used together. To explain this observation, further investigation is needed. As sodium thiosulphate will not be used in analyses of real samples, the problem will not exist.

The ANOVA results of the third experiment (Table 5) indicate that humic acid (A) and water pH (B) have significant effects on the recovery, among which humic acid is the most important factor ($RC = 60\%$). The interaction effect between pH and NaCl ($B \times C$) is near the significant level. The two elution methods (back-flush and front-forward elution) make no difference in recovery when C_{18} cartridges are used. When the

concentration of dissolved organic substances was increased from 2 to 10 mg l^{-1}, the recovery dropped from 81 to 61%. When the pH was lowered from 8.5 to 3.5, the recovery increased from 65% to 77%. At pH 3.5 addition of sodium chloride can decrease the recovery and at pH 8.5 addition of sodium chloride can increase the recovery. Although the effects of humic acid and pH can be explained based on the results of Johnson *et al.* [6] and Liska *et al.* [2], the interaction between pH and salinity can only be an observation here. As there are no significant interactions between humic acid and pH and between humic acid and sodium chloride, it is impossible to decrease the adverse effects of humic acid through adjustment of the pH and the concentration of salt.

Based on the results of the three experiments, the conditions for extraction of pesticides from water were chosen as follows: C_{18} as extraction cartridge, methanol as preconditioning solvent (10 ml) and as eluent (5 ml), elution by the front-forward method, air-drying time 0.5 min and addition of sodium thiosulphate when the recoveries of pesticides from tap water are to be determined.

Table 6
Recoveries of pesticides from water by solid-phase extraction (duplicated results)

Pesticide	Retention time (min)	Recovery (%)[a]		
		A	B	C
Simazine	3.96	96, 112	94, 97	88, 84
Isoprocarb	5.70	73, 61	64, 108	84, 83
Fenobucarb	7.70	84, 103	93, 125	106, 110
Methyldymiron	8.80	95, 105	83, 113	89, 99
Napropamide	10.1	85, 95	87, 91	94, 97
Isoprothiolane	11.2	86, 95	90, 106	99, 123
Mepronil	13.4	81, 93	82, 83	88, 99
Flutolanil	14.6	93, 107	94, 122	103, 106
Diazinon	16.4			84, 85
Thiobencarb	22.0	84, 96	84, 87	84, 87
Iprodione	23.5	26, 49	84, 89	85, 89
Terbutol	25.0	88, 103	90, 98	90, 95
Isofenphos	28.7	121, 132	122, 123	119, 129
Pencycuron	30.9	99, 108	99, 101	96, 103
Butamifos	33.0	98, 101	96, 97	99, 106
EPN	37.3	77	87	83, 90
Pendimethalin	54.4	70, 79	73, 79	59, 67
Chlorpyrifos	56.4	49, 71	71, 79	65, 69
Balan	70.9	63, 73	66, 69	61, 64
Dichlorvos	3.85	82, 123	49, 89	67, 88
Thiram	5.50	2, 20	0, 3	15, 17
Captan	9.25	19, 25	13, 13	0, 0
Pyridaphenthion	11.2	75, 95	79, 95	101, 112
Chloroneb	12.7	77, 106	79, 106	62, 78
Proamide	13.4	66, 105	90, 109	90, 98
Chlorothalanil	15.2	57	83	82, 91
Etridiazole	16.8	49, 82	20, 76	32, 85
Bensulfite	30.4	122, 138	99, 156	110, 117
Tolclofos	32.1	85, 105	81, 96	75, 83
Isoxathion	39.4	60, 60	108, 143	115, 139

[a] A = Extracted from tap water with graphitized carbon black cartridge; B = extracted from tap water with C_{18} cartridges; C = extracted from sea water with C_{18} cartridges.

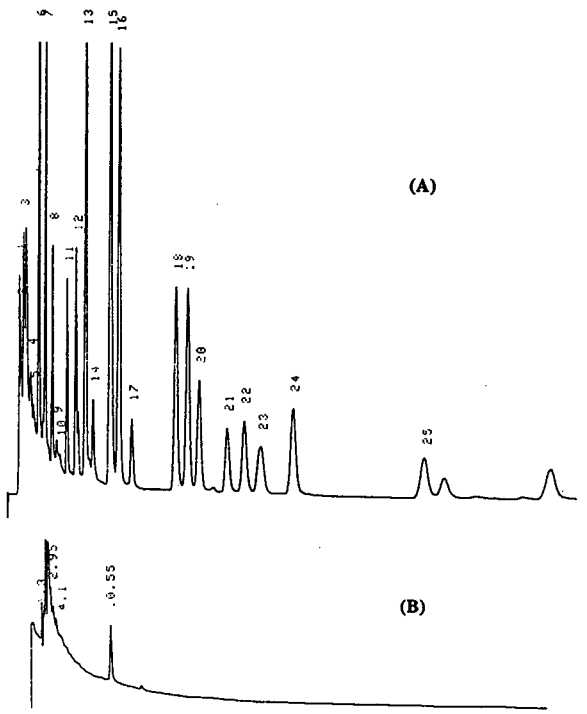

Fig. 2. Chromatograms of sea water samples. (A) Fortified with group 1 pesticides at 10 μg l^{-1} level (6 = simazine; 8 = isoprocarb; 11 = fenobucarb; 12 = methyldymiron; 13 = napropamide; 14 = isoprothiolane; 15 = mepronil; 16 = flutolanil; 17 = diazinon; 18 = thiobencarb; 19 = aprodione; 20 = terbutol; 21 = isophenfos; 22 = pencycuron; 23 = butamifos; 24 = EPN; 25 = pendimethalin; 26 = chlorpyrifos; 27 = balan). (B) Blank sea water (0.5 l) extracted with a C_{18} cartridge following the same procedures as fortified samples.

Under the optimum conditions, the recoveries of the pesticides from tap water and sea water at the 10 μg l^{-1} level were determined. The results are given in Table 6. The chromatograms of fortified and blank sea water samples are given in Fig. 2.

4. Conclusions

The concept of the optimum in systematic optimization is a conditional one; it depends on the goals one wants to achieve and the experimental conditions available. In this study, the recoveries of some pesticides were not satisfactory under the selected conditions. It is possible that some variables that may affect the extraction of these pesticides have not been studied or some important levels have been missed. In the case of the sorbent type, more levels may be tested to improve the recoveries of the pesticides. Although the optimization by factorial designs is regarded as a simultaneous method, the optimum is actually located step by step as in sequential approaches. In this study, the second experiment was designed based on the results of the first experiment, and the third experiment was based on the first and the second experiments. This process can be continued with new variables and more accurate levels to achieve better results. It should be mentioned that orthogonal array designs, as with other factorial designs, cover a predefined region. Problems appear in situations where the initial values of the effects are too close together to give a significant difference, or are too far apart, giving a large but useless significant difference. Therefore, it is necessary to rely on previous knowledge of the system, past experience and intuition when the levels of the variables are chosen [16]. Previous knowledge is also necessary in interpreting the results, otherwise certain observations will remain mere observations.

Acknowledgement

H.B.W. and W.G.L. thank the National University of Singapore for the award of research scholarships.

References

[1] A. Balinova, *J. Chromatogr.*, 643 (1993) 203.
[2] I. Liska, E.R. Bronwer, H. Lingeman and U.A.Th. Brinkman, *Chromatographia*, 37 (1993) 13.
[3] A. Di Corcia and M. Marchetti, *Anal. Chem.*, 63 (1991) 580.
[4] A. Di Corcia, R. Samperi, Marcomini and S. Stelluto, *Anal. Chem.*, 65 (1993) 907.
[5] J.M. Vinuesa, J.C.M. Cortes, C.I. Canas and G.F. Perez, *J. Chromatogr.*, 472 (1989) 365.
[6] W.E. Johnson, N.J. Fendinger and J.R. Plimer, *Anal. Chem.*, 63 (1991) 1510.

[7] G. Font, J. Manes, J.C. Molto and Y. Pico, *J. Chromatogr.*, 642 (1993) 135.
[8] J. Sherma and C. Rolfe, *J. Chromatogr.*, 643 (1993) 337.
[9] D. Barcelo, *J. Chromatogr.*, 643 (1993) 117.
[10] C.L. Hsu and R.R. Walters, *J. Chromatogr.*, 629 (1993) 61.
[11] J. Sherma, *Anal. Chem.*, 65 (1993) 40R.
[12] C.K. Bayne and I.B. Rubin, *Practical Experimental Designs and Optimization Methods for Chemists*, VCH, Deerfield Beach, FL, 1986.
[13] S.D. Brown, R.S. Bear, Jr. and T.B. Blank, *Anal. Chem.*, 64 (1992) 22R.
[14] F.H. Walters, L.R. Parker, S.L. Morgan and S.N. Deming, *Sequential Simplex Optimization*, CRC Press, Boca Raton, FL, 1991.
[15] S.M. Sultan and F.E.O. Suliman, *Analyst*, 118 (1993) 573.
[16] D.C. Montgomery, *Design and Analysis of Experiments*, Wiley, New York, 3rd ed., 1991, pp. 197–291.
[17] G.A. Zachariadis and J. Stratis, *J. Anal. At. Spectrom.*, 6 (1991) 239.
[18] H.B. Wan, W.G. Lan, M.K. Wong and C.Y. Mok, *Anal. Chim. Acta*, 289 (1994) 371.
[19] P.J. Ross, *Taguchi Techniques for Quality Engineering*, McGraw-Hill, New York, 1988.
[20] G. Taguchi, *System of Experimental Design*, Vols. 1 and 2, Kraus International, New York, 1987.

ELSEVIER

Journal of Chromatography A, 677 (1994) 265–272

JOURNAL OF CHROMATOGRAPHY A

Detailed analysis of crude oil group types using reversed-phase high-performance liquid chromatography

Mohammed Shahid Akhlaq*, Petra Götze

German Petroleum Institute, Walther-Nernst-Strasse 7, D-38678 Clausthal-Zellerfeld, Germany

First received 11 February 1994; revised manuscript received 22 April 1994

Abstract

Different HPLC methods were developed for characterizing the one-, two-, three- and four-ring aromatic compounds from crude oils. The crude oils are separated in five different fractions and these fractions are then analysed by reversed-phase HPLC. This method of analysing crude oil could be of help in evaluating the origin of the corresponding oil. The methods described were applied to some crude oils.

1. Introduction

For the mineral oil industry and for research purposes it is very important to know the different group types in a given crude oil [1–5], which will contain different amounts of aliphatics, naphthenes, aromatics, naphthenoaromatics, heteroaromatics, polar compounds and colloids [6–10]. Efforts have been made to determine all of these groups quantitatively [11–14].

From the geochemical point of view, it is not enough to know the exact amounts of group types present in a crude oil. It is important to know the detailed constituents of the crude oil [10]. On the other hand, polycyclic aromatic hydrocarbons (PAHs) are well known components of petroleum and petroleum-derived products. PAHs are important environmental pollutants because of their carcinogenicity [15,16]. These compounds are routinely determined in industrial waste water, drinking water and ground water. Regulations on these toxic chemicals are already in effect in North America and Europe.

Many GC and HPLC methods are currently used for PAH determinations, most of which involve time-consuming extraction and clean-up steps [17–19]. The determination of PAHs from crude oil is usually a difficult task [20]; the mixtures are complex and the isolation of PAHs prior to analysis requires multi-step procedures [21], often involving tedious and time-consuming open-column chromatography and liquid–liquid extractions [22,23].

This paper describes improved methods based on (1) the preparative HPLC separation of group types from crude oils [14] and (2) the detailed analysis of collected group types fraction by reversed-phase HPLC. These HPLC methods allow the qualitative characterization of crude oils.

* Corresponding author.

0021-9673/94/$07.00
SSDI 0021-9673(94)00395-P

2. Experimental

2.1. Solvents and chemicals

The solvents used were distilled *n*-hexane, chloroform, methanol and acetonitrile, all from Riedel-de Haën. Water was purified with a Millipore Q-filter system. The quality of this water is equal to that of triply distilled water. Standard model compounds were purchased from Aldrich and were used as received. The crude oils investigated were Suria, Shingli, Jakarta Arco and two north German crude oils. To compare the crude oils with fuels, a diesel fuel was also investigated. The specially prepared diesel fuel sample contains about 1% of sulphur compounds.

2.2. Instrumentation

We used a multi-step analysis. First the preparative separation of crude oils was performed based on previously published work [14], which was modified for preparative analysis. Five fractions were collected. The collected fractions were dried and dissolved in methanol or tetrahydrofuran and then fractions analysed on an analytical column.

The preparative HPLC system consisted of two pumps (Model 510), a UV detector (Model 484) and a refractive index (RI) detector (Model 410) (all from Millipore–Waters). Maxima 820 chromatography workstation software (Millipore–Waters) controlled the overall HPLC instrument. A high-pressure gradient system and an electronic backflush valve were used. The gradient system is shown in Table 1. The column used was LiChrosorb NH_2 from Merck (Darmstadt, Germany) (250 mm × 10 mm I.D.) with a particle size of 7 μm. To eliminate the resins and asphaltenes, the column was washed with chloroform in the backflush mode. This procedure was repeated once a day for about 2 h.

The analytical HPLC apparatus consisted of quaternary pump (1050 Ti-Series), an autosampler (1050 Series) and a degasser (1050 Series), all from Hewlett-Packard, and a UV detector (Merck–Hitachi L-4000). HPLC ChemStation (DOS Series) software (Hewlett-Packard) controlled the overall HPLC instrument. The gradient systems are shown in Table 2. The columns used were Nucleosil C_{18} (Macherey–Nagel) (125 mm × 4.0 mm I.D.) with a 30-mm precolumn (Macherey–Nagel) with a particle size of 5 μm (column system I) and Nucleosil C_{18} PAH (Macherey–Nagel) (150 mm × 4.0 mm I.D.) with an 11-mm precolumn from the same supplier with a particle size of 5 μm (column system II).

Table 1
HPLC gradient system (linear) for the preparative separation of crude oils

Time (min)	Stage	Flow-rate (ml/min)
0		3.0
17		3.0
20	Backflush	6.0
40		6.0
45	Re-equilibration	3.0
60		3.0

Column, NH_2 phase (250 mm × 10.0 mm I.D.); particle size, 7 μm; mobile phase, *n*-hexane.

3. Results

The major problem in the analysis of crude oils and crude oil fractions is the complexity of this natural mixture, containing hundreds of different compounds [14,24,25]. For example, one can find in the monoaromatic fraction all the possible substitutions on the aromatic ring and also the whole variety of chains with respect to type and length. A very limited selection of these compounds that belong to a single group type fraction (monoaromatics fraction) is given in Table 3. Separation of all the possible compounds present in crude oil is not possible [10,25].

To characterize a crude oil in detail, one has to analyse its group-type fractions to some extent [26,27]. RP-HPLC and GC are suitable for this purpose. The advantage of RP-HPLC over GC is its ability to separate even more condensed

Table 2
HPLC gradient system (linear) for the separation of crude oil fractions

Method	Time (min)	Mobile phase		Flow-rate (ml/min)	Column system
		Water (%)	Acetonitrile (%)		
1	Start	30	70	0.70	I
	5	30	70	0.70	
	10	20	80	0.70	
	25	0	100	0.70	
	50	0	100	0.70	
		Re-equilibration			
	55	30	70	0.70	
	70	30	70	0.70	
2	Start	40	60	1.00	II
	15	40	60	1.00	
	20	35	65	0.75	
	60	0	100	0.75	
	100	0	100	0.75	
		Re-equilibration			
	105	40	60	1.00	
	120	40	60	1.00	
3	Start	30	70	1.00	II
	12	30	70	1.00	
	15	15	85	1.00	
	25	15	85	1.00	
	30	0	100	1.00	
	45	0	100	1.00	
		Re-equilibration			
	50	30	70	1.00	
	65	30	70	1.00	
4	Start	20	80[a]	1.00	II
	25	20	80	1.00	
	50	0	100	1.00	
	70	0	100	1.00	
		Re-equilibration			
	75	20	80	1.00	
	90	20	80	1.00	
5	Start	20	80	1.00	II
	15	20	80	1.00	
	25	10	90	1.00	
	50	0	100	1.00	
	70	0	100	1.00	
		Re-equilibration			
	75	20	80	1.00	
	90	20	80	1.00	

[a] Mobile phase methanol.

aromatic compounds and long-chain aliphatic substituted aromatics. These compounds could not be measured using GC.

For studying the group-type fractions of crude oil, we analysed the crude oils on a preparative NH_2 column [14] and collected the five different fractions (see Fig. 1). The zero fraction (0) contains aliphatic compounds that can easily be

Table 3
HPLC retention times of monoaromatic model compounds

Substance	No. of substituents	No. of carbon atoms	Retention time (min)
Benzene	0	6	3.96
Toluene	1	7	4.74
Ethylbenzene	1	8	5.60
p-Xylene	2	8	5.72
Isopropylbenzene	1	9	6.55
1,2,3-Trimethylbenzene	3	9	6.79
o-Ethyltoluene	2	9	6.84
m-Ethyltoluene	2	9	7.19
p-Ethyltoluene	2	9	7.19
1,2,4-Trimethylbenzene	3	9	7.19
n-Propylbenzene	1	9	7.27
1,3,5-Trimethylbenzene	3	9	7.56
tert.-Butylbenzene	1	10	7.84
o-Diethylbenzene	2	10	8.43
1,2,3,4-Tetramethylbenzene	4	10	8.54
p-Isopropyltoluene	2	10	8.68
sec.-Butylbenzene	1	10	8.73
m-Diethylbenzene	2	10	8.82
p-Diethylbenzene	2	10	8.91
1,2,3,5-Tetramethylbenzene	4	10	8.96
1,2,4,5-Tetramethylbenzene	4	10	8.96
Isobutylbenzene	1	10	9.12
n-Butylbenzene	1	10	9.45
p-tert.-Butyltoluene	2	11	10.03
Pentamethylbenzene	5	11	10.61
2,2-Dimethylpropylbenzene	1	11	10.85
4-Methylbutylbenzene	1	11	11.32
1,3-Diisopropylbenzene	2	12	11.75
5-*tert*-.Butyl-*m*-xylene	3	12	11.75
n-Pentylbenzene	1	11	11.87
1,4-Diisopropylbenzene	2	12	12.11
Hexamethylbenzene	6	12	12.38
1,2,4-Triethylbenzene	3	12	12.39
1,3,5-Triethylbenzene	3	12	12.68
n-Hexylbenzene	1	12	14.37
1,4-Di-*tert.*-butylbenzene	2	14	14.64
3,5-Di-*tert.*-butyltoluene	3	15	15.89
1,3,5-Triisopropylbenzene	3	15	16.31
n-Heptylbenzene	1	13	17.00
1,3,5-Tri-*tert.*-butylbenzene	3	18	19.33
1,2,4,5-Tetraisopropylbenzene	4	18	19.35
n-Octylbenzene	1	14	19.58
n-Nonylbenzene	1	15	22.12
n-Decylbenzene	1	16	24.43
n-Dodecylbenzene	1	18	28.34

Column, C_{18} phase (125 mm × 4.0 mm I.D.); particle size, 5 μm; mobile phase, water–acetonitrile (see Table 2, method 1).

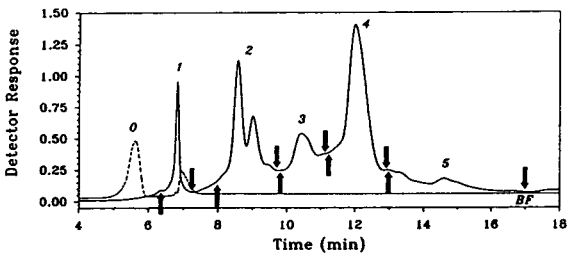

Fig. 1. Preparative HPLC of crude oil A dissolved in chloroform and filtered with a 0.25-μm filter. A 250-μl volume of the solution was injected. HPLC conditions are given in the text and Table 1. Solid line, UV detection (254 nm); dotted line, RI detection. ↑, Start of collecting the fraction; ↓, end of collecting the fraction.

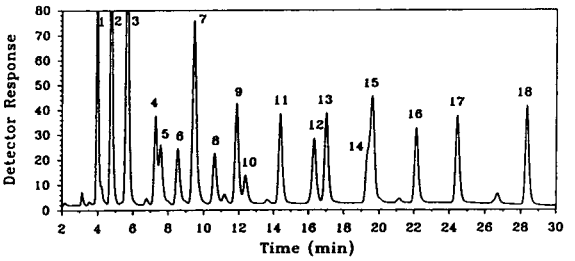

Fig. 2. HPLC of the monoaromatic model compounds. Solvent, methanol. A 10-μl volume of the solution was injected. Peaks: 1 = benzene; 2 = toluene; 3 = xylene and ethylbenzene; 4 = *n*-propylbenzene; 5 = 1,3,5-trimethylbenzene; 6 = 1,2,3,4-tetramethylbenzene; 7 = *n*-butylbenzene; 8 = pentamethylbenzene; 9 = *n*-pentylbenzene; 10 = hexamethylbenzene; 11 = *n*-hexylbenzene; 12 = 1,3,5-triisopropylbenzene; 13 = *n*-heptylbenzene; 14 = 1,3,5-tri-*tert.*-butylbenzene; 15 = *n*-octylbenzene; 16 = *n*-nonylbenzene; 17 = *n*-decylbenzene; 18 = *n*-dodecylbenzene. HPLC method 1 (see test and Table 2). UV detection at 254 nm.

determined by GC. The separation of this fraction has been published previously [14]. The first fraction (1) isolated in this work contains monoaromatic compounds, the second (2) contains diaromatic substances, the third (3) has a maximum amount of heteroaromatic compounds and the fourth (4) and the fifth (5) contain three- and four-ring aromatic hydrocarbon compounds [14].

For better reproducibility of the results, we collected the whole fractions manually as indicated in Fig. 1. The eluent was removed from these fractions carefully under vacuum to minimize the loss of compounds during the drying process.

Because in each fraction compounds with different chain length and substitution are present [5,14], we first investigated the chromatographic behaviour of some standard compounds. Table 3 gives retention data for some standard monoaromatic compounds along with the number of substituents and total number of carbon atoms (N_C). The HPLC traces of the substances are given in Figs. 2 and 3.

Most of the standard compounds are well separated. There is a noticeable substituent dependence of the retention time. The *ortho*-substituted compounds elute earlier than the corresponding *meta*- and *para*-substituted compounds. The straight-chain alkyl-substituted compounds elute later than most of the compounds having the same carbon number (see C_4-substituted benzene, e.g., tetra-, *sec.*-, iso- and *n*-butylbenzene all with $N_C = 10$). Similarly, *n*-octylbenzene ($N_C = 14$) elutes even later than 1,3,5-tri-*tert.*-butylbenzene and 1,2,4,5-tetraisopropylbenzene (both $N_C = 18$).

These few examples make it clear that the identification of all compounds present in a crude oil fraction just by comparing the retention times of the standard compounds is not possible. Even HPLC–MS would have problems in identifying hundreds of these compounds. For this

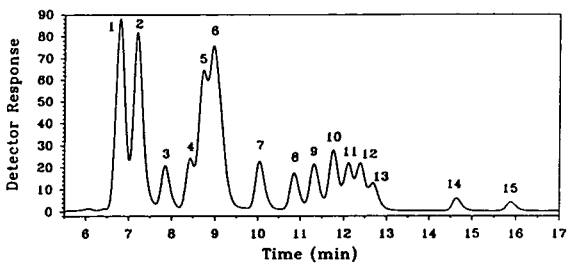

Fig. 3. HPLC of the monoaromatic model compounds. Solvent, methanol. A 10-μl volume of the solution was injected. Peaks: 1 = *o*-ethyltoluene; 2 = *m*-+*p*-ethyltoluene; 3 = *tert.*-butylbenzene; 4 = *o*-diethylbenzene; 5 = *sec.*-butylbenzene; 6 = *m*-+*p*-diethylbenzene; 7 = *p*-*tert.*-butyltoluene; 8 = 2,2-dimethylpropylbenzene; 9 = 3-methylbutylbenzene; 10 = 1,3-diisopropylbenzene; 11 = 1,4-diisopropylbenzene; 12 = 1,2,4-triethylbenzene; 13 = 1,3,5-triethylbenzene; 14 = 1,4-di-*tert.*-butylbenzene; 15 = 3,5-di-*tert.*-butyltoluene. HPLC method 1 (see text and Table 2). UV detection at 254 nm.

reason, we did not make any attempt to identify and quantify the peaks from crude oil fractions.

Our goal was to show the qualitative differences in crude oil fractions. Fig. 4 shows the differences in the compositions of a diesel fuel and two crude oils regarding monoaromatic compounds. We believe that each peak present in the chromatogram does not represent a single compound but contains many different substituted compounds.

Similarly, Figs. 5–8 show the differences for the two- three- and four-ring aromatic compounds and for the heteroaromatic compounds present in diesel fuel and in both crude oils. Fig. 6 shows the differences in the polar aromatic content of the samples. The diesel fuel contains, as mentioned above, about 1% of sulphur, crude oil A has 2.7% and crude oil B about 1.8% of sulphur. Fig. 6 includes not only the sulphur heteroaromatic compounds but also oxygen heteroaromatic compounds [28].

The preparative HPLC traces of diesel fuel, crude oil A and crude oil B do not differ very much (data not shown). On the other hand, the RP-HPLC traces (see Figs. 4–8) show substantial differences.

Fig. 4 shows, as expected, that not very many monoaromatic compounds are present in crude oils, compared with diesel fuel. The loss of short-chain substituted monoaromatic compounds is high because they are volatile (the oils used were not fresh oils). Diesel fuel is a distillation product, so it is rich in monoaromatic compounds.

It is worth mentioning that crude oil A is a so-called "heavy oil". This is also evident from Figs. 5–8. There are few peaks present in the shorter retention time region as compared with the diesel fuel and crude oil B, which indicates the absence of low-molecular-mass compounds.

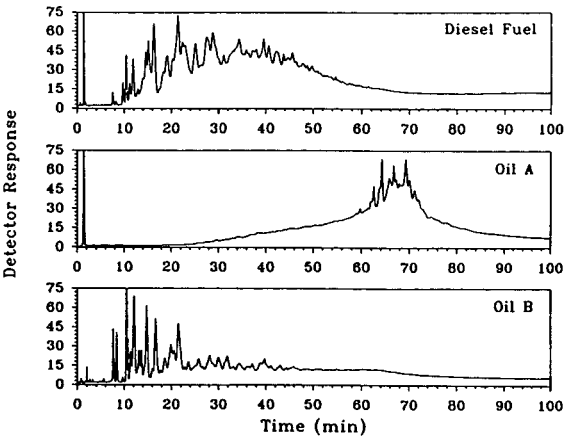

Fig. 5. HPLC of the second preparative fraction (two-ring aromatic compounds). Solvent, methanol. A 25-μl volume of the solution was injected. HPLC method 2 (see text and Table 2). UV detection at 254 nm.

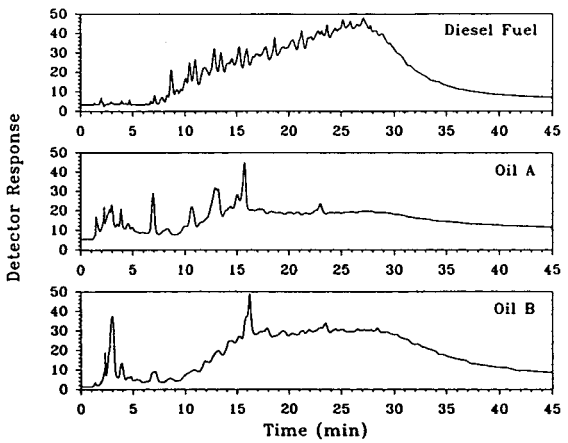

Fig. 4. HPLC of the first preparative fraction (monoaromatic compounds). Solvent, methanol. A 25-μl volume of the solution was injected. HPLC method 1 (see text and Table 2). UV detection at 254 nm.

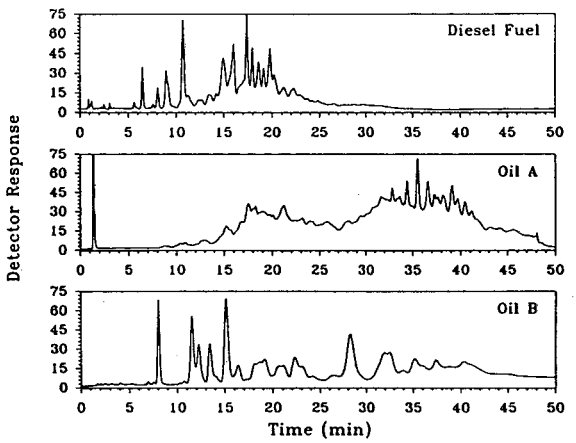

Fig. 6. HPLC of the third preparative fraction (heteroaromatic compounds). Solvent, methanol. A 25-μl volume of the solution was injected. HPLC method 3 (see text and Table 2). UV detection at 254 nm.

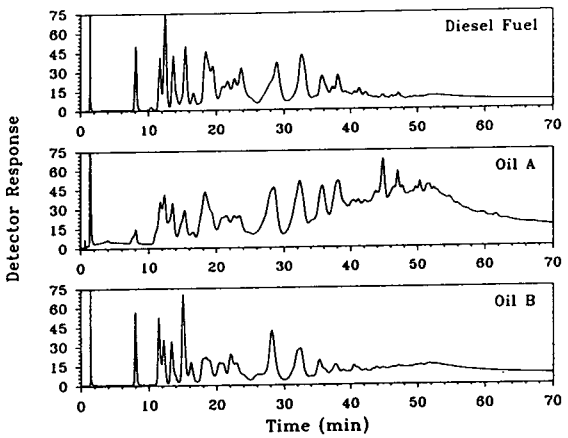

Fig. 7. HPLC of the fourth preparative fraction (three-ring aromatic compounds). Solvent, methanol. A 25-μl volume of the solution was injected. HPLC method 4 (see text and Table 2). UV detection at 254 nm.

It is obvious from the chromatograms that this oil produces more peaks at the higher retention time, which is in agreement with its higher molecular mass compounds.

4. Conclusions

The HPLC methods described allow the detailed separation of crude oils. The results help to characterize a crude oil. The crude oils are preparatively separated into the group types. The preparative chromatograms differ mostly in the peak area and not very much in shape [14]. The RP-HPLC methods with C_{18} and C_{18} PAH columns reflect the physical and chemical properties of the crude oils (molecular mass, contents of heteroaromatic compounds and the chain length of the substituents).

Efforts are in progress to establish a data bank of crude oils characterized with these methods. With the help of this data bank, it would be possible to establish the origin of an unknown crude oil sample, which is important in cases of soil and water pollution with crude oils. On the basis of these results, it should become possible to evaluate the environmentally relevant impact of soil and water contamination with crude oil.

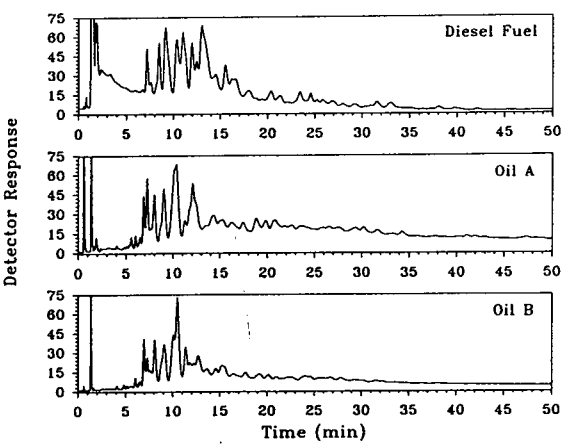

Fig. 8. HPLC of the fifth preparative fraction (four-ring aromatic compounds). Solvent, methanol. A 25-μl volume of the solution was injected. HPLC method 5 (see text and Table 2). UV detection at 254 nm.

References

[1] J.C. Suatoni, H.R. Garber and B.E. Davis, *J. Chromatogr. Sci.*, 13 (1975) 367–371.
[2] J.C. Suatoni and H.R. Garber, *J. Chromatogr. Sci.*, 14 (1976) 546–548.
[3] R.L. Miller, L.S. Ettre and N.G. Johannsen, *J. Chromatogr.*, 264 (1983) 19–32.
[4] J.M. Colin and G. Vion, *J. Chromatogr.*, 280 (1984) 152–158.
[5] M.S. Akhlaq, *Proceedings of the 11. Königsteiner Chromatographietage, Neuss, October 1991*, GIT, Darmstadt, 1991, pp. 392–397.
[6] J.C. Suatoni and R.E. Swab, *J. Chromatogr. Sci.*, 14 (1976) 535–537.
[7] H. Engelhardt, *Erdöl Kohle Erdgas Petrochem.*, 30 (1977) 405–411.
[8] I.L. Davies, K.D. Bartle, G.A. Andrews and P.T. Williams, *J. Chromatogr. Sci.*, 26 (1988) 125–130.
[9] S.C. Lamey, P.A. Hesbach and K.D. White, *Energy Fuels*, 5 (1991) 222–226.
[10] C.S. Hsu and K. Qian, *Energy Fuels*, 7 (1993) 268–272.
[11] N.J. Tate, in G.B. Crump (Editor), *Advances in Analytical Chemistry in the Petroleum Industry 1975–1982; Petroanalysis '81*, Wiley, Chichester, 1982, pp. 268–284.
[12] R.L. Miller, L.S. Ettre and N.G. Johannsen, *J. Chromatogr.*, 259 (1983) 393–412.
[13] P.C. Hayes Jr. and S.D. Anderson, *J. Chromatogr.*, 387 (1987) 333–346.
[14] M.S. Akhlaq, *J. Chromatogr.*, 644 (1993) 253–258.
[15] D. Hoffman and C.E. Wynder, *Chemical Carcinogens (ACS Monograph Series*, No. 173), American Chemical Society, Washington, DC, 1976.

[16] R.D. Harvey (Editor), *Polycyclic Aromatic Hydrocarbons and Carcinogenesis (ACS Monograph Series*, No. 283), American Chemical Society, Washington, DC, 1985.
[17] F. Munari, A. Trisciani, G. Mapelli, S. Trestianu, K. Grob, Jr., and J.M. Colin, *J. High Resolut. Chromatogr. Chromatogr. Commun.*, 8 (1985) 601–606.
[18] H.J. Cortes, B.E. Richter, C.D. Pfeiffer and D.E. Jensen, *J. Chromatogr.*, 349 (1985) 55–61.
[19] S. Coulombe and H. Sawatzky, *Fuel*, 65 (1986) 552–557.
[20] P.R. Fielden and A.J. Packham, *Anal. Chem.*, 62 (1990) 2594–2599.
[21] J.A. Apffel and H. McNair, *J. Chromatogr.*, 279 (1983) 139–144.
[22] C.E. Östman and A.L. Colmsjö, *Fuel*, 68 (1989) 1248–1250.
[23] M.W. Dong, *Int. Labmate*, 18, No. 4 (1993) 21–24.
[24] P.L. Grizzle and J.S. Thomson, *Anal. Chem.*, 54 (1982) 1071–1078.
[25] J. Bundt, W. Herbel, H. Steinhart, S. Franke and W. Francke, *J. High Resolut. Chromatogr.*, 14 (1991) 91–97.
[26] I.L. Davies, M.W. Raynor, P.T. Williams, G.E. Andrews and K.D. Bartle, *Anal. Chem.*, 59 (1987) 2579–2583.
[27] I.L. Davies, K.D. Bartle, P.T. Williams and G.E. Andrews, *Anal. Chem.*, 60 (1988) 204–209.
[28] L.G. Galya and J.C. Suatoni, *J. Liq. Chromatogr.*, 3 (1980) 229–242.

ELSEVIER

Journal of Chromatography A, 677 (1994) 273–278

JOURNAL OF CHROMATOGRAPHY A

High-performance liquid chromatographic determination of dietary fibre in raw and processed carrots☆

A. Redondo*, M.J. Villanueva, M.D. Rodríguez

Departamento de Nutrición y Bromatología II, Facultad de Farmacia, Universidad Complutense, Ciudad Universitaria, 28040-Madrid, Spain

First received 8 September 1993; revised manuscript received 3 April 1994

Abstract

An HPLC method was developed to determine dietary fibre in carrots (*Daucus carota* L.). Primary hydrolysis of dietary fibre residue was performed with 12 *M* H_2SO_4 for 2 h at 40°C and secondary hydrolysis with 0.414 *M* H_2SO_4 for 3 h at 100°C. For the neutralization step prior to injection, AG4-X4 resin (Bio-Rad) was used. Neutral monosaccharides were separated using an HPX-87P column (Bio-Rad). This method was applied for evaluation of the quantitative variation of dietary fibre content in carrots during autoclaving.

1. Introduction

There are several definitions of dietary fibre which differ mainly in the components considered. One of them refers to this component of food as non-starch polysaccharides (NSP) [1]. This definition has been traditionally defended by Englyst and Cummings [1] in terms of providing a clear scope for the analyst: NSP can be clearly measured and are responsible of some physiological effects.

Dietary fibre has been related to some beneficial effects against several diseases, e.g., constipation, diabetes, cancer of the colon and high levels of cholesterol. Some of the mechanisms are not well defined at present, but some others such as absorption of fibre in the foregut, modification of sterol metabolism and caecal fermentation [2] are being elucidated nowadays.

There have been numerous studies on the determination of dietary fibre in carrots by different types of methods, e.g. spectrophotometric, gravimetric and gas chromatographic (GC). HPLC methods for the determination of dietary fibre are very scarce, and the existing ones use refractive index detection. Although cell wall hydrolysates were determined by this technique nearly 20 years ago [3], dietary fibre was not measured by HPLC until some time later. One of the first studies was carried on by Barton et al. [4] and related to the determination of neutral detergent fibre (NDF) in forages. For human food Slavin and Marlett [5] developed an interesting method for the analysis of different kinds of materials. All these HPLC systems

* Corresponding author.

☆ Presented at the symposium *Applications of HPLC and CE in the Biosciences, Verona and Soave, September 7–10, 1993.*

0021-9673/94/$07.00
SSDI 0021-9673(94)00398-S

included refractive index detection and silica, ion-exchange and amino columns.

In this work, we developed a method for the determination of dietary fibre by HPLC that is fundamentally similar to those of Englyst and Cummings [1] and Garleb et al. [6]. We used it to evaluate quantitative changes produced during autoclaving of carrots (*Daucus carota* L.).

2. Experimental

2.1. Equipment

The chromatographic equipment consisted of a Waters chromatograph equipped with a Model 6000 A pump, a U6K injector and a Data Module Model 701 recorder. An Erma ERC-7522 refractive index detector was incorporated (attenuation of sensitivity ×4). A Haake W_{19} water-bath with a Haake D_8 thermostat was used. An HPX-87P column (300 × 7.8 mm I.D.) (Bio-Rad, Richmond, CA, USA) with particle size 9 μm was used. The mobile phase was deionized water filtered through a Millipore membrane (0.45 μm) and degassed in an ultrasonic bath. The optimum temperature was 85°C and the flow-rate was 0.5 ml/min.

2.2. Preparation of sample

Three different lots of carrots were purchased at local markets in Madrid. The samples were peeled in the laboratory and cut into pieces of similar mass. They were separated into three groups and each group was divided into two parts, one of which was kept to be analysed raw and the other was processed. As a result, thermal processing was applied three times to each lot. The conditions of autoclaving were 121°C for 15 min. When thermal treatment was finished, the processed sample and liquid were separated. Raw and processed samples were freeze-dried (Terruzzi Mevilsa TP-3 freeze-drier), homogenized and kept in hermetically closed bottles.

2.3. Procedure

The method is divided into three steps: isolation of dietary fibre residue from the original material, chemical hydrolysis of the residue and neutralization of the hydrolysate for determination of each component by HPLC.

Isolation of dietary fibre residue

The method of Englyst and Cummings [1] was applied, using 300 mg of freeze-dried sample. Starch was dispersed by adding 2 ml of dimethyl sulfoxide (DMSO) and hydrolysed by enzymatic treatment with α-amylase (EC 3.2.1.1) and pullulanase (EC 3.2.1.41) for 16 h. The residue free from starch was washed with ethanol and acetone and then dried.

Chemical hydrolysis of dietary fibre residue

The residue was hydrolysed with 0.3 ml of 12 *M* H_2SO_4 on a hot magnetic plate with stirring for 2 h at 40°C (primary hydrolysis). A volume of 8.4 ml of deionized water was added, followed by stirring for 3 h in a boiling water-bath (secondary hydrolysis).

Neutralization of hydrolysate and chromatographic conditions

An aliquot of 5 ml of hydrolysate was passed through a column of resin (Bio-Rad) 4 cm high and 0.9 cm wide. After the hydrolysate had eluted from the column the latter was washed with 5 ml of deionized water three times. The combined eluates were evaporated to dryness and the residue was dissolved with 2 ml of water. The liquids were filtered through a Millex filter of pore size 0.45 μm and through a Sep-Pak C_{18} cartridge. The purified liquids were kept in a vial and a volume of 75 μl was injected.

Extraction of pectic substances

Galacturonic acid was extracted from freeze-dried samples with hot oxalic acid–ammonium oxalate (pH 4) in two steps following the method described by Dekker and Richards [7].

Determination of galacturonic acid

Pectic substances were measured as galacturonic acid by spectrophotometry using 3,5-dimethylphenol as the chromogenic reagent [8], the method being adapted to carrot samples in our laboratory [9].

3. Results and discussion

Enzymatic treatment for the isolation of a dietary fibre residue free of starch and protein has frequently been studied. In this work, α-amylase and pullulanase were used as highly effective enzymes for starch hydrolysis [1]. In some recent studies [10] the incubation times were drastically reduced owing to the incorporation of Termamyl in the enzymatic treatment in all kinds of food. The elimination of enzymatic treatment in samples with a low proportion of starch has also been proposed [11], because the results obtained were very similar for treated and untreated samples.

In this work, the mass of freeze-dried sample to be used was studied. An amount of 300 mg of carrot proved to give satisfactory results. This is the maximum amount considered in the method for the indicated concentration of enzymes.

For validating the method different assays were carried out and different hydrolysis conditions were compared [12]. Those chosen for the analysis of carrots were applied to standards of cellulose (Sigmacell Type 20) and xylan (Fluka Biochemika), resulting in good recoveries of 91.88 ± 2.50 g/100 g for cellulose and 81.09 ± 2.38 g/100 g for xylan.

An important percentage of unrecovered cellulose corresponds to cellobiose (approximately 6%) and a minor percentage to a different oligosaccharide, probably cellotriose, but unconfirmed owing to lack of a standard [5]. Incomplete hydrolysis of cellulose requires further investigation in order to understand it better. With respect to xylan, the lower recovery obtained is probably due to the important degree of degradation experienced by xylose during secondary hydrolysis. This was clearly revealed during the study of the recovery of monosaccharides in this work and has also been reported by several other workers [5,6,13,14].

Table 1
Monomeric composition of polysaccharides that constitute dietary fibre in raw carrot (g per 100 g dry matter)

Constituent	Mean[a]	R.S.D.[a]
Cellobiose	0.5567	0.5064
Glucose	3.9375	0.1844
Xylose	0.4180	0.0947
Galactose/rhamnose	2.2252	0.1587
Arabinose	1.6330	0.2718
Mannose	0.3546	0.1153
Galacturonic acid	5.1833	0.0868
Total	14.3083	0.0936

[a] $n = 18$.

The resolution of the column was checked using mixtures of standard sugars in different proportions. All the monosaccharides were well separated except rhamnose and galactose, which co-eluted.

It has been reported that the extent of losses of monosaccharides varies depending on the hydrolysis conditions [13]. A solution of standard monosaccharides was treated under selected hydrolysis conditions, obtaining satisfactory recoveries for all the sugars: cellobiose 89.21%, glucose 91.24%, xylose 88.39%, galactose/rhamnose 89.34%, arabinose 95.28% and mannose 98.12%. This assay was carried out in parallel with each batch of samples and the correction

Table 2
Monomeric composition of polysaccharides that constitute dietary fibre in processed carrots (g per 100 g dry matter)

Constituent	Mean[a]	R.S.D.
Cellobiose	0.8123	0.3882
Glucose	5.2812	0.1158
Xylose	0.5399	0.5051
Galactose/rhamnose	3.9278	0.2910
Arabinose	3.3835	0.2773
Mannose	0.4130	0.1770
Galacturonic acid	5.8344	0.1121
Total	20.1921	0.0990

[a] $n = 18$.

Table 3
Comparison of values for monomeric components of dietary fibre in raw and processed carrots (g per 100 g fresh matter)

	Raw				Processed			
	Lot A	Lot B	Lot C	Overall	Lot A	Lot B	Lot C	Overall
Cellobiose	0.037 ± 0.002	0.039 ± 0.002	0.108 ± 0.027	0.061 ± 0.039	0.043 ± 0.007	0.059 ± 0.015	0.069 ± 0.031	0.057 ± 0.014
Glucose	0.449 ± 0.039	0.286 ± 0.020	0.531 ± 0.014	0.422 ± 0.122	0.411 ± 0.065	0.366 ± 0.039	0.347 ± 0.034	0.374 ± 0.032
Xylose	0.044 ± 0.007	0.039 ± 0.002	0.049 ± 0.002	0.044 ± 0.049	0.025 ± 0.005	0.028 ± 0.003	0.061 ± 0.010	0.038 ± 0.020
Galactose/rhamnose	0.247 ± 0.005	0.178 ± 0.012	0.287 ± 0.054	0.237 ± 0.054	0.208 ± 0.003	0.267 ± 0.041	0.353 ± 0.056	0.276 ± 0.071
Arabinose	0.168 ± 0.020	0.113 ± 0.015	0.248 ± 0.048	0.176 ± 0.066	0.214 ± 0.032	0.194 ± 0.032	0.308 ± 0.041	0.238 ± 0.059
Manose	0.033 ± 0.003	0.033 ± 0.003	0.047 ± 0.002	0.038 ± 0.008	0.036 ± 0.005	0.027 ± 0.005	0.026 ± 0.005	0.030 ± 0.005
Galacturonic acid	0.551 ± 0.025	0.514 ± 0.037	0.571 ± 0.044	0.545 ± 0.029	0.471 ± 0.017	0.425 ± 0.014	0.347 ± 0.034	0.414 ± 0.061

Results are mean values ± standard deviations ($n = 6$), corresponding to three processings in duplicate applied to each lot of carrot.

factors obtained in each instance were applied to the sample.

The efficacy of the extraction of pectic substances with oxalic acid–ammonium oxalate was tested and satisfactory results were obtained [15]. The accuracy, precision and inteferences with neutral sugars were also tested. 3,5-Dimethylphenol gave a better sensitivity and selectivity than *m*-phenylphenol, frequently used in the determination of galacturonic acid [9].

Dietary fibre of raw and processed carrots was characterized by HPLC and a spectrophotometric method. Mean values corresponding to the three lots and general statistics are summarized in Tables 1 and 2. The component monosaccharides were expressed as polysaccharides (×0.88 pentoses; ×0.90 hexoses and galacturonic acid and ×0.95 cellobiose). Results are expressed in grams per 100 g of dry matter.

Table 1 shows that glucose is the major monosaccharide in raw carrot samples, followed by galactose/rhamnose, arabinose, cellobiose, xylose and mannose. Galacturonic acid is the most representative monomer in the dietary fibre fraction in this product.

The results for processed carrot samples, summarized in Table 2, show that the values for different sugars are higher than in the raw product. However, the order of quantitative importance is maintained: glucose, galactose/rhamnose, arabinose, cellobiose, xylose and mannose. Galacturonic acid is, as in raw product, the most representative monomer.

Studying both materials (grams per 100 g dry matter) and calculating the proportion of each sugar in NSP, the increase observed in each sugar could be explained in terms of the different nature of raw and processed materials. If the sum of all sugars plus galacturonic acid is considered (NSP), the distribution of each component in both materials is as follows: glucose, raw 27.52% and processed 26.15%; galactose/rhamnose, raw 15.55% and processed 19.45%; arabinose, raw 11.41% and processed 16.76%; cellobiose, raw 3.89% and processed 4.02%; xylose, raw 2.92% and processed 2.67%; mannose, raw 2.48 and processed 2.04%; and galacturonic acid, raw 36.23% and processed 28.89%.

The comparative distribution of monomers shows that galacturonic acid is the main component in both raw and processed carrots, but in the latter the proportion of galacturonic acid has diminished in relation to the unprocessed material, giving a large increase in the proportion of galactose/rhamnose and arabinose.

For studying the influence of thermal treatment on carrots, the results are expressed in grams per 100 g of fresh matter (Table 3). Losses of soluble solids during processing result in an increase in the concentration of insoluble components. Among the soluble compounds is galacturonic acid, which is the most abundant monomer of pectic polysaccharides. This explains why this monomer did not experience the same increase as neutral monosaccharides. To establish a correct comparison with the results for processed samples, a correction factor was applied to avoid errors due to the losses of soluble solids mentioned above.

The experimental design developed to study modifications in carrots during processing allows statistical treatment with the analysis of variance (ANOVA) test to determine significant differences that could be attributed to the autoclaving conditions. Although some differences were observed when comparing raw and processed material in each lot, these were not statistically significant (level of significance, $\alpha = 0.05$) because they are small and the different characteristics of each lot of material should be considered. From a quantitative point of view no statistical differences were observed when the global mean value for raw material was compared with the global mean value for processed material in any monosaccharide. For galacturonic acid the differences observed were statistically significant ($\alpha = 0.05$). This component is solubilized during autoclaving of carrots. Similar results were found by Waldron and Selvendran [16] during boiling of other vegetables. The monosaccharide fraction of NSP of carrots remained unmodified during processing under the conditions mentioned above and the value of NSP considered as the sum of monosaccharides plus galacturonic acid did not experience any variation as a result of autoclaving.

Other workers did not find any difference in cooked or tinned carrots using a GC method for the determination of monosaccharides and a spectrophotometric method for the determination of galacturonic acid [17].

The HPLC method developed here for dietary fibre determination is rapid and easy to perform and gives good results for samples with different amounts of monomeric components of NSP. This method shows no statistically significant changes in dietary fibre during autoclaving of carrots.

References

[1] H.N. Englyst and J.H. Cummings, *J. Assoc. Off. Anal. Chem.*, 71 (1988) 808.
[2] M.A. Eastwood and E.R. Morris, *Am. J. Clin. Nutr.*, 55 (1990) 436.
[3] E.C. Conrad and J.K. Palmer, *Food Technol.*, October (1976) 84.
[4] F.E. Barton, W.R. Windham and D.S. Himmelsbach, *J. Agric. Food Chem.*, 34 (1982) 1119.
[5] J.L. Slavin and J.A. Marlett, *J. Agric. Food Chem.*, 31 (1983) 467.
[6] K.A. Garleb, L.D. Bourquin and G.C. Fahey, Jr., *J. Agric. Food Chem.*, 37 (1989) 1287.
[7] R.F.H. Dekker and G.N. Richards, *J. Sci. Food. Agric.*, 23 (1972) 475.
[8] R.W. Scott, *Anal. Chem.*, 51 (1979) 936.
[9] M.D. Rodríguez, A. Redondo and M.J. Villanueva, *Alimentaria*, 232 (1992) 79.
[10] H.N. Englyst, M.E. Quigley, G.J. Hudson and J.H. Cummings, *Analyst*, 117 (1992) 1707.
[11] B.W. Li and M.S. Cardozo, *J. AOAC Int.*, 45 (1992) 372.
[12] M^a.D. Rodríguez, A. Redondo and M^a.J. Villanueva, in D.A.T. Southgate, K. Waldron, I.T. Johnson and G.R. Fenwick (Editors), *Dietary Fibre: Chemical and Biological Aspects*, Royal Society of Chemistry, Cambridge, 1990, Part 3, p. 130.
[13] J.H. Sloneker, *Anal. Biochem.*, 43 (1971) 539.
[14] R.R. Selvendran, J.F. March and S.G. Ring, *Anal. Biochem.*,, 96 (1979) 282.
[15] M.J. Villanueva, A. Redondo and M.D. Rodríguez, *Anal. Bromatol.*, 42 (1990) 57.
[16] K.W. Waldron and R.R. Selvendran, in D.A.T. Southgate, K. Waldron, I.T. Johnson and G.R. Fenwick (Editors), *Dietary Fibre: Chemical and Biological Aspects*, Royal Society of Chemistry, Cambridge, 1990, Part 2, p. 44.
[17] H.N. Englyst, S.A. Bingham, S.A. Runswick, E. Collinson and J.H. Cummings, *J. Hum. Nutr. Diet.*, 1 (1988) 247.

ELSEVIER

Journal of Chromatography A, 677 (1994) 279–288

JOURNAL OF CHROMATOGRAPHY A

Two-step chromatographic procedure for the purification of hen egg white ovomucin, lysozyme, ovotransferrin and ovalbumin and characterization of purified proteins

A.C. Awadé[a,*], S. Moreau[a,b], D. Mollé[a], G. Brulé[b], J.-L. Maubois[a]

[a]*Laboratoire de Recherches et de Technologie Laitière, Institut National de la Recherche Agronomique, 65 Rue de St.-Brieuc, 35042 Rennes Cedex, France*

[b]*Laboratoire de Technologie Alimentaire, Ecole Nationale Supérieure d'Agronomie, 65 Rue de St.-Brieuc, 35042 Rennes Cedex, France*

First received 24 February 1994; revised manuscript received 25 March 1994

Abstract

An improved procedure is described involving gel permeation and anion-exchange chromatography for the purification of four major hen egg white proteins. The procedure involves a first-step purification of ovomucin and lysozyme by gel permeation on a Superose 6 Prep Grade column. In the second step, anion-exchange chromatography on Q Sepharose Fast Flow led to the isolation of ovotransferrin and ovalbumin from a gel permeation chromatographic peak. The purities were estimated as *ca.* 80, 100, 80 and 100% for ovomucin, lysozyme, ovotransferrin and ovalbumin, respectively. The purification yield was over 60% for each protein. Further characterization of purified lysozyme revealed that it was fully active and homogeneous in relation to the electrospray ionization mass spectrum. The electrospray ionization mass spectrum showed different ovotransferrin species. The amino acid composition of purified ovomucin was compared to those published previously.

1. Introduction

In the last 10 years, egg production in industrialized countries has remained almost constant. The value of egg components is becoming increasingly necessary for the poultry product industry. With this in view, the isolation and purification of such components, particularly proteins, appears to be promising.

Over two decades, different methods [1] including protein precipitation by salts or by ionic strength reduction and liquid chromatography have been developed for purifying major egg white proteins. Almost all of these procedures were affected by the lack of emphasis on the importance of the co-product resulting from each step.

In this paper, we discuss a serial procedure that allows the purification of four major egg white proteins: ovalbumin (*ca.* 54% of egg white), ovotransferrin (*ca.* 13%), lysozyme (*ca.* 3.5%) and ovomucin (*ca.* 1.5%). Ovomucin is a highly polymerized glycoprotein with a molecular mass (M_r) ranging between *ca.* $0.22 \cdot 10^6$ and $270 \cdot 10^6$, depending on the sample preparation conditions [2]. This protein is assumed to play a

* Corresponding author.

0021-9673/94/$07.00
SSDI 0021-9673(94)00401-T

preponderant role in the structure of the egg white, and is largely implicated in its foaming properties [3]. It has been proposed by Van Boeckel [4] as a possible source of glycopeptides and oligosaccharides for antibiotic preparations. The function of ovotransferrin is generally accepted to be that of iron transport. This glycoprotein with $M_r \approx 78\,000$ can also exhibit antimicrobial activity [5,6]. Lysozyme ($M_r = 14\,300$) is an enzyme (EC 3.2.1.17) that is used in the food and pharmaceutical industries [7] on account of its antimicrobial activity. Ovalbumin, which constitutes over half of the egg white proteins by mass, is a glycoprotein with $M_r \approx 45\,000$. This protein presents functional properties in egg white that are related to foaming and gelling. Although no biological function has been proposed for ovalbumin, its role in the immunological and allergenic properties of egg white has been investigated [1]. Moreover, this protein can be assumed to be useful in nutrition.

The object of our work is to purify a maximum number of proteins from the same sample. The procedure presented here includes gel permeation and anion-exchange chromatography and it was tried out on a laboratory scale. The activity of the purified lysozyme was determined and the amino acid composition of the ovomucin was compared with those published previously. Moreover, purified lysozyme and ovotransferrin were characterized by electrospray mass-spectrometry.

2. Experimental

2.1. Materials and reagents

The system for sample concentration, Amicon 8200, Centricon-3 and Centriprep-3, was obtained from Amicon (Epernon, France). A Superose 6 HR 10/30 column was purchased from Pharmacia Biotechnology (St.-Quentin-Yvelines, France). Reference lysozyme, ovotransferrin, ovomucoid, ovalbumin and *Micrococcus lysodeikticus* cells were obtained from Sigma (L'Isle d'Abeau Chenes, France). Superose 6 Prep Grade, Q Sepharose Fast Flow and protein M_r markers were supplied by Pharmacia Biotechnology. All other reagents were of analytical-reagent grade.

2.2. Egg white preparation

Egg white was diluted with 2 volumes of 0.05 *M* Tris–HCl (pH 9) containing 0.4 *M* NaCl and 10 m*M* β-mercaptoethanol and gently stirred overnight.

2.3. Lysozyme activity assay

Lysozyme activity was determined by the turbidimetric method as proposed by Weaver *et al.* [8].

2.4. Amino acid composition

Amino acid composition was determined as described by Spackman *et al.* [9] using a Pharmacia–LKB (Alpha Plus) analyser. Protein samples (1–2 mg) were dried and hydrolysed under vacuum in 6 *M* HCl for 24, 48 or 96 h at 110°C. In order to determine cysteine and methionine residues, protein samples were first subjected to performic acid oxidation and then hydrolysed at 110°C in 6 *M* HCl according to Moore [10].

2.5. Other methods

Protein determination

Protein concentrations were determined according to the method of Bradford [11], using the Bio-Rad protein assay with bovine serum albumin as standard.

Polyacrylamide gel electrophoresis

Sodium dodecyl sulfate polyacrylamide gel electrophoresis (SDS-PAGE) was performed according to Laemmli [12], using 7.5% or 15% separation gels and 4% stacking gel containing 0.1% SDS. Protein bands were stained with Coomassie Brilliant Blue.

Analytical chromatography

Isolated fractions were rechromatographed on a TSK-G3000 SW gel permeation column

(Supelco, St.-Germain-en-Laye, France) using 0.01 *M* sodium phosphate buffer (pH 2.4) containing 0.2 *M* NaCl as the eluent. The ovomucin fraction was analysed at pH 7 instead of pH 2.4. The flow-rate was 0.4 ml/min.

Electrospray mass spectrometry

Electrospray mass spectrometry was conducted with a single-quadripole mass spectrometer (API I; Sciex, Toronto, Canada) equipped with an atmospheric-pressure ionization ion source (ion spray). Sample solutions (diluted in water containing 0.1% trifluoroacetic acid), delivered to the sprayer by a syringe infusion pump (generally at a flow-rate of 5 μl/min), were sprayed through a stainless-steel capillary held at a high voltage between +5 and +5.2 kV. The concentrations of the samples were *ca.* 56 μM for lysozyme and 20 μM for ovotransferrin. Solutions were sprayed at 55°C. The liquid nebulization was aided by a coaxial air flow along the sprayer, the nebulizer pressure being adjusted between 0.3 and 0.4 MPa. The interface between the sprayer and the mass analyser consisted of a conical orifice of 100 μm I.D.; the potential on the orifice was 100 V. A gas curtain formed of a continuous nitrogen flow was used in the interface to break up the ion cluster formation. The instrument was calibrated with ammonium adduct ions of polypropylene glycols (PPG) [13]. The unit resolution was maintained across the entire mass range for singly charged PPG calibrant ions, according to the 55% valley definition.

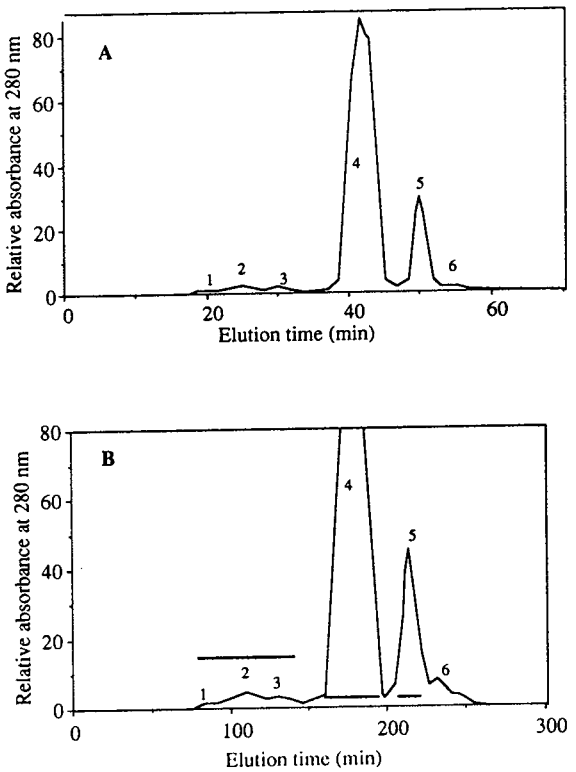

Fig. 1. (A) Chromatography of hen egg white proteins on a Superose 6 HR column (30 × 1 cm I.D.): 100 μl of the egg white preparation containing *ca.* 6 mg of protein were applied to the column previously adjusted with 0.05 *M* Tris–HCl buffer (pH 9) containing 0.2 *M* NaCl, using the Pharmacia FPLC system at room temperature. Proteins were eluted with the same buffer at a flow-rate of 0.4 ml/min. (B) Chromatography of hen egg white proteins on a Superose 6 Prep Grade column (90 × 2.6 cm I.D.), using 0.05 *M* Tris–HCl buffer (pH 9) containing 0.02 *M* NaCl: 10 ml of egg white preparation containing *ca.* 615 mg of proteins were loaded on the column and protein elution was performed at a flow-rate of 2 ml/min.

3. Results and discussion

3.1. Gel permeation chromatography allowing simultaneous isolation of ovomucin and lysozyme

Preliminary experiments on the fractionation of egg white proteins were carried out using a Superose 6 HR column (30 × 1 cm I.D.). As shown in Fig. 1A, six major chromatographic peaks (1–6) were obtained from the whole egg white sample. Aliquots of preparations containing reference proteins from Sigma were subsequently added to egg white sample before loading on the column. This indicated that peak 4 may contain ovalbumin, ovotransferrin and ovomucoid as major proteins, while lysozyme may be present in peak 5. According to its M_r (see above), we assumed that ovomucin was eluted in either peak 1, 2 or 3. Subsequent preparative-scale experiments were performed on a 90 × 2.6 cm I.D. Superose 6 Prep Grade column using the same fast protein liquid chro-

matographic (FPLC) system at room temperature. As shown in Fig. 1B, the chromatographic protein profile was similar to that obtained with the smaller column. Each peak was recovered and concentrated by gel filtration. SDS-PAGE analysis of peaks 1, 2 and 3, taken separately (data not shown), revealed that the principal polypeptides present corresponding to those previously reported for ovomucin [14]. Therefore, in further experiments, the three fractions were pooled. However, for other experiments it may be interesting to study these fractions separately, e.g., in order to determine their actual composition. Thus, SDS-PAGE analysis (Fig. 2) of different fractions revealed that the pool of proteins contained in peaks 1, 2 and 3 essentially correspond to ovomucin that was contaminated with small amounts of polypeptides corresponding to ovalbumin and ovotransferrin. This analysis also showed that peak 4, which contains the largest amount of proteins, is mainly composed of polypeptides corresponding to ovalbumin and ovotransferrin. The polypeptide band obtained from the peak 5 corresponded to that of lysozyme. The recovery of ovomucin in three different adjacent peaks may be explained by the different degrees of polymerization of this protein. Indeed, it has been shown by gel filtration that native ovomucin exhibited different apparent M_r in relation to its elution profile on Sepharose 4B [15].

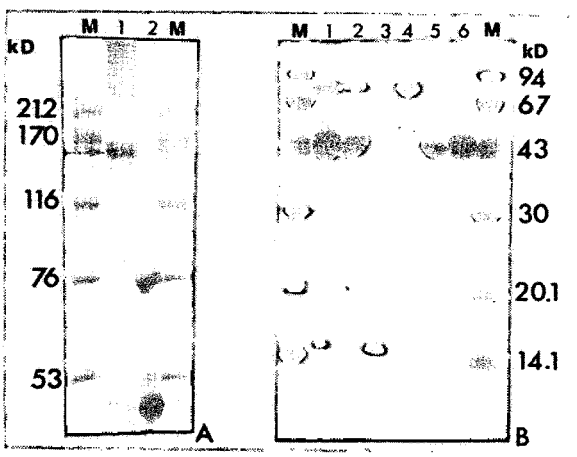

Fig. 2. (A) SDS-PAGE (7.5%) of egg white proteins (100 μg) (lane 2) and proteins (40 μg) contained in the pooled fractions from gel permeation peaks 1, 2 and 3 (see Fig. 1). The arrow indicates a protein band that may contain ovomucin and ovostatin subunits. (B) SDS-PAGE (15%) of egg white proteins (100 μg) (lane 1), and proteins contained in peak 4 from gel permeation (40 μg) (lane 2), peak 5 from gel permeation (5 μg) (lane 3), peak A from Q Sepharose Fast Flow (see Fig. 4) (10 μg) (lane 4), peak B from Q Sepharose Fast Flow (10 μg) (lane 5) and peak C from Q Sepharose Fast Flow (40 μg) (lane 6). M denotes M_r markers kD = kilodalton.

The purity of the fractions corresponding to ovomucin and lysozyme was further investigated with an analytical gel permeation column (TSK-G 3000 SW) using an HPLC system. As shown in Fig. 3, lysozyme was purified to homogeneity. However, the ovomucin fraction was purified only to *ca.* 80% if we assume that it was contaminated with ovostatin (see below). Other workers have isolated ovomucin from egg white by adding egg white slowly to three volumes of water and adjusting the pH to 6 [15,16]. This procedure had the advantage of being rapid and applicable in industry. However, it was difficult to resolubilize the ovomucin obtained. In addition, the ovomucin obtained by this procedure was contaminated with lysozyme, which interacts with ovomucin at low pH and ionic strength [15,16]. Conversely, no contamination with lysozyme was observed in the ovomucin prepared in our laboratory by gel permeation. However, the ovomucin preparation may be contaminated with ovostatin if we refer to the M_r of this protein (780 000) [17]. Our supposition is strengthened by the studies of Nagase *et al.* [17] on the purification of ovostatin by a procedure including gel filtration. This may be confirmed unambiguously, for example, by Western blot experiments, using antibodies raised against ovostatin. The ovomucin we prepared can be used more easily for further studies as it is soluble. Gel permeation was previously used by Young and Gardner [18] to purify soluble ovomucin from egg white. However, their fractions were less separated than ours. They showed that another peak was included in the ovomucin peak from total egg white, using chromatographic analysis of ovomucin-depleted egg white; in our opinion, this peak may correspond to ovostatin. Gel permeation has also

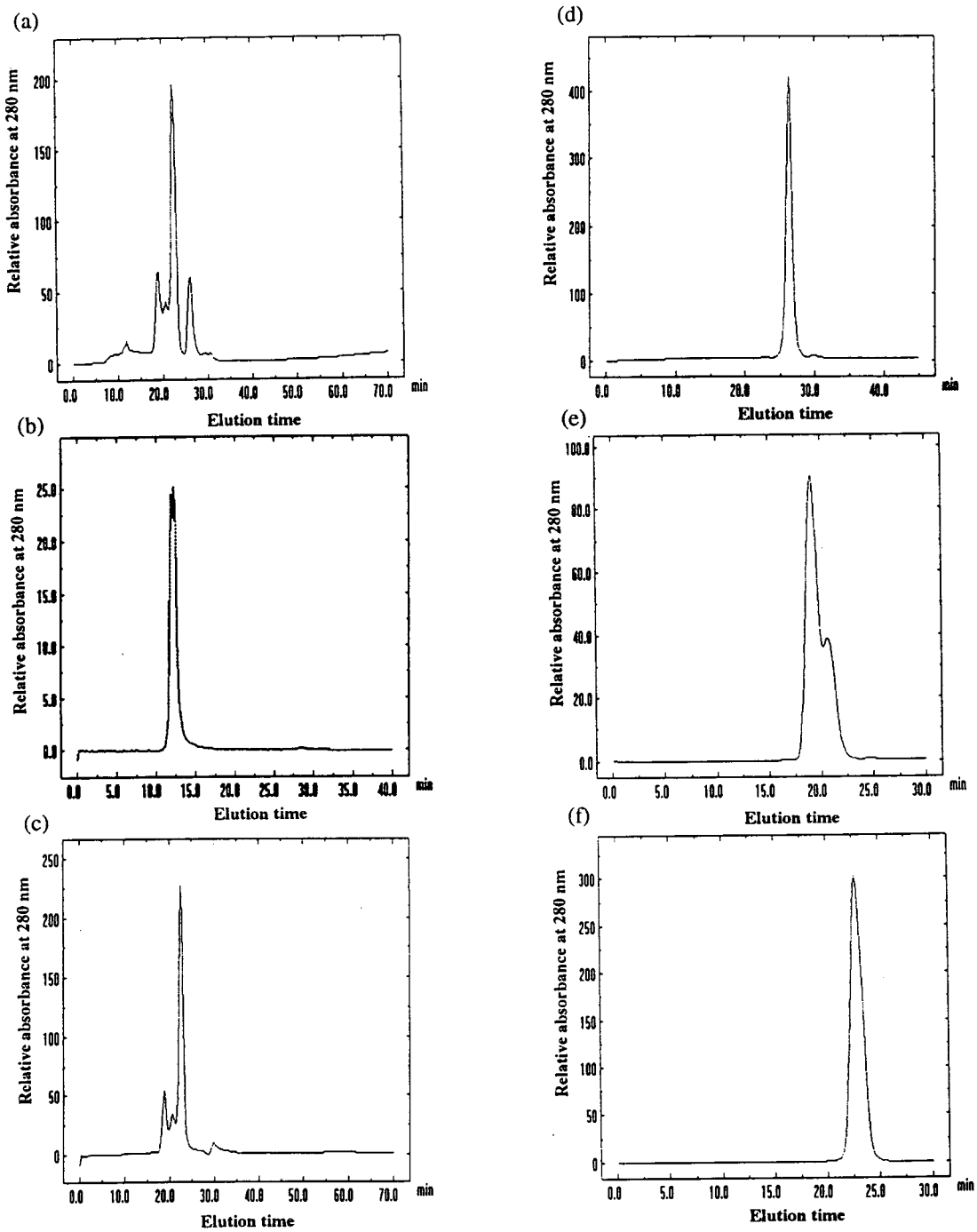

Fig. 3. Rechromatography using a TSK-G3000 SW gel filtration column (see Experimental) of fractions eluted from Superose 6 Prep Grade gel permeation column (see Fig. 1) or fractions eluted from Q Sepharose Fast Flow (see Fig. 2). (a) Whole egg white; (b) ovomucin fractions (peaks 1, 2 and 3 from gel permeation); (c) proteins contained in peak 4 from gel permeation; (d) lysozyme fraction (peak 5 from gel permeation); (e) ovotransferrin fraction (peak A from the anion-exchange column); (f) ovalbumin fractions (peak B or C from the anion-exchange column).

been used for the isolation of lysozyme [19]. However, to our knowledge, this is the first report on the simultaneous purification of ovomucin and lysozyme by gel permeation chromatography.

Protein quantification assay showed that from *ca.* 615 mg of total egg white protein, *ca.* 9 mg of ovomucin and 14 mg of lysozyme were isolated in one step; *ca.* 520 mg of protein were recovered in peak 4. The purification yields were estimated to be *ca.* 80% for ovomucin and 70% for lysozyme.

3.2. Purification of ovotransferrin and ovalbumin by using an anion-exchange column

Following the serial purification procedure, the proteins present in gel filtration peak 4 (see above) were pooled, concentrated, dialysed against 0.05 *M* Tris–HCl buffer (pH 9) and chromatographed on a Q-Sepharose Fast Flow column (Table 1). As shown in Fig. 4, the elution profile revealed three major peaks whose aspect suggests that they contain several proteins. SDS-PAGE analysis of proteins contained in these peaks indicated that the ovotransferrin protein band ($M_r \approx 78\,000$) (in peak A) was contaminated by a protein band with $M_r \approx$ 50 000. This protein band may contain at least one of the two minor glycoproteins with $M_r =$ 52 000, recently isolated from hen egg white by heparin affinity chromatography by Itoh *et al.* [20]. Peaks B and C contain only ovalbumin. Hence it is noteworthy that two distinct peaks of ovalbumin were separated in our procedure. The form contained in peak B may correspond to the S-ovalbumin that comes from a conversion of ovalbumin during storage [21,22]. This may be verified by heat-stability studies on ovalbumins recovered in the two peaks. It has been shown that S-ovalbumin was more heat stable than ovalbumin [23]. Kurisakai *et al.* [24] concluded that as there was no difference in the electrophoretic and ion-exchange chromatographic profiles of fresh and stored ovalbumin, the increased heat stability of S-ovalbumin could not be explained by an increase in net negative charge. The fact that two chromatographic peaks of ovalbumin (one probably corresponding to S-ovalbumin) were obtained in our procedure by anion-exchange chromatography may lead to a revision of this statement. Rechromatography of fractions from Q Sepharose Fast Flow as shown in Fig. 4 indicated that ovalbumin fractions were purified near to homogeneity, whereas ovotransferrin was purified to only *ca.* 80% The aspect of the peaks may be due to the heterogeneity in

Table 1
Parameters for the elution of gel permeation peak 4 proteins from Q Sepharose Fast Flow column

Time (min)	A (%)	B (%)
0	100	0
25	100	0
40	60	40
85	60	40
95	55	45
115	55	45
125	50	50
175	50	50
185	45	55
235	45	55
280	0	100

Two buffers, (A) 0.05 *M* Tris–HCl (pH 9) and (B) A containing 0.3 *M* NaCl, were used for increasing stepwise and gradients from 100% A to 100% B. Flow-rate: 7.5 ml/min.

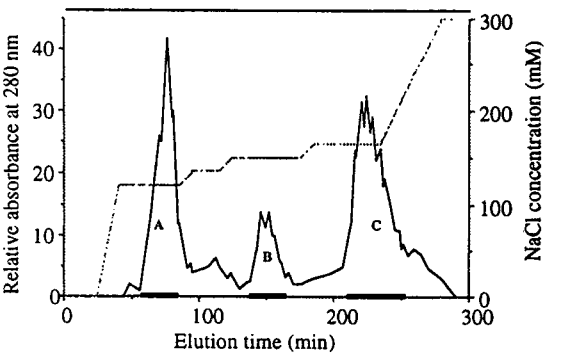

Fig. 4. Chromatography of proteins contained in peak 4 from gel permeation (see Fig. 1) on a Q Sepharose Fast Flow column (10 × 5 cm I.D.). Protein sample was dialysed in 0.05 *M* Tris–HCl buffer (pH 9) (A) and applied to the column previously adjusted with the same buffer. After thoroughly washing the column (25 min) with buffer A the proteins were eluted as presented in Table 1.

ovotransferrin and ovalbumin. That may be related in part to the heterogeneity in glycans bound to the proteins, in the case of ovotransferrin. For ovalbumin, this could be explained by the presence of components that differ in phosphorus content [25–27].

From *ca.* 500 mg of the proteins present in the gel permeation peak 4, *ca.* 91 and 220 mg of proteins were recovered in the ovotransferrin and the ovalbumin peak, respectively. Hence, the final recovery of proteins, according to the theoretical ratios of these proteins in egg white, was estimated to be *ca.* 90% and 66% for ovotransferrin and ovalbumin, respectively.

An anion-exchange column (DE 92) has been used for egg white fractionation, principally to separate ovalbumin [28]. However, proteins were better separated and certainly purer in the present work. Q Sepharose Fast Flow has recently been used by Jacobs *et al.* [29], who studied the selenium contents of the fractions obtained by chromatography of the whole diluted egg white on a column made of this resin. With regard to the chromatographic profiles, their fractions may be less pure than those obtained in this work. For instance, the two ovalbumin peaks were not separated.

3.3. Further characterization of purified proteins

The M_r of purified lysozyme and ovotransferrin were determined by electrospray ionization mass spectrometry (ESI-MS). The mass spectra for lysozyme and ovotransferrin are shown in Figs. 5 and 6, respectively. The average M_r for lysozyme was calculated from five multiply charged molecular ions (Fig. 5, Table 2). The M_r for lysozyme, 14 303.4 (±0.6), is consistent with that expected from the polypeptide chain (14 304.2). The corresponding spectrum revealed that the molecule was homogeneous, although the presence of sodium adducts (mass 14 325.7 ± 0.9) could be observed. Three major species were detected for ovotransferrin. The major population, average M_r 77 513 ± 8.3, calculated from fifteen multiply charged molecular ions, is presented in Fig. 6A, Table 3. The other M_r values of 77 659.4 ± 8.7 and 77 324.2 ± 9.1 were

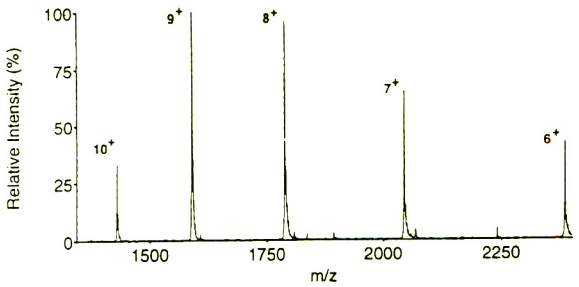

Fig. 5. Electrospray ionization mass spectrum of purified lysozyme; 326 pmol were consumed in acquiring the spectrum. Scan accumulation and mass calculation were performed with Tune 2.3 and Macspec 3.2 programs, respectively. The protonation states are indicated above the peaks. Average M_r: 14 303.4 ± 0.6.

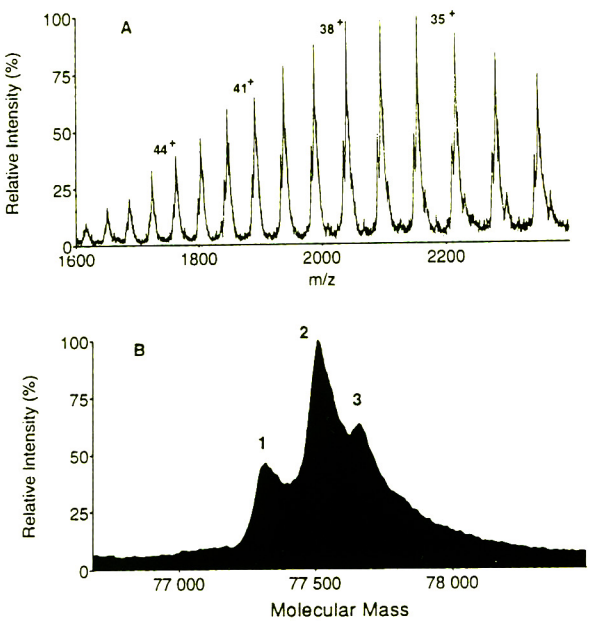

Fig. 6. (A) Electrospray ionization mass spectrum of purified ovotransferrin. The spectrum was acquired by using 384 pmol on the basis of ovotransferrin M_r = 78 000. Scan accumulation and mass calculation were performed with Tune 2.3 and Macspec 3.2 programs respectively. Protonation states of the three major species are indicated above some peaks. The fourth less important form of ovotransferrin belongs to another protonation states series. (B) M_r spectrum reconstructed from the mass spectrum by using the Macspec 3.2 program. Peak 1, 2 and 3 correspond to calculated M_r values of 77 324.2 ± 9.1, 77 513.9 ± 8.3 and 77 659.4 ± 8.7, respectively.

Table 2
ESI-MS determination of lysozyme M_r by HyperMass method

Actual peak (m/z)	Intensity	Predicted peak (m/z)	Charge	Compound mass
1431.40	735 000	1433.40	10	14 303.92
1590.20	2 228 000	1590.33	9	14 302.73
1789.00	2 131 000	1789.00	8	14 303.94
2044.40	1 445 000	2044.43	7	14 303.74
2384.80	929 000	2385.00	6	14 302.75

The primary charge agent was H, mass 1.0079. The average compound M_r calculated from five estimates was 14 303.42 with a standard deviation of 0.62.

determined from fourteen and twelve multiply charged molecular ions, respectively. Another less important species with average M_r = 75 795.3 was also detected. The multiply charged ions for this last species belongs to a series different from that of the three major forms which belong to the same series. M_r values of 76 000 or 77 500 have been determined previously by ESI-MS for ovotransferrin [30,31]; we assume that only one species of the ovotransferrin population was characterized in these cases. The mass reconstruct obtained from the mass spectrum and presented in Fig. 6B illustrates the heterogeneity in the glycans bound to this protein. The different ovotransferrin forms are not evidenced by polyacrylamide gel electrophoresis even though they were slightly separated by chromatography on a Q Sepharose Fast Flow column (see Fig. 4).

The amino acid composition of the purified ovomucin was compared to that of the protein purified by gel permeation, reported by Young and Gardner [18], and by precipitation, reported by Guérin and Brulé [32] (Table 4). Ovomucin

Table 3
ESI-MS determination of the ovotransferrin major population M_r by HyperMass method

Actual peak (m/z)	Intensity	Predicted peak (m/z)	Charge	Compound mass
1650.40	64 000	1650.07	47	77 521.43
1686.20	78 000	1685.92	46	77 518.84
1723.60	125 000	1723.37	45	77 516.64
1762.80	149 000	1762.51	44	77 518.85
1803.60	179 000	1803.48	43	77 511.46
1846.80	229 000	1846.39	42	77 523.27
1891.40	247 000	1891.40	41	77 506.08
1938.80	299 000	1938.66	40	77 511.69
1988.80	334 000	1988.34	39	77 523.89
2041.00	371 000	2040.64	38	77 519.70
2095.80	374 000	2095.77	37	77 507.31
2154.40	381 000	2153.96	36	77 522.12
2215.40	366 000	2215.47	35	77 503.73
2280.60	317 000	2280.60	34	77 506.14
2349.40	282 000	2349.68	33	77 496.94

The primary charge agent was H, mass 1.0079. The average M_r of the compound from fifteen estimates was 77 513.87 with a standard deviation of 8.32.

Table 4
Amino acid composition of ovomucins from different purification procedures

Amino acid	Ovo A[a]	Ovo B[a]	Ovo C[a]
Asx	12.3	10.2	9.3
Thr	7.1	7.9	8.5
Ser	8.5	8.4	7.8
Glx	8.8	8.1	12.0
Pro	5.1	5.9	5.8
Gly	7.2	5.8	3.7
Ala	6.2	3.9	4.0
Cys	5.9	6.0	7.7
Val	6.2	6.4	6.0
Met	0.9	1.3	0.8
Ile	4.7	4.9	4.7
Leu	7.0	6.9	7.5
Tyr	2.9	4.4	4.1
Phe	4.9	7.6	4.9
His	1.7	2.3	2.4
Lys	5.6	6.4	6.4
Arg	4.9	3.7	4.5
Trp	ND	ND	ND

[a] Values are mol per 100 mol of residues. Ovo A = ovomucin prepared by the method of Guérin and Brulé [24]; Ovo B = ovomucin presented in this work; Ovo C = ovomucin isolated by Young and Gardner [17].

obtained by the two gel permeation procedures showed similar compositions, even though some striking differences were observed for the Phe, Glx and Gly composition. This might be due to the differences in contamination.

The specific activity of the purified lysozyme was estimated at *ca.* 60 000 U/mg of protein. This value is slightly higher than those stated by manufacturers or, for example, that obtained by Guérin and Brulé [32]. This indicates that the lysozyme preparation obtained by filtration on Superose 6 Prep Grade was purer and more active than the latter preparations. In fact, even though lysozyme is presented as a relatively stable protein, the native conformation of the enzyme might be better conserved with the gel permeation procedure than with the other procedures such as precipitation by salt addition or ion-exchange chromatography. Determination of the lysozyme activity from original egg white indicated that the enzyme was purified with a yield of *ca.* 60%. This value is in line with the yield deduced from protein quantification (see above) and confirms the quasi-absence of enzyme degradation during purification.

4. Conclusions

Several procedures have been developed for the separation of major egg albumen protein, usually on a laboratory scale and, to a lesser extent, on a process scale [33–43]. It is noteworthy that ovomucin is generally isolated as a precipitate by adding to egg white three volumes of water at an acidic pH [15,16]. The resolubilization of this precipitate in non-denaturing conditions is not evident. Soluble ovomucin has been prepared from egg white diluted in a saline solution at a relatively basic pH, by using gel permeation chromatography [18].

The past procedures used for egg white protein isolation have usually suffered from a lack of importance being attributed to the co-product. In keeping with the idea of maximum value of the egg white, we set up a procedure that allows the purification of several egg white proteins from the same sample. This has been tried previously by Guérin and Brulé [32], who developed a method involving ovomucin precipitation and separation of lysozyme and ovotransferrin from the co-product, by using cation-exchange chromatography. This procedure has the advantage of probably being applicable in industry. However, as mentioned above, the ovomucin obtained by this method was insoluble. In addition, as this protein coprecipitates with lysozyme, this led to a substantial decrease in the yields with lysozyme preparations. The two-step purification procedure proposed here allows the isolation of ovomucin purified to *ca.* 80% with a yield of 80%, lysozyme purified to homogeneity with a yield of *ca.* 65%, ovotransferrin purified to *ca.* 80% with a yield of 90% and ovalbumin purified to homogeneity with a yield of *ca.* 66%. Moreover, gel permeation chromatography allowed the separation of three peaks containing ovomucin. It will be interesting

to investigate the actual composition of proteins present in these peaks.

Although the gel permeation chromatography may not be easily transferrable to industry, the procedure we have developed constitutes a good means of preparing highly purified proteins with relatively good yields, especially for laboratory use. One advantage is that our purification scheme takes into account the maximum value of the egg white, by purifying several proteins from the same sample. The combination of this method with that of Guérin and Brulé [32] may allow the setting up of a procedure more easily adaptable to industry.

Acknowledgements

We are grateful to M. Piot for the determination of the ovomucin amino acid composition. We thank Dr. W. Nasser for valuable discussions. S. Moreau was funded by the Ministère de la Recherche et de l'Espace.

References

[1] E. Li-Chan and S. Nakai, *Crit. Rev. Poult. Biol.*, 2 (1989) 21.
[2] Y. Tomimatsu and J.W. Donovan, *J. Agric. Food Chem.*, 20 (1972) 1067.
[3] L. Stevens, *Comp. Biochem. Physiol.*, 100B (1991) 1.
[4] C.A.A. Van Boeckel, *Recl. Trav. Chim. Pays-Bas*, 105 (1986) 35.
[5] P. Valenti, G. Antonini, M.R.R. Fanelli, N. Orsi and E. Antonini, *Antimicrob. Agents Chemother.*, 21 (1982) 840.
[6] P. Valenti, G. Antonnini, C. Von Hunolstein, P. Visca, N. Orsi and E. Antonini, *Int. J. Tissue React.*, 5 (1983) 97.
[7] V.A. Proctor and F.E. Cunningham, *CRC Crit. Rev. Food Sci. Nutr.*, 29 (1988) 359.
[8] G.L. Weaver, M. Kroger and F. Katz, *J. Food. Sci.*, 42 (1977) 1084.
[9] D.H. Spackman, W.H. Stein and S. Moore, *Anal. Chem.*, 30 (1958) 1190.
[10] S.C. Moore, *J. Biol. Chem.*, 283 (1963) 235.
[11] M.M. Bradford, *Anal. Biochem.*, 72 (1976) 248.
[12] U.K. Laemmli, *Nature*, 277 (1979) 680.
[13] S.F. Wong, C.K. Meng and J.B. Fenn, *J. Phys. Chem.*, 92 (1988) 546.
[14] S. Hayakawa and Y. Sato, *Agric. Biol. Chem.*, 40 (1976) 2397.
[15] A. Kato, K. Ogino, N. Matsudoni and K. Kobayashi, *Agric. Biol. Chem.*, 41 (1977) 1925.
[16] A. Kato, S. Oda, Y. Yamanaka, N. Matsudoni and K. Kobayashi, *Agric. Biol. Chem.*, 49 (1985) 3501.
[17] H. Nagase, E.D. Harris, J.F. Woessner, Jr., and K. Brew, *J. Biol. Chem.*, 258 (1983) 7481.
[18] L.L. Young and F.A. Gardner, *J. Food Sci*, 37 (1972) 8.
[19] J.M. Fernandez-Sousa, R. Perez-Castells and R. Rodriguez, *Biochim. Biophys. Acta*, 523 (1978) 430.
[20] T. Itoh, S. Takeuchi and T. Saito, *Biosci. Biotechnol. Biochem.*, 57 (1993) 1018.
[21] M.B. Smith, *Aust. J. Biol. Sci.*, 17 (1964) 261.
[22] M.B. Smith and J.F. Back, *Aust. J. Biol. Sci.*, 18 (1965) 365.
[23] W.J. Stadelman and O.J. Cotterill, *Egg Science and Technology*, Macmillan, London, 3rd ed., 1986.
[24] J. Kurisakai, Y. Murata, S. Kaminogawa and K. Yamauchi, *J. Agric. Food Chem.*, 30 (1982) 349.
[25] J.R. Cann, *J. Am. Chem. Soc.*, 71 (1949) 907.
[26] L.G. Longsworth, R.K. Cannan and D.A. McInnes, *J. Am. Chem. Soc.*, 62 (1940) 2580.
[27] G.E. Perlman, *J. Gen. Physiol.*, 25 (1952) 711.
[28] P.R. Levison, S.E. Badger, D.W. Toome, M.L. Koscielny, L. Lane and E.T. Butts, *J. Chromatogr.* 590 (1992) 49.
[29] K. Jacobs, L. Shen, H. Benemariya and H. Deelstra, *Z. Lebensm.-Unters.-Forsch.*, 196 (1993) 236.
[30] J.B. Fenn, M. Mann, C.K. Meng, S.F. Wong and C.M. Whitehouse, *Science*, 249 (1989) 64.
[31] R.D. Smith, J.A. Loo, C.G. Edmonds, C.J. Barinaga and H.R. Udseth, *Anal. Chem.*, 62 (1990) 882.
[32] C. Guérin and G. Brulé, *Sci. Aliments*, 12 (1992) 705.
[33] A. Furka and F. Sebestyén, *Acta Biochim. Biophys. Acad. Sci. Hung.*, 4 (1969) 379.
[34] R.C. Warner and I. Weber, *J. Biol. Chem.*, 191 (1951) 173.
[35] M.B. Rhodes, P.R. Azari and R.E. Feeney, *Biochem. J.*, 83 (1958) 355.
[36] P. Azari and P.F. Baugh, *Arch. Biochem. Biophys.*, 118 (1967) 138.
[37] E. Antonini, *US Pat.*, 4 029 711 (1977).
[38] S.A. Al-Mashikhi and S. Nakai, *Agric. Biol. Chem.*, 51 (1987) 2881.
[39] H. Lineweaver and C.W. Murray, J. Biol. Chem., 171 (1947) 565.
[40] G. Alderton and H.L. Fevold, *J. Biol. Chem.*, 164 (1946) 1.
[41] P. Bailon and A.H. Nishikawa, *Prep. Biochem.*, 7 (1977) 61.
[42] R. Ahvenainen, M. Heikonen, M. Linko and P. Linko, *Food Process Eng.*, 2 (1979) 301.
[43] E. Li-Chan, S. Nakai, J. Sim, D.B. Bragg and K.V. Lo, *J. Food Sci.*, 51 (1986) 1032.

ELSEVIER

Journal of Chromatography A, 677 (1994) 289–299

JOURNAL OF CHROMATOGRAPHY A

Purification of recombinant ricin A chain with immobilised triazine dyes

Wendy K. Alderton[a,1], Christopher R. Lowe[a,*], David R. Thatcher[b]

[a]*Institute of Biotechnology, University of Cambridge, Tennis Court Road, Cambridge CB2 1QT, UK*

[b]*Zeneca Pharmaceuticals, Alderley Park, Macclesfield, Cheshire SK10 4TG, UK*

First received 29 December 1993; revised manuscript received 26 April 1994

Abstract

Immunotoxins, such as those based on ricin A chain, must be rigorously purified before they can be administered in vivo. The work described in this paper investigates the interaction between recombinant ricin A chain and several triazine dyes and other ligands that may be of value in its purification. All ligands displayed a high affinity (dissociation constants 3–20 μM) and are displaced from their binding sites on the protein by polynucleotides, heparin and synthetic polyphosphates, but not by mono- or dinucleotides. Affinity chromatography on the immobilised dyes, Procion Red H-3B, Procion Red HE-3B, Procion Red HE-7B and Procion Yellow HE-4R, resulted in a one-step purification of recombinant ricin A chain from an *Escherichia coli* fermentation extract to 94–98% purity and with a >95% yield. These materials are far superior to purification on the conventional dye, Cibacron Blue F-3GA, and show promise for the isolation of immunotoxins from immunoconjugation mixtures.

1. Introduction

Ricin, a potent cytotoxin from the seeds of the castor bean (*Ricinus communis*), is a heterodimer consisting of a ribosome-inactivating A chain, linked by a disulphide bond to a cell-surface receptor binding (B) chain [1]. The B chain binds ricin to cell surfaces through galactose-containing receptors, triggering endocytosis of the toxin [2]. The disulphide bond between the two chains is broken, and once within the cytosol, ricin A chain enzymatically inactivates the 60S ribosomal subunit, inhibiting protein synthesis and causing the death of the cell [3]. Ricin A chain is an N-glycosidase, which hydrolyses a specific adenine base from a highly conserved loop region of 28S rRNA [4]. A comparison of the amino acid sequence of ricin A with other ribosome-inactivating proteins revealed thirteen conserved residues [5]. The three-dimensional structure of ricin has been solved by X-ray crystallography [6] revealing that many of these invariant residues are clustered in a putative active site cleft. Site-directed muta-

* Corresponding author.

[1] Present address: Molecular Sciences, Wellcome Foundation Research Laboratories, South Eden Park Road, Beckenham, Kent BR3 3BS, UK.

0021-9673/94/$07.00
SSDI 0021-9673(94)00409-3

genesis of some of these residues [7–9] has led to a proposed mechanism of ricin A chain action [10]. Around the putative active site cleft of ricin A chain are several patches of arginine residues; such arginine-rich clusters are commonly found in RNA-binding proteins and may also play an important role in specific RNA recognition [11].

The toxicity of ricin A chain within the cytosol has led to its use in immunotoxins for the treatment of certain cancers [12]. However, glycosylation of native ricin A chain can result in the rapid clearance of immunotoxins from the bloodstream by the liver [13]. The cDNA encoding ricin has been cloned and expressed in *Escherichia coli* [14] and the non-glycosylated recombinant ricin A chain has been used in the construction of second-generation immunotoxins [15].

Immunotoxins must be rigorously purified before they can be administered in vivo and affinity chromatography on immobilised dyes has proved to be a convenient method for this [16–18]. Immobilised triazine dye adsorbents are increasingly being used for protein purifications [19], the low cost of reactive dyes combined with their resistance to chemical and biological degradation and ease of immobilisation, has led to affinity adsorbents that are more stable and less expensive than those based on natural biological ligands. The most commonly used dye, Cibacron Blue F-3GA, has been shown to interact with native ricin A chain but not with ricin B chain or intact ricin, both in solution [20] and with the dye immobilised onto agarose [21]. Cibacron Blue F-3GA was found to reduce the ability of native ricin A chain to inactivate ribosomes in an in vitro translation assay suggesting that the dye interacted at, or near, the active site [22].

This work describes an investigation into the interaction of a recombinant ricin A chain (r-ricin A) with a range of reactive dyes in order to improve the specificity and efficiency of their use in the purification of ricin A. The use of these dyes immobilised onto agarose in the purification of r-ricin A from an *E. coli* fermentation extract is compared with the more conventional immobilised Cibacron Blue F-3GA.

2. Experimental

2.1. Chemicals

C.I. Reactive Blue 2 and Procion dyes Red H-3B, Red H-E3B, Red H-E7B and Yellow H-E4R were supplied by ICI Organics Division (Blackley, Manchester, UK). r-Ricin A samples were supplied by Zeneca Pharmaceuticals (Macclesfield, UK). Sephadex LH-20 and Sepharose CL-4B, deoxy-CTP and polynucleotides poly(A), poly(C), poly(G) and poly(U) were obtained from Pharmacia (Uppsala, Sweden). Heparin and polyphosphates were obtained from Sigma (Poole, UK). ATP, $NADP^+$ and NAD^+ were obtained from Boehringer Mannheim (Lewes, UK). Herring testes DNA and yeast RNA were supplied by Dr. J.A.H. Murray, Institute of Biotechnology, Cambridge, UK. Heparin agarose was obtained from Affinity Chromatography Ltd. (Ballasalla, Isle of Man, UK). All other reagents and solvents were of analytical grade and were obtained from UK suppliers.

2.2. Spectral difference titrations

The dissociation constants (K_d) of triazine dyes with r-ricin A were determined by difference spectral titrations at 25°C. A stock solution (approximately 0.5 mg ml^{-1}) of r-ricin A (filtered through a 0.45-μm pore size filter) in 2-(N-morpholino)ethanesulphonic acid (MES)–3-(N-morpholino)propanesulphonic acid (MOPS)–N-[tris(hydroxymethyl)methyl]glycine (Tricine)·NaOH buffer, pH 7.5 (33.3 or 3.33 m*M* in each buffering species, to give a total anion concentration of 0.1 or 0.01 *M*) was prepared and the protein concentration was determined from the absorbance at 280 nm using an extinction coefficient of 1.1 ml mg^{-1} cm^{-1} and a subunit M_r of 29 900 [23]. A stock solution of r-ricin A (10–20 nmol; 1 ml) was added to black-walled silica cuvettes (10 mm pathlength) and placed in the sample beam of a Perkin-Elmer Lambda 7 spectrophotometer. A buffer blank was placed in a similar cuvette in the reference beam and a background correction was performed between

700 and 450 nm. Identical aliquots (2–10 μl) of purified dye solution (1 mM) were added to both cells and the difference spectrum recorded after each pair of additions. The difference absorption, $\Delta\lambda_{max}$, was estimated. Data were corrected for the effect of dilution and the K_d value was calculated by fitting the data to the following equation on an ENZFITTER program [24] using a non-linear regression analysis in an identical manner to that described by Cleland [25]:

$$K_d = \frac{[P_T] - [PD]([D_T] - [PD])}{[PD]}$$

where $[P_T]$ is the total protein concentration, $[D_T]$ is the total dye concentration and [PD] is the concentration of the protein–dye complex.

2.3. Competitive binding experiments

A complex of r-ricin A and dye was formed in solution and the ability of mono-, di- and polynucleotides or other ligands to displace the dye was measured as follows. A 10 mm pathlength black-walled silica cuvette containing r-ricin A (0.3 mg, 10 nmol) and Procion Red H-3B (11.6 ng, 15 nmol) in 1 ml MES–MOPS–Tricine · NaOH buffer, pH 7.5 (3.33 mM in each anion, to give a total anion concentration of 10 mM) was placed in the sample beam of a UV–Vis spectrophotometer. A buffer blank contained the same concentration of dye. The absorption maximum was recorded after the addition of 2–10 μl increments of mono-, di- or polynucleotide, or synthetic ligand as a 5 or 10 mg ml^{-1} solution in deionised water, to both the sample and reference cuvette. Subsequently, identical volumes of dye solution were added to both sample and reference cuvettes. The ligands used were: mononucleotides (ATP, deoxy-CTP), dinucleotides (NAD^+, $NADP^+$), polynucleotides [herring testes DNA, yeast RNA, poly(A), poly(C), poly(G), poly(U)] and other ligands (heparin, polyphosphate glasses of the general formula P_nO_{3n+1}/Na_{n+2} where n is the average number of phosphorous atoms in the chain for $n = 3, 4, 5, 15, 65$).

Data were presented as the absorbance at $\Delta\lambda_{max}$ against amount of ligand added (μg).

2.4. Immobilisation of triazine dyes to agarose by direct coupling

Monochlorotriazine dyes were directly coupled to a cross-linked agarose (Sepharose CL-4B, Pharmacia) according to the method of Lowe et al. [26]: to exhaustively washed agarose (5 g moist mass) was added a solution of purified dye (50 mg) in water (5 ml), followed by NaCl solution (22%, w/v; 1 ml). The mixture was agitated for 30 min at room temperature before adding solid sodium carbonate (50 mg), followed by agitation overnight at 60°C. The dyed gels were washed sequentially with water (200 ml), 1 M NaCl solution (100 ml), water (100 ml), 50% (v/v) dimethyl sulphoxide solution (20 ml) and water (200 ml) to ensure complete removal of any uncoupled dye, and stored in sodium azide solution (0.02%, w/v) at 4°C until required.

2.5. Determination of immobilised dye concentration

Dyed agarose (30 mg moist mass) was hydrolysed at 60°C for 5 min with HCl solution (5 M; 0.6 ml). The hydrolysate was neutralised by the addition of NaOH solution (10 M; 0.3 ml) and potassium phosphate buffer, pH 7.6 (1 M; 2.1 ml). The absorbance at the λ_{max} of the hydrolysate was read against an agarose blank treated in an equivalent manner. Molar extinction coefficients were determined from hydrolysed dye solution (1–25 μM) prepared in a manner identical to that of the hydrolysed gel. Immobilised dye concentrations were calculated as μmol dye per gram moist mass gel.

2.6. Determination of molar capacity of immobilised ligands for r-ricin A chain

Adsorbent (approximately 0.15 ml) was fully equilibrated with Tris · HCl buffer (0.1 M, pH 7.0) before r-ricin A (0.45–0.75 mg, 15–25 nmol) was added in equilibration buffer (1 ml)

and gently agitated for 5 min. The adsorbent was allowed to settle and the supernatant removed for protein determination. Protein was determined by the method of Bradford [27], and a standard curve for r-ricin A prepared for the range 0–0.75 mg ml^{-1} from dilutions of a solution of known concentration. This procedure was repeated until significant amounts of r-ricin A were found in the supernatant. The molar capacity of adsorbents was calculated as mol r-ricin A bound per mol of immobilised ligand.

2.7. Purification of r-ricin A from an E. coli fermentation extract by chromatography on immobilised triazine dyes

Column chromatography experiments were performed using a Pharmacia fast protein liquid chromatography (FPLC) system at 20–25°C. Dyes immobilised onto agarose were packed into Pharmacia HR 5/10 columns to a volume of approximately 1 ml, and equilibrated with Tris·HCl buffer, pH 7.0 (100 m*M*). A solution of r-ricin A *E. coli* fermentation extract was filtered (0.45-μm pore size filter) and loaded onto the column via a 0.2-ml injection loop at a flow-rate of 1 ml min^{-1}. After all unbound protein had washed through, r-ricin A chain adsorbed was eluted by a stepwise gradient of 0.25 *M* NaCl (for 8 min) to 0.55 *M* NaCl (for 9 min) in 100 m*M* Tris·HCl, pH 7.0. Eluted protein was monitored by absorbance at 280 nm. The collected fractions were analysed by sodium dodecyl sulphate–polyacrylamide gel electrophoresis (SDS-PAGE).

2.8. Analysis of purified r-ricin A by SDS-PAGE

The general procedure employed was SDS-discontinuous PAGE previously described by Laemmli [28]. Stacking gel (4%, w/v; 0.125 *M* Tris·HCl, pH 6.8) and separating gel (12%, w/v; 0.375 *M* Tris·HCl, pH 8.8) were used to electrophorese the loaded samples (1–50 μg). The gels were run at 200 V, 40 mA for approximately 1 h before staining with either silver stain according to the method described by Merril et al. [29] or with Coomassie Blue R-250. Molecular mass markers (low range) were used and consisted of rabbit muscle phosphorylase *b* (M_r 97 400), bovine serum albumin (M_r 66 200), hen egg white ovalbumin (M_r 45 000), bovine carbonic anhydrase (M_r 31 000), soybean trypsin inhibitor (M_r 21 500) and hen egg white lysozyme (M_r 14 400). The stained gels were scanned and bands were quantified using whole band analysis on a Bio Image system (Millipore, MI, USA)

3. Results

Commercial dye preparations frequently contain impurities such as reaction intermediates, hydrolysis products, buffer salts and de-dusting agents [30], and it is essential to remove these before studying dye–protein interactions [31]. The reactive dyes used in this study were purified by Sephadex LH-20 column chromatography and the degree of purification assessed by high-performance liquid chromatography (HPLC) as previously described [32]. In all cases, the purified dyes were estimated by peak integrations to be >96% pure.

Difference spectroscopy is a useful technique for studying the interactions between dyes and proteins [33]. The dye Cibacron Blue F-3GA has been most commonly used for such studies and found to be a sensitive spectroscopic probe for the binding sites of enzymes [34]. The dyes chosen for this study were polyaromatic, polysulphonated molecules that might prove useful mimics of the repeating patterns of heterocyclic bases and ribose-polyphosphate backbones of polynucleotides such as RNA. Fig. 1 shows an example of a spectral difference titration for r-ricin A with Procion Red H-3B. The difference spectra show maxima at 558 nm (a "red shift" of 24 nm from the absorbance maximum of the unbound dye), minima at 490 and 528 nm and an isosbestic point at 542 nm. The maxima at 558 nm were used to calculate the K_d value of r-ricin A for the dye using a non-linear regression analysis. Table 1 shows the structure, λ_{max} and molar extinction coefficient of this and several

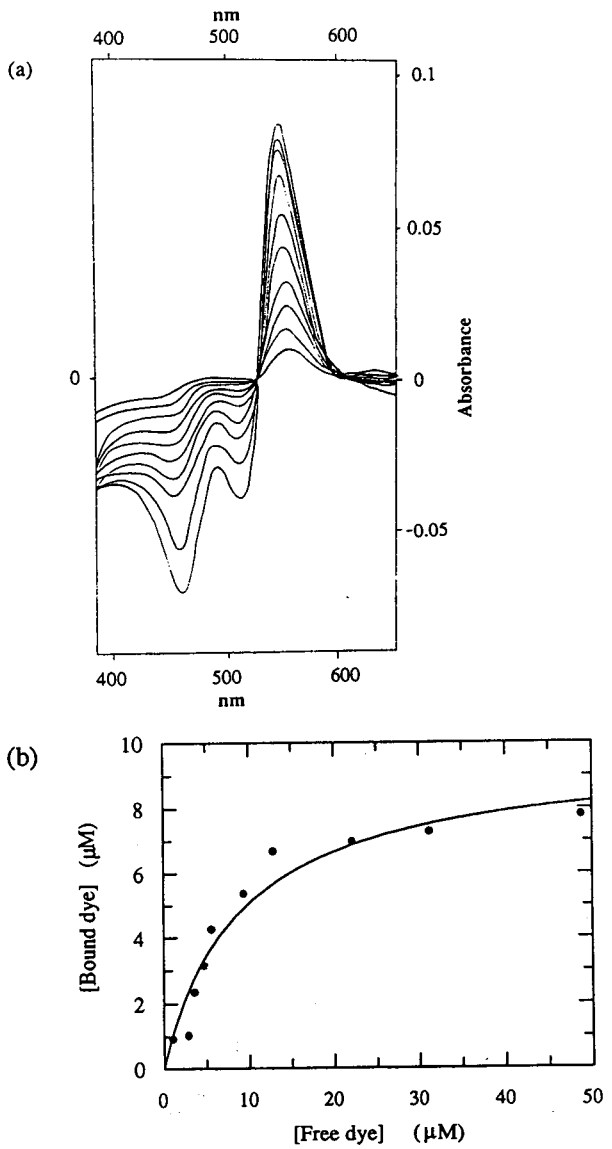

Fig. 1. Determination of the dissociation constant for r-ricin A and Procion Red H-3B in solution. r-Ricin A (0.33 mg, 10.4 nmol subunits) in 1 ml MES–MOPS–Tricine · NaOH buffer, pH 7.5 (0.01 *M*) and a buffer reference were titrated with aliquots (2–10 μl) of Procion Red H-3B solution (1 m*M*); the difference spectra were recorded at 25°C following each pair of additions. (a) The spectral difference titration of r-ricin A (10.4 μ*M*) with Procion Red H-3B (2–9.9 μ*M*). (b) The difference absorbance spectrum plotted as a function of the bound dye versus the free dye concentrations. The K_d value for the complex was determined from these data according to the method of Thompson and Stellwagen [34] and calculated using a non-linear regression analysis.

other dyes and their dissociation constants with r-ricin A determined at pH 7.5 in 10 m*M* buffer. The K_d values were all in the μ*M* range and varied little from dye to dye despite widely differing structures. In general, the values of K_d for the dye–r-ricin A complexes were two to sixfold greater in higher-ionic-strength buffer (results not shown), indicating that electrostatic interactions are important in dye–r-ricin A interactions. These observations suggest that the dyes may bind electrostatically at the arginine-rich clusters on the surface of r-ricin A. The value of the dissociation constant for Cibacron Blue F-3GA with r-ricin A determined in this work (5.6 μ*M*) is considerably higher than that calculated by Watanabe and Funatsu [22] (0.77 μ*M*) and may be due to differences between native and recombinant ricin A chain.

The effect of a variety of mono-, di- and polynucleotides and other ligands on r-ricin A–dye complexes was studied by competitive binding experiments. The results for Procion Red H-3B are shown in Fig. 2 and were typical for all the dyes. Mononucleotides (ATP and deoxy-CTP) and dinucleotides (NAD^+ and $NADP^+$) did not displace the dye from the dye–r-ricin A complex (Fig. 2a) while polynucleotides [RNA, DNA and poly(U)] did displace the dye (Fig. 2b). Readdition of the dye after displacement with polynucleotides restored the difference peak at 558 nm, suggesting that the dye and polynucleotide were competing for the same site on r-ricin A. These results agree with those of a similar experiment by Watanabe and Funatsu [22] for Cibacron Blue F-3GA. Control experiments confirmed that the spectrum of the dye alone was not altered by the addition of any of the ligands used. In addition, it was found that the polyanionic ligands heparin and synthetic polyphosphates also displaced Procion Red H-3B from a dye–r-ricin A complex. A range of polyphosphates of the general formula P_nO_{3n+1}/Na_{n+2} where n is the number of phosphate units in the chain varying between 3 and 65 were used in competitive binding experiments with Procion Red H-3B for r-ricin A (Fig. 2c). The data are presented as absorbance at 558 nm against concentration of phosphate units (PO_4^{2-}) to offset

Table 1
Spectral difference titrations of r-ricin A chain with Cibacron Blue F-3GA and Procion dyes

Ligand	Structure	λ_{max} (nm)	Molar extinction coefficient[a] ($l\ mol^{-1}\ cm^{-1}$)	$\Delta\lambda_{max}$ (nm)	K_d (μM)
Procion Red H-3B	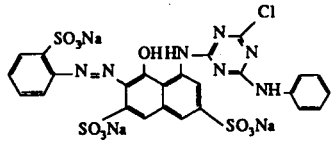	534	23 315	558	8.9 ± 2.1
Procion Red HE-3B	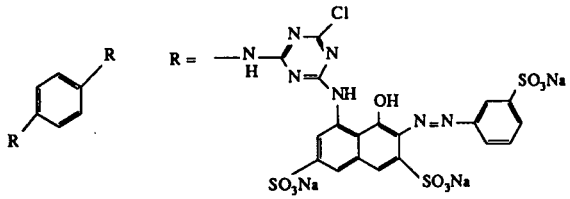	535	40 796	552	3.7 ± 0.7
Procion Red HE-7B	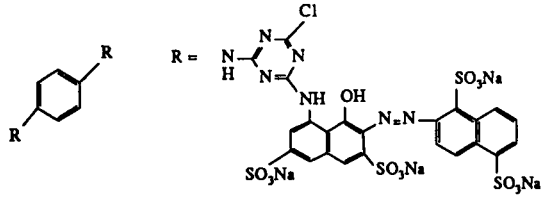	543	53 250	575	18.0 ± 2.5
Procion Yellow HE-4R	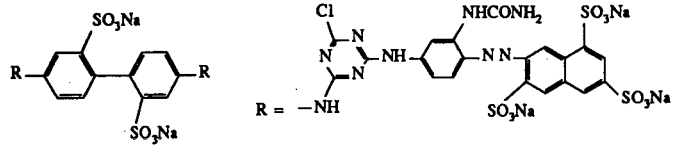	402	34 205	457	19.1 ± 2.9
Cibacron Blue F-3GA	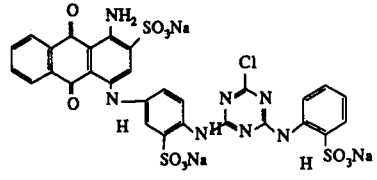	617	12 600	683	5.6 ± 1.4

[a]In deionised water.

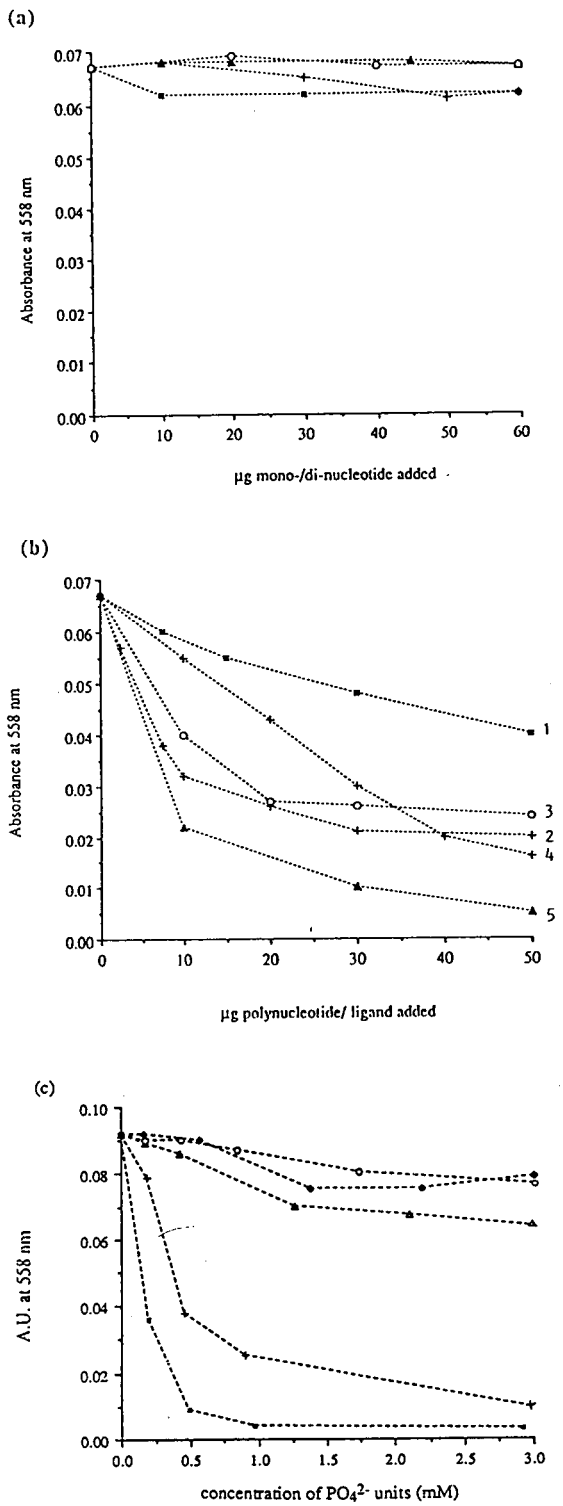

Fig. 2. The effect of various (a) mono- and dinucleotides, (b) polynucleotides and other ligands, and (c) polyphosphate glasses of general formula $P_nO_{3n+1}Na_{n+2}$ with between $n = 3$ and $n = 65$ phosphate units in a linear chain, on the maximum difference absorbance of Procion Red H-3B in the presence of r-ricin A. The sample cuvette initially contained r-ricin A (10 nmol) and 15 nmol dye in 1 ml of MES–MOPS–Tricine · NaOH buffer, pH 7.5 (0.01 *M*), and the reference cuvette contained the same concentration of dye in 1 ml of buffer. The maximum difference absorptions were recorded after the addition of 2–10-µl increments of ligand. (a) ○ = $NADP^+$; ▲ = NAD^+; + = ATP^+; □ = deoxy-CTP. (b) 1 = DNA; 2 = RNA; 3 = poly(U); 4 = heparin; 5 = polyphosphate ($n = 65$). (c) (◆) $n = 3$; (△) $n = 4$; (○) $n = 5$; (+) $n = 15$; (□) $n = 65$.

the effects of displacement by ionic strength increase alone. Polyphosphates of 3 to 5 units were unable to displace the dye from a complex with Procion Red H-3B, but polyphosphates of 15 and 65 units did displace the dye. The ability of polyphosphates to displace effectively dyes suggests the importance of the interactions between negatively charged dye sulphonates and positively charged protein groups in the interaction with r-ricin A. It is not clear why phosphate ligands of different lengths have different effects on the r-ricin A–dye complex. It may be that polyphosphates of 15 to 65 units are better analogues of the RNA substrate, or they may induce a conformational change in r-ricin A.

The affinity of proteins for dyes immobilised onto a chromatographic support can sometimes vary considerably from the K_d values determined in solution studies [31]. Therefore, the interaction between r-ricin A and immobilised dyes was also studied. The immobilised dye concentration is an important determinant of the affinity of a protein for a dye adsorbent and the use of lightly substituted gels (approximately 2 µmol dye per g moist mass gel) lead to more satisfactory purifications [35]. The Procion dyes Red H-3B, Red HE-3B, Red HE-7B and Yellow HE-4R and Cibacron Blue F-3GA, were immobilised onto Sepharose CL-6B, a cross-linked agarose, by direct coupling and the immobilised dye concentrations were determined to be between 2.3 and 2.8 µmol dye per g moist mass gel (Table 2). The molar capacities of immobilised

Table 2
Comparison of molar capacity for r-ricin A chain of triazine dyes and heparin immobilised on agarose

Immobilised ligand	Ligand concentration (μmol ligand per g moist mass gel)	Molar capacity (μmol r-ricin A per μmol immobilised ligand)
Procion Red H-3B	2.8	0.06
Procion Red HE-3B	2.7	0.07
Procion Red HE-7B	2.7	0.07
Procion Yellow HE-4R	2.3	0.13
Cibacron Blue F-3GA	2.7	0.03
Heparin	1	0.09

dyes and of heparin agarose for r-ricin A were determined batchwise (Table 2). Procion Red H-3B, Procion Red HE-3B and Procion Red HE-7B exhibited a twofold higher molar capacity for r-ricin A than immobilised Cibacron Blue F-3GA, while immobilised Procion Yellow HE-4R exhibited a fourfold increase in molar capacity over Cibacron Blue F-3GA and a 1.5-fold higher capacity than heparin agarose. Recombinant ricin A was not retained on Sepharose CL-6B alone. Molar capacities of approximately 10% of the total ligand are typical for immobilised dyes [36].

The selectivity of dyes immobilised onto agarose for r-ricin A was examined by the purification of r-ricin A from an *E. coli* fermentation extract by FPLC. A non-selective desorption technique was adopted (NaCl, 0.25–1 *M*) so that an indication of adsorbent specificity could be obtained. An example of the FPLC purification of r-ricin A from an *E. coli* fermentation extract on immobilised Procion Red HE-7B is shown in Fig. 3. Crude extract (lanes 3 and 8) was applied to the column and protein that did not bind to the column appeared at the void volume (2.5 ml, fraction I; lane 4), adsorbed proteins were eluted with a stepwise gradient of 0.25 *M* and 0.55 *M* NaCl in Tris · HCl buffer, pH 7.0 (0.1 *M*). r-Ricin A was eluted with 0.55 *M* NaCl (fraction III) and showed few contaminating proteins on the silver-stained SDS-PAGE gel (lane 6). It was estimated by band quantification that r-ricin A was purified to approximately 95% purity with a yield of >95% from a crude extract containing 10% r-ricin A. A comparison by Coomassie-stained SDS-PAGE of the purification of r-ricin A from an *E. coli* fermentation extract by dyes immobilised on agarose and by heparin agarose is shown in Fig. 4. Both Procion Yellow HE-4R and Procion HE-7B show good purifications of r-ricin A (lanes 4 and 5, respectively, both 98% purity) with only a few minor contaminants remaining from the crude extract (lanes 3 and 10). Heparin agarose and immobilised Cibacron Blue F-3GA gave less satisfactory purifications [lane 6 (85% purity) and lane 7 (40% purity), respectively], with both ligands retaining *E. coli* proteins. Analysis by silver-stained SDS-PAGE of the purification of r-ricin A from an *E. coli* fermentation extract by Procion Red H-3B and Procion Red HE-3B immobilised on agarose [Fig. 5, lane 5 (98% purity) and lane 7 (94% purity), respectively] showed that these dyes also gave good, one-step purifications comparable to that obtained on Procion Red HE-7B (Fig. 3). Heparin agarose (lane 10, 75% purity) performed poorly in comparison.

4. Discussion

A recombinant ricin A (expressed in *E. coli)* is increasingly being used in the construction of immunotoxins. Immobilised dyes could be exploited in two procedures in the production of ricin-based immunotoxins —for the purification of ricin A chain from the recombinant *E. coli* extract and for the purification of ricin A—

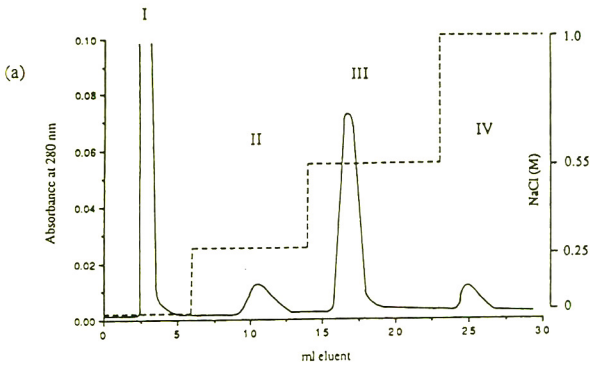

Fig. 3. The purification of r-ricin A from an *E. coli* fermentation extract on Procion Red HE-7B immobilised on agarose. (a) A sample (200 μl) of *E. coli* fermentation extract was loaded onto a column (1 ml) of Procion Red HE-7B immobilised onto agarose, equilibrated in Tris · HCl buffer (0.1 *M*), pH 7.0, at a flow-rate of 1 ml ml^{-1}. After unbound protein had washed through, a stepwise gradient was employed at 25, 55 and 100% (v/v) of NaCl (1 *M*) in Tris · HCl buffer, pH 7.0 (0.1 *M*). Eluted protein was measured at 280 nm and fractions (0.5 ml) were collected and analysed by SDS-PAGE. (b) Silver-stained SDS-PAGE gel of the purification of r-ricin A from an *E. coli* fermentation extract on Procion Red HE-7B-agarose. Lanes: 1, 10 = Molecular mass markers (kDa = kilodalton); 2 = r-ricin A standard; 3, 8 = *E. coli* extract; 4 = fraction I, not retained on Procion Red HE-7B column; 5 = fraction II, eluted with 0.25 *M* NaCl; 6 = fraction III, r-ricin A eluted with 0.55 *M* NaCl; 7 = fraction IV, eluted with 1 *M* NaCl; 9 = blank; 10 = r-ricin A purified on heparin agarose.

containing immunotoxins from immunoconjugation mixtures. This work describes the first example of the purification of r-ricin A from crude extracts using immobilised dyes.

Purification of r-ricin A from an *E. coli* fermentation extract on immobilised ligands Procion Red H-E3B, Procion Red H-E7B and Procion Yellow H-E4R resulted in a one-step purification of r-ricin A with high yield (94–98% purity with >95% yield, as only minor contaminants were visualised by silver staining of an SDS-PAGE gel). In comparison, heparin agarose

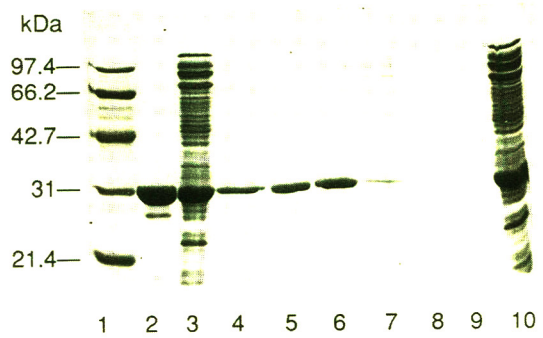

Fig. 4. Coomassie-stained SDS-PAGE gel of the purification of r-ricin A from an *E. coli* fermentation extract on dyes immobilised onto agarose. Lanes: 1 = Molecular mass markers (kDa = kilodalton); 2 = r-ricin A standard; 3, 10 = *E. coli* fermentation extract; 4 = r-ricin A purified on immobilised Procion Yellow HE-4R; 5 = r-ricin A purified on immobilised Procion Red HE-7B; 6 = r-ricin A purified on heparin agarose; 7 = r-ricin A purified on immobilised Cibacron Blue F-3GA; 8, 9 = blank.

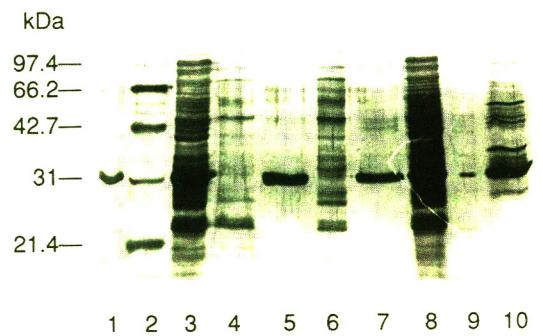

Fig. 5. Silver-stained SDS-PAGE gel of the purification of r-ricin A from an *E. coli* fermentation extract on dyes immobilised on agarose. Lanes: 1, 9 = r-ricin A standard; 2 = Molecular mass markers (kDa = kilodalton); 3, 8 = *E. coli* fermentation extract; 4 = protein not retained on immobilised Procion Red HE-3B column; 5 = r-ricin A purified on immobilised Procion Red HE-3B; 6 = protein not retained on immobilised Procion Red H-3B column; 7 = r-ricin A purified on immobilised Procion Red H-3B; 10 = r-ricin A purified on heparin agarose.

and immobilised Cibacron Blue F-3GA performed poorly. Immobilised Procion Yellow H-E4R had the highest molar capacity for r-ricin A (0.13 μmol r-ricin A per μmol immobilised ligand; 9 mg r-ricin A per g moist mass gel) of the ligands examined. Consequently, Procion Red H-E3B, Procion Red H-E7B and Procion Yellow H-E4R are novel ligands for the purification of r-ricin A and these new adsorbents show considerable potential for the large-scale purification of recombinant ricin A from *E. coli* fermentation extracts and for the purification of immunotoxins from immunoconjugation mixtures. In a recent publication, Li et al. [37] report the high level expression and simplified purification of a recombinant ricin A chain from *E. coli*. However, this procedure required further S-200 gel filtration to achieve equivalent purity. The overall yields of recovered protein also appeared to be considerably lower than those reported here. The similarities between ricin A and other ribosome-inactivating proteins such as abrin and modeccin [38] may also enable effective purifications of these other proteins to be achieved. Furthermore, the purification of the recently developed fusion toxins (wholly recombinant immunotoxins consisting of toxins and antibody fragments produced by genetic fusion [39,40]) may also prove possible.

The site of dye-binding to r-ricin A has yet to be firmly established. However, preliminary results presented in this paper suggest that the dyes bind to a site competitive with polynucleotides and their polyanionic analogues (heparin and polyphosphates). It appears that this interaction is largely electrostatic in nature, as evidenced by the reduced affinity of all dyes tested at higher ionic strength. For example, the dissociation constant of Cibacron Blue F3G-A was increased from 5.6 ± 1.4 μM in 10 mM buffer pH 7.5 to 33.1 ± 14.7 μM in 100 mM buffer pH 7.5. A plausible explanation for this is that the dyes bind r-ricin A at the arginine-rich clusters involved in co-ordinating RNA. Further work is in progress to identify the detailed nature of the interaction and the binding site topography in order to design a novel ligand based on these dyes for the purification of r-ricin A and its immunoconjugates [41]. Furthermore, these studies should rationalize the selective elution strategy based on the competitive interactions between the dyes and known competitive ligands, such as heparin and polyphosphates. It is anticipated that these studies will lead to a comprehensive purification strategy for ricin A and its immunoconjugates.

Acknowledgements

We would like to thank the Biotechnology Directorate of the Science and Engineering Research Council and Zeneca Pharmaceuticals for their financial support.

References

[1] F. Stirpe and L. Barbieri, *FEBS Lett.*, 195 (1986) 1–8.
[2] B. van Deurs, O.W. Pederson, A. Sundan, S. Olsnes and K. Sandvig, *Exp. Cell. Res.*, 159 (1985) 287.
[3] S. Olsnes and A. Pihl, in P. Cohen and S. van Heyningens (Editors), *Molecular Action of Toxins and Viruses*, Elsevier, Amsterdam, 1982, pp. 51–105.
[4] Y. Endo and K. Tsurugi, *J. Biol. Chem.*, 262 (1987) 8128–8130.
[5] G. Funatsu, M.R. Islam, Y. Minami, K. Sung-Sil and M. Kimura, *Biochimie*, 73 (1991) 1157–1161.
[6] E. Rutenber, B.J. Katzin, E.J. Collins, D. Mlsna, S. Ernst, M.P. Ready and J.D. Robertus, *Proteins*, 10 (1991) 240–250.
[7] P. Schlossman, D. Withers, P. Welsh, A. Alexander, J.D. Robertus and A.E. Frankel, *Mol. Cell Biol.*, 9 (1989) 5012–5021.
[8] A.E. Frankel, P. Welsh, J. Richardson and J.D. Robertus, *Biochem. J.*, 278 (1990) 1–23.
[9] M.P. Ready, Y. Kim and J.D. Robertus, *Proteins*, 10 (1991) 260–269.
[10] J.D. Robertus, *Seminars Cell Biol.*, 2 (1991) 23–30.
[11] D. Lazinski, A. Grzadzielska and A. Das, *Cell*, 59 (1989) 207–218.
[12] E.S. Vitetta and P.E. Thorpe, *Seminars Cell Biol.*, 2 (1991) 47–58.
[13] D.C. Blakey, D.N. Skilleter, R.J. Price and P.E. Thorpe, *Biochim. Biophys. Acta*, 968 (1988) 172–178.
[14] M. O'Hare, L.M. Roberts, P.E. Thorpe, G.J. Watson, B. Prior and J.M. Lord, *FEBS Lett.*, 216 (1987) 73–78
[15] E.J. Wawrzynczak, A.J. Cumber, R.V. Henry and G.D. Parnell, *Int. J. Cancer*, 47 (1991) 130–135.
[16] P.P. Knowles and P.E. Thorpe, *Anal. Biochem.*, 160 (1987) 440–443.

[17] V. Ghetie, M.-A. Ghetie, J.W. Uhr and E.S. Vitetta, *J. Immunol. Methods*, 112 (1988) 267–277.
[18] V. Ghetie, M.A. Till, M.-A. Ghetie, J.W. Uhr and E.S. Vitetta, *J. Immunol. Methods*, 126 (1990) 135–141.
[19] S.B. McLoughlin and C.R. Lowe, *Rev. Prog. Colouration*, 18 (1988) 16–28.
[20] P.S. Appukuttan and B.K. Bachhawat, *Biochim. Biophys. Acta*, 580 (1979) 10–14.
[21] S. Sperti, L. Montanano, F. Rambelli and M. Zamboni, *Biosci. Rep.*, 6 (1986) 1035–1040.
[22] K. Watanabe and G. Funatsu, *Biochim. Biophys. Acta*, 914 (1987) 177–184.
[23] D.R. Thatcher, Zeneca Pharmaceuticals, unpublished results.
[24] R.J. Leatherbarrow, ENZFITTER, Elsevier, Amsterdam, 1987.
[25] W.W. Cleland, *Methods Enzymol.*, 63A (1979) 103–138.
[26] C.R. Lowe, M. Hans, N. Spibey and W.T. Drabble, *Anal. Biochem.*, 10 (1980) 23–28.
[27] M.M. Bradford, *Anal. Biochem.*, 72 (1976) 248–254.
[28] U.K. Laemmli, *Nature*, 227 (1970) 680–685.
[29] C.R. Merril, D. Goldman, S.A. Sedman and M.H. Ebert, *Science*, 211 (1981) 1437–1438.
[30] C.R. Lowe, *Top. Enzyme Ferment. Biotechnol.*, 9 (1984) 78–161.
[31] S.J. Burton, C.V. Stead and C.R. Lowe, *J. Chromatogr.*, 455 (1988) 201–216.
[32] S.J. Burton, S.B. McLoughlin, C.V. Stead and C.R. Lowe, *J. Chromatogr.*, 435 (1988) 127–137.
[33] J.E.C. McArdell and C.J. Bruton, in Y.D. Clonis, A. Atkinson, C.J. Bruton and C.R. Lowe (Editors), *Reactive Dyes in Protein and Enzyme Technology*, Macmillan, Basingstoke, 1987, pp. 161–187.
[34] S.T. Thompson and E. Stellwagen, *Proc. Natl. Acad. Sci U.S.A.*, 73 (1976) 361–365.
[35] E. Gianazza and P. Arnaud, *Biochem. J.*, 201 (1982) 129–136.
[36] P.A. Anderson and L. Jervis, *Biochem. Soc. Trans.*, 6 (1978) 263–266.
[37] B.-Y Li, A.E. Frankel and S. Ramakrishnan, *Protein Expr. Purif.*, 3 (1992) 386–394.
[38] J.M. Lord, M.R. Hartley and L.M. Roberts, *Seminars Cell. Biol.*, 2 (1991) 15–22.
[39] R.A. Spooner and J.M. Lords, *Trends Biotechnol.*, 8 (1990) 189–193.
[40] I. Paston, V. Chaudhray and D.J. Fitzgerald, *Ann. Rev. Biochem.*, 61 (1992) 331–354.
[41] C.R. Lowe, S.J. Burton, N.P. Burton, J.M. Pitts and J.A. Thomas, *Trends Biotechnol.*, 10 (1992) 442–448.

ELSEVIER

Journal of Chromatography A, 677 (1994) 301–306

JOURNAL OF CHROMATOGRAPHY A

High-performance liquid chromatographic resolution of dinophysistoxin-1 and free fatty acids as 9-anthrylmethyl esters

Toshiyuki Suzuki

Tohoku National Fisheries Research Institute, 3-27-5 Shinhama, Shiogama, Miyagi 985, Japan

First received 2 February 1994; revised manuscript received 26 April 1994

Abstract

Resolution of a mixture of dinophysistoxin-1 (DTX1) and free fatty acids (FFAs) including eleven components which are the dominant FFAs in mussels and scallops was carried out by high-performance liquid chromatography (HPLC) with fluorimetric detection after their derivatization with 9-anthryldiazomethane (ADAM). Clear separation was obtained for a mixture of DTX1 and FFAs. As an application of the HPLC resolution of both DTX1 and FFAs, hydrolysis products of dinophysistoxin-3 (DTX3), a mixture of 7-O-acyl esters of DTX1, were separated as a replacement of direct HPLC analysis of DTX3. Determination of FFAs in scallops by HPLC–fluorometry is also described.

1. Introduction

Diarrhetic shellfish poisoning (DSP) was first described in Japan by Yasumoto et al. [1] as a new type of a seafood disease resulting from ingestion of shellfish infested with dinoflagellate toxins. In recent years, reports concerning DSP have been markedly increasing both in number and in geographical distribution with the general recognition of a new type of marine toxin [2].

Among DSP toxins, all being lipophilic compounds, the most important responsible for diarrheal symptoms are okadaic acid (OA) and its derivatives, dinophysistoxin-1 (35-methylokadaic acid; DTX1) and dinophysistoxin-3 (7-O-acyl-35-methylokadaic acid; DTX3) [3–5] (Fig. 1). The relative ratio of the individual toxins in shellfish shows significant annual and regional variations. In contrast to the predominant presence of OA in European mussels, with a few exceptions, the major toxin of Japanese mussels is DTX1, and scallops cultured in northern Japan occasionally contain DTX3 as a principal toxin [6–8].

Routine monitoring of shellfish for DSP toxins is generally done using rat or mouse bioassay [9], but instrumental methods are required for confirmation. The most common method for OA and DTX1 is high-performance liquid chromatography (HPLC) with precolumn derivatization with 9-anthryldiazomethane (ADAM) or 4-

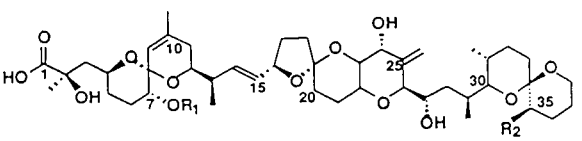

okadaic acid (OA) : $R_1 = H$ $R_2 = H$

dinophysistoxin-1 (DTX1) : $R_1 = H$ $R_2 = CH_3$

dinophysistoxin-3 (DTX3) : R_1 = acyl $R_2 = CH_3$

Fig. 1. Structures of DSP toxins.

SSDI 0021-9673(94)00410-B

bromomethyl-7-methoxycoumarin (Br-Mmc) [10,11]. On the other hand, confirmation of DTX3 by instrumental means has been carried out by detection of DTX1 obtained from DTX3 via alkaline hydrolysis, as DTX3 can be separated from other DSP toxins (OA and DTX1) by partitioning between 80% methanol (OA and DTX1) and *n*-hexane (DTX3) or isolated by column chromatography [12]. However, the biological activities of the toxins associated with DTX3 increase with increasing degree of unsaturation of the acyl chain [5], and therefore the true toxicity of a particular sample would depend on the distribution of acyl derivatives in the DTX3 mixture. Hence HPLC separation of free fatty acids (FFAs) derived from DTX3 coupled with the determination of DTX1 (from DTX3) is necessary to obtain more detailed information in analysis of DTX3.

In this study, resolution of a mixture of DTX1 and FFA standards was carried out by gradient HPLC after derivatization with ADAM to determine DTX3. As an application of the proposed HPLC separation, HPLC analyses of hydrolysis products obtained from DTX3 standard and FFAs which are regarded as interferences in mouse bioassays [13] are described.

2. Experimental

2.1. 9-Anthryldiazomethane

9-Anthryldiazomethane (ADAM) was obtained from Funakoshi Pharmacy (Tokyo, Japan).

2.2. FFA standards

Myristic acid (C14:0), palmitic acid (C16:0), stearic acid (C18:0), oleic acid (C18:1), linoleic acid (C18:2), and arachidic acid (C20:0) were obtained from Wako (Osaka, Japan). Palmitoleic acid (C16:1), *cis*-6,9,12,15-octadecatetraenoic acid (C18:4) and arachidonic acid (C20:4) were purchased from Sigma (St. Louis, MO, USA). *cis*-5,8,11,14,17-Eicosapentaenoic acid (C20:5) and *cis*-4,7,10,13,16,19-docosahexaenoic acid (C22:6) were supplied by Dr. Y. Itabashi of Hokkaido University (Hakodate, Japan).

2.3. DSP toxin standards

Authentic DTX1 and DTX3 obtained from midgut glands of scallops (*Patinopecten yessoensis*) collected at Mutsu Bay, Japan, were provided by Professor T. Yasumoto of Tohoku University (Sendai, Japan).

2.4. Sample material

Non-toxic scallops *Patinopecten yessoensis* were collected at Mutsu Bay, Japan, in September 1993. The specimens were kept frozen at −70°C until used.

2.5. Hydrolysis of DTX3 standard

DTX3 (1 μg) was hydrolysed by heating in 100 μl of 0.2 *M* NaOH–MeOH (10:90) at 75°C for 1 h in a 1-ml coloured vial. After removing the methanol from the reaction mixture under nitrogen, the aqueous layer was acidified with 200–300 μl of 0.1 *M* HCl and then extracted with diethyl ether (400 μl × 3). The combined ether layers which contain the DTX1 and FFAs were washed with 200 μl of water, then reacted with ADAM according to the previous method [10] after evaporating the solvent.

2.6. Derivatization and purification

Derivatization by labelling the carboxylic group of DTX1, FFAs and hydrolysis products of DTX3 with ADAM were performed essentially according to the method of Lee et al. [10].

DTX1 (1 μg), standard FFA mixture including 100 ng of the respective components and hydrolysis products from 1 μg of DTX3 were reacted with 100 μl of 0.1% ADAM–MeOH for 1 h in the dark at ambient temperature. A 200-μl volume of 0.1% ADAM–MeOH was used for derivatization of FFAs from scallops. For purification of the 9-anthrylmethyl (9-AM) ester of DTX1, the ADAM reaction mixture was placed on an ordinary Sep-Pak silica cartridge column

(Waters, Milford, MA, USA), then washed with 5 ml of *n*-hexane–dichloromethane (1:1, v/v) and subsequently eluted with 8 ml of pure dichloromethane. Finally, fractions of 9AM-DTX1 were obtained with 5 ml of dichloromethane–methanol (9:1, v/v) [10]. Purification of the 9AM esters of FFAs and the hydrolysis products of DTX3 was not carried out.

2.7. HPLC

HPLC separation was carried out with a Hitachi (Tokyo, Japan) L-6200/L-6000 gradient system equipped with a Develosil ODS-5 column (250 mm × 4.6 mm I.D.) (Nomura Chemical, Seto, Japan) with a stepwise gradient of solvent A (acetonitrile–methanol–water, 8:1:1, v/v/v) and solvent B (methanol) at ambient temperature and a flow-rate of 1.1 ml/min. The following linear gradient was used: segment 1, 100% A for 20 min, i.e., as reported for the resolution of OA and DTX1 by Lee et al. [10]; segment 2, initial conditions changed to 100% B over 30 min; and segment 3, 100% B for 50 min. The peaks of fluorescent derivatives were monitored with a Hitachi F-1050 spectrofluorimeter. The excitation and emission wavelengths were set at 365 and 412 nm, respectively. The FFA content in the midgut glands of scallop extracts was determined by comparing the peak areas of each of FFA with those of the standard.

3. Results and discussion

Fig. 2 shows the HPLC separation of a mixture of DTX1 and eleven FFAs, i.e., the available major FFAs of mussels and scallops [14], as their ADAM derivatives on the Develosil ODS-5 column. Injection was carried out by co-injection of DTX1 and a mixture of FFAs. 9AM-DTX1 and -FFAs were separated into eleven peaks within 80 min with a separation factor (α) from 1.01 to 2.06 (Table 1). 9AM esters of FFA were eluted in order of increasing carbon number and decreasing number of double bonds after elution of 9AM-DTX1. Linearity of peak area with increasing concentration of FFAs or DTX1 was

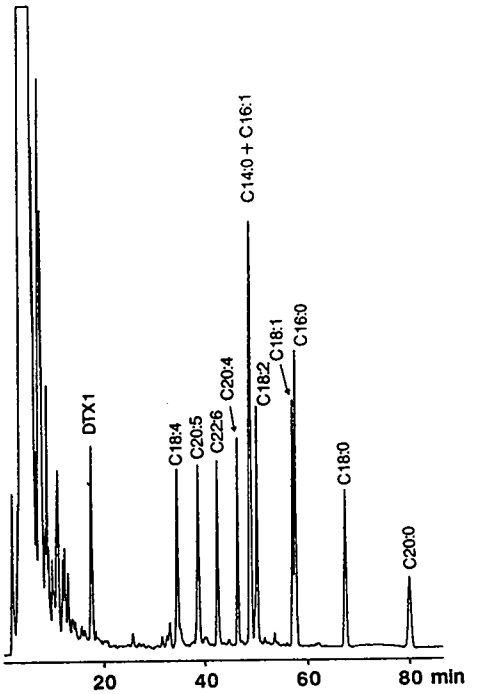

Fig. 2. HPLC separation of the 9AM esters of DTX1 and FFAs on the Develosil ODS-5 column. Amounts of 50 ng of DTX1 and 10 ng of each FFA were co-injected. For derivatization procedure and chromatographic conditions, see text.

confirmed over a wide range of concentrations, showing that the reaction of ADAM with FFAs or DTX1 was quantitative and reproducible.

Chromatographic data for the separation of a mixture of DTX1 and FFAs are given in Table 1. Because the retention times for the individual peaks were very sensitive to slight differences in the temperature and constitution of mobile phase, the relative retention times (RRTs) of respective peaks with respect to C18:0 were preferred for peak identification.

The FFA profile and DTX1 arising after hydrolysis of 1 μg of DTX3 standard is shown in Fig. 3. This demonstrates that the hydrolysis of DTX3 is connected with the release of FFAs and DTX1. The amount of DTX1 contained in the reaction mixture was 1020 ng, which was calculated from the HPLC data. This is slightly high compared with the theoretical amount (about 800 ng) estimated in the hydrolysis products resulting from 1 μg of DTX3 standard.

Table 1
Chromatographic data obtained on the separation of 9-anthrylmethyl esters of dinophysistoxin-1 and free fatty acids on a Develosil ODS-5 column

DTX1[a] and FFAs[b]	t_R[c]	k'[d]	α[e]
DTX1	0.26	13.0	2.06
C18:4	0.52	26.8	1.12
C20:5	0.58	30.1	1.10
C22:6	0.64	33.1	1.09
C20:4	0.69	36.2	1.05
C14:0 + C16:1	0.73	38.2	1.03
C18:2	0.75	39.1	1.14
C18:1	0.85	44.6	1.01
C16:0	0.86	45.1	1.17
C18:0	1.00	52.7	1.19
C20:0	1.19	62.9	

[a] DTX1 = dinophysistoxin-1.
[b] FFAs: free fatty acids are expressed as the number of carbon atoms: number of double bonds.
[c] Relative retention time with respect to C18:0.
[d] Capacity factor.
[e] Separation factor (the ratio of capacity factors).

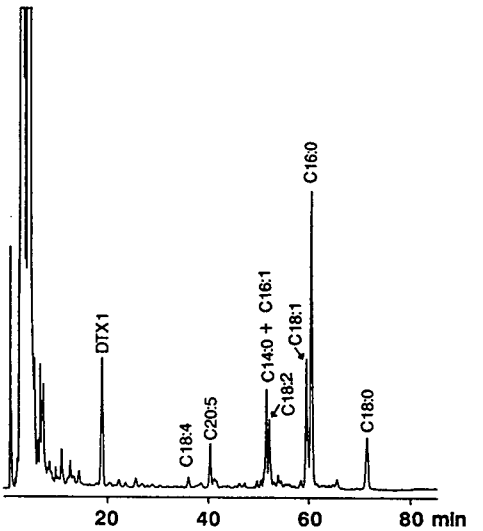

Fig. 3. HPLC separation of the 9AM esters of DTX1 and FFAs resulting from hydrolysis of DTX3 standard on the Develosil ODS-5 column. An aliquot (one tenth) of the hydrolysis products obtained from 1 μg of DTX3 standard was injected. The peak of DTX1 corresponds to 102 ng. For derivatization procedure and chromatographic conditions, see text.

The proportion of FFAs obtained from the DTX3 standard is given in Table 2. The most prominent FFA was C16:0. These results show directly the percentages of particular DTX3 homologues differing in acyl groups, and therefore the amount of each DTX3 homologue is calculable from the amount of DTX1 (from DTX3) and the percentage of each FFA obtained from DTX3. Although 1 μg of DTX3 standard was subjected to hydrolysis reaction, the total amount of DTX3 homologues calculated from the HPLC data was high (Table 2). This discrepancy may arise from the errors in subdivision of standard toxins.

Takagi et al. [13] pointed out a significant disadvantage of the official mouse bioassay test, that is, the false-positive results caused by the presence of large amounts of FFAs in samples not contaminated by DSP toxins: 3–14 mg of FFAs per gram of midgut glands showed positive results in the official mouse bioassay. They also indicated differences in interfering property of

Table 2
Proportion of free fatty acids and amount of particular dinophysistoxin-3 obtained from HPLC of hydrolysis products of 1 μg of dinophysistoxin-3 standard

FFA[a]	t_R[b]	Composition (mol%)	DTX3[c] (ng)
C18:4	0.53	1.6	22
C20:5	0.59	5.5	76
C22:6	–	–	–
C20:4	–	–	–
C14:0 + C16:1	0.74	6.8	88
C18:2	0.75	9.7	131
C18:1	0.85	20.5	277
C16:0	0.86	43.5	573
C18:0	1.00	12.4	168
C20:0	–	–	–
Total		100.0	1335

[a] FFAs: free fatty acids are expressed as the number of carbon atoms: number of double bonds.
[b] Relative retention time with respect to C18:0.
[c] DTX3 containing FFAa (mass) = DTX1 (mass, from DTX3) × mol% FFAa/100 × $[M_r(\text{DTX1}) + M_r(\text{FFAa}) - M_r(H_2O)]/M_r(\text{DTX1})$ where M_r indicates molecular mass.

FFAs for the mouse intraperitoneal (i.p.) test and suggested that polyunsaturated fatty acids (PUFAs), especially C20:4 and C20:5, are active agents as mouse lethal material.

Fig. 4 shows the FFA profile extracted from midgut glands of non-toxic scallops by the procedure described in the official method for mouse bioassay [9]. Whereas C14:0 and C16:1 were not separated, again a fair separation of the other principal FFAs was achieved. Table 3 gives the concentrations of the individual FFAs in the midgut glands of the scallops determined as 9AM esters by fluorescence detection after HPLC separation. The total amount of FFAs of 270 μg/g midgut glands found in the samples is close to that in mussels collected in the Gulf of Trieste [15]. This basic FFA content is not sufficient to interfere in the mouse bioassay.

It has been proposed that DTX3 may be the result of acylation of DTX1 in the midgut glands of scallops because DTX3 has not been detected in dinoflagellates [16], and similar FFA constituents in DTX3 and midgut glands in scallops have therefore been suggested. The DTX3 standard used in this study was obtained from midgut glands of scallops collected at Mutsu Bay. The FFA composition derived from the DTX3 standard under investigation was simpler than that obtained from midgut glands of scallops collected at the same location (Tables 2 and 3). The similarity of high percentages of C16:0 in FFAs from the DTX3 standard and the midgut gland of scallops is noteworthy. On the other hand, the percentages of PUFAs differed; the absence of C20:4 and C22:6 and the low proportion of C18:4 and C20:5 in the DTX3 standard (Table 2) were notably different from the results obtained for scallops (Table 3). The absence of C20:4 and C22:6 and the low level of C18:4 and C20:5 are due to degradation of the DTX3 esterified by these PUFAs during the extraction and purification of DTX3 standard from scallops owing to its instability [12].

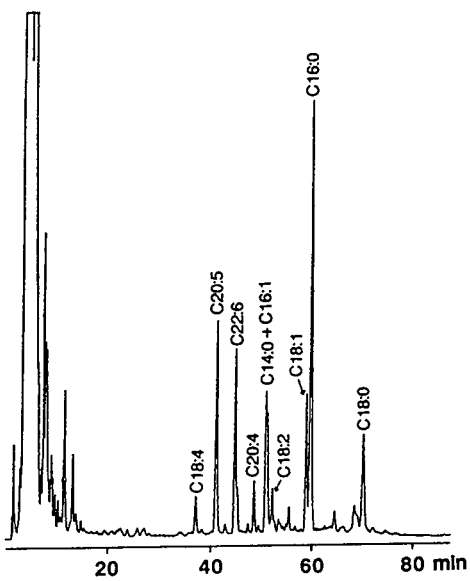

Fig. 4. HPLC separation of the 9AM esters of FFAs from midgut glands of scallops collected at Mutsu Bay, Japan, in September 1993, on the Develosil ODS-5 column. An aliquot (1/8000 of 0.91 g of midgut glands of scallops) of the extract was injected. The peak of C16:0 corresponds to 9.4 ng. For derivatization procedure and chromatographic conditions, see text.

Table 3
Individual free fatty acid contents of 1 g of midgut glands of scallops collected at Mutsu Bay in September 1993

FFA[a]	t_R[b]	Concentration (μg/g MG)[c]	Composition (mol%)
C18:4	0.53	9	3.5
C20:5	0.59	46	15.8
C22:6	0.64	36	11.3
C20:4	0.69	10	3.5
C14:0 + C16:1	0.73	23	9.9
C18:2	0.75	11	3.9
C18:1	0.85	32	11.5
C16:0	0.86	83	33.3
C18:0	1.00	20	7.3
C20:0	–	–	–
Total		270	100.0

[a] FFAs: free fatty acids are expressed as the number of carbon atoms: number of double bonds.
[b] Relative retention time with respect to C18:0.
[c] Midgut gland.

4. Conclusions

This study demonstrates that the clear elution profile for a mixture of DTX1 and FFAs obtained by HPLC with programmed gradient

elution and fluorometric detection is applicable to the analysis of the hydrolysis products of DTX3 standard. The most prominent component of DTX3 standard obtained from midgut glands of scallops collected at Mutsu Bay was that containing C16:0, which was the major FFA in midgut glands of scallops collected in the same location.

The concentration of FFAs obtained from midgut glands of scallops was also determined by HPLC–fluorometry. The FFA content found in scallops collected at Mutsu Bay in September 1993 was far below that reported to cause death in mice. The HPLC separation of FFAs described here will allow a more accurate interpretation of DSP because the determination of FFAs is very important in scallops from late spring to early summer, as they contain FFAs at levels high enough to give false-positive results. Although the peaks of C14:0 and C16:1 overlapped, they can be separated by subjecting of these overlapping peaks collected in the first HPLC run to a second HPLC run using a different column, if detailed percentages of C14:0 and C16:1 are required.

A problem with this HPLC method is interferences that prevent the sensitive and unambiguous analysis of a sample and instability of the 9AM ester [10,11,17]. We found that the 9AM esters of DTX1 and FFAs were stable for at least 1 month when stored at −40°C in methanol, showing no change in fluorescence intensity. Although clear detection was obtained for an aliquot (one tenth) of individual 9AM esters derived from hydrolysis products of 1 μg of DTX3 standard, clean-up of ADAM derivatives was required when the amount of DTX3 standard subjected to the hydrolysis reaction was below 200 ng. Clean-up of 9AM-DTX1 and -FFAs was investigated by using a Sep-Pak silica cartridge column to avoid interferences from ADAM reagent in peak detection, but satisfactory results were not obtained owing to the difference in the adsorption properties of DTX1 and FFAs on Sep-Pak silica. We are now examining the clean-up of 9AM-DTX1 and -FFAs and modification of the HPLC equipment [11] to achieve the detection of 9AM esters.

Acknowledgements

I express my gratitude to Professor T. Yasumoto of Tohoku University for providing DTX1 and DTX3 and comments on the manuscript. I am also grateful to Dr. Y. Itabashi of Hokkaido University for supplying C20:5 and C22:6.

References

[1] T. Yasumoto, Y. Oshima and M. Yamaguchi, *Bull. Jpn. Soc. Sci. Fish.*, 44 (1978) 1249.
[2] G.M. Hallegraeff, *Phycologia*, 32 (1993) 79.
[3] Y. Hamano, Y. Kinoshita and T. Yasumoto, in D.M. Anderson, A.W. White and D.G. Baden (Editors), *Toxic Dinoflagellates*, Elsevier, New York, 1985, Ch. 4, p. 383.
[4] K. Terao, E. Ito, T. Yanagi and T. Yasumoto, *Toxicon*, 24 (1986) 1141.
[5] T. Yanagi, M. Murata, K. Torigoe and T. Yasumoto, *Agric. Biol. Chem.*, 53 (1989) 525.
[6] M. Kumagai, T. Yanagi, M. Murata, T. Yasumoto, M. Kat, P. Lassus and J.A. Rodriguez-Vazquez, *Agric. Biol. Chem.*, 50 (1986) 2853.
[7] J.S. Lee, K. Tangen, E. Dahl, P. Hovgaard and T. Yasumoto, *Bull. Jpn. Soc. Sci. Fish.*, 54 (1988) 1953.
[8] J. Zhao, G. Lembeye, G. Cenci, B. Wall and T. Yasumoto, in T.J. Smayda and Y. Shimizu (Editors), *Toxic Phytoplankton Blooms in the Sea*, Elsevier, Amsterdam, 1993, p. 587.
[9] T. Yasumoto, *Food Sanit. Res.*, 31 (1981) 515.
[10] J.S. Lee, T. Yanagi, R. Kenma and T. Yasumoto, *Agric. Biol. Chem.*, 51 (1987) 877.
[11] B. Luckas, *J. Chromatogr.*, 624 (1992) 439.
[12] T. Yasumoto, M. Murata, Y. Oshima, M. Sano, G.K. Matsumoto and J. Clardy, *Tetrahedron*, 41 (1985) 1019.
[13] T. Takagi, K. Hayashi and Y. Itabashi, *Bull. Jpn. Soc. Sci. Fish.*, 50 (1984) 1413.
[14] J.D. Joseph, *Prog. Lipid Res.*, 21 (1982) 109.
[15] F. Zonta, B. Stancher, P. Bogoni and P. Masotti, *J. Chromatogr.*, 594 (1992) 137.
[16] J.S. Lee, M. Murata and T. Yasumoto, in S. Natori, K. Hashimoto and Y. Ueno (Editor), *Mycotoxins and Phycotoxins '88 – Papers presented at the 7th International IUPAC Symposium on Mycotoxins and Phycotoxins, Tokyo, August 1988*, Elsevier, Amsterdam, 1989, p. 327.
[17] O.B. Stabell, V. Hormazabal, I. Steffenak and K. Pedersen, *Toxicon* 29 (1991) 21.

ELSEVIER

Journal of Chromatography A, 677 (1994) 307–318

JOURNAL OF CHROMATOGRAPHY A

Influence of integrator parameters on estimates calculated with the statistical model of overlap

DeWayne Bowlin, Christian Hott, Joe M. Davis*

Department of Chemistry and Biochemistry, Southern Illinois University at Carbondale, Carbondale, IL 62901, USA

First received 22 September 1993; revised manuscript received 26 April 1994

Abstract

The effect of the slope and area thresholds of a digital integrator on the calculation of component numbers with the statistical model of overlap (SMO) is critiqued. As these thresholds increase, the numbers of maxima recognized by the integrator and components calculated with the SMO both decrease. With modest changes in threshold, the maxima and component numbers decrease proportionally, such that their ratio remains constant. For larger changes in threshold, the number of components usually decreases more rapidly than the number of maxima. Computer simulations are developed that confirm the general trend of these observations. The implications of these variations are discussed.

1. Introduction

The statistical model of overlap (SMO) has been used by this [1–3] and other groups [4–8] to estimate the quality of separation in chromatograms of complex mixtures. These estimations are based on either an interpretation of the numbers of maxima in a series of chromatograms of different peak capacity [2,4,6,8], or an interpretation of the distribution of intervals between adjacent maxima in a single chromatogram [1–3,5–7]. By either interpretation, several statistical parameters can be calculated, including the expected number of mixture components, the expected numbers of singlet and multiplet peaks, and the probability of resolving components as single-component peaks. The SMO and its applications have been reviewed recently [9].

Because these parameters are calculated from the numbers of, or intervals between, chromatographic maxima, they depend intimately on the mechanics of peak detection and processing. Commonly, both the numbers of peaks and their retention times (from which intervals between peaks are calculated easily) are determined by digital integrators. Regardless of their commercial origin, these integrators process chromatographic signals in a similar manner. Furthermore, many integrator settings are adjustable by the scientist. Thus, the scientist has considerable influence over the number of peaks determined.

The subject of this paper is the dependence of the most important statistical parameter, the number of mixture components, on the processing of peaks by a commercial integrator. The stimulus for this work was a previously reported observation based on gas chromatograms of a coal-tar extract [3]. When retention times were

* Corresponding author.

0021-9673/94/$07.00
SSDI 0021-9673(94)00412-3

determined by an integrator, the numbers of maxima and estimates of component number increased with increasing flow-rate. In contrast, when retention times were determined by visual inspection and manual digitization, the numbers of maxima decreased slightly with increasing flow-rate and estimates of component number were largely independent of flow-rate. It was suggested (but not proven) that the slope threshold of the integrator was responsible for this difference. The most important observation was that the means of peak processing —in one case by a digital integrator and in the other by eye— had a pronounced effect on the value of statistical parameters.

To our knowledge, a systematic experimental study of the effects of peak processing on SMO predictions has not been reported. The closest related work is by Dondi et al. [6], who interpreted computer-simulated chromatograms containing 50 major components and from 0 to 500 minor components. The latter were added to determine if their presence affected the statistical interpretation of the number of major components (the effect was small). In that study, however, all maxima below a certain amplitude were ignored. This differs from the study here, in which maxima are detected in some chromatograms but not in others.

Integrators have qualitative and especially quantitative limitations, which have been discussed by several authors [10–13]. Because integrators are fairly ubiquitous in the separation laboratory, we have examined the effect of two major parameters on the predictions of the SMO. In brief, 30 gas chromatograms of lime oil were developed under conditions appropriate to interpretation by the SMO. These chromatograms were processed differently, however, by varying systematically the electrometer amplification of the gas chromatograph and the slope and area thresholds of the integrator. The principal effect of this processing was to cause the retention times and areas of small maxima to be determined in some chromatograms but not in others. Thus, the sequence of determined retention times varied from chromatogram to chromatogram. The numbers of components detected then were estimated from these retention-time sequences by a well established procedure. Because these sequences differed for different processing conditions, the number of detected components also differed. In total, 480 different sequences of retention times were interpreted.

To lend credence to the interpretation of these sequences, we also determined retention times in 480 computer-simulated chromatograms using an in-house algorithm superficially similar to that of the integrator. The results of those interpretations closely, although not identically, paralleled those determined by experiment.

It should be noted that the word "detected" is used loosely here to indicate signals that are recognized and interpreted by the integrator. Signals that were truly detectable (i.e., statistically above the noise level) consequently will be described as undetected, if they were not so recognized and interpreted.

2. Theory

The expected number $\overline{m}$ of single-component peaks (SCPs) detected by the integrator was determined by the so-called single-chromatogram method, which is based on the SMO and is described elsewhere [5,14]. In brief, the differences between the retention times of adjacent maxima in an interval of temporal span X were compared to a series of arbitrary times. The numbers p' of intervals between adjacent maxima greater than x_0' were determined and graphed against x_0'/X as

$$\ln p' = \ln \overline{m} - \overline{m} x_0'/X \quad (1)$$

For SCPs distributed in accordance with Poisson statistics (i.e., distributed randomly throughout the chromatogram), values of $\ln p'$ are constant for small x_0'/X values but then decrease linearly as x_0'/X increases [14]. In this case, a line fit to the linear region has a slope equal to $-\overline{m}$ and an intercept equal to $\ln \overline{m}$. The two $\overline{m}$ estimates so determined are designated m_{sl} and m_{in}, respectively, and are pooled to obtain a weighted estimate of $\overline{m}$, which is designated m_{ave}. The

algorithm for pooling m_{sl} and m_{in} is outlined elsewhere [1]. The resultant estimate, m_{ave}, is an estimate to the actual number m of detectable SCPs.

To obtain accurate estimates, m_{sl} and m_{in} should agree closely, the graph of ln p' vs. x'_0/X should be linear (except for small x'_0/X values), the density of maxima in region X should be constant, and α should be less than 0.5 or so, when determined as

$$\alpha = -\ln \frac{p_m}{m_{ave}} \quad (2)$$

where p_m is the number of maxima detected by the integrator [2,14]. Unless noted otherwise, these criteria were satisfied fairly well in this study.

3. Procedures

3.1. Protocol

A cold-pressed lime oil (A.M Todd Co., Kalamazoo, MI, USA) was diluted 10-fold with HPLC-grade methylene chloride (Fisher Scientific, St. Louis, MO, USA). The mixture was stored in the refrigerator when not in use.

Chromatograms of this mixture were developed on a 30 m × 0.320 mm I.D. DB-1701 fused-silica capillary (J & W Scientific, Folsom, CA, USA) having a phase thickness of 0.25 μm. The capillary was incorporated into a Shimadzu GC-9AM modular gas chromatograph (Columbia, MD, USA) equipped with flame ionization detection (FID) and a SPL-G9 split–splitless injector. The electrometer output was sent to a CR-6A integrator (Shimadzu) for digital processing, as detailed below.

Two of four possible amplifications of FID current by the electrometer were used in this study. The full-scale electrometer currents at these amplifications were 10 and 100 pA; the chromatograms so developed will be designated 10-pA and 100-pA chromatograms. The other two amplifications generated either too few or too many maxima for interpretation. In the former case, too few (e.g., 20 or less) were detected to obtain reliable statistics; in the latter case, the saturation α substantially exceeded 0.5.

For both amplifications, 15 replicate chromatograms were developed as outlined below over a two-day period. The short interval of time favored the development of highly reproducible chromatograms, which was essential to our purpose. Thus, a total of 30 chromatograms (15 chromatograms per amplification × 2 amplifications) was generated.

Each of these chromatograms then was processed repetitively by integrator software to generate files of retention times for statistical interpretation. Two of four adjustable integrator parameters were varied. The width parameter was fixed for all chromatograms at 5 s to reduce noise, and the baseline-drift parameter was set to its default value. In contrast, the area threshold A_t was varied over the four values, 5, 50, 125 and 625 μV s, and the slope threshold S_t was varied over the four values, 200, 400, 600 and 800 μV/min. For any chromatogram, the retention time of a maximum was recorded, only if the experimental slope and area exceeded S_t and A_t, respectively. For each amplification, each of the 15 replicate chromatograms was processed at all 16 possible combinations of S_t and A_t, such that $16 \times 15 = 240$ retention-time files were obtained. These combinations of S_t and A_t will be represented here by the coordinates, (S_t, A_t). Thus, a total of 480 retention-time files were generated (240 files per amplification × 2 amplifications).

Precautions were taken to minimize the detection of spurious maxima. To ensure that solvent impurities were not detected as maxima, the solvent periodically was chromatographed at the most sensitive coordinate, (200, 5). No maxima were detected, other than the solvent peak. In addition, for any new coordinate, the capillary first was programmed through its temperature sequence to verify that no maxima were detectable. This precaution also was carried out at the beginning of each day.

The data acquired by the integrator were converted to ASCII files of the digitized chromatogram and retention times by Chromatopac data archiving utility (Shimadzu). These files

were downloaded to a 386 PC compatible computer (Northgate Computer Systems, Minneapolis, MN, USA) and then transferred to a Macintosh SE (Apple Computer, Cupertino, CA, USA) for editing, graphing and analysis. The communications software between the PC and Macintosh computers were PROCOMM PLUS (DataStorm Technologies, Columbia, MO, USA) and VersaTerm (Synergy Software, Reading, PA, USA).

3.2. Chromatography

The chromatographic conditions were: carrier, helium at average flow-rate of 4.25 ml/min (range, 4.23–4.32 ml/min); split flow, 42 ml/min; purge flow, 2.1 ml/min; make-up gas, 40 ml/min; air flow-rate to FID, 320 ml/min, hydrogen flow-rate to FID, 35 ml/min; injector and detector temperatures, 270°C; and sample size, 0.2 μl. The split–splitless ratio was controlled by and measured from the chromatograph. The carrier flow-rate was reproduced closely to ensure that the maximum slope of a given peak varied little among replicate chromatograms; such variation might have affected the number of detected peaks.

An empirically determined series of heating rates was used to develop chromatograms containing randomly distributed SCPs at the most sensitive (S_t, A_t) coordinate, (200, 5), and the 10-pA amplification. The temperature program developed at flow-rate $F = 4.25$ ml/min was: isothermal period, 65°C for 2.82 min; first ramp, 10.6°C/min to 95°C; second ramp, 21.4°C/min to 120°C ; third ramp, 3.6°C/min to 140°C; isothermal period, 140°C for 4.71 min; fourth ramp, 40°C/min to 220°C; isothermal period, 220°C for 9.41 min. The purpose of the final ramp was to flush high-boiling components from the capillary. The fraction of the chromatogram interpreted statistically is shown in Fig. 1.

We note in passing that theory was developed recently to circumvent the need of developing elution patterns consistent with constant-density Poisson statistics [15]. The theory shows much promise in statistically interpreting chromatograms more simply than performed here. However, the present study was initiated prior to this development.

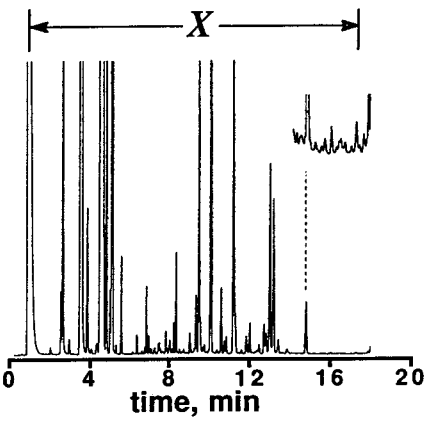

Fig. 1. Region X of lime-oil chromatogram interpreted by graphs of ln p' vs. x_0'/X.

3.3. Computer simulations

To add credibility to our interpretation, computer-simulated chromatograms were generated and interpreted by an algorithm superficially similar to that of the integrator. The retention-time sequences so generated then were interpreted by Eq. 1 as were the experimental sequences. The standard deviation of SCPs in these simulations was set arbitrarily to 2 s. The amplitudes of chromatograms were computed at intervals of 0.5 s to mimic the integrator's storage of digitally smoothed data at intervals equal to 1/10th of the width parameter (equal to 5 s; see above). Other details are deferred to the Results and discussion section.

It is important to recognize that we did not attempt to reproduce by simulation the experimental chromatograms exactly. Such a reproduction is not possible. In the experimental chromatograms, for example, SCP widths change systematically with changes in heating rate, and detailed theory is needed to model this variation. Even if this modeling were implemented, the SCP amplitude distribution is unknown, and consequently the relative amplitudes one should assign SCPs are unknown. Furthermore, baseline drift and noise are present in experimental

chromatograms but not the simulated ones. Instead, what we sought to verify by simulation was that the experimental variation of p_m and m_{ave} with S_t and A_t was an expected and reasonable result and not an artifact of our interpretation. In other words, we sought trends, not an exact agreement.

The following "rules" were adopted to mimic an integrator:

(a) A maximum was judged as detectable if and only if the slope on its front edge exceeded S_t, if the absolute value of the slope on its back edge exceeded S_t, and if the slope at one or more subsequent points on its back edge exceeded $-S_t$. Maxima that did not satisfy all these conditions were ignored.

(b) For each maximum, the integration limits were chosen from among the 10 amplitudes preceding (on the front edge) or following (on the back edge) the point at which the slope threshold was crossed. Among those values, the limit was identified with a valley between two maxima, a return to baseline, or the 10th value. The use of 10 values was not arbitrary but mimicked the integrator. Areas were evaluated with Simpson's rule.

(c) If the area of the maximum exceeded A_t, then the retention time was recorded. The retention time was determined by parabolic interpolation of the local maximum amplitude and the two adjacent amplitudes. If more than one maximum was found (a rare occurrence), then the retention time of the largest maximum was recorded (this action also mimicked the integrator).

The recorded retention times comprised the retention-time file for that simulated chromatogram.

3.4. Analysis of retention-time files

The retention-time files of both experimental and simulated chromatograms were interpreted by a series of FORTRAN programs written in Language Systems FORTRAN (Language Systems Corp., Herndon, VA, USA) and executed on an SE Macintosh (Apple) or Outbound Macintosh. The first program generated the data pairs, $(x_0'/X, \ln p')$, for graphs of $\ln p'$ vs. x_0'/X; the second computed values of m_{sl}, m_{in}, and m_{ave}; and the third generated simulated chromatograms for purposes of comparison to experimental ones. The third program was executed only periodically to verify a resemblance between experimental and simulated chromatograms.

For both experimental and simulated chromatograms, graphs of $\ln p'$ vs. x_0'/X and plots of simulated chromatograms were generated with KaleidaGraph (Synergy Software). Each graph of $\ln p'$ vs. x_0'/X was examined to exclude from the fitting those coordinates at small x_0'/X values that did not fall on a straight line. Three-dimensional graphs were generated with DeltaGraph Professional (DeltaPoint, Monterey, CA, USA).

4. Results and discussion

4.1. Dependence of ln p′ graphs on A_t and S_t

Fig. 2 shows graphs of $\ln p'$ vs. x_0'/X developed from the 10-pA chromatograms at various coordinates (S_t, A_t). The numbers p_m of maxima recognized by the integrator varied from 58 to 85; the numbers m_{ave} of components detected by the integrator varied from 102 to 171. The circles represent experimental data; the filled circles represent data fit to Eq. 1 by least-squares theory; the solid lines represent theoretical fits. Although chromatographic conditions were chosen to develop linear graphs only at the most sensitive coordinate, (200, 5), the graphs are fairly linear for all coordinates. From the graphs alone, one cannot tell that approximately one-third of the maxima detectable at the smallest (S_t, A_t) coordinate are not detected at the largest (S_t, A_t) coordinate.

4.2. Experimental variation of m_{ave} with S_t and A_t

In Fig. 3a and c three-dimensional graphs are shown of the average numbers $\bar{p}_m$ of maxima determined from 10- and 100-pA chromatograms, respectively, vs. S_t and A_t. Here, $\bar{p}_m$ represents the mean number of maxima determined from 15 replicate chromatograms by inte-

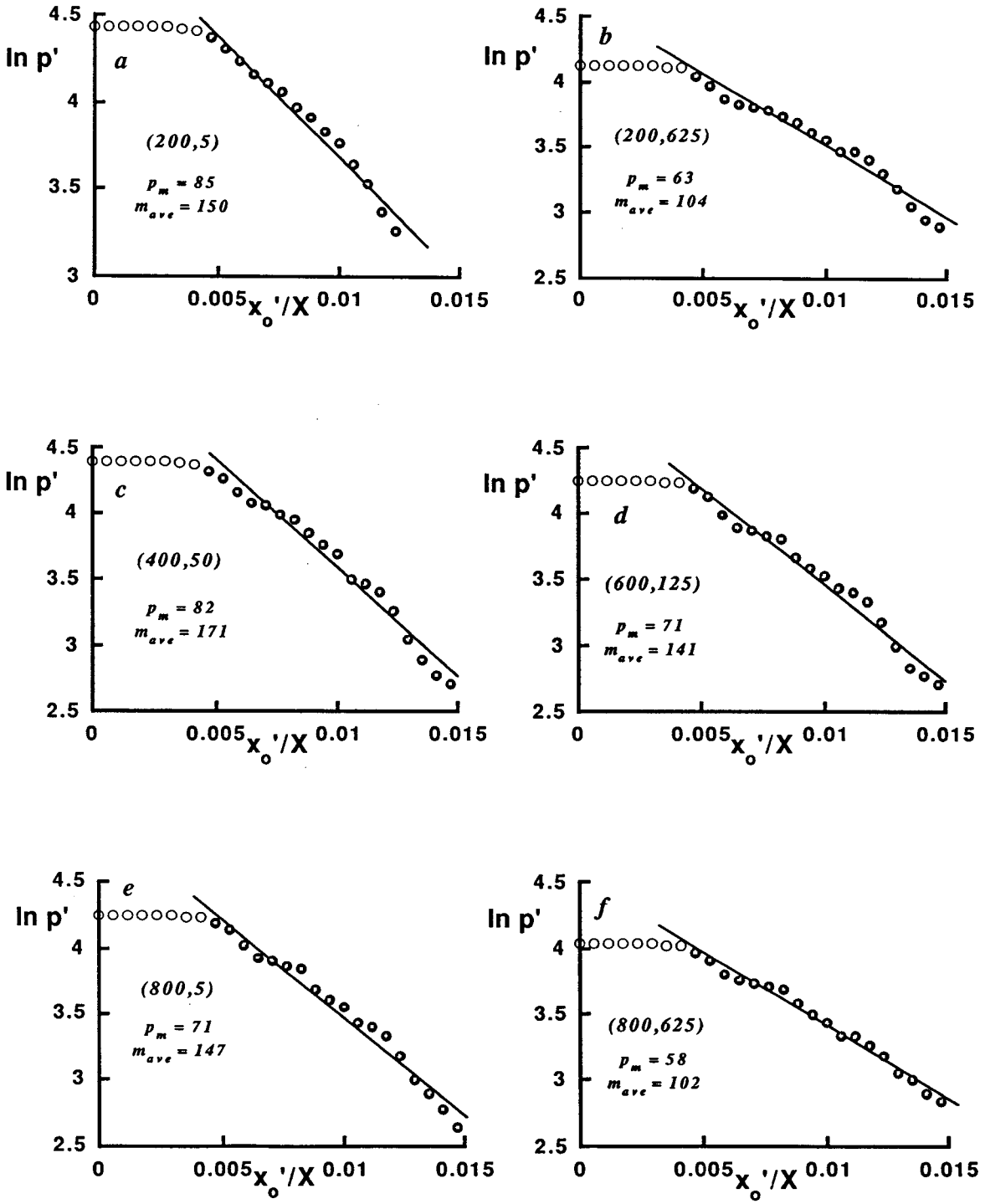

Fig. 2. Graphs of ln p' vs. x_0'/X developed from 10-pA chromatograms interpreted at different (S_t, A_t) coordinates. All symbols represent experimental data; filled symbols represent data fit to Eq. 1; solid lines represent theory.

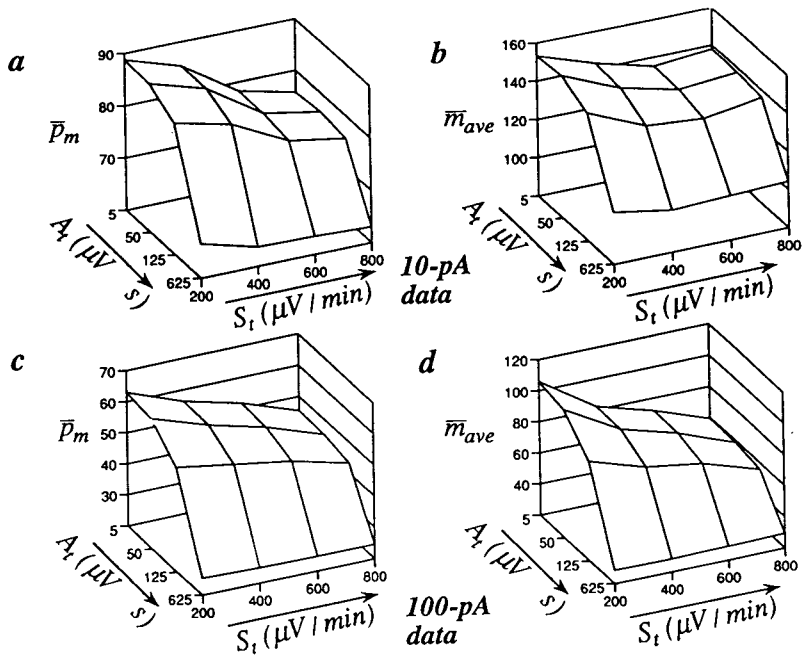

Fig. 3. Graphs of the average number $\overline{p}_m$ of maxima vs. S_t and A_t in the (a) 10-pA and (c) 100-pA chromatograms. Graphs of the average number $\overline{m}_{ave}$ of components calculated from Eq. 1 vs. S_t and A_t for the (b) 10-pA and (d) 100-pA chromatograms. Each datum represents the average of p_m or m_{ave} determined from 15 replicate chromatograms.

grator software at any coordinate, (S_t, A_t). Unsurprisingly, this number decreases with increasing S_t and A_t and with increasing full-scale current output. In Fig. 3b and d three-dimensional graphs are shown of the average numbers $\overline{m}_{ave}$, computed from these chromatograms with Eq. 1, vs. S_t and A_t. Here, $\overline{m}_{ave}$ represents the mean number of components estimated from the 15 retention-time files processed at the coordinate, (S_t, A_t). In general, these estimates track the variation of $\overline{p}_m$ with S_t and A_t, but this tracking is only roughly proportional.

For example, in Fig. 4a and b graphs are shown of the ratio $\overline{p}_m/\overline{m}_{ave}$, computed from the data comprising Fig. 3a–d. In both figures, this ratio is about 0.58–0.60 for small values of S_t and A_t but varies with increasing S_t and A_t (it usually increases). In particular, the $\overline{p}_m/\overline{m}_{ave}$ ratio at $A_t = 625$ is quite large for the 100-pA chromatograms. In general the rate of increase is larger for the 100-pA chromatograms than for the 10-pA chromatograms.

4.3. Generation and analysis of computer-simulated chromatograms

To lend credibility to these observations, computer simulations were generated and interpreted by an algorithm mimicking the digital integrator. These simulations were generated to gauge if the graphs in Fig. 3 reflected realistic and expected experimental behaviors, as opposed to artifacts.

A brief outline of these simulations' generation is given here. The simulatory equivalents of S_t and A_t corresponding to the experimental coordinate, (800, 625), were determined for both the 10- and 100-pA chromatograms, such that the numbers of maxima in the simulatory and experimental chromatograms were identical at this coordinate. All remaining simulatory S_t and A_t values then were scaled relative to these values and their experimental counterparts. To implement the scaling, however, the true number of components, corresponding to what one

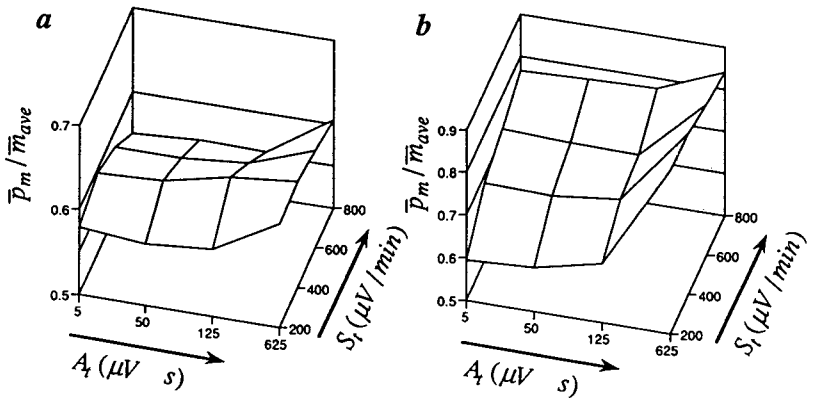

10-pA data *100-pA data*

Fig. 4. Graphs of the ratio $\bar{p}_m/\bar{m}_{ave}$ vs. S_t and A_t for the (a) 10-pA and (b) 100-pA chromatograms.

would detect at $S_t = 0$ and $A_t = 0$, was required. This number was estimated very simply from the data by appropriate expansions.

The normalization of simulations for the 10-pA chromatograms is described here in some detail. A first-order estimate of m was made by extrapolating via two-dimensional Taylor-series expansions [16] the $\bar{m}_{ave}$ values in Fig. 3b to the coordinate, (0, 0), the coordinate at which all components would be detected. A similar extrapolation was made for the $\bar{p}_m$ values in Fig. 3a. The extrapolated $\bar{m}_{ave}$ and $\bar{p}_m$ values were 163.2 and 92.2, respectively. This value of $\bar{m}_{ave}$ then was corrected for the deterministic error resulting from saturation. This error depends on the SCP amplitude distribution; evidence exists that this distribution is approximately exponential [17]. Relative to the coordinate, (0, 0), α was calculated from Eq. 2 as $-\ln(\bar{p}_m/\bar{m}_{ave}) = -\ln(92.2/163.2) = 0.571$. As shown elsewhere, the approximate percentage error PE expected in m under these conditions is [3]

$$PE = 100\left(\frac{m_{ave}}{m} - 1\right)$$
$$= 108.8\alpha^2 - 173.1\alpha + 49.7 \quad (3)$$

From Eq. 3, a corrected estimate of m, equal to 189, was calculated. This value was interpreted as the best estimate of m as S_t and A_t approach zero.

To determine the simulatory thresholds corresponding to the experimental coordinate, (800, 625), the average number of maxima in 50 simulations containing $m = 189$ SCPs with exponential amplitudes and a mean amplitude of 10 units was determined for various arbitrary but proportional S_t and A_t values. These thresholds were increased systematically from zero, until the average number of maxima (here, equal to 63.0) determined from the simulations equalled that determined at the experimental coordinate, (800, 625). These thresholds were increased proportionally, such that the ratio A_t/S_t equalled 46.9 s^2, the ratio determined by the coordinate, (800, 625) [i.e., 625 μV s/(800 μV/min · 1 min/60 s) = 46.9 s^2]. It was found that 63 maxima were detected in the simulations, when $A_t = 43.75$ unit · s and $S_t = 0.933$ unit/s (or 56.0 unit/min). The remaining simulatory A_t and S_t values then were scaled relative to these values, e.g., the simulatory area threshold corresponding to $A_t = 50$ μV s was calculated as (50/625)43.75 = 3.5 unit · s.

In Fig. 5a and b three-dimensional graphs are shown of the average numbers $\bar{p}_m$ of maxima and $\bar{m}_{ave}$ of detected components, respectively, determined from 15 computer simulations vs. the S_t and A_t simulatory thresholds. The number of simulations interpreted at any (S_t, A_t) coordinate was identical to the number of interpreted experimental chromatograms. Unlike for the

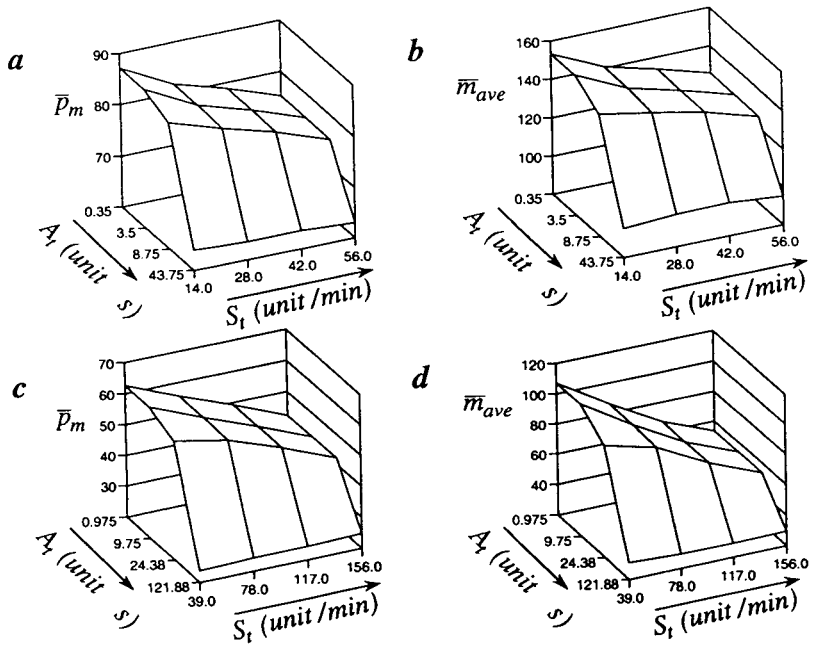

Fig. 5. Graphs of the average number $\overline{p}_m$ of maxima vs. S_t and A_t in scaled computer simulations of the (a) 10-pA and (c) 100-pA chromatograms. Graphs of the average number $\overline{m}_{ave}$ of components calculated from Eq. 1 vs. S_t and A_t for scaled computer simulations of the (b) 10-pA and (d) 100-pA chromatograms. Each datum represents the average of p_m or m_{ave} determined from 15 computer simulations. Values of S_t and A_t were determined by simulation.

experimental chromatograms, however, the simulations were not replicates but rather were generated from different sequences of retention times and amplitudes (replicate simulations simply would have generated identical p_m and m_{ave} values). The (S_t, A_t) coordinates reported in the figure differ from their experimental counterparts, because of scaling. However, the $\overline{p}_m$ and $\overline{m}_{ave}$ axes in Figs. 3a and 5a, and 3b and 5b, are scaled identically to facilitate easy comparison. This comparison shows that experimental and simulatory graphs of $\overline{p}_m$ and $\overline{m}_{ave}$ vs. S_t and A_t are qualitatively identical and quantitatively similar. Some differences do exist; in particular, m_{ave} values for the experimental 10-pA data increase slightly for large S_t and small A_t values, in contrast to the results from simulation. Mostly, however, a good agreement exists.

Indeed, in light of all the assumptions we were forced to make in generating the simulations, and also of the fact that $\overline{p}_m$ was "fixed" at only one of the 16 (S_t, A_t) coordinates and $\overline{m}_{ave}$ was "fixed" at none of them, the agreement is actually quite profound. The agreement strongly suggests that the trends illustrated in Fig. 3a and b are real.

The 100-pA chromatograms were mimicked similarly. The first-order estimates of $\overline{m}_{ave}$ and $\overline{p}_m$ at the coordinate, (0, 0) were again determined by Taylor-series expansions and were 130.2 and 70.0, respectively, with $\alpha = 0.619$. This estimate was corrected for saturation to the value, $m = 154$. The simulation thresholds S_t and A_t corresponding to the experimental coordinate, (800, 625), were determined as before and were 156.0 unit/min and 121.88 unit·s. These thresholds are larger than for the 10-pA data, because more maxima (and thus more maxima having small areas) existed in that case. Fig. 5c and d are three-dimensional graphs of $\overline{p}_m$ and $\overline{m}_{ave}$ determined from these simulations. As before, a strong correlation between the results of simulation and experiment (cf. Fig. 3c and d) is observed.

We note that it would have been desirable to interpret at least a fraction of these simulations by the integrator software itself to test the integrity of our in-house algorithm. Unfortunately the integrator software generates a proprietary binary code, whose encryptation we could not break.

4.4. Interpretation of results

Two observations can be made with respect to these experiments, analyses, and simulations. Prerequisite to these observations are the postulates that detectable SCPs are Poisson distributed, α is sufficiently small that reliable m_{ave} values can be calculated from graphs of ln p' vs. x_0'/X, and detectable SCPs may not be detected, if integrator thresholds are sufficiently large. Further, we presume that the value of neither p_m nor $\overline{m}$ is as important as the ratio, $p_m/\overline{m}$, which is a measure of the extent of separation [18].

The first observation is that the probability $p_m/\overline{m}$ that any detectable maximum is an SCP is identical for all maxima and that this probability is not altered by the exclusion of maxima from detection by high thresholds. Thus, the actual $p_m/\overline{m}$ ratio for a chromatogram does not change, even as maxima are excluded from detection; both maxima and components are excluded proportionally. The second observation is that approximation of $p_m/\overline{m}$ by p_m/m_{ave} can be erroneous, if the maxima distribution from which m_{ave} is calculated via ln p' vs. x_0'/X graphs is distorted by the selective exclusion of maxima. Thus, even though $p_m/\overline{m}$ is constant, the measurable ratio $p_m/\overline{m}_{ave}$ can vary, and misleading conclusions can be drawn about the extent of separation.

These behaviors are evident in our experimental results. At sufficiently small (S_t, A_t) coordinates, $\overline{p}_m/\overline{m}_{ave}$ is about 0.6 for both 10- and 100-pA chromatograms, even though $\overline{p}_m$ differs by about 26 between the two chromatogram sets. For larger coordinates, however, $\overline{p}_m/\overline{m}_{ave}$ varies systematically (it usually increases) for both the 10- and 100-pA chromatograms. The reasons for this behavior are not understood at this time. In general, the behavior occurs because the detectable maxima density, which is Poisson at small (S_t, A_t) coordinates, is distorted by the exclusion of maxima at large (S_t, A_t) coordinates.

The above assertion that $p_m/\overline{m}$ is identical for all maxima applies, if one considers only the Poisson distribution of components along the time axis. As shown by others [17,19], the probability that a peak is chemically pure actually depends on amplitude; in particular, small peaks are more likely to be pure than peaks of intermediate size. This finding does not explain our data, however, since the integrator's failure to detect small pure (or nearly pure) peaks should cause p_m to decrease more rapidly than $\overline{m}$, when $p_m \ll \overline{m}$. In fact, the opposite behavior is observed, i.e., $\overline{m}$ decreases more rapidly than p_m.

Thus it appears that experimental conditions consistent with development of Poisson-distributed retention times are restrictive not only in terms of chromatographic specifics (e.g., temperature program and flow-rate) but also detective specifics (e.g., S_t and A_t thresholds). In other words, the alteration of integrator thresholds can distort significantly a Poisson distribution that was established at other thresholds. This study shows that only minor threshold adjustments can be made without distortion.

From this study, one can conclude that integrator thresholds cannot be adjusted extensively, once separation conditions are found to develop a Poisson distribution. The converse also is likely; i.e., separation conditions cannot be substantially altered, once integrator thresholds consistent with a Poisson distribution are adopted. This imposes some difficulties on systematic investigations by the SMO and other statistical theories.

An illustration of the converse scenario is reported here. To test a new theory of overlap that relaxes the constraint of randomness from a global to a local domain [15], gas chromatograms were developed at simple heating rates r between 2 and 10°C/min [20]. Instead of systematically decreasing because of non-equilibrium effects, p_m initially increased with r and decreased only when r exceeded 7°C/min. The

anomalously detected maxima all had small areas (e.g., <500 μV s) and most probably were detected, because they eluted rapidly enough at high heating rates to cross an S_t threshold not crossed at lower heating rates. Since $\overline{m}$ increases as p_m increases, the anomalous detection of these maxima complicated the testing.

It is ironic that very small maxima, which often are of little or no interest, cause these difficulties. Fortunately, they cause complications only if one systematically varies separation conditions. At any single (S_t, A_t) coordinate, conditions appropriate to the SMO can usually be found. One should bear in mind, though, that those conditions are detective as well as separatory.

5. Conclusions

This paper shows that the number of components predicted by the SMO is a relative and not absolute quantity, because it is estimated from only those maxima recognized by the integrator. This number, in turn, varies with conditions of signal processing. Maxima that are not detected, or that are detected but are ignored by processing software for one or more reasons, make no contribution to the interpretation.

It is clear that a systematic protocol for adjusting integrator thresholds must be developed, if their effects on estimates of $\overline{m}$ and other statistical parameters are to be isolated from effects due to separation conditions. This may prove to be a formidable challenge. Nevertheless it is necessary for systematic studies of the kind pursued by this group.

It should be noted that other integrator parameters, e.g., baseline drift, width, etc., also are adjustable. The importance of these parameters, however, is secondary to that of slope and area thresholds, as indicated by the close agreement between experiment and simulation.

Other factors may be relevant in some instances. If one were interested in trace analysis, for example, one might normalize all peak areas to the area of the largest peak. Relative to the study reported here, fewer maxima would be detected at a given (S_t, A_t) coordinate, since peak area is smaller. This coordinate itself also could be scaled, however, such that the area normalization had no effect. Clearly, the results one obtains from any experiment will depend on the magnitudes of the signal, S_t, and A_t. However, only a relative, and not absolute, magnitude is important, as also was demonstrated by the computer simulations.

Finally, this study calls into question a guideline suggested in previous publications for gauging chromatographic saturation by comparing experimental chromatograms to published simulated ones [14]. In such simulations, all visible maxima contribute to saturation, but in an experimental chromatogram, only detected maxima contribute to saturation. Specifically, maxima that are visible to the eye but are not detected by an integrator create a misleading impression of high saturation. The converse also is true; maxima that are detected by an integrator but are not visible to the eye create a misleading impression of low saturation. The only way this guideline can be applied correctly is to attenuate or amplify a chromatogram to a level where maxima that are not detected by the integrator are not visible and maxima that are detected are visible; for practical reasons, this is not always possible.

Acknowledgements

The authors thank Lee Olszewski and Jim Mott of the Delta Instrument Company for instructive comments on the operation of the GC-9AM chromatograph and CR-6A integrator. The assistance of Eric Fletcher in processing the computer-generated chromatograms is gratefully acknowledged. This work was supported by the National Science Foundation (CHE-9215908).

References

[1] J.M. Davis, *J. Chromatogr.*, 449 (1988) 41.
[2] S.L. Delinger and J.M. Davis, *Anal. Chem.*, 62 (1990) 436.

[3] F.J. Oros and J.M. Davis, *J. Chromatogr.*, 550 (1991) 135.
[4] D.P. Herman, M.-F. Gonnord and G. Guiochon, *Anal. Chem.*, 56 (1984) 995.
[5] J.M. Davis and J.C. Giddings, *Anal. Chem.*, 57 (1985) 2178.
[6] F. Dondi, Y.D. Kahie, G. Lodi, M. Remelli, P. Reschiglian and C. Bighi, *Anal. Chim. Acta*, 191 (1986) 261.
[7] S. Coppi, A. Betti and F. Dondi, *Anal. Chim. Acta*, 212 (1988) 165.
[8] F. Dondi, T. Gianferrara, P. Reschiglian, M.C. Pietrogrande, C. Ebert and P. Linda, *Anal. Chim. Acta*, 485 (1990) 631.
[9] J.M. Davis, *Adv. Chromatogr.*, 34 (1994) 109.
[10] L.R. Snyder, *J. Chromatogr. Sci.*, 10 (1972) 200.
[11] J.P. Foley, *J. Chromatogr.*, 384 (1987) 301.
[12] E. Grushka and D. Israeli, *Anal. Chem.*, 62 (1990) 717.
[13] N. Dyson, *Chromatographic Integration Methods*, Royal Society of Chemistry, Cambridge, 1990.
[14] J.M. Davis and J.C. Giddings, *Anal. Chem.*, 57 (1985) 2168.
[15] J.M. Davis, *Anal. Chem.*, 66 (1994) 735.
[16] J.M. Davis, F.-R.F. Fan and A.J. Bard, *J. Electroanal. Chem.*, 238 (1987) 9.
[17] L.J. Nagels, W.L. Creten and P.M. Vanpeperstraete, *Anal. Chem.*, 55 (1983) 216.
[18] M. Martin and G. Guiochon, *Anal. Chem.*, 57 (1985) 289.
[19] M.Z. El Fallah and M. Martin, *J. Chromatogr.*, 557 (1991) 23.
[20] M. Johll, D. Bowlin and J.M. Davis, *Anal. Chim. Acta*, submitted for publication.

ELSEVIER

Journal of Chromatography A, 677 (1994) 319–329

JOURNAL OF CHROMATOGRAPHY A

Concept of additivity for a non-polar solute–solvent criterion log L^{16} Non-aromatic compounds

Pavel Havelec, Jiří G.K. Ševčík*

Department of Analytical Chemistry, Charles University Albertov 2030, CZ-128 40 Prague 2, Czech Republic

First received 8 February 1994; revised manuscript received 5 April 1994

Abstract

An additivity principle was formulated for functional and atom groups and their structural and interactional contributions to the log L^{16} criterion, expressing apolar solute–solvent interactions in gas–liquid chromatography. Numerical values were calculated for the contributions of 27 groups and 9 structural and 10 interactional contributions. The correlation coefficients between recalculated and measured values of log L^{16} for two sets, consisting of 336 monofunctional and 481 both mono- and polyfunctional compounds, were 0.998 and 0.997, respectively. The precision of the prediction of the log L^{16} criterion was tested on an independent data set, obtaining a correlation coefficient of 0.988.

1. Introduction

Since the early days of gas–liquid chromatography (GLC) much effort has been dedicated to obtaining a quantitative description of solute–solvent interactions (e.g., [1]). Among the criteria describing apolar interactions is log L^{16}, yielding a value of the solute partition coefficient in a gas–hexadecane system at 298 K [2]. This criterion includes both general dispersion interactions and the cavity term and has become an essential characteristic in linear solvation energy relationships (LSER) [2–7]. The importance of LSER concepts lies in the possibility of characterizing solute–solvent systems and predicting retention behaviour in them.

The numerical values of log L^{16} have so far been determined experimentally on both packed [2] and capillary columns [8]. In the experimental methods, attention was paid to the contributions of gas–solid, liquid–solid and gas–liquid interfacial adsorption as a source of the differences between reported values. It was shown [8] that there is a good fit for values of log L^{16} for a remeasured set of 105 non-polar and polar solutes between both experimental methods. Still, if an experimental value of log L^{16} was not available, the LSER concept could not be applied, the retention behaviour could not be predicted and an optimization procedure, i.e., the selection of a stationary phase, could not be performed in a general manner.

The concept of additivity of partial contribu-

* Corresponding author. Present address: Analytical Laboratory Systems, GmbH, Franz-von-Buhl-Strasse 2, D-67143 Deidesheim, Germany.

0021-9673/94/$07.00
SSDI 0021-9673(94)00376-K

tions has already been applied and verified in GLC for the prediction of some retention parameters, e.g., retention indices [9,10], but not for the calculation of the log L^{16} criterion. Abraham [11] demonstrated a calculation of the contributions of substituents (X) on the phenyl ring to log L^{16} for PhX compounds and the contribution of the carbon chain length in *n*-alkyl benzoate homologues, but a general approach to additivity of the log L^{16} criterion has not yet been presented.

This work was aimed at proving the validity of the principle of additivity for the calculation of log L^{16} values and demonstrating it on sets of monofunctional and polyfunctional non-aromatic compounds.

2. Results and discussion

It is assumed that the retention behaviour of compound X is the result of three contributions comprising the number of particular groups forming compound X and their structural and interactional contributions. The value of the log L^{16} criterion is then described by

$$\log(L^{16}X) = \sum_i l_i FG_i + \sum_j m_j SC_j + \sum_k n_k IC_k \quad (1)$$

where i, j, k are identification numbers of the groups (i) (see Table 1), structural contributions (j) (see Table 2) and interaction contributions (k) (see Table 3), l, m, n are the values of the regression coefficients in Eq. 1 for the contribution of a particular group (l) (see Table 1), a structural contribution (m) (see Table 2) and an interactional contribution (n) (see Table 3) and FG, SC, IC are the numbers of particular groups (FG) forming compound X (see Table 1), structural (SC) (see Table 2) and interactional (IC) (see Table 3) contributions.

Published data on log L^{16} [3,4] were used for the analysis of the additivity hypothesis according to Eq. 1. Two data sets were formed to prove the effect of interactional contributions on the additive model of log L^{16}. The first data set (set A) contained only monofunctional compounds, a total of 336 compounds, and the second data set (set B) contained both mono- and polyfunctional compounds, a total of 481 compounds (see Appendix). For these data sets A and B, 27 types of group contributions FG (see Table 1), 9 types of structural contributions SC (see Table 2) and 10 types of interactional contributions IC (see Table 3) were specified.

The method of multi-linear correlation was applied to solve Eq. 1 by means of the matrix according to Eq. 2 for both data sets of 336 compounds (set A) and 481 compounds (set B). In Eq. 2 $FG_{x,i}$ are integral numbers of particular groups i forming compound X (see Table 1), $SC_{x,j}$ are integral numbers of particular structural contributions j in compound X (see Table 2) and $IC_{x,k}$ are integral numbers of interactional contributions k within compound X (see Table 3).

The results of the analysis of the matrix (Eq. 2) are sets of formal regression coefficients l_1 to l_{27}, m_1 to m_9 and n_1 to n_{10} such as given in Table 1 (the effect of group contributions), Table 2 (the effect of structural contributions) and Table 3 (the effect of interactional contributions).

log ($L^{16}X$)	i 1 to 27	j 1 to 9	k 1 to 10
X 1 to 336 or 1 to 481	$FG_{1,1} \cdots FG_{1,27}$	$SC_{1,1} \cdots SC_{1,9}$	$IC_{1,1} \cdots IC_{1,10}$
	$\vdots$	$\vdots$	$\vdots$
	$FG_{x,i}$	$SC_{x,j}$	$IC_{x,k}$
	$\vdots$	$\vdots$	$\vdots$
	$FG_{481,1} \cdots FG_{481,27}$	$SC_{481,1} \cdots SC_{481,9}$	$IC_{481,1} \cdots IC_{481,10}$

(2)

Table 1
Regression coefficients l_i, their standard deviations s_l and frequencies x_l for group i calculated form Eq. 1 for data sets A and B

i	Structure	Set A			Set B		
		l_i	s_l	x_l	l_i	s_l	x_l
1	CH_3—	0.333	0.009	620	0.358	0.009	834
2	—CH_2—	0.504	0.002	1256	0.499	0.002	1492
3		0.488	0.016	129	0.437	0.017	193
4		0.456	0.029	30	0.350	0.032	46
5	H_2C=	0.198	0.027	13	0.280	0.020	59
6	—HC=	0.471	0.022	21	0.450	0.017	77
7		0.567	0.050	4	0.609	0.024	20
8	HC≡	0.085	0.034	11	0.063[a]	0.046	13
9	—C≡	0.595	0.035	11	0.558	0.046	13
10	F—	−0.114	0.045	4	−0.121	0.060	11
11	Cl—	0.894	0.030	9	0.786	0.020	50
12	Br—	1.293	0.027	11	1.319	0.036	13
13	I—	1.766	0.034	7	1.756	0.046	8
14	—O—	0.302	0.026	16	0.346	0.016	114
15	—CHO	0.982	0.026	13	1.014	0.030	18
16	—CO—	1.098	0.023	22	1.087	0.025	34
17	HCOO–	1.078	0.028	11	1.070	0.035	12
18	—COO—	1.108	0.019	43	1.105	0.020	65
19	—COOH	1.589	0.024	15	1.590	0.032	15
20	—CN	1.213	0.029	10	1.209	0.039	10
21	—NH_2	0.798	0.032	8	0.791	0.043	8
22		0.746	0.047	4	0.711	0.062	4
23		0.575	0.068	2	0.508	0.089	2
24	—NO_2	1.524	0.034	7	1.518	0.046	7
25	—OH	0.739	0.015	52	0.762	0.015	101
26	—SH	1.312	0.026	13	1.323	0.033	14
27	—S—	1.435	0.037	7	1.406	0.048	7

[a] Statistically not significant.

The value of the regression coefficient l_i describes the significance of the contribution of a particular group to the retention behaviour of compound X. The numerical values of l_i vary from −0.121 for fluorine to 1.756 for iodine, and the value of the statistical error of estimation of the regression coefficient varies from 0.002 to 0.060 for the whole data set (see Table 1). The best precision of estimation was attained for the –CH_2– group (0.4%), and the worst for the HC≡ group (75%). The values of the regression coefficient l_i have been ordered according to their absolute values and it was found that there are significant differences between the groups, especially between those containing oxygen and those without oxygen atom (see Fig. 1). The results presented in Fig. 1 demonstrate the relative importance of a particular group to the

Table 2
Regression coefficients m_j, their standard deviations s_m and frequencies x_m of specified structural contributions j calculated from Eq. 1 for data sets A and B

j	Structure	Set A			Set B		
		m_j	s_m	x_m	m_j	s_m	x_m
1	3-Ring				0.117[a]	0.064	6
2	4-Ring				0.182	0.092	2
3	5-Ring	0.001[a]	0.037	8	0.060[a]	0.040	12
4	6-Ring	0.040[a]	0.033	14	0.084	0.035	18
5	7-Ring	0.169	0.042	6	0.207	0.052	6
6	8-Ring	0.299	0.090	1	0.337	0.121	1
7	*trans*	−0.090[a]	0.079	2	−0.027[a]	0.046	9
8	*cis*	0.074[a]	0.062	3	0.094[a]	0.061	5
9	Oxygen atom in ring				0.051[a]	0.030	22

[a] Statistically not significant.

Table 3
Regression coefficients n_k, their standard deviations s_n and frequencies x_n of interactional contributions k calculated from Eq. 1 for data sets A and B

k	Structure	Set A			Set B		
		n_k	s_n	x_n	n_k	s_n	x_n
1					0.152	0.073	4
2					−0.117	0.025	24
3					0.715	0.041	4
4					1.602	0.128	1
5					−0.012[a]	0.043	6
6	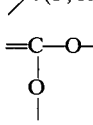				−0.083	0.033	31
7	—COCO—				−0.128[a]	0.088	2
8	—$COCH_2CO$—				0.471	0.122	1
9	—$COOC_nH_{2n}$— —OOC— (n=1—3)				1.163	0.063	4
10	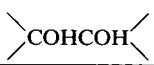				0.146	0.060	5

[a] Statistically not significant.

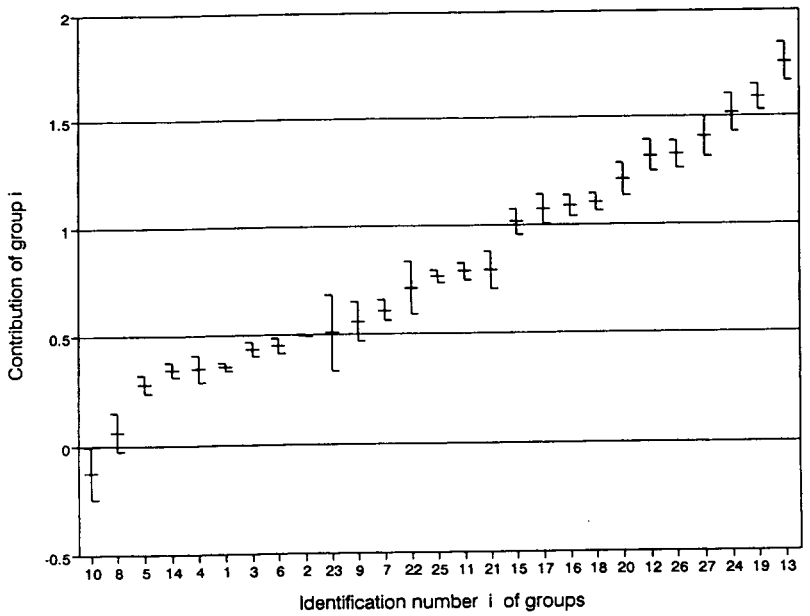

Fig. 1. Values of regression coefficient l_i vs. magnitude of contribution of group FG_i for data set B as given in Table 1. The bar length represents the precision of estimation ($l_i \pm s_l$).

retention behaviour of compound X in a GLC system where apolar solute–solvent interactions predominate. It is of interest that the smallest value of the regression coefficient l_i was found for fluorine and the highest value for iodine. This effect could possibly be related to the polarizability of these atoms. A detailed examination of this observation will be the subject of further physico-chemical studies.

The value of the regression coefficient m_j describes the role of the structural arrangement, especially the size of the ring in compound X. The numerical values of coefficient m_j are smaller then those of l_i and thus the role of the structural, cyclic arrangement is less important for the retention behaviour than the role of the group contributions. The precision of the estimated regression coefficients m_j was significantly poorer (around 50%) than that for group contribution l_i and it could only be speculated that either an insufficient number of input data were used or that the selected structural contributions specified in Table 2 were of limited significance.

The value of the regression coefficient n_k describes the role of interactional contributions between neighbouring groups bonded to a common carbon atom. The values of the coefficient n_k are both positive and negative, as can be expected from general theories of interactions. The numerical value of n_k varies over a broad range (see Table 3), similar to the range of coefficient l_i, and it can be interpreted as an indication that interactional contributions are highly important for the description of additivity of the log L^{16} criterion. Based on the differences between the calculated and measured values of log L^{16} for polyfunctional compounds, it can be assumed that there are some cross-linked interactions over the carbon chain length. This effect was not proved by the data sets used and it would be a subject of further studies.

A test of the significance of the differences in the regression coefficients l_i and m_j between data set A and data set B was used to assess the importance of the individual contributions. Only monofunctional compounds were selected for data set A, whereas data set B consisted of both mono- and polyfunctional compounds. Hence if

Table 4
Test of statistical significance of differences in regression coefficients l_i and m_j for data sets A and B

Coefficient	Structure	Result of σ-test[a]	Significance level (%)
l_1	CH_3—	1.919	94.5
l_2	—CH_2—	1.831	93.3
l_3	—CH<	2.257	97.6
l_4	>C<	2.445	98.6
l_5	H_2C=	2.466	98.6
l_6	—HC=	0.725	53.2
l_7	>C=	0.740	54.1
l_8	HC≡	0.384	29.9
l_9	—C≡	0.644	48.0
l_{10}	F—	0.093	7.4
l_{11}	Cl—	2.995	99.7
l_{12}	Br—	0.570	43.2
l_{13}	I—	0.176	14.0
l_{14}	—O—	1.408	84.1
l_{15}	—CHO	0.813	58.4
l_{16}	—CO—	0.342	26.8
l_{17}	HCOO—	0.167	13.3
l_{18}	—COO—	0.080	6.4
l_{19}	—COOH	0.027	2.2
l_{20}	—CN	0.070	5.6
l_{21}	—NH_2	0.145	11.5
l_{22}	>NH	0.455	35.1
l_{23}	—N<	0.603	45.3
l_{24}	—NO_2	0.115	9.2
l_{25}	—OH	1.055	70.9
l_{26}	—SH	0.266	21.0
l_{27}	—S—	0.482	37.0
m_3	5-Ring	1.071	71.6
m_4	6-Ring	0.910	63.7
m_5	7-Ring	0.568	43.0
m_6	8-Ring	0.253	19.9
m_7	*trans*	0.686	50.8
m_8	*cis*	0.239	18.9

[a] The σ-test was carried out according to the following expressions:

$$\sigma = \frac{|l_i(\mathrm{A}) - l_i(\mathrm{B})|}{[s_l(\mathrm{A})^2 + s_l(\mathrm{B})^2]^{0.5}}$$

or

$$\sigma = \frac{|m_j(\mathrm{A}) - m_j(\mathrm{B})|}{[s_m(\mathrm{A})^2 + s_m(\mathrm{B})^2]^{0.5}}.$$

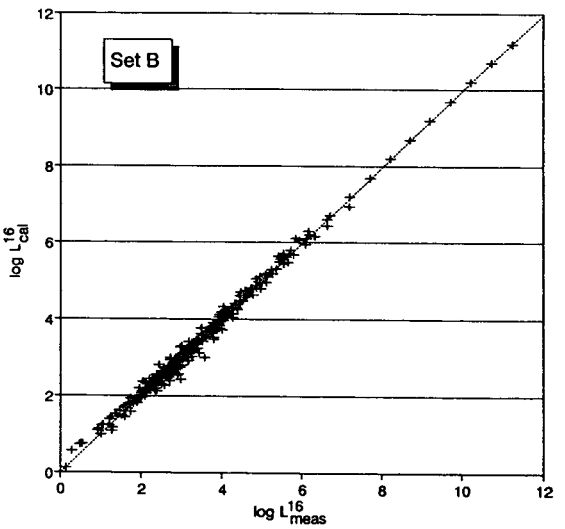

Fig. 2. Functional dependence of criterion log L^{16}_{cal} vs. log L^{16}_{meas} for data set B (see Appendix). Total number of analysed compounds $X = 481$; slope = 1; correlation coefficient $r = 0.997$.

there is a statistically significant difference $[(l_i)_{\text{set A}} <> (l_i)_{\text{set B}}]$, the interactional contributions n_k will be of importance, in addition to the group and structural contributions. The results of the test are given in Table 4. It was found that

Table 5
Summarized data of linear regression analysis of calculated and measured values of the criterion log L^{16} for monofunctional (set A) and mono- and polyfunctional (set B) compounds according to Eq. 3

Characterization of sets	Set A	Set B
No. of compounds	336	481
Degrees of freedom	303	435
Log L^{16}_{min}	0.15	0.15
Log L^{16}_{max}	11.25	11.25
Log L^{16}_{mean} ($\bar{x}_{set}$)	3.57	3.40
No. of functional groups	27	27
No. of structural contributions	6	9
No. of interaction contributions	0	10
Correlation coefficient (r)	0.998	0.997
Standard deviation (s)	0.089	0.120
Maximum error (me)	0.309	0.573
Mean statistical error (v, %)	2.491	3.518

$$me = \max|\log L^{16}_{\text{estimated}} - \log L^{16}_{\text{measured}}|.$$

$$v = 100 \cdot \frac{s_{\text{set A (B)}}}{\bar{x}_{\text{set A (B)}}}.$$

the regression coefficient l_i differs between data sets A and B at different statistical levels, and a significance higher than 95% was found for groups such as —CH<, >C<, H_2C= and Cl, i.e., groups providing a large numbers of different interactional contributions. Hence the description of additivity principle of log L^{16} according to Eq. 1, consisting of three types of contribution, group, structural and interactional, is correct.

Based on the calculated values of the regression coefficients l_i, m_j and n_k (see Tables 1, 2 and 3, respectively), the values of log L^{16}_{cal} were calculated for the original sets of input compounds and the significance of their fit to the measured data was estimated from linear regression analysis: see Eq. 3a for set A, Eq. 3b for set B and Eq. 3c for set C.

$$\log L^{16}_{cal(A)} = 1.000(\pm 0.001)\log L^{16}_{meas(A)} \quad (3a)$$

$$\log L^{16}_{cal(B)} = 0.999(\pm 0.001)\log L^{16}_{meas(B)} \quad (3b)$$

$$\log L^{16}_{cal(C)} = 0.993(\pm 0.006)\log L^{16}_{meas(C)} \quad (3c)$$

The difference between the slope values found with Eqs. 3a, 3b and 3c and the predefined value of 1.00 are statistically not significant and further

Table 6
Examples of prediction of log L^{16}_{pred} values and their comparison with the measured values

Compound[a]	Log L^{16}_{meas}	Contribution		Log L^{16}_{pred}	
		Type	Amount	Partial	Total
Adamantane		*l*2	6	6 · 0.499	
		*l*3	4	4 · 0.437	
		*m*4	4	4 · 0.084	
	5.095				5.078
Methoxyflurane		*l*1	1	1 · 0.358	
		*l*3	1	1 · 0.437	
		*l*4	1	1 · 0.350	
		*l*10	2	2 · (−0.121)	
		*l*11	2	2 · 0.786	
		*l*14	1	1 · 0.346	
		*n*1	1	1 · 0.152	
		*n*2	1	1 · (−0.117)	
	2.864				2.856
3,4-Dihydropyran		*l*2	3	3 · 0.499	
		*l*6	2	2 · 0.450	
		*l*14	1	1 · 0.346	
		*m*4	1	1 · 0.084	
		*m*9	1	1 · 0.051	
	2.910				2.876

[a] Structures of the compounds are as follows:

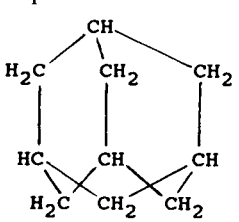

adamantane

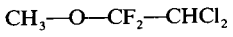

methoxyflurane

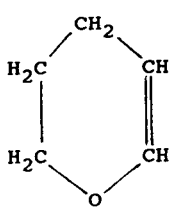

3,4-dihydropyran

Table 7
List of compounds in data set C and their evaluation

Compound	Log L^{16}_{meas} [a]	Log L^{16}_{pred} [b]	Difference
Ethylcyclohexane	3.877	3.873	0.004
Cyclohexylcyclohexane	6.434	6.032	0.402
Adamantane	5.095	5.076	0.019
cis-2-Methyldecaline	5.550	5.329	0.221
2-Methyl-2-butene	2.226	2.132	0.094
2-Methyl-2-pentene	2.588	2.631	−0.043
3-Methylcyclohexene	3.379	3.276	0.103
4-Methylcyclohexene	3.372	3.276	0.096
Cyclooctene	4.119	4.232	−0.113
1,3-Cyclohexadiene	2.917	2.884	0.033
1,4-Cyclohexadiene	3.132	2.884	0.284
1,3-Cycloheptadiene	3.607	3.506	0.101
1,5-Cyclooctadiene	4.300	4.135	0.165
1,3,5-Cycloheptatriene	3.442	3.408	0.034
1,3,5,7-Cyclooctatetraene	3.884	3.940	−0.056
α-Pinene	4.200	4.620	−0.420
Dicyclopentadiene	4.651	4.726	−0.075
Fluorocyclohexane	3.215	2.894	0.321
Iodocyclohexane	4.785	4.772	0.013
1-Chlorocyclohexene	3.990	3.925	0.065
1-Bromocyclohexene	4.350	4.458	−0.108
1-Bromo-4-methylcyclohexene	4.669	4.753	−0.084
1-Iodocyclohexene	4.838	4.895	−0.057
Fluorotrichloromethane	1.995	2.200	−0.205
Methyl cyclohexyl ether	3.861	3.719	0.142
1,2-Dimethoxyethane	2.565	2.405	0.160
trans-2-Hexen-1-al	3.400	3.244	0.156
trans-2-Hepten-1-al	3.897	3.743	0.154
Carvone	5.330	5.269	0.061
Ethyl trimethylacetate	3.481	3.386	0.095
Cyanocyclohexane	4.333	4.225	0.108
Isopentylamine	3.058	2.941	0.117
Cyclohexylamine	3.796	3.806	−0.010
3-Methylcyclohexylamine	4.125	4.102	0.023
Diisobutylamine	3.901	4.014	−0.113
Tripropylamine	4.229	4.576	−0.347
Nitrocyclohexane	4.826	4.533	0.293
3,4-Dihydropyran	2.910[c]	2.878	0.032
Cyclooctanone	4.981[c]	4.917	0.064
Allylamine	2.268[c]	2.021	0.247
Cyclopropylcarbinol	2.675[c]	2.813	−0.138
Diallyl sulphide	3.750[c]	3.866	−0.116
1,1,1,2-Tetrachloroethane	3.641[d]	3.641	0.000
Isopentyl isopentanoate	4.580[e]	4.907	−0.327
Methyl heptanoate	4.356[f]	4.316	0.040
Methyl octanoate	4.838[f]	4.815	0.023
Methyl nonanoate	5.321[f]	5.314	0.007
Methyl decanoate	5.803[f]	5.813	−0.010
Methyl undecanoate	6.285[f]	6.312	−0.027

[a] Measured values of log L^{16}_{meas} are from [11], except where indicated otherwise.
[b] Predicted values of log L^{16}_{pred} were calculated from sets of regression coefficients l_i (Table 1), m_j (Table 2) and n_k (Table 3).
[c] From [3].
[d] From [12].
[e] From [5].
[f] From [13].

statistical evaluations, such as given in Tables 5 and 8, were carried out under this assumption.

The analysis results in correlation coefficients of 0.998 for data set A and 0.997 for data set B. These data demonstrate that the functional dependence is statistically significant and thus lead to confirmation of the hypothesis of additivity of partial contributions for calculation of the criterion log L^{16}. Fig. 2 demonstrates this dependence and Table 5 lists the data for the regression analysis according to Eqs. 3. It should be pointed out that the errors of estimation of the log L^{16}_{cal} values are small (about 3%) and can probably be further minimized by using additional data sets and describing the particular contributions to the log L^{16} criterion is more detail.

The predictive power of the additivity concept of the criterion log L^{16} and the precision of prediction were tested on an independent data set C for compounds that were not used for the calculation of the regression coefficients (the compounds were not included in either data set A or B). The compounds in set C were split into elementary contributions of groups, structural and interactional contributions (see Tables 1, 2 and 3, respectively) and their values of log L^{16}_{pred} were calculated (examples are given in Table 6). The predicted values of log L^{16}_{pred} were compared with the measured log L^{16}_{meas} values for data set C by means of linear regression according to Eq. 3c. A list of the compounds in data set C and the measured and predicted values of log L^{16} are given in Table 7 and summarized data of the regression analysis in Table 8 and Fig. 3. It can be seen that the prediction based on Eq. 1 yields good results for a whole set of complex compounds exhibiting all kinds of contributions. A correlation coefficient of 0.987 was found for the function log L^{16}_{pred} = log $L^{16}_{meas\ c}$ and thus applicability of the additivity principle to the prediction of the values of the criterion log L^{16} was verified. Comparing the correlation coefficients for functional dependences log L^{16}_{cal} = log L^{16}_{meas} ($r = 0.997$) and log L^{16}_{pred} = log L^{16}_{meas} ($r = 0.988$), it can be seen that both data sets B and C could be merged and used for confirmation of predictability of the criterion log L^{16} on the principle of additivity of partial contributions.

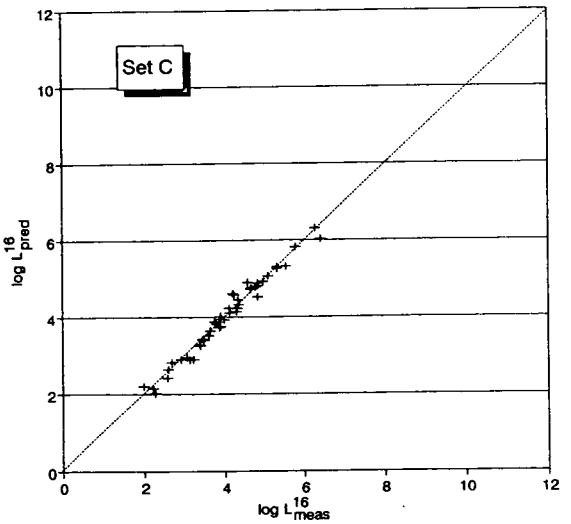

Fig. 3. Functional dependence of criterion log L^{16}_{pred} vs. log L^{16}_{meas} for data set C (see Table 7). Total number of predicted values of log $L^{16}_{pred} = 49$; slope = 1; correlation coefficient $r = 0.988$.

Table 8
Summarized data of regression analysis of functional dependence of log L^{16}_{pred} vs. log L^{16}_{meas} according to Eq. 3 for data set C (see Table 7)

Characterization of set	Set C
No. of compounds	49
Log L^{16}_{min}	1.995
Log L^{16}_{max}	6.434
Log L^{16}_{mean} ($\bar{x}_{set}$)	4.017
Correlation coefficient (r)	0.988
Standard deviation (s)	0.163
Maximum error (me)	0.402
Mean statistical error (v, %)	4.05

For definitions of me and v, see Table 5.

3. Conclusions

The results of the analysis of data sets containing 336 and 481 compounds confirm the hypothesis of additivity of partial contributions for calculation of the log L^{16} criterion, as a measure of apolar solute–solvent interactions in GLC. It was shown that, in addition to the

contribution of groups, there are important structural and interactional contributions. The significant correlation between the calculated and measured values of log L^{16} (a correlation coefficient of 0.997) demonstrates that the proposed additivity form according to Eq. 1 is correct.

The mean statistical relative errors of the estimation of log L^{16}_{cal} for data sets A and B (see Appendix) were 2.49% and 3.52%, respectively. In other words, the error of calculation is of about the same order of magnitude as the experimental errors [11].

The prediction power of the present concept was tested on an independent data set and a correlation coefficient of 0.988 between the predicted and measured values of log L^{16} was found. We are convinced that it is an unequivocal advantage to have an access to one of the general criteria of solute–solvent interactions by means of calculation, especially from the point of view of optimization procedures carried out by GLC expert systems.

Appendix

A list of compound types and their abundance in data sets A and B used for testing of additivity character of the log L^{16} criterion is given below

Type of compound	Set A	Set B
Alkanes	41	41
Cycloalkanes	11	11
Alkenes	13	13
Cycloalkenes	6	6
Alkadienes		3
Alkynes	11	11
Monofluoroalknes	4	4
Monochloroalkanes	8	8
Chlorocycloalkanes	1	1
Polychloroalkanes		8
Polychloroalkenes		4
Monobromoalkanes	10	10
Bromocycloalkanes	1	1
Polybromoalkanes		2
Monoiodoalkanes	7	7
Polyiodoalkanes		1
Dialkyl ethers	16	17
Cycloalkyl ethers		12
Alkyl alkyl diethers		23
Cycloalkyl diethers		2
Alkyl alkyl triethers		2
Cycloalkyl triethers		2
Alkyl alkenyl ethers		4
Dialkenyl ethers		1
Alkyl alkenyl diethers		1
Difluorotetrachloroalkanes		2
Alkanals	13	13
Alkenals		4
Alkadienals		1
Alkanones	19	19
Cycloalkanones	3	3
Alkenones		4
Alkadiones		3
Alkyl formates	11	11
Alkyl acetates	19	20
Cycloalkyl acetates	1	1
Alkyl propanoates	10	10
Alkyl butanoates	10	10
Alkyl isobutanoates	3	3
Alkyl acrylates		6
Alkenyl carboxylates		8
Alkoxy carboxylates		4
Alkylenedicarboxylates		4
Cyanoalkanes	10	10
Alkylamines	8	8
Dialkylamines	4	4
Trialkylamines	2	2
Nitroalkanes	7	7
Carboxylic acids	15	15
Alkanols	48	48
Cycloalkanols	4	4
Alkanediols		8
Alkenols		12
Alkynols		2
Chloroalkanols		1
Alkoxyalkanols		11
Alkenoxyalkanols		1
Hydroxyalkanones		5
Trifluoroalkanols		1
Alkanethiols	13	13
Alkenethiols		1
Dialkyl sulphides	7	7

References

[1] L. Rohrschneider, *J. Chromatogr.*, 22 (1966) 6.
[2] M.H. Abraham, P.L. Grellier and R.A. McGill, *J. Chem. Soc., Perkin Trans.* 2, (1987) 797.
[3] M.H. Abraham, G.S. Whiting, R.M. Doherty and W.J. Shuely, *J. Chromatogr.*, 587 (1991) 213.
[4] M.H. Abraham, *Chem. Soc. Rev.*, 110 (1993) 73.
[5] M.H. Abraham, G.S. Whiting, R.M. Doherty and W.J. Shuely, *J. Chem. Soc., Perkin Trans. 2*, (1990) 1451.
[6] M.H. Abraham, G.S. Whiting, R.M. Doherty and W.J. Shuely, *J. Chem. Soc. Perkin Trans. 2*, (1990) 1851.
[7] M.H. Abraham, G.S. Whiting, R.M. Doherty and W.J. Shuely, *J. Chromatogr.*, 518 (1990) 329.
[8] Y. Zhang, A.J. Dallas and P.W. Carr, *J. Chromatogr.*, 638 (1993) 43.
[9] V. Tekler, G. Tarjan and J.M. Takacs, *J. Chromatogr.*, 406 (1987) 131.
[10] P.H. Weiner and D.G. Howery, *Anal. Chem.*, 44 (1972) 1189.
[11] M.H. Abraham, *J. Chromatogr.*, 644 (1993) 95.
[12] M.H. Abraham, G.S. Whiting, R.M. Doherty and W.J. Shuely, *J. Chromatogr.*, 587 (1991) 229.
[13] M.H. Abraham, J. Andonian-Haftvan, I. Hamerton, C.F. Poole and T.O. Kollie, *J. Chromatogr.*, 646 (1993) 351.

ELSEVIER

Journal of Chromatography A, 677 (1994) 331–343

JOURNAL OF CHROMATOGRAPHY A

Fast and accurate method for the automatic prediction of programmed-temperature retention times

S. Vezzani, P. Moretti, G. Castello*

Istituto di Chimica Industriale, Corso Europa 30, 16132 Genova, Italy

First received 22 February 1994; revised manuscript received 6 April 1994

Abstract

Six calculation methods for the prediction of the retention times in programmed-temperature gas chromatography by starting from isothermal data were applied to capillary column analysis. The minimum number of isothermal runs necessary to obtain accurate results was evaluated. The application of the various methods and the accuracy of the prediction are discussed. A quadratic interpolation method which requires only three isothermal retention values as the starting data was found suitable and easily applied to computer programs.

1. Introduction

The prediction of retention times in programmed-temperature gas chromatography (PTGC) by using computer programs which employ as input data retention values measured under isothermal analytical conditions is a procedure of considerable interest in routine work. To predict the retention times of the component of a sample in all the possible programmed runs permits one to select the best conditions for the separation, mainly when the different polarities of the compounds result in peak coincidence or inversion of the elution order. The conditions yielding the shortest possible analysis time can also be found.

Many methods have been suggested [1–21] and a comparison of the precisions of four of them was published previously [22]. The simplest methods can be easily applied by BASIC programming on a personal computer, by inputting a few initial data: the retention times in few isothermal analyses, the initial temperature of the programmed run, the length of the initial isothermal stage and the temperature gradient.

The increasing computerization of GC instruments, obtained by on-line connection to integrators and data systems or by direct use of built-in microprocessors, nowadays enables one to perform quantitative analysis and to calculate some parameters useful for the correct separation, e.g., the carrier gas velocity and the dead time [23,24]. Dedicated software is also available for this equipment, applied to simulated distillation, retention index calculation, peak deconvolution, gel permeation calculation, etc. It therefore seems possible to add to these software packages some options that automatically predict the PTGC retention times by starting from isothermal runs, whose parameters and results are directly transferred from the data system memory to the input section of the prediction program.

* Corresponding author.

0021-9673/94/$07.00
SSDI 0021-9673(94)00375-J

For easy application, such a program should follow a systematic approach, permit the choice of a few initial parameters by the operator, give accurate results and require a limited number of initial isothermal analyses. In order to establish what is the minimum number of isothermal runs that permit a suitable accuracy in the prediction of PTGC retention times, and to select the simplest, most accurate and fastest program, several different prediction methods were tested, by using as the starting values a variable number of isothermal data (from 3 to 25). The results obtained with six methods are discussed and some suggestions on their application to automatic prediction programs are given.

2. Experimental

A Model 3600 gas chromatograph (Varian, Palo Alto, CA, USA) equipped with a split–splitless injector and a flame ionization detector was used for isothermal (IT) and programmed-temperature (PT) analyses. Fused-silica capillary columns (30 m × 0.32 mm I.D.) were used (Supelco, Bellefonte, PA, USA): a non-polar polydimethylsiloxane (SPB-1), a polar polyglycol (Supelcowax-10) and a carbon layer open-tubular (CLOT) column partially deactivated with polyglycol [20,21].

The analyses were carried out on the three columns in the range 60–190°C, at 10°C intervals for SPB-1 and Supelcowax-10 columns and at 5°C intervals for the CLOT column, by using samples containing all the compounds listed in Tables 2–4. They were selected in order to represent the different polarity classes [25], containing both electron-donor atoms and active hydrogen (chloroanilines), donor atoms but not active hydrogen (nitro- and chloronitrobenzenes), π-electrons of the aromatic ring (naphthalene) more or less influenced by the inductive effect of halogens in different positions (chlorobenzenes). Linear alkanes (C_7–C_{22}) and alcohols (C_5–C_{13}) were also added to the sample to represent the two classes of low-polarity (purely dispersive forces) and high hydrogen bonding capacity, respectively. The presence of linear alkanes and alcohols also permitted the determination of the polarity of the columns with the ΔC method [26,27]. PT analyses were made with different initial temperatures, T_i, initial length of the isothermal stage, t_i, and programming temperature rate, g.

The built-in flow control of the instrument was designed in order to maintain the inlet pressure to the column constant during both isothermal and programmed-temperature analyses. As temperature increases, the gas viscosity and column resistance increase, thus changing the flow-rate. Constant mass flow pneumatic controllers, designed to maintain a constant carrier gas input during the programme, are not reliable in this instance. In fact, differential systems sense the flow-rate and increase the upward pressure on a diaphragm in order to compensate for the increase in column back-pressure with increasing temperature. The available systems installed in many commercial GC instruments can maintain a constant flow-rate over a wide temperature range when packed columns are used at relatively high gas flow-rates (20–60 $cm^3\ min^{-1}$). We checked experimentally that, when wide-bore capillary columns are installed without splitting systems so that all the carrier gas stream is dispatched to the column, commercially available differential controllers can maintain a constant flow-rate as low as 3 $cm^3\ min^{-1}$ over the temperature programming range 50–250°C.

However, when narrow-bore columns are used in conjunction with a splitting system, the column back-pressure due to the increase in gas viscosity with temperature has a negligible effect with respect of the prevailing amount of gas flowing through the splitter line. Therefore, the mass flow controllers which keep the overall flow-rate constant do not ensure constancy of the linear velocity into the column.

Further, split–splitless systems, which open and close the split line when the sample is injected, cause fluctuations in the flow regulator that influence the carrier velocity at the beginning of the analysis. It is easier to keep the inlet pressure constant and therefore this solution is generally selected by many producers of capillary GC instruments. When the column inlet and

outlet pressures are known, the use of Poiseuille's law permits one to calculate the linear gas velocity in the column at any temperature and to obtain the gas hold-up time which is used in the calculation described below.

The prediction of the PT retention times was carried out by BASIC programming on IBM and COMPAQ personal computers with all the calculation methods described under Theory. As the starting values were used the IT retention times measured with a precision of ±0.001 min, using a Varian DS-650 data system in all the isothermal runs or in three of them selected at the lowest, the highest and one intermediate temperature. The predicted PT values were compared with those measured experimentally during many programmed-temperature runs with different initial temperatures and various programming rates. The built-in BASIC option of the DS-650 can also be programmed in order to capture the raw data recorded by the integration system during isothermal analyses and to apply on-line the prediction procedures.

3. Theory

The general equation used for the prediction of programmed-temperature retention times, $PT t_R$, is [1,2,7,8]

$$g = \int_{T_i}^{T_f} \frac{dT}{t_R(T)} \quad (1)$$

where T_i is the initial temperature of the programmed run, T_f is the temperature at which a given compound is eluted from the column, g is the temperature gradient and $t_R(T)$ is the function which represents the dependence of the retention time of that compound on the change in temperature. The main problems of the prediction are to find the function $t_R(T)$ which gives the best approximation to the experimental values of t_R with changing temperature and to solve the integral of Eq. 1 for a value of T_f that satisfies the equation.

For all the methods used, except that suggested by Said [7,8], the integration of Eq. 1 was carried out with the trapezoid method [22,28–31], and the difference between the various procedures is due only to the choice of the function $t_R(T)$. Three different expressions of this function were selected:

$$t_R(T) = A + \exp\left(\frac{B}{T} + C\right) \quad (2)$$

$$t_R(T) = t_M(T)\left[1 + \exp\left(\frac{B'}{T} + C'\right)\right] \quad (3)$$

$$t_R(T) = t_M(T)\left[1 + \exp\left(\frac{A''}{T} + B'' + C''T\right)\right] \quad (4)$$

where $t_M(T)$ is the gas hold-up time (or dead time) necessary for the carrier gas to travel along the column, and introduces into the equations the dependence of the retention time on temperature, through the change of the dynamic viscosity of the carrier gas $\mu(T)$. The different methods that can be used for the determination of $t_M(T)$ were described previously [24,32–36].

The gas hold-up time can be measured by manual or electronic flow meters, deduced by the retention time of methane or calculated theoretically as follows.

When the pressure at the column inlet is constant and exactly known, the application of Poiseuille's law permits one to obtain the $t_M(T)$ (min) value:

$$t_M(T) = \frac{16L^2\mu(T)}{60jr^2} \cdot \frac{P_o}{P_i^2 - P_o^2} \quad (5)$$

where L = column length (cm), r = column radius (cm), P_o = column outlet pressure (absolute) (dyn cm^{-2}), P_i = column inlet pressure (absolute) (dyn cm^{-2}), j = pressure gradient correction factor of James and Martin [37] and $\mu(T)$ = dynamic viscosity of the carrier gas used (poise). $\mu(T)$ depends on temperature and can be obtained from tabulated data or calculated with exponential or quadratic expressions [24,38].

The various procedures used for solving Eq. 1 are briefly described below; for a full description and discussion, the reader should consult the listed references.

3.1. Said's method

Said's method [7,8] (indicated with the subscript X in the text and in the tables) is essentially based on the function reported in Eq. 2. The coefficients A, B and C were calculated by using the values of the isothermal retention times (IT_{R}) measured at three temperatures only: the lowest, the highest and an intermediate value in the temperature range of the column used.

3.2. Trapezoids method

The trapezoids method (subscript T) [22,25–28] also employs the function of Eq. 2 and the same coefficients as in Said's method, but the integral of Eq. 1 was solved by using the trapezoids rule, and IT_{R} values measured at three temperatures only were used.

3.3. Interpolation method

This method (subscript I) was applied by using the function of Eq. 3 whose coefficients B' and C' were obtained by linear interpolation with the least-squares method of all the experimental IT_{R} values obtained at 5 or 10°C intervals within the range 60–190°C. The functions of Eq. 3 and that of Eq. 4 discussed below describe the dependence of the retention time on the values of t_{M} and of the capacity factor k' [39–46]:

$$t_{R}(T) = t_{M}(T)(1 + k') \tag{6}$$

where k' is expressed by

$$k' = \beta \exp(\Delta G/RT) \tag{7}$$

where β is the phase ratio of the column, ΔG is the free energy of solution or partition of a given compound between the gas and liquid phases, R is the universal gas constant and T the absolute temperature. By taking into account the classical thermodynamic equation

$$\Delta G = \Delta H - T\,\Delta S \tag{8}$$

Eq. 7 can be rewritten as

$$k' = \exp\left(\ln \beta + \frac{\Delta H}{RT} - \frac{\Delta S}{R}\right) \tag{9}$$

The term β can be considered as a constant while both ΔH and ΔS depend on temperature [40,41,47,48]. If these thermodynamic parameters are taken as constants, the combination of Eqs. 6 and 9 is equivalent to the function of Eq. 3. The values of PT_{R} predicted with method I differ from the experimental values more that those obtained with the Said (X) and trapezoids (T) methods, notwithstanding the greater number of IT_{R} values used for interpolation. This confirms that the hypothesis of ΔH and ΔS being completely independent of temperature cannot be accepted. One can suppose that this dependence can be neglected for small temperature intervals and, by using a great number of isothermal runs differing by only 5 or 10°C, calculate the values of the coefficients B' and C' for every small temperature interval. The integral of Eq. 1 was therefore solved by using for each temperature step the corresponding pair of B' and C' coefficients. This procedure, differing from the linear interpolation method (I), is indicated with the subscript S (step) and, as shown below, predicts PT_{R} with a good approximation to the experimental results.

Further, as the procedure yields a large number of B' and C' pairs, each of them corresponding to a narrow temperature range or, to a first approximation, to the average temperature for that interval, their values can be correlated with thermodynamic functions, with the polarity of the column and with its dependence on temperature. The main difficulty in the application of the step interpolation method (S) for routine work is that it requires a large number of isothermal runs and therefore is more time consuming than the Said and trapezoids methods.

Our experimental results, however, show that the ΔH and ΔS can be considered with a suitable approximation to depend linearly on temperature. Fig. 1 shows for some compounds taken as examples the linear dependence of B' and C' on temperature. As these coefficients are proportional to ΔH and ΔS, respectively, as follows:

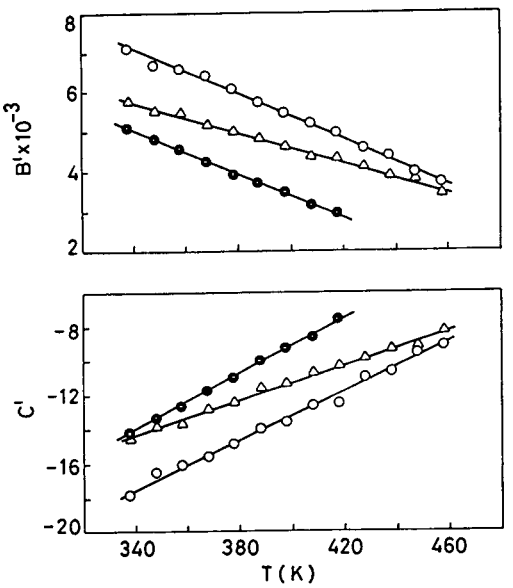

Fig. 1. Experimental values of the coefficients of Eq. 3, B' (upper graph) and C' (lower graph), as a function of temperature, for (●) *n*-dodecane, (○) *n*-octanol and (△) 1,4-dichlorobenzene on a Supelcowax 10 column. The slope of the regression lines are given in Table 1.

$$B' = \Delta H/R \tag{10}$$

$$C' = \ln \beta - (\Delta S/R) \tag{11}$$

β and R being constants, the thermodynamic parameters also vary linearly with the column temperature.

Table 1 shows the values of the slope and of the correlation coefficient of B' and C' versus absolute temperature for eight compounds representative of the various polarity classes on the three columns. The linearity is fair and the slopes depend on the polarity of the compound and of the column. All the other compounds tested show linear behaviour. Therefore, by taking into account the linear dependence of ΔH and ΔS on temperature, by combination of Eqs. 6 and 9 an equation equivalent to the function of Eq. 4 is obtained. The method, indicated as QI (quadratic interpolation), employs the function of Eq. 4, whose coefficients A'', B'' and C'' were obtained by interpolating with the least-squares method all the experimental values of IT_{t_R} obtained in the range 60–190°C.

These coefficients are valid within the whole temperature range of the column, while those obtained with the S method change for every temperature interval of the programmed run. This method has the same disadvantage as the S method, because a large number of isothermal runs are used in order to obtain the coefficients A'', B'' and C''. However, by taking into account the linearity of the coefficients B' and C', an attempt was made to obtain the coefficients of Eq. 4 by using the same three IT_{t_R} values used for the calculation with the Said and trapezoids methods. This procedure, indicated as the Q (quadratic) method, allows one to predict the PT_{t_R} values with an approximation nearly equivalent to that obtained with the more complex and time-consuming QI method and is therefore suitable for routine use.

4. Results and discussion

Tables 2, 3 and 4 show examples of the results obtained by predicting the PT_{t_R} on the three columns: in the first column of each table all the compounds contained in the samples are listed in order of increasing retention times obtained in isothermal analysis at 60°C on the three columns. The experimental retention times PT_{t_R}(exp) obtained in a programmed-temperature run taken as an example (initial temperature T_i = 60°C; initial isothermal time t_i = 2 min; programming rate g = 5°C min^{-1}, and the same for the three columns, are listed. The percentage differences between the predicted and experimental PT_{t_R} values, calculated with the equation

$$E = \frac{PT_{t_R}(\text{calc}) - PT_{t_R}(\text{exp})}{PT_{t_R}(\text{exp})} \cdot 100 \tag{12}$$

are reported for all the calculation methods used. The subscripts refer to the various methods described in the Theory section, as follows: three methods use the IT_{t_R} of all the isothermal runs in the range 60–190°C: I = linear interpolation method, S = step method and QI = quadratic interpolation method.

The other methods use as the starting data

Table 1
Slope, s, and correlation coefficient, r, of the straight lines showing the dependence of the coefficients B' and C' of Eq. 3 on the absolute temperature of the column for various compounds (see also Fig. 1)

Compound	Coefficient	SPB-1		Supelcowax-10		CLOT	
		s	r	s	r	s	r
n-Dodecane	B'	−24.10	0.996	−27.74	0.997	−27.40	0.993
	C'	0.061	0.995	0.080	0.998	0.066	0.997
n-Octanol	B'	−30.43	0.991	−28.87	0.990	−16.37	0.986
	C'	0.077	0.993	0.071	0.992	0.039	0.993
Naphthalene	B'	−20.11	0.994	−15.22	0.996	−7.51	0.951
	C'	0.052	0.995	0.038	0.995	0.017	0.966
1,4-Dichlorobenzene	B'	−24.30	0.991	−19.24	0.996	−11.49	0.974
	C'	0.062	0.993	0.050	0.996	0.029	0.972
1,3,5-Trichlorobenzene	B'	−21.45	0.997	−17.62	0.998	−13.25	0.997
	C'	0.055	0.998	0.045	0.998	0.031	0.997
Nitrobenzene	B'	−23.31	0.994	−15.67	0.994	−21.49	0.977
	C'	0.060	0.995	0.038	0.994	0.050	0.979
1-Chloro-4-nitrobenzene	B'	−21.24	0.984	−14.56	0.992	−24.02	0.994
	C'	0.054	0.987	0.635	0.990	0.055	0.995
4-Chloroaniline	B'	−24.37	0.995	−10.89	0.999	−26.96	0.999
	C'	0.062	0.995	0.025	0.999	0.062	0.997

three isothermal runs at the lowest, the highest and an intermediate temperature: X = Said's method [7,8], T = trapezoid method [22,28–31] and Q = quadratic method.

The average errors $E_{ave}(tot)$ and the absolute average errors $E_{abs}(tot)$ are also reported, taking into account all the compounds contained in the sample, and calculated as

$$E_{ave}(N) = \frac{\sum_{0}^{n} E_M(N)}{N} \quad (13)$$

$$E_{abs}(N) = \frac{\sum_{0}^{n} |E_M(N)|}{N} \quad (14)$$

where the subscript M refers to the symbols of the methods listed above. Table 5 shows the values of $E_{ave}(N)$ and $E_{abs}(N)$ for programmed runs with different T_i, t_i and g and the overall averages of all these runs for each method, $E_{ave}(tot)$ and $E_{abs}(tot)$, calculated with the same method shown in Eqs. 13 and 14. The values of $E_{abs}(tot)$ in Table 5 are plotted in Fig. 2 for the various prediction methods, indicated on the abscissa.

The data in Tables 2–4 show that the three columns tested elute the analysed compounds in different orders. The elution order in various isothermal analyses does not change on the gas–liquid SPB-1 and Supelcowax-10 columns, whereas some inversions were observed on the gas–liquid–solid CLOT column [20,21]. This is due to the polarity of the column, which, calculated with the ΔC method [26,27], is constant in the range 60–190°C for GLC columns (2.70 for SPB-1 and 7.52 for Supelcowax-10) but changes linearly from 6.00 to 6.45 for the CLOT column.

Notwithstanding the different characteristics of the columns and their dependence on temperature, the prediction methods tested permitted an acceptable approximation to the experimental results. In fact, the values of the deviation between the predicted and calculated PTt_R values are small for the methods tested, excluding the linear interpolation (I) method (see Fig. 2).

Table 2
Percentage difference between predicted and experimental PTt_R values, E, calculated by Eq. 11 for the SPB-1 column

No. Compound	PTt_r (min)	E_X	E_T	E_I	E_S	E_{QI}	E_Q
1 *n*-C_7	1.177	−0.93	−0.93	−0.34	−0.93	−0.99	−0.93
2 *n*-C_8	1.658	−0.72	−0.72	4.40	−0.72	−0.79	−0.72
3 Chlorobenzene	1.904	−0.16	−0.16	5.88	−0.16	−0.17	−0.16
4 *n*-C_9	2.683	−0.79	−0.26	8.42	−0.75	−0.97	−0.67
5 Bromobenzene	2.825	−0.20	−0.18	7.58	−0.14	−0.35	−0.07
6 1,3-Dichlorobenzene	4.049	−0.04	−0.02	9.53	−0.30	0.30	−0.44
7 1,4-Dichlorobenzene	4.148	0.09	−0.05	9.43	−0.36	0.07	−0.36
8 *n*-C_{10}	4.409	−0.45	−0.93	7.08	−1.00	−1.04	−0.82
9 1,2-Dichlorobenzene	4.571	0.14	0.02	8.58	−0.35	0.00	−0.39
10 Nitrobenzene	5.404	0.48	−0.11	7.75	−0.31	−0.20	−0.17
11 2-Chloroaniline	6.491	0.26	−0.29	5.73	−0.25	−0.12	−0.09
12 *n*-C_{11}	6.702	−0.32	−1.01	4.61	−0.82	−0.67	−0.73
13 1,3,5-Trichlorobenzene	6.842	−0.08	−0.70	4.52	−0.42	−0.37	−0.34
14 1,2,4-Trichlorobenzene	7.825	0.00	−0.58	2.84	−0.20	−0.13	−0.03
15 Naphthalene	7.945	0.06	−0.57	2.84	−0.20	−0.05	0.08
16 3-Chloroaniline	8.117	−0.19	−0.90	3.01	−0.10	0.00	−0.10
17 4-Chloroaniline	8.191	0.09	−0.48	2.93	−0.07	0.05	0.20
18 1,2,3-Trichlorobenzene	8.636	0.05	−0.39	2.00	−0.15	0.01	0.24
19 1-Chloro-3-nitrobenzene	8.723	−0.16	−0.77	2.02	−0.11	0.02	0.07
20 1-Chloro-4-nitrobenzene	8.914	−0.03	−0.63	1.76	−0.10	0.06	0.24
21 1-Chloro-2-nitrobenzene	9.080	−0.33	−0.77	1.40	−0.12	−0.03	−0.06
22 *n*-C_{12}	9.271	−0.41	−1.07	0.91	−0.47	−0.30	−0.04
23 *n*-C_{13}	11.874	2.02	1.38	0.43	0.67	1.19	2.42
$E_{ave}(N)$		−0.07	−0.44	4.49	−0.32	−0.20	−0.13
$T_{abs}(N)$		0.35	0.56	4.52	0.38	0.34	0.41

Analytical parameters of the temperature-programmed run: $T_i = 60°C$; $t_i = 2$ min; $g = 5°C\ min^{-1}$. The values averaged over all the compounds are also shown (see Eqs. 12 and 13). Subscripts to E refer to the prediction methods.

Further, by comparing the values of E for the various compounds obtained with many temperature programs and the average values in Table 5, one can see that the deviations between the predicted and experimental PTt_R values are stochastic and do not depend on the method used or on the compound analysed. The greater values of the deviation for the linear interpolation method (E_I) are due, as seen in the Theory section, to the hypothesis applied for the calculation that ΔH and ΔS values do not depend on temperature. On the contrary, as shown in Fig. 1 and Table 1, both thermodynamic functions depend linearly on the column temperature.

This is better shown by Fig. 3, where the Arrhenius plots ($\ln k'$ vs. $1/T$) for *n*-nonanol on the three columns of different polarity are reported (upper graph). All these plots show an appreciable curvature, greater for the SPB-1 column, as confirmed by the behaviour of the first derivative (lower graph), i.e., of the slope of the various tracts. Therefore, the linear interpolation of method I predicts PTt_R values differing from the experimental values to an extent depending on the curvature of the Arrhenius plot. The same behaviour was observed for all the compounds tested, as shown by the greater values in the E_I column in Tables 2–5. Fig. 3 shows that the best linearity of the $\ln k'$ vs. $1/T$ plot was given by the CLOT column, notwithstanding its change of polarity with temperature. The other prediction methods, which are independent of the linearity of the Arrhenius plot or interpolate step by step by taking into account its curvature, are therefore more accurate than the I method,as shown in Fig. 2.

Table 3
Percentage difference between predicted and experimental PTt_R values, E, calculated by Eq. 11 for the Supelcowax-10 column

No.	Compound	PTt_r (min)	E_X	E_T	E_I	E_S	E_{QI}	E_Q
22	n-C_{12}	2.901	−1.03	−1.00	5.58	−0.97	−0.76	−0.90
3	Chlorobenzene	3.152	−0.85	−0.57	7.14	−0.79	−0.79	−0.73
23	n-C_{13}	4.440	−1.08	−1.58	5.43	−1.60	−1.46	−1.37
5	Bromobenzene	5.229	−1.37	−1.93	4.40	−1.30	−1.11	−1.76
24	n-C_{14}	6.394	−1.40	−2.13	3.24	−1.64	−1.49	−1.67
6	1,3-Dichlorobenzene	6.597	−1.30	−1.71	2.82	−1.36	−1.18	−1.55
7	1,4-Dichlorobenzene	7.224	−1.39	−2.02	1.87	−1.34	−1.20	−1.51
9	1,2-Dichlorobenzene	8.108	−1.51	−2.00	0.43	−1.27	−1.25	−1.49
25	n-C_{15}	8.556	−1.98	−2.73	−0.41	−1.62	−1.60	−1.81
13	1,3,5-Trichlorobenzene	8.683	−1.61	−2.15	−0.44	−1.20	−1.27	−1.57
26	n-C_{16}	10.798	0.25	−0.48	5.25	−0.31	−0.82	−0.95
14	1,2,4-Trichlorobenzene	11.432	0.08	−0.33	3.26	−0.22	−0.55	−0.62
18	1,2,3-Trichlorobenzene	13.229	−0.25	−0.61	1.19	−0.48	−0.62	−0.68
10	Nitrobenzene	13.542	−0.26	−0.50	0.92	−0.45	−0.58	−0.63
15	Naphthalene	13.542	−0.26	−0.50	0.92	−0.45	−0.58	−0.63
27	n-C_{18}	15.168	−0.32	−1.07	−0.51	−0.88	−0.89	−0.82
19	1-Chloro-3-nitrobenzene	17.073	−0.23	−0.57	0.01	−0.47	−0.62	−0.64
20	1-Chloro-4-nitrobenzene	17.902	−0.27	−0.72	−0.32	−0.53	−0.65	−0.69
11	2-Chloroaniline	18.045	−0.10	−0.69	−0.35	−0.50	−0.62	−0.64
21	1-Chloro-2-nitrobenzene	19.237	−0.11	−0.59	−0.50	−0.41	−0.51	−0.55
28	n-C_{20}	19.237	−0.02	−0.90	−1.05	−0.74	−0.80	−0.81
17	4-Chloroaniline	22.659	0.76	0.13	0.48	0.22	−0.05	−0.05
16	3-Chloroaniline	22.833	0.73	0.10	0.45	0.19	−0.07	−0.07
29	n-C_{22}	23.062	0.75	−0.21	0.05	−0.12	−0.38	−0.38
	$E_{ave}(N)$		−0.53	−1.03	1.66	−0.76	−0.83	−0.94
	$E_{abs}(N)$		0.75	1.05	1.96	0.79	0.83	0.94

Analytical parameters of the temperature-programmed run: $T_i = 60°C$; $t_i = 2$ min; $g = 5°C\ min^{-1}$. The values averaged over all the compounds are also shown (see Eqs. 12 and 13). Subscripts to E refer to the prediction methods.

The two methods QI and Q, which both apply the expression of Eq. 4, and whose coefficients A'', B'' and C'' are obtained by using many ITt_R values at small temperature intervals (QI) or three ITt_R values only (Q), show a comparable accuracy (Fig. 2). The exponential section of Eq. 4 containing the three coefficients is similar to the familiar Van Deemter expression; in fact, the dependence of the exponent on temperature follows the same behaviour as the dependence of HETP on the gas velocity: a constant value (B''), a linear dependence ($C''T$) and an hyperbolic function (A''/T). Fig. 4 shows as an example the dependence of A'', B'' and C'' for linear alkanes on SPB-1, Supelcowax-10 and CLOT columns. The trend for the last column differs markedly from that observed on gas–liquid partition systems, and this difference was also observed for other homologous series tested.

5. Application of Q method to automatic prediction

As shown above, the Q method permits the prediction of PTt_R values to be carried out by starting from three isothermal runs, with an accuracy similar to that given by the more complex S and QI methods. Its application, which can be off-line, by manually transferring

Table 4
Percentage difference between predicted and experimental PTt_R values, E, calculated by Eq. 11 for the CLOT column

No. Compound	PTt_r (min)	E_X	E_T	E_I	E_S	E_{QI}	E_Q
8 n-C_{10}	3.990	−0.98	−1.50	3.38	0.83	−0.53	−1.38
12 n-C_{11}	6.266	−1.68	−2.30	2.19	1.36	−1.29	−2.70
3 Chlorobenzene	5.545	−0.58	−1.17	2.13	1.01	−1.08	−1.51
22 n-C_{12}	8.870	−3.03	−3.83	−1.05	1.48	−1.72	−3.12
5 Bromobenzene	8.482	−2.22	−2.45	−1.38	1.73	−1.92	−2.86
23 n-C_{13}	11.527	−1.22	−1.93	0.83	1.13	−1.18	−1.74
6 1,3-Dichlorobenzene	10.455	−1.97	−2.25	−1.59	1.28	−1.30	−1.74
7 1,4-Dichlorobenzene	11.154	−1.05	−1.40	0.58	1.10	−1.21	−1.34
9 1,2-Dichlorobenzene	12.184	−1.23	−1.53	−0.11	1.16	−1.24	−1.39
24 n-C_{14}	14.109	0.02	−0.57	2.35	0.44	−0.72	−0.89
13 1,3,5-Trichlorobenzene	13,451	−0.51	−0.74	1.81	0.58	−1.03	−1.04
25 n-C_{15}	16,601	1.04	0.43	2.70	−0.59	0.00	0.02
14 1,2,4-Trichlorobenzene	16,402	−0.07	−0.29	1.88	0.08	−0.75	−0.71
10 Nitrobenzene	17.665	−0.32	−0.48	0.93	0.38	−0.82	−0.80
26 n-C_{16}	18.977	0.29	−0.49	0.66	0.37	−0.73	−0.74
18 1,2,3-Trichlorobenzene	18.319	−0.40	−0.61	0.72	0.52	−0.92	−0.93
15 Naphthalene	18.319	−0.34	−0.50	0.68	0.41	−0.78	−0.79
19 1-Chloro-3-nitrobenzene	21.403	−1.30	−1.62	−1.03	0.80	−2.04	−1.81
11 2-Chloroaniline	21.799	0.01	−0.42	0.22	−0.02	−0.83	−0.68
20 1-Chloro-4-nitrobenzene	22.533	−0.11	−0.43	0.01	−0.01	−0.79	−0.70
21 1-Chloro-2-nitrobenzene	23.485	−0.20	−0.53	−0.28	0.19	−0.79	−0.70
27 n-C_{18}	23.457	0.24	−0.82	−0.40	0.57	−0.99	−0.99
17 4-Chloroaniline	26.431	0.06	−0.60	−0.53	0.53	−0.75	−0.75
16 3-Chloroaniline	26.562	0.05	−0.63	−0.56	0.48	−0.78	−0.78
28 n-C_{20}	27.605	0.24	−0.96	−0.89	0.96	−1.10	−1.03
$E_{ave}(N)$		−0.61	1.11	0.53	0.67	−1.01	−1.24
$E_{abs}(N)$		0.77	1.14	1.16	0.72	1.01	1.25

Analytical parameters of the programmed-temperature run: $T_i = 60°C$; $t_i = 2$ min; $g = 5°C\ min^{-1}$. The values averaged over all the compounds are also shown (see Eqs. 12 and 13). Subscripts to E refer to the prediction methods.

the ITt_R values to a personal computer, or online, if the integrator used is directly programmable in BASIC or is interfaced to a separate computer, require the following steps.

(a) Three isothermal runs covering the expected temperature range of the programmed-temperature analysis are carried out. Automatic samplers can be employed in order to repeat the injection three or four times at every temperature.

(b) The average ITt_R values at the three temperatures are used to solve a system of three equations deduced from Eq. 4, in order to calculate the values of A'', B'' and C'':

$$\ln k'_{(i)} = \frac{A''}{T_i} + B'' + C''T_i \quad (15)$$

where i refers to the different isothermal runs.

(c) The values of the coefficients are substituted in the integral

$$g = \int_{T_i}^{T_f} \frac{dT}{t_M(T)\left[1 + \exp\left(\frac{A''}{T} + B'' + C''T\right)\right]}$$

which is solved with the trapezoids method [22,28–31]. The values of T_f (elution temperature of every compound) are obtained and, the

Table 5
Average and absolute average percentage differences between predicted and calculated PTt_R values, E, calculated with Eqs. 12 and 13 for various programmed-temperature runs on the three columns

Column	T_i (°C)	t_i (min)	g (°C min^{-1})	E_X	E_T	E_I	E_S	E_{QI}	E_Q
SPB-1	45	0	4	0.89	1.23	7.03	0.69	0.76	0.76
	50	0	2	1.04	0.46	10.27	0.56	0.38	0.41
	80	0	3	0.90	0.95	1.27	0.45	0.68	0.80
	50	3	5	0.80	1.30	7.44	1.02	0.87	0.87
	60	2	5	0.35	0.56	4.52	0.38	0.34	0.41
	60	6	2	0.56	0.59	10.19	0.47	0.52	0.52
E_{abs}(tot)				0.76	0.85	6.79	0.60	0.59	0.63
	45	0	4	−0.15	−1.12	7.03	−0.25	−0.65	−0.56
	50	0	2	0.49	−0.09	10.27	0.54	0.23	0.34
	80	0	3	0.90	0.50	−1.16	0.41	0.66	0.71
	50	3	5	−0.66	−1.24	7.44	−0.23	−0.73	−0.64
	60	2	5	−0.07	−0.44	4.49	−0.32	−0.20	−0.13
	60	6	2	0.33	0.30	10.19	0.42	0.46	0.50
E_{ave}(tot)				0.14	−0.35	6.38	0.10	−0.04	0.04
Supelcowax-10	45	0	4	1.03	1.05	3.19	0.75	0.91	1.01
	60	0	4	0.87	1.14	1.44	0.85	0.86	0.98
	80	0	3	1.36	1.40	2.45	0.75	0.79	0.96
	45	2	5	0.94	1.30	3.04	0.92	1.26	1.36
	60	2	5	0.75	1.05	1.96	0.79	0.83	0.94
	100	4	2	1.26	1.00	3.46	0.66	0.32	0.57
E_{abs}(tot)				1.04	1.16	2.59	0.79	0.83	0.97
	45	0	4	0.42	−1.00	3.12	−0.66	−0.91	−1.01
	60	0	4	−0.60	−1.11	1.13	−0.80	−0.87	−0.98
	80	0	3	−1.36	−1.24	−1.43	−0.68	−0.79	−0.94
	45	2	5	−0.13	−1.30	2.77	0.92	−1.27	−1.36
	60	2	5	−0.53	−1.03	1.66	−0.76	−0.83	−0.94
	100	4	2	−1.12	−0.73	−2.71	0.13	−0.20	−0.36
E_{ave}(tot)				−0.55	−1.07	0.76	−0.31	−0.81	−0.93
CLOT	45	0	4	0.98	1.01	1.57	0.74	0.98	1.15
	70	0	5	0.97	0.97	1.53	0.72	0.52	0.88
	80	0	3	1.30	1.24	2.18	0.79	0.87	1.29
	60	2	5	0.77	1.14	1.16	0.72	1.01	1.25
	80	2	7	0.96	0.95	1.57	0.80	0.60	0.91
	90	10	10	1.44	1.43	2.68	1.03	0.78	1.28
E_{abs}(tot)				1.07	1.12	1.78	0.80	0.79	1.13
	45	0	4	0.37	1.00	1.22	−0.59	−0.95	−1.11
	70	0	5	0.00	−0.29	0.64	−0.35	0.01	0.40
	80	0	3	−1.17	−1.02	0.23	0.20	0.80	−1.21
	60	2	5	−0.61	−1.11	0.53	0.67	−1.01	−1.24
	80	2	7	0.22	0.09	0.60	−0.67	0.33	−0.03
	90	10	10	−0.22	−0.23	0.57	0.64	0.21	−0.34
E_{ave}(tot)				−0.23	−0.26	0.63	−0.02	−0.10	−0.59

The overall averages are also shown. Subscripts to E refer to the prediction methods.

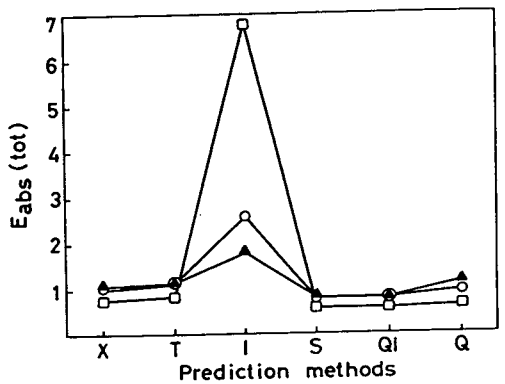

Fig. 2. Absolute percentage difference between predicted and experimental PTt_R values, averaged over all the analysed compounds and different programmed runs, E_{abs}(tot), for the various calculation methods (see Table 5).

programming rate g and the initial temperature T_i being known, permit the calculation of the retention time:

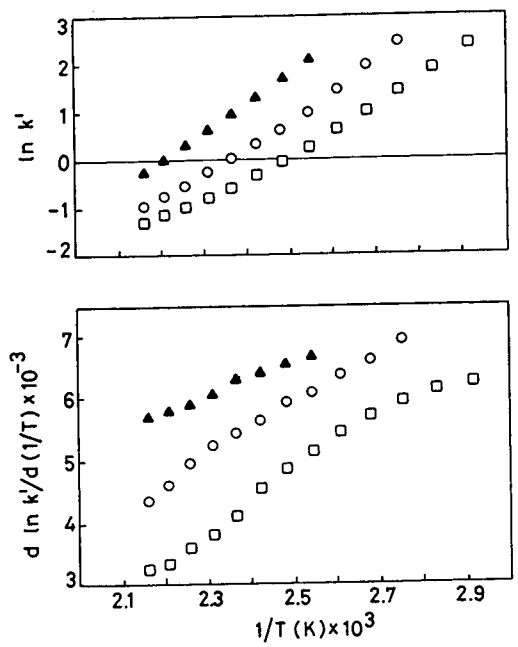

Fig. 3. Upper graph: Arrhenius plots (ln k' vs. $1/T$) for n-nonanol on the three columns (□ = SPB-1; ○ = Supelcowax-10; ▲ = CLOT). Lower graph: values of the first derivative that show the change of slope of the upper curves with temperature.

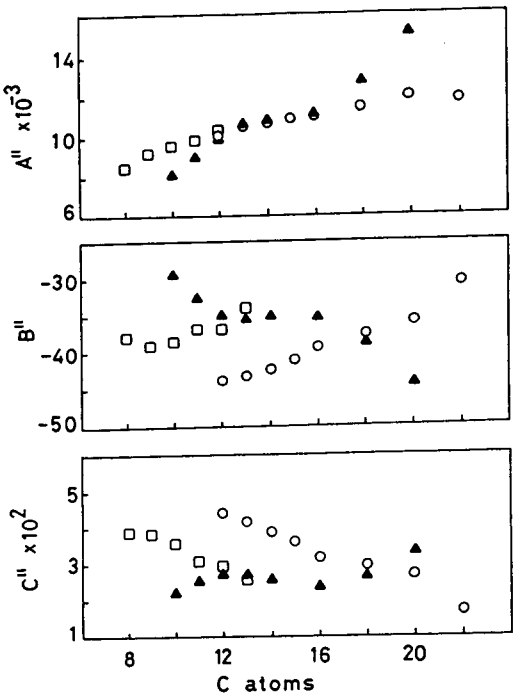

Fig. 4. Values of the coefficients of Eq. 4, A'', B'' and C'', for linear alkanes on (□) SPB-1, (○) Supelcowax-10 and (▲) CLOT columns.

$$PTt_R(\text{calc}) = (T_f - T_i)/g \quad (16)$$

6. Conclusions

The comparison of the various prediction methods tested showed that, for some of them, an increase in the number of starting isothermal data results in a better approximation of predicted to experimental PTt_R values, whereas for others, when the linearity is poor, appreciable deviations are observed. The step (S), quadratic interpolation (QI) and quadratic (Q) methods permit the same degree of confidence to be obtained as found previously with the Said and trapezoids methods. A further advantage of the Q method is that it can be applied by using only three isothermal data and is suitable of easy application to automatic data acquisition and calculation. The constants of Eqs. 3 and 4, which can be calculated by using experimental isother-

mal retention values, are correlated with the classical thermodynamic functions and may therefore be used to obtain their values and to investigate the solute–solvent interaction mechanism.

Acknowledgements

This research was supported by the Italian Ministry of University and Scientific Research (MURST). The authors thank Miss Carla Parodi for her help in preparing the manuscript.

References

[1] H.W. Habgood and W.E. Harris, *Anal. Chem.*, 32 (1960) 450.
[2] W.E. Harris and H.W. Habgood, *Programmed Temperature Gas Chromatography*, Wiley, New York (1966).
[3] D.W. Grant and M.G. Hollis, *J. Chromatogr.*, 158 (1978) 3.
[4] J. Culvers, J. Rijks, C. Cramers, K. Knauss and P. Larson, *J. High Resolut. Chromatogr. Chromatogr. Commun.*, 8 (1985) 607.
[5] E.E. Akporhonor, S. Le Vent and D.R. Taylor, *J. Chromatogr.*, 405 (1987) 67.
[6] P.Y. Shrotri, A. Mokashy and D. Hukesh, *J. Chromatogr.*, 387 (1987) 399.
[7] A.S. Said, in P. Sandra (Editor), *Proceedings of the 8th International Symposium on Capillary Chromatography, Riva del Garda, Italy*, Vol. I, Hüthig, Heidelberg, 1987, p. 85.
[8] A.S. Said, in P. Sandra and G. Redant (Editors), *Proceedings of the 10th International Symposium on Capillary Chromatography, Riva del Garda, Italy*, Hüthig, Heidelberg, 1989, p. 163.
[9] F. Helaimiam, M. Bourmahraz, H. Sissaoni and M.D. Messadi, *Analysis*, 17 (1989) 596.
[10] E.E. Akporhonor, S. Le Vent and D.R. Taylor, *J. Chromatogr.*, 463 (1989) 271.
[11] J.Y. Zhang, G.M. Wang and R. Qian, *J. Chromatogr.*, 521 (1990) 71.
[12] Y. Guan and L. Zhou, *J. Chromatogr.*, 552 (1991) 187.
[13] L.H. Wright and J.F. Walling, *J. Chromatogr.*, 540 (1991) 311.
[14] Y. Guan, P. Zheng and L. Zhou, *J. High Resolut. Chromatogr.*, 15 (1992) 18.
[15] N.H. Snow and H.M. McNair, *J. Chromatogr. Sci.*, 30 (1992) 271.
[16] T.C. Gerbino and C. Castello, in P. Sandra (Editor), *Proceedings of the 14th International Symposium on Capillary Chromatography, Baltimore, MD, 1992*, Foundation for the International Symposium on Capillary Chromatography, Miami, FL, 1992, p. 70.
[17] T.C. Gerbino and G. Castello, *J. High Resolut. Chromatogr.*, 16 (1993) 46.
[18] T.C. Gerbino, G. Castello and G. Pettinati, *J. Chromatogr.*, 634 (1993) 338.
[19] T.C. Gerbino and G. Castello, in P. Sandra (Editor), *Proceedings of the 15th International Symposium on Capillary Chromatography, Riva del Garda, Italy*, Hüthig, Heidelberg, 1993, p. 60.
[20] G. Castello and S. Vezzani, in P. Sandra (Editor), *Proceedings of the 15th International Symposium on Capillary Chromatography, Riva del Garda, Italy*, Hüthig, Heidelberg, 1993, p. 68.
[21] G. Castello, S. Vezzani and P. Moretti, *J. High Resolut. Chromatogr.*, 17 (1994) 31.
[22] G. Castello, P. Moretti and S. Vezzani, *J. Chromatogr.*, 635 (1993) 103.
[23] S.S. Stafford (Editor), *Electronic Pressure Control in Gas Chromatography*, Hewlett-Packard, Wilmington, DE, 1993.
[24] G. Castello, S. Vezzani and P. Moretti, *J. Chromatogr. A*, 677 (1994) 95.
[25] R.H. Ewell, J.M. Harrison and L. Berg, *Ind. Eng. Chem.*, 36 (1944) 871.
[26] G. Castello and G. D'Amato, *J. Chromatogr.*, 623 (1992) 289.
[27] G. Castello, G. D'Amato and S. Vezzani, *J. Chromatogr.*, 646 (1993) 361.
[28] C. Caratheodory, *Algebraic Theory of Measure and Integration*, Chelsea, New York, 1963.
[29] F. Ayres, Jr., *Theory and Problems of Differential and Integral Calculus*, Schaum, New York, 1964.
[30] E.J. McShane, *Unified Integration*, Academic Press, Orlando, FL (1983).
[31] J.L. Kelley and T.P. Srinmivasan, *Measure and Integral*, Springer, New York, 1988.
[32] L.S. Ettre, *Chromatographia*, 13 (1980) 73.
[33] M.S. Wainwright and J.K. Haken, *J. Chromatogr.*, 184 (1980) 1.
[34] M.S. Wainwright, C.S. Nieass, J.K. Haken and R.P. Chaplin, *J. Chromatogr.*, 321 (1985) 287.
[35] R.J. Smith, J.K. Haken, M.S. Wainwright and B.G. Madden, *J. Chromatogr.*, 328 (1985) 11.
[36] B. Koppenhoefer, G. Laupp and M. Humel, *J. Chromatogr.*, 547 (1991) 239.
[37] A.P. James and A.J.P. Martin, *Biochem. J.*, 50 (1952) 679.
[38] L.S. Ettre, *Chromatographia*, 18 (1984) 243.
[39] R. Kaiser, *Gas Phase Chromatography*, Vol. 1, Butterworths, London, 1963.
[40] M.H. Guermouches and J.M. Vergnaud, *J. Chromatogr.*, 94 (1971) 169.

[41] M.H. Guermouches and J.M. Vergnaud, *J. Chromatogr.*, 94 (1974) 25.
[42] R.L. Grob, *Modern Practice of Gas Chromatography*, Wiley, New York, 1977.
[43] L. Podmaniczky, L. Szepesy, K. Lakzner and G. Schomburg, *Chromatographia*, 20 (1985) 591.
[44] L. Podmaniczky, L. Szepesy, K. Lakzner and G. Schomburg, *Chromatographia*, 20 (1985) 623.
[45] K. Kuningas, S. Rang and T. Kailas, *Chromatographia*, 27 (1989) 544.
[46] H. Rotzsche, *Stationary Phases in Gas Chromatography*, Elsevier, Amsterdam, 1991.
[47] R.W. Dwyer, *J. Chromatogr. Sci.*, 15 (1977) 450.
[48] A.N. Korol and T.I. Dovbush, *J. Chromatogr.*, 209 (1981) 21.

ELSEVIER

Journal of Chromatography A, 677 (1994) 345–354

JOURNAL OF CHROMATOGRAPHY A

Analytical strategy by coupling headspace gas chromatography, atomic emission spectrometric detection and mass spectrometry Application to sulfur compounds from garlic

D. Deruaz*, F. Soussan-Marchal, I. Joseph, M. Desage, A. Bannier, J.L. Brazier

Laboratoire d'Etudes Analytiques et Cinétiques du Médicament, Institut des Sciences Pharmaceutiques et Biologiques, 8 Avenue Rockefeller, 69393 Lyon, France

First received 20 January 1994; revised manuscript received 13 April 1994

Abstract

Numerous sulfur-containing molecules are present in garlic cloves, alliine being the most important. The characteristic aroma of garlic is obtained after the reaction of the enzyme alliinase which converts alliine into allicine. This very unstable molecule is rapidly converted into a series of numerous other odorous sulfur-containing molecules. This complex mixture of volatile compounds was analysed using GC–atomic emission spectrometric detection and GC–MS after introduction with a headspace device. The analysed products were non-peeled and peeled whole garlic cloves, peeled and crushed garlic cloves and garlic juice obtained by crushing the cloves. A comparison was made between the heating times of the headspace device (5 and 45 min). The two-stage analytical strategy used for this kind of analysis is described: (i) location of the sulfur-containing compounds from the specific sulfur chromatograms obtained by monitoring the sulfur atomic emission line with an atomic emission spectrometer coupled to a gas chromatograph and (ii) structural analysis of the located and selected compounds by mass spectrometry after transposing the chromatographic method to GC–MS.

1. Introduction

Garlic, *Allium sativum* L. [1–3] has been known since antiquity for its medicinal properties and its characteristic flavour. The chemical composition of garlic cloves has been described in numerous studies and its pharmacological properties have been documented and established. These properties are associated with the presence of sulfur-containing molecules which are the main components of garlic. Their formation and degradation processes remained unknown for a long time because of the complexity of the chemical mechanisms giving rise to their formation during garlic use. Alliine [4–9], which is the major component, is converted into allicine by alliinase [10], an enzyme released when the garlic cloves are crushed. Allicine, which is very unstable chemically, allows the formation of a complex mixture of volatile sulfur-containing compounds.

The influence of the starting product was studied by measuring quantitatively and qualitatively the various mono-, di- and trisulfides formed from the garlic cloves. Their identification was carried out simultaneously by measure-

* Corresponding author.

SSDI 0021-9673(94)00382-J

ment of the C/S and H/C inter-element ratios using both atomic emission and mass spectrometry. The results shown here demonstrate the use of the dual analytical strategy of applying both atomic and mass spectrometric methods.

2. Experimental

2.1. Headspace device

The headspace device used was an HP 19395A from Hewlett-Packard. The temperature of the oil-bath was set at 70°C and that of the injector valve at 85°C. Two time intervals (5 and 45 min) were used for sample heating. The injector cycle was set as follows: pressurization, 10 s; ventilation, 10 s; injection, 130 s.

2.2. Gas chromatograph

The gas chromatographs used were HP 5890 Series II models. They were equipped with a capillary column (HP5, 25 m × 0.31 mm I.D., film thickness 0.53 μm, diphenylpolysiloxane 5%, dimethylpolysiloxane 95%). Helium (99.999%) was used as the mobile phase. The injector temperature was set at 220°C. Injection was performed according to the split mode (splitting ratio 1:40). The oven temperature was programmed as follows: 40°C for 2 min, then increased at 3°C/min up to 70°C, 7.5°C/min up to 205°C and 25°C/min up to 250°C. The temperature of the transfer line was 250°C.

2.3. Atomic emission spectrometric detector

The atomic emission spectrometric (AES) detector was an HP 5921A equipped with a Beenakker-type resonant cavity. The frequency of the microwave beam was 2.75 GHz and the plasma energy was 70 W. The plasma induced by microwaves was generated from helium (99.9999%). Oxygen and hydrogen were used as reactant gases under a pressure of 100 kPa (purity 99.998% for both gases). The discharge tube was cooled by water (60°C). The data were processed using an HP 59970 Chemstation. For atomic emission detection the following emission lines were monitored: carbon, 193.03 nm; sulphur, 180.7 nm; and hydrogen, 486.1 nm.

2.4. Mass-selective detector

The analytical system used was an HP 5970 B mass-selective detector with a quadrupole mass filter, operating in the electron impact mode (ionization energy 70 eV). Mass spectra were recorded in the scan mode (one scan per second from m/z 35 to 300). The data were processed using an HP 59970 Chemstation.

3. Results

3.1. Elemental chromatograms: comparisons of carbon and sulfur profiles

AES detection when coupled with GC allows elemental chromatograms to be obtained from the detection and continuous monitoring of the specific atomic line of an atom or isotope [11,12]. Fig. 1 displays the chromatograms recorded by monitoring the 193-nm line for carbon and the 181-nm line for sulfur from the compounds evaporated from a peeled garlic clove placed inside the headspace device. The heating time of the sample was 45 min. The carbon chromatogram is a non-specific chromatogram and allows the detection of all the organic compounds that are present in the sample.

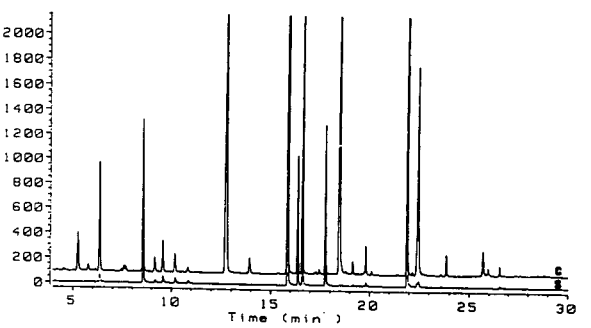

Fig. 1. Elemental chromatograms of carbon (193.03 nm) and sulfur (180.7 nm) for a whole peeled garlic clove.

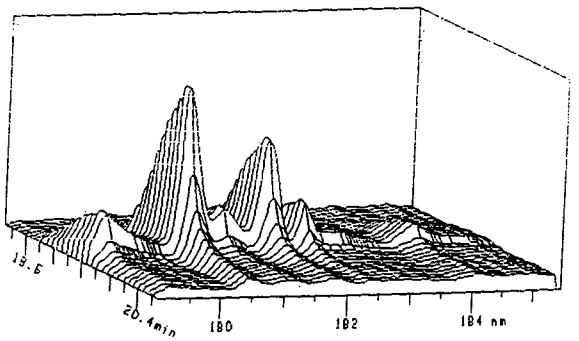

Fig. 2. Spectrum of the sulfur-containing compound eluted at 19.8 min.

When detection is carried out with the 180.7-nm line, which is characteristic of sulfur, only the sulfur-containing compounds are specifically detected. The presence of sulfur is verified by recording the three-dimensional emission spectrum of the chromatographic peak (Fig. 2) using the potential of an HP 5921A diode-array spectrophotometer [13,14]. On this spectrum the three characteristic emission lines of sulfur can be observed at 180.7, 182.0 and 182.7 nm.

Fig. 3 shows carbon and sulfur chromatograms obtained from the aroma of a crushed garlic clove. It can be observed that the compound with a retention time of 2.4 min contains sulfur atoms whereas that at 3.5 min does not contain sulfur because of the absence of a peak at 180.7 nm. This sulfur elemental chromatogram reveals

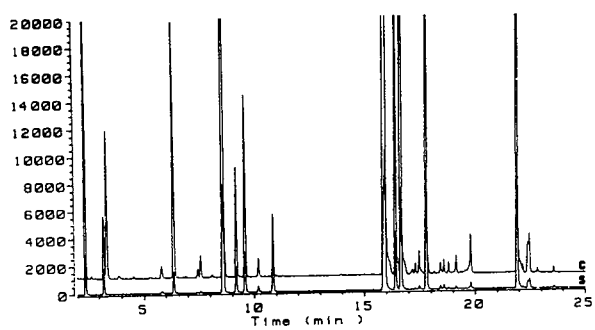

Fig. 3. Elemental chromatograms of carbon (193.03 nm) and sulfur (180.7 nm) for a crushed garlic clove.

nineteen sulfur-containing compounds. The compositions of the garlic effluvium from peeled cloves, non-peeled whole cloves, crushed cloves and garlic juice were compared. The results are given in Tables 1 and 2 and Figs. 4 and 5.

Table 1 (and Fig. 4) allows one to compare the relative compositions (%) of sulfur-containing compounds for the four types of sample according to the two heating conditions (5 and 45 min). Table 2 (and Fig. 5) gives the normalized results, the more abundant compounds being taken as the 100% value. These results show that both the type of sample and the heating time have an influence on the qualitative and quantitative composition of the garlic aroma.

Whole non-peeled garlic clove

When the heating time in increased from 5 to 45 min, new sulfur-containing compound are formed and eluted from the whole non-peeled clove. A significant variation in the relative proportions of each component can be observed with an important decrease in the principal compound with a retention time of 15.9 min (Table 1). Increasing the heating time inside the headspace device allows more sulfur-containing compounds to be generated with different relative proportions. The dry envelope partially prevents the sulfur-containing molecules from escaping from the clove.

Whole peeled clove

In the whole peeled garlic glove, most of the sulfur-containing compounds are detected with a heating time of 5 min at 70°C in the headspace device. The variations induced by a longer heating time are less important than those obtained from a non-peeled garlic clove. Increasing the heating time decreases this screening effect.

Crushed garlic clove

Important quantitative variations can be observed according to the heating time when crushed cloves are analysed. Qualitative differences can also be observed: five new sulfur-containing compounds are located on the elemental chromatograms and the overall area of all the chromatographic peaks corresponding to

Table 1
Relative percentages of the sulfur-containing compounds eluted, with heating for 5 and 45 min

t_r (min)	Non-peeled clove		Peeled clove		Crushed clove		Juice	
	5 min	45 min	5 min	45 min	5 min	45 min	5 min	45 min
2.4	12.91	2.98	15.61	11.73	0.74	3.64	5.2	4.35
3.2	0	0	0	0.32	1.76	2.25	1.82	1.68
5.8	0	0	0	0	0	0.28	0	0
6.4	5.84	2.69	1.67	4.94	0.52	2.1	6.35	5.87
8.6	8.83	14.64	7.85	8.86	18.05	12.96	1.93	2.58
9.2	0	0	0	0.22	0.32	2.56	0.62	0.68
9.6	0	0	0	0.24	3.31	4.11	6.08	5.77
10.2	0	0	0	0.23	0.5	0.63	0	0
10.9	0	0	0	0.21	0.25	3.97	2.79	2.85
15.9	66.93	57.81	69.06	53.54	35.17	21.87	13.89	14.74
16.4	0	1.87	1.03	1.82	1.68	5.42	2.25	2.68
16.7	0	4.19	2.05	3.29	20.32	11.38	15.59	15.76
17.5	0	0	0	0	0.9	0.32	0	0
17.8	0	3.86	0	2.43	3.01	12.33	15.97	15.77
19.14	0	0	0	0	1.77	0.35	0	0
19.8	0	0	0	0.21	3.12	0.76	0	0
21.9	5.49	11.95	2.72	11.7	7.71	13.19	26.26	25.87
22.4	0	0	0	0.28	0.48	0.62	0	0
22.5	0	0	0	0	1	1.03	0.68	0.73
23.6	0	0	0	0	0	0.24	0.48	0.57
Sample code	S1	S2	S3	S4	S5	S6	S7	S8

the sulfur containing molecules is multiplied fourfold. Hence crushing the clove allows the release of a larger amount of volatile sulfur compounds.

Garlic juice

The number of volatile compounds is qualitatively lower than when the crushed clove is analysed. The compounds with retention times at 5.8, 10.2, 17.5, 19.2, 19.8 and 22.4 min are either evaporated or decomposed before analysis. The two compounds with retention times of 10.2 and 19.8 min (Tables 1 and 2) are absent from the juice. The variation of the relative proportions of the various compounds with the heating time of the sample is smaller than with the other samples studied. After a 45-min heating time, the quantitatively major compounds are those with the longer retention times.

3.2. Recording of mass spectra corresponding to the retention times of sulfur-containing compounds

Chromatograms obtained under the same conditions by the spectrometric sulfur emission at 180.7 nm and by mass-selective detection were compared. Fig. 6 shows the chromatogram obtained from a crushed garlic clove after a heating time of 45 min. Fig. 7 shows the total ion current recorded by GC from the same sample. Comparing the retention times from both profiles allows one to locate the sulfur-containing compounds on the AES profile and record the mass spectra at the various retention times of the previously located peaks.

The flow-rate inside the chromatograph column has to be optimized according to the type of detector used in order to obtain the same retention times because the pressures at the end of

Table 2
Absolute intensities of the sulfur-containing compounds eluted, with heating for 5 and 45 min

t_r (min)	Non-peeled clove		Peeled clove		Crushed clove		Juice	
	5 min	45 min	5 min	45 min	5 min	45 min	5 min	45 min
2.4	19.29	5.15	22.60	21.91	2.10	16.64	19.80	16.81
3.2	0.00	0.00	0.00	0.60	5.00	10.29	6.93	6.49
5.8	0.00	0.00	0.00	0.00	0.00	1.28	0.00	0.00
6.4	8.73	4.65	2.42	9.23	1.48	9.60	24.18	22.69
8.6	13.19	25.32	11.37	16.55	51.32	59.26	7.35	9.97
9.2	0.00	0.00	0.00	0.41	0.91	11.71	2.36	2.63
9.6	0.00	0.00	0.00	0.45	9.41	18.79	23.15	22.30
10.2	0.00	0.00	0.00	0.43	1.42	2.88	0.00	0.00
10.9	0.00	0.00	0.00	0.39	0.71	18.15	10.62	11.02
15.9	100.00	100.00	100.00	100.00	100.00	100.00	52.89	56.98
16.4	0.00	3.23	1.49	3.40	4.78	24.78	8.57	10.36
16.7	0.00	7.25	2.97	6.14	57.78	52.03	59.37	60.92
17.5	0.00	0.00	0.00	0.00	2.56	1.46	0.00	0.00
17.8	000	6.68	0.00	4.54	8.56	56.38	60.81	60.96
19.14	0.00	0.00	0.00	0.00	5.03	1.60	0.00	0.00
19.8	0.00	0.00	0.00	0.39	8.87	3.48	0.00	0.00
21.9	8.20	20.67	3.94	21.85	21.92	60.31	100.00	100.00
22.4	0.00	0.00	0.00	0.52	1.36	2.83	0.00	0.00
22.5	0.00	0.00	0.00	0.00	2.84	4.71	2.59	2.82
23.6	0.00	0.00	0.00	0.00	0.00	1.10	1.83	2.20
Sample code	S1	S2	S3	S4	S5	S6	S7	S8

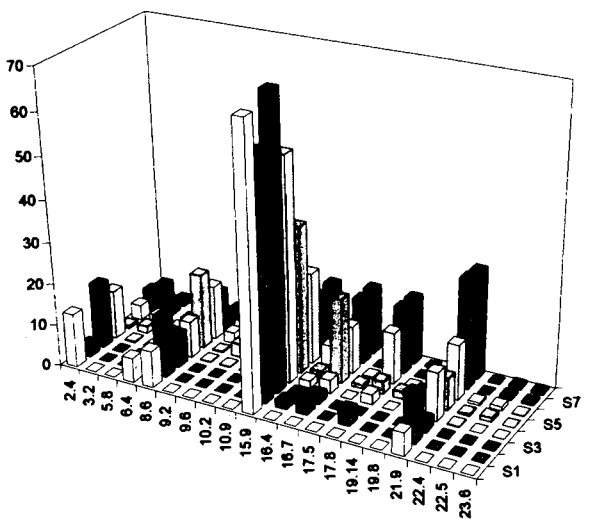

Fig. 4. Histogram of relative percentages of sulfur-containing compounds eluted. S1 = non-peeled garlic clove (5 min); S2 = non-peeled garlic clove (45 min); S3 = peeled garlic clove (5 min); S4 = peeled garlic clove (45 min); S5 = crushed garlic clove (5 min); S6 = crushed garlic clove (45 min); S7 = garlic juice (5 min); S8 = garlic juice (45 min). *y*-Axis represents %, *x*-axis: time in min.

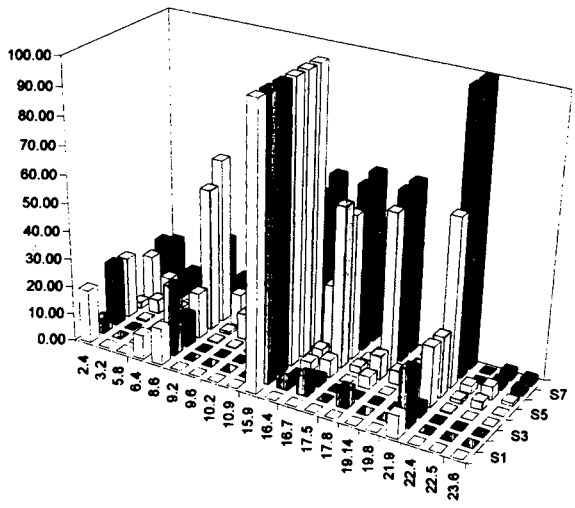

Fig. 5. Histogram of the absolute intensity of the sulfur-containing compounds eluted. S1–S8 as in Fig. 4. *y*-Axis represents %, *x*-axis: time in min.

the column are different when AES and MS detectors are connected. The characteristic ions of the compounds eluted from the whole garlic

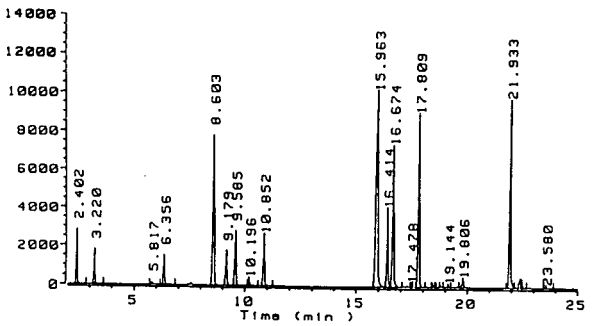

Fig. 6. Elemental chromatograms of sulfur (180.7 nm) from a crushed garlic clove. Heating time in the headspace device: 45 min.

clove and crushed cloves are given in Tables 3 and 4, respectively. Two compounds were easily identified from these spectra, at a retention time of 5.97 min allyl sulfide ($m/z = 114$; $C_6H_{10}S$) and at 16.28 min diallyl disulfide ($m/z = 146$; $C_6H_{10}S_2$). The identification of all other sulfur-containing molecules was achieved using data from both AES (inter-element ratios) and MS.

3.3. Inter-element ratio

The analytical response of the AES detector is proportional to the concentration and to the number of emitting atoms present in the analysed sample. When two elements are simultaneously monitored, their relative response depends only on the number of atoms. The ratio between the response areas of these atoms affords the inter-element ratio [15–17].

For each of the eluted compounds the C/S and the H/C elemental ratios were calculated. In order to calculate these ratios accurately, two compounds whose composition was given by mass spectrometry were taken as standards in order to obtain the coefficient of proportionality, K, between the elements. The $K_{C/S}$ value calculated from allyl disulfide was 2.12 and the value of $K_{H/C}$ calculated from allyl sulfide was 2.34 (means of three measurements). These values were calculated according to the following equation:

$$K_{C/S} = (\text{No. of S atoms}) \cdot (\text{area of carbon peak}) / (\text{No. of C atoms}) \cdot (\text{area of sulphur peak})$$

The inter-element ratios of all other compounds were calculated using these coefficients of proportionality in the following relationship:

$$\text{No. of S atoms/No. of C atoms} = K_{C/S} \cdot (\text{area of sulfur peak})/(\text{area of carbon peak})$$

The calculated and theoretical values are given in Tables 5 and 6. The identification of the other

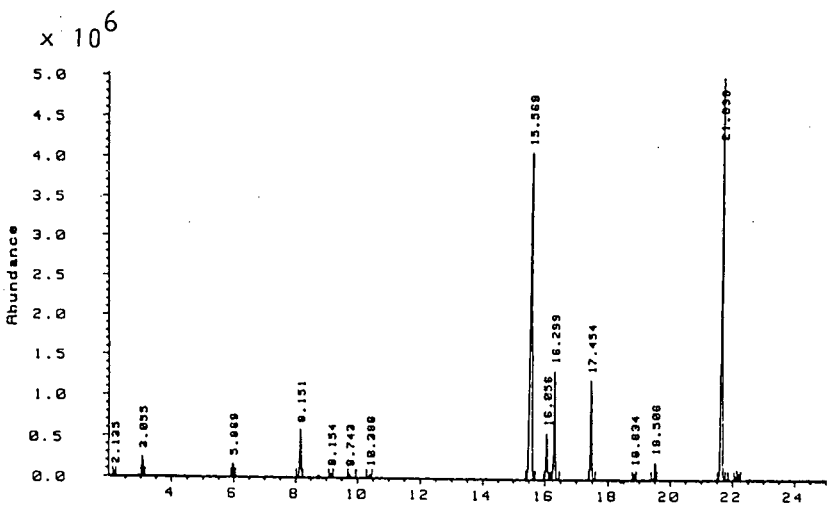

Fig. 7. Total ion current from a crushed garlic clove. Heating time in the headspace device: 45 min. x-Axis represents time in min.

Table 3
Retention times and characteristic ions (m/z and abundance, %) for sulfur-containing compounds from a whole peeled garlic clove

t_r (min) (MS)	No.	M_r	More abundant ions
2.14	1	88	88 (61), 73 (61), 61(20), 47 (32), 45 (100), 41 (62), 39 (86)
3.05	2	94	94 (75), 84 (29), 79 (52), 64 (20), 61 (16), 55 (32), 47 (37), 46 (47), 45 (100)
5.97	3	114	114 (13), 99 (14), 81 (8), 73 (33), 72 (25), 47 (19), 45 (100)
8.16	4	120	120 (31), 79 (10), 64 (11), 47 (13), 46 (13), 45 (48), 41 (100)
	5		
9.16	6	120	120 (52), 80 (21), 72 (33), 71 (25), 58 (13), 48 (17), 47 (31), 45 (100), 41 (36)
9.74	7		
10.39	8	126	126 (60), 79 (49), 64 (37), 47 (44), 46 (31), 45 (100), 44 (17)
15.58	9	146	146 (3), 113 (4), 105 (5), 81 (10), 79 (5), 76 (3), 72 (3), 71 (5), 47 (7), 45 (31), 41 (100)
16.04	10	146	146 (14), 105 (12), 81 (22), 79 (5), 73 (34), 72 (13), 71 (19), 61 (15), 47 (20), 45 (99), 41 (100), 39 (80)
16.28	11	146	146 (13), 105 (12), 81 (21), 73 (34), 71 (16), 61 (18), 58 (7), 47 (14), 45 (95), 41 (100), 39 (77)
17.45	12	152	152 (2), 120 (4), 111 (9), 105 (2), 87 (66), 79 (16), 64 (21), 47 (41), 45 (100), 41 (83), 39 (67)
18.83	13	144	144 (55), 111 (80), 97 (66), 85 (20), 79 (50), 77 (58), 71 (60), 58 (19), 45 (100), 39 (73)
19.5	14	144	144 (30), 111 (34), 72 (100), 71 (95), 45 (82), 39 (42)
21.83	15	178	178 (2), 113 (34), 105 (3)k, 73 (62), 71 (9), 64 (9), 47 (14), 45 (68), 41 (100), 39 (86)
22.17	16	NI[a]	

[a] Not identified.

Table 4
Retention times and characteristic ions (m/z and abundance, %) of sulfur-containing compounds from a crushed garlic clove

t_r (min) (MS)	No.	M_r	More abundant ions
2.14	1	88	88 (61), 73 (61), 61(20), 47 (32), 45 (100), 41 (62), 39 (86)
2.91	2	94	94 (75), 84 (29), 79 (52), 64 (20), 61 (16), 55 (32), 47 (37), 46 (47), 45 (100)
5.97	3	114	114 (13), 99 (14), 81 (8), 73 (33), 72 (25), 47 (19), 45 (100)
8.16	4	120	120 (31), 79 (10), 64 (11), 47 (13), 46 (13), 45 (48), 41 (100)
ND[a]	5		
9.16	6	120	120 (52), 80 (21), 72 (33), 71 (25), 58 (13), 48 (17), 47 (31), 45 (100), 41 (36)
ND	7		
10.39	8	126	126 (60), 79 (49), 64 (37), 47 (44), 46 (31), 45 (100), 44 (11)
15.58	9	146	146 (3), 113 (4), 105 (5), 81 (10), 79 (5), 76 (3), 72 (3), 71 (5), 47 (7), 45 (31), 41 (100)
16.04	10	146	146 (14), 105 (12), 81 (22), 79 (5), 73 (34), 72 (13), 71 (19), 61 (15), 47 (20), 45 (99), 41 (100), 39 (80)
16.28	11	146	146 (13), 105 (12), 81 (21), 73 (34), 71 (16), 61 (18), 58 (7), 47 (14), 45 (95), 41 (100), 39 (77)
17.45	12	152	152 (2), 120 (4), 111 (9), 105 (2), 87 (66), 79 (16), 64 (21), 47 (41), 45 (100), 41 (83), 39 (67)
ND	13		
ND	14		
21.61	15	178	178 (2), 113 (34), 105 (3), 73 (62), 71 (9), 64 (9), 47 (14), 45 (68), 41 (100), 39 (86)
22.17	16	NI[b]	

[a] Not detected.
[b] Not identified.

Table 5
Retention times and calculated and theoretical C/S and H/C ratios from a whole peeled garlic clove

Parameter	t_r (min) (GC–AES)										
	2.4	3.22	6.35	8.56	9.18	10.19	15.86	16.38	16.61	17.76	21.89
Calculated C/S	4.14	1.53	6.14	2.05	1.85	ND[a]	2.98	3	2.84	1.32	2.08
Theoretical C/S	4	1	6	2	2	0.66	3	3	3	1.33	2
Calculated H/C	2.34	2.6	1.67	2.22	1.79	2.65	1.99	1.61	1.66	2.19	1.85
Theoretical H/C	2	3	1.67	2	2	3	1.66	1.67	1.67	2	1.67
Formula	C_4H_8S	$C_2H_6S_2$	$C_6H_{10}S$	$C_4H_8S_2$	$C_4H_8S_2$	$C_2H_6S_3$	$C_6H_{10}S_2$	$C_6H_{10}S_2$	$C_6H_{10}S_2$	$C_4H_8S_3$	$C_6H_{10}S_3$

[a] Not detected.

Table 6
Retention times and calculated and theoretical C/S and H/C ratios from a crushed garlic clove

Parameter	t_r (min) (GC–AES)										
	2.4	3.22	6.35	8.56	9.18	10.85	15.96	16.41	16.67	17.81	19.81	21.93
Calculated C/S	4.11	1.53	6.13	2.05	1.85	0.55	2.98	3	2.84	1.33	3.25	2.15
Theoretical C/S	4	1	6	2	2	0.66	3	3	3	1.33	3	2
Calculated H/C	2.34	2.6	1.67	2.22	1.79	2.65	1.99	1.61	1.66	2.19	ND[a]	1.85
Theoretical H/C	2	3	1.67	2	2	3	1.66	1.67	1.67	2	1.33	1.67
Formula	C_4H_8S	$C_2H_6S_2$	$C_6H_{10}S$	$C_4H_8S_2$	$C_4H_8S_2$	$C_2H_6S_3$	$C_6H_{10}S_2$	$C_6H_{10}S_2$	$C_6H_{10}S_2$	$C_4H_8S_3$	$C_6H_8S_2$	$C_6H_{10}S_3$

[a] Not detected.

Table 7
Characteristic ions mostly encountered

Ion m/z	Formula
39	$CH_2{=}CHCH^+$
41	$^+CH_2CH{=}CH_2$ or $CH_2{=}CHCH_2^+$
45	$^+CH{=}S$
47	CH_3S^+
73	$^+SCH_2CH{=}CH_2$
79	CH_3SS^+ or $CH_3S^+{=}S$
105	$^+SSCH_2CH{=}CH_2$ or $S{=}S^+CH_2CH{=}CH_2$
111	$^+SSSCH_3$ or $S{=}S^+SCH_3$

sulfur-containing was carried out using their mass spectra and elemental data given by AES detection.

Most of the analysed molecules are unsaturated mono-, di- or trisulfides. Several noticeable fragment ions are characteristic of the various chemical groups: $m/z = 39$ and 41 (allyl), $m/z = 73$ (allyl sulfide), $m/z = 105$ (allyl disulfide), $m/z = 47$, 79, 111 for mono-, di- and trisulfides, respectively (Table 7). All the identified compounds are given in Table 8 [18].

4. Conclusions

The detection by AES of sulfur from aromas obtained by the headspace method from various garlic samples (whole non-peeled cloves, peeled cloves, crushed cloves and juices) allowed their sulfur-containing components to be located and compared. These results show the influence of the sample conditions and of the experimental conditions (temperature) on the analytical response when aromas containing very labile and unstable molecules react chemically or enzymatically during sample handling and analytical processes. These observations have to be taken in account for the correct interpretation of the data observed from samples such as garlic and for the use of this kind of product where sulfur-containing molecules are mostly responsible of the flavour and also of the pharmacological properties. The use of elemental profiles obtained from the same sample allows the calculation of inter-element ratios and the determination of the number of C, S and H atoms present in each of the molecules eluted from the GC column when AES data are coupled with MS data. These elemental data are very useful for the determination of the structures and compositions of molecules from complex mixtures such as aromas and natural extracts.

This example shows that a dual analytical strategy can be developed. The first step is the location of the compounds of interest by the specific detection of the atomic emission of one or several of their characteristic elements. In the second step, mass spectra of the selected compounds are recorded, then both mass spectrometric and elemental data are used simultaneously for the accurate determination of the unknown compounds.

Table 8
Identification of sulfur-containing compounds eluted by the headspace device

No.	M_r	Formula	Name
1	88	C_4H_8S	Allyl methyl sulfide
2	94	$C_2H_6S_2$	Methyl disulfide
3	114	$C_6H_{10}S$	Allyl sulfide
4	120	$C_4H_8S_2$	Allyl methyl disulfide
5			
6	120	$C_4H_8S_2$	Methyl *trans*-propenyl disulfide
7			
8	126	$C_2H_6S_3$	Dimethyl trisulfide
9	146	$C_6H_{10}S_2$	Dipropenyl disulfide
10	146	$C_6H_{10}S_2$	Allyl propenyl disulfide
11	146	$C_6H_{10}S_2$	Allyl disulfide
12	152	$C_4H_8S_3$	Allyl methyl trisulfide
13	144	$C_6H_8S_2$	3-Vinyl-1,2-dithiin
14	144	$C_6H_8S_2$	2-Vinyl-1,3-dithiin
15	178	$C_6H_{10}S_3$	Allyl trisulfide

References

[1] G. Garnier, L. Bezanger-Beaucquesnel and G. Debraux, *Ressources Médicinales de la Flore Française*, Vigot, Paris, 1961, p. 1511.
[2] F. Soussan-Marchal, *Thèse de Doctorat en Pharmacie*, No. 49, Institut des Sciences Pharmaceutiques et Biologiques, Lyon, 1993.
[3] I. Joseph, *Thèse de Doctorat en Pharmacie*, No. 34, Institut des Sciences Pharmaceutiques et Biologiques, Lyon, 1993.
[4] A. Stoll and E. Seebeck, *Adv. Enzymol.*, 11 (1951) 377.
[5] M. Mutsch-Eckner, B. Meir, A.D. Wright and O. Sticher, *Phytochemistry*, 31 (1992) 2389.

[6] S.J. Ziegler and O. Sticher, *Planta Med.*, 58, Suppl. (1989) 37.
[7] E. Block, S. Nagathan, D. Putman and S.H. Zhao, *J. Agric. Food Chem.*, 40 (1992) 2418.
[8] L. Lawson and B.G. Hugues, *Planta Med.*, 58 (1992) 345.
[9] B. Iberl, G. Winkler and K. Knobloch, *Planta Med.*, 56 (1990) 202 and 320.
[10] H. Jansen, B. Muller and K. Knobloch, *Planta Med.*, 55 (1989) 440.
[11] D. Deruaz and J.M. Mermet, *Analusis*, 174 (1986) 107.
[12] D. Deruaz and J.L. Brazier, *Spectra 2000*, 161 (1991) 8.
[13] B.D. Quimby and J.J. Sullivan, *Anal. Chem.*, 62 (1990) 1027.
[14] J.J. Sullivan and B.D. Quimby, *Anal. Chem.*, 62 (1990) 1034.
[15] P.L. Wylie and R. Oguchi, *J. Chromatogr.*, 517 (1990) 131.
[16] A.L.P. Valente and P.C. Uden, *Analyst*, 115 (1990) 525.
[17] C. Bicchi, C. Frattini, G. Pellegrino, P. Rubiolo, V. Raverdino and G. Soupras, *J. Chromatogr.*, 609 (1992) 305.
[18] T.H. Yu, C.M. Wu and Y.C. Liou, *J. Agric. Food. Chem.*, 37 (1989) 725.

ELSEVIER

Journal of Chromatography A, 677 (1994) 355–364

JOURNAL OF CHROMATOGRAPHY A

Determination of sodium polyacrylate by pyrolysis–gas chromatography

Walter C. Buzanowski*, Sergio S. Cutié, Robert Howell, Richard Papenfuss, Charles G. Smith

Analytical Sciences, Dow USA, 1897D Building, Midland, MI 48667, USA

First received 11 January 1994; revised manuscript received 8 April 1994

Abstract

The use of sodium polyacrylate superabsorbent polymers continues to grow for the disposable baby and adult diapers market. The fate of these materials in the environment is of continuing interest for the producers and users of these polymers. A method was previously described for the determination of polyacrylic acid in environmental samples after derivatization by pyrolysis–gas chromatography (GC) and by size-exclusion chromatography. However, much of the polymer exists in the neutralized form as sodium polyacrylate which interferes with the derivatization procedures. This paper describes a pyrolysis–GC technique that can be applied to the determination of sodium polyacrylate in the environment without derivatization. Proposed mechanisms for the pyrolysis of the polymer are included as well as identification of the primary pyrolytic products.

1. Introduction

As discussed in a previous paper [1] polyacrylic acid may be determined in environmental samples by pyrolysis–gas chromatography (Py–GC) after derivatization of the polymeric acid to the methyl ester. However, in most commercial forms, polyacrylic acid actually exists as the sodium salt or sodium polyacrylate. Attempts to derivatize the acid groups in the presence of the salt, however, did not proceed with the expected results. When pyrolyzed, the sodium form of the polyacrylic acid gave several unique products including cyclopentadiene that can be used to determine soluble sodium polyacrylate in environmental samples. This paper presents the conditions for the determination of sodium polyacrylate and supporting Py–GC–mass spectrometry (MS) and Py–GC–infrared (IR) spectroscopy data to confirm the identity of the observed pyrolysis products. Literature reference to the formation of cyclopentadiene as a product from pyrolysis of polyacetylene [2] and other references [3–20] were used to propose mechanisms for the formation of the observed pyrolysis products.

2. Experimental

2.1. Sample preparation

Linear polyacrylic acid (weight-average molecular mass, $M_w \approx 243\,000$ and 0% neutralization)

* Corresponding author.

SSDI 0021-9673(94)00383-K

was obtained from Scientific Polymer Products, Ontario, NY, USA. Sodium polyacrylate was prepared at different levels of neutralization by adding known amounts of sodium hydroxide to water solutions of this polyacrylic acid. The water was then removed by freeze drying, and the solid polymer was placed in a quartz tube for Py–GC analysis. Methyl esters of the sodium polyacrylate were prepared as described in a previous paper [1] using Methyl-8 derivatizing reagent (Pierce, Rockford, IL, USA). The methyl esters were prepared by adding 250 μl of Methyl-8 (dimethylformamide solution of dimethyl acetal) to the dried sample. The sample was heated at 160°C for 16 h after which residual solvent was evaporated with a heat lamp and a nitrogen purge. The residue was then dissolved in 0.5 ml of methanol and analyzed by Py–GC. The sample could then be quantitated using the resulting methyl acrylate peak.

2.2. Pyrolysis–gas chromatography

Samples of sodium polyacrylate and methylated sodium polyacrylate solids were weighed into quartz tubes and equilibrated 5 min in a 200°C interface connected to the injection port of an HP5890 gas chromatograph equipped with flame ionization detection (FID). Samples were pyrolyzed (CDS 120 Pyroprobe Pt coil) at a set temperature of 700°C with the maximum heating rate and a 20-s interval. The pyrolysis products were split in the 220°C injection port, separated on a fused-silica capillary column (J & W DBWAX, 60 m × 0.25 mm I.D., 0.25-μm film) using a linear temperature program (50°C for 4 min then 6°C/min ramp to 220°C and a 16-min hold), and detected by FID.

2.3. Py–GC–MS

A 300-μg portion of 60% neutralized polyacrylic acid was weighed into a quartz boat and equilibrated 10 min in a 215°C interface connected to the injection port of a VG TRIO-1 GC–MS system. The sample was pyrolyzed at a set temperature of 700°C (CDS Pyroprobe Pt coil) with a ramp of 20°C per ms and a pyrolysis interval of 20 s. Using splitless injection through a 220°C injection port, pyrolysis products were separated on a 60-m fused-silica capillary column (J & W DBWAX; 0.2-μm film) programmed from 40°C/4 min to 220°C at 6°C/min. Electron impact mass spectra were obtained every second over the range of 29–350 u with the detector multiplier at 330 V, a scanning electron current of 150 μA, a source temperature of 180°C, and the transfer line between the gas chromatograph and the mass spectrometer set at 200°C.

Table 1
Infrared spectrometer conditions

Transfer line temperature (°C)	200
Background scans	100
Sample scans	100
Nominal resolution (cm^{-1})	4
Detector	MCT[a]
Apodization function	Triangular
Iris	0
Zerofill	1 ×

[a] MCT = Mercury cadmium telluride.

2.4. Py–GC–IR

Approximately 0.40 mg of sample was weighed into a quartz tube and pyrolyzed in a helium atmosphere using a CDS Pyroprobe Pt coil. The pyrolysis products were separated using a Hewlett-Packard 5890 gas chromatograph, fitted with a 60-m fused-silica capillary column (J & W DBWAX, 0.2-μm film), interfaced with a Mattson Instruments Cryolect 4800 matrix isolation IR detector. Pyrolysis and chromatographic conditions for the Py–GC–IR experiment were the same as those previously described for the Py–GC–MS experiment. The spectrophotometer conditions used to obtain the IR spectra of the isolated pyrolysis products are shown in Table 1.

3. Results and discussion

3.1. Pyrolysis experiments and identification of pyrolysis products

Fig. 1 compares pyrograms (FID) of derivatized sodium polyacrylate at different levels of neutralization. The arrow designates the reten-

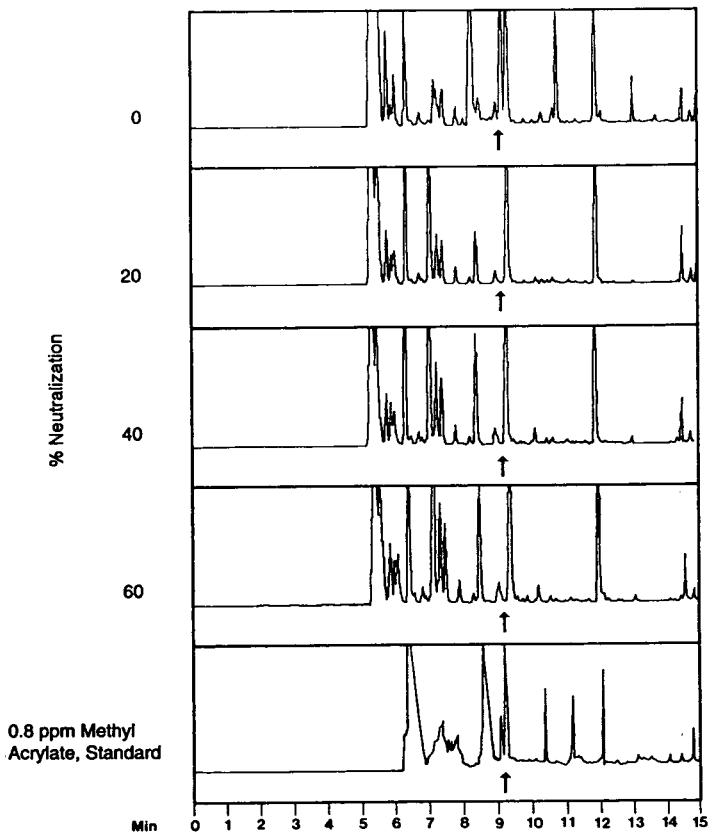

Fig. 1. Derivatization Py–GC of sodium polyacrylate at different levels of neutralization.

tion time for the methyl acrylate product from pyrolysis of polyacrylic acid (no neutralization). This peak is noticeably absent in the pyrograms of the sodium polyacrylate at higher levels of neutralization.

Pyrograms of underivatized sodium polyacrylates at different levels of neutralization are compared in Fig. 2. The peak identified as cyclopentadiene, distinctly absent in the pyrogram of un-neutralized polyacrylic acid, is present in all of the other pyrograms regardless of the level of neutralization. Note that the intensity of the other peaks decreases with increased level of neutralization. As shown in Fig. 3, this peak for cyclopentadiene is present in pyrograms of a 60% neutralized polymer with or without derivatization. Absence of this peak in the pyrogram of un-neutralized, un-derivatized polymer mixed with 60% NaCl indicates that the mechanism for formation of this pyrolysis product is related to the neutralization process and not just the presence of ionic sodium.

The Py–GC–MS experiment was used to verify the identification of cyclopentadiene as a major product from pyrolysis of 60% neutralized polyacrylic acid. Fig. 4 shows the total ion current pyrogram from a 60% neutralized polyacrylic acid sample.

Peak assignments based on the mass spectral data are summarized in Table 2. Fig. 5 represents the mass spectrum of the pyrolysis product peak at scan 339 and this spectrum matches NBS Library reference spectra for cyclopentadiene.

Pyrolysis–GC–IR was subsequently used to verify the identification of cyclopentadiene as a primary product from 700°C pyrolysis of 60% neutralized polyacrylic acid. The phase-sensitive IR reconstructed chromatogram for products

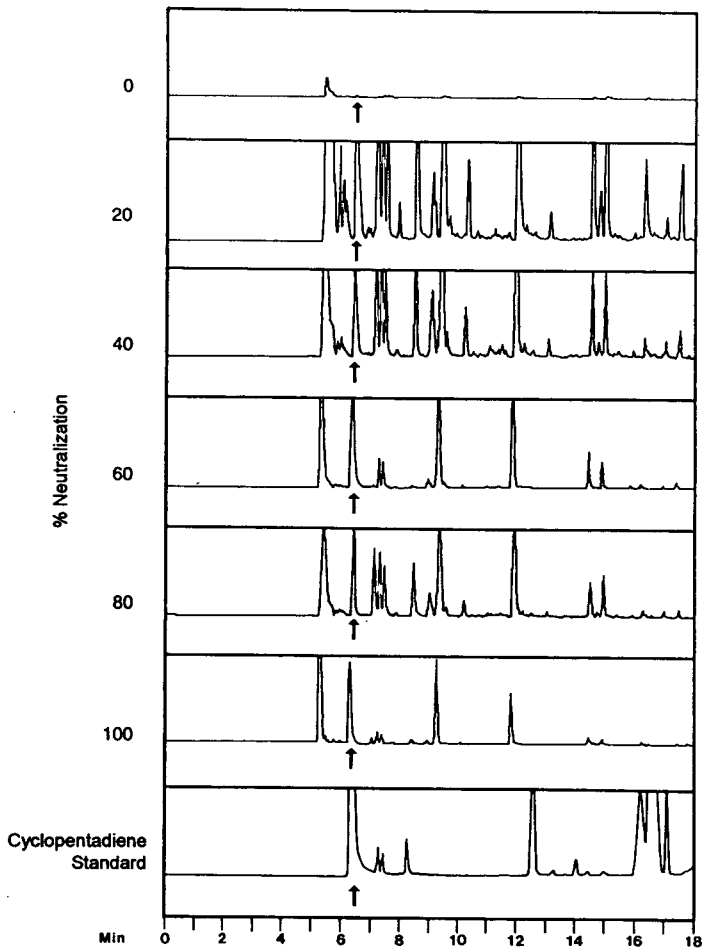

Fig. 2. Underivatized Py–GC of sodium polyacrylate at different levels of neutralization.

from pyrolysis of that sample is shown in Fig. 6 while the IR spectrum of the peak eluting at about 5.53 min is shown in Fig. 7. The major compounds present in this spectrum are methane and carbon dioxide. An expanded spectrum of the peak eluting at 5.53 min is shown in Fig. 8. This expanded spectrum strongly suggests the presence of ethane and ethene as minor components eluting alone with the carbon dioxide and methane. In addition there is evidence for vinyl twisting and wagging vibrations which suggests the possible presence of propene.

The IR spectrum of the material eluting at about 6.53 min is shown in Fig. 9. This spectrum is consistent with that of a standard spectrum of 1,3-cyclopentadiene, and it supports the data obtained by Py–GC–MS.

3.2. Mechanisms for formation of cyclopentadiene

Because of the commercial importance of acrylate polymers, the thermal degradation characteristics (thermal stability) of polyacrylic acid [3–9] and salts [10–18] have received much attention. Although the degradation of these materials has repeatedly been investigated the thermally stimulated processes which occur have not yet been fully delineated. In fact, the mode of degradation seems to be influenced by the

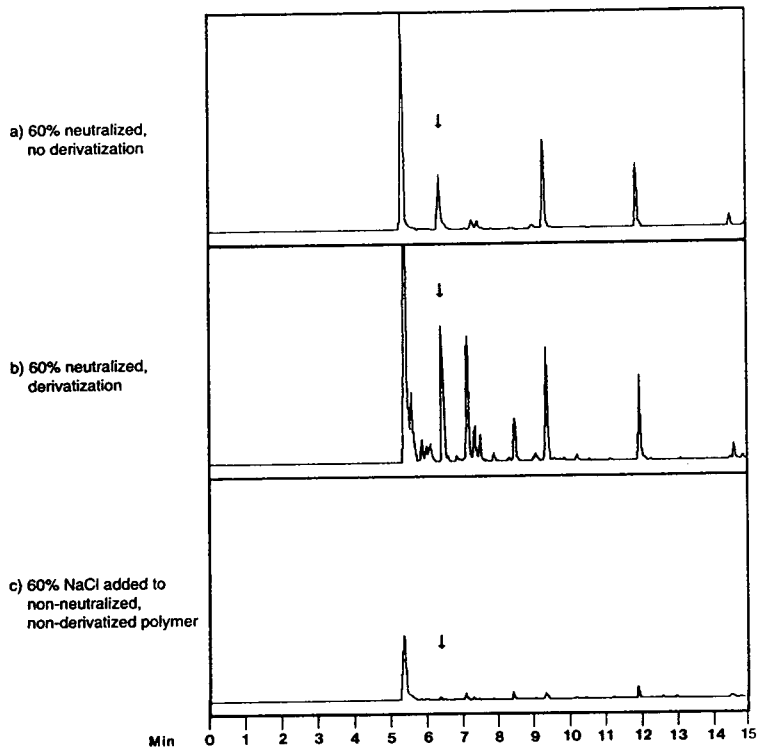

Fig. 3. Py–GC of sodium polyacrylate.

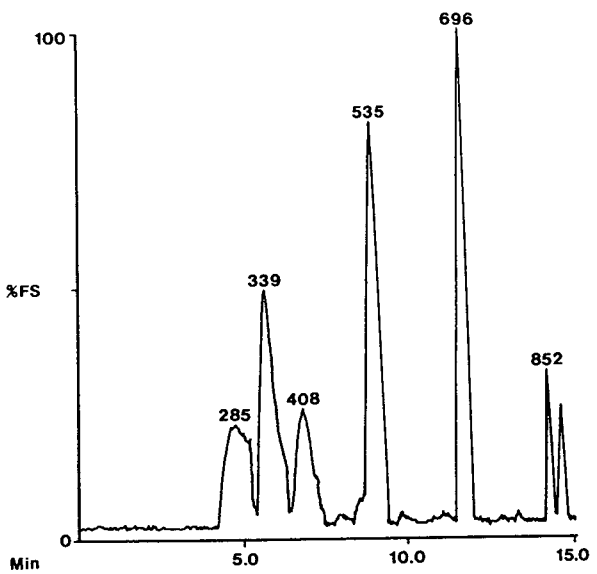

Fig. 4. GC–MS total ion current pyrogram of 60% neutralized polyacrylic acid.

means of sample preparation and the techniques used to study the decomposition. Some prominent features of the decomposition seem to be reasonably well established. The processes most often studied have been those which occur at low or moderate temperature (130–450°C) [3–18].

At approximately 150°C polyacrylic acid undergoes dehydration to form anhydrides [3–9]. Under most conditions anhydride formation is an intramolecular process to form a six-membered cyclic anhydride [7–9]. However, under film-forming conditions substantial intermolecular anhydride formation apparently occurs [10–14]. The nature of the anhydride formed may be influenced by the temperature at which the dehydration occurs [4]. At somewhat higher temperature (250–300°C), the anhydrides undergo decarboxylation to form keto structures [8–10]. The nature of the ketone formed is dependent upon the anhydride from which it originates. Initial intramolecular anhydride formation leads to the generation of cyclobutanone-type

Table 2
Mass spectra of products from pyrolysis of 60% neutralized polyacrylic acid

Scan	Retention time (min)	Prominent m/z [a]	Assignment
285	4.75	(44)	Carbon dioxide
		41, 40, (42), 39	Propylene
339	5.65	(66), 65, 39, 40	1,3-Cyclopentadiene
408	6.80	79, (80), 77, 39, 51, 52	Methyl-1,3-cyclopentadiene
535	8.92	(78), 77, 51, 52, 50	Benzene
696	11.60	91, (92), 65	Toluene
852	14.20	91, (106), 51, 65, 77	Ethylbenzene or dimethylbenzene isomer

[a] Ions listed in order of decreasing intensity with the parent ion in parentheses.

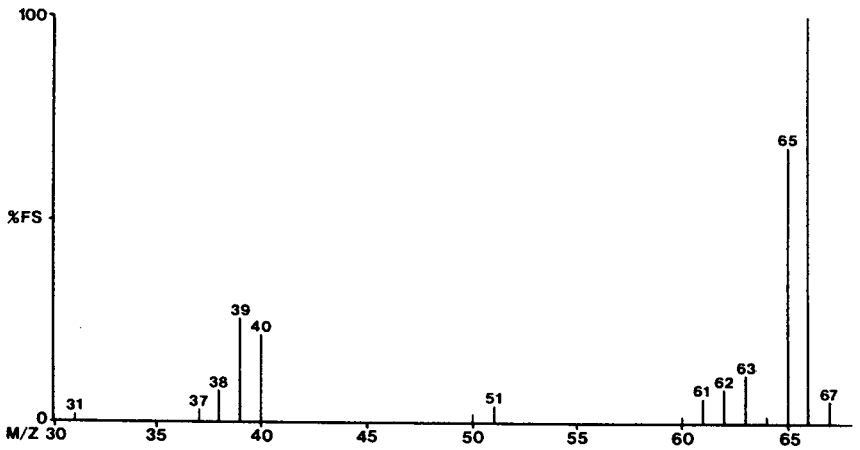

Fig. 5. Mass spectrum of peak 339 (identified as 1,3-cyclopentadiene).

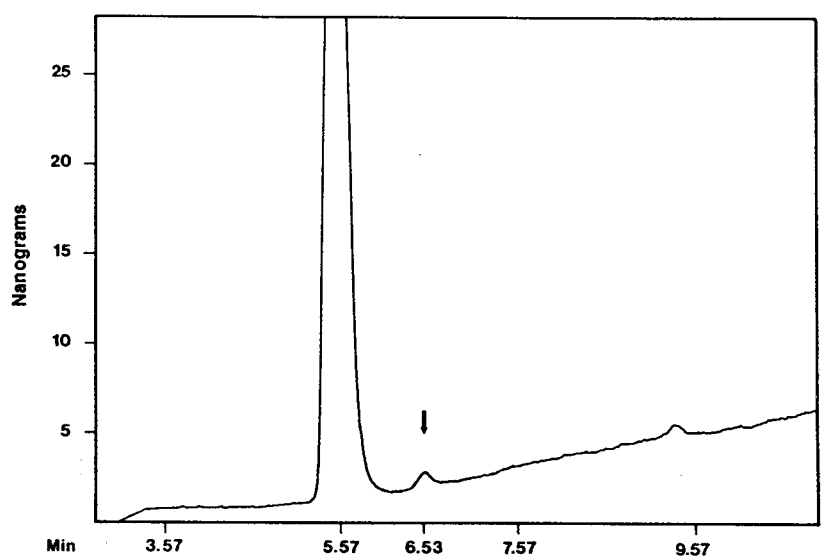

Fig. 6. Phase-sensitive IR reconstructed chromatogram of 60% neutralized polyacrylic acid.

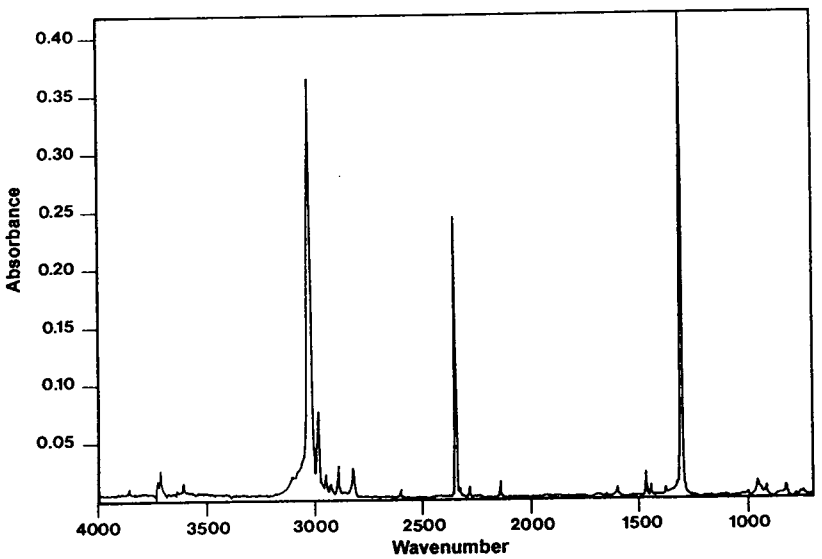

Fig. 7. IR spectrum of peak eluting at 5.53 min in Fig. 6.

structures [8,9] while intermolecular anhydride formation results in the establishment of keto cross-links [10–14] which may be utilized in the generation of superior films. Decarboxylation may be accompanied by some chain scission and ene formation [7,8,19].

Decarboxylation of cyclobutanone units within the degrading polymer may generate cyclopropyl structures [8]. It might be anticipated that such structures would be thermally unstable and could lead to the evolution of unsaturated hydrocarbon fragments. At temperatures above 350°C significant aromatization occurs and a residual char containing phenolic functionality is formed [7].

Anhydride formation is significantly facilitated by partial neutralization of the carboxy groups of

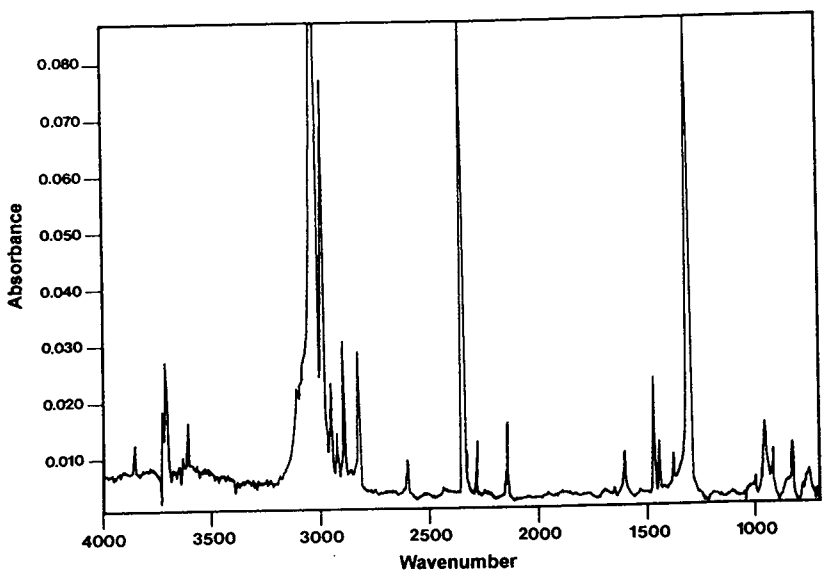

Fig. 8. Enlarged IR spectrum of peak eluting at 5.53 min.

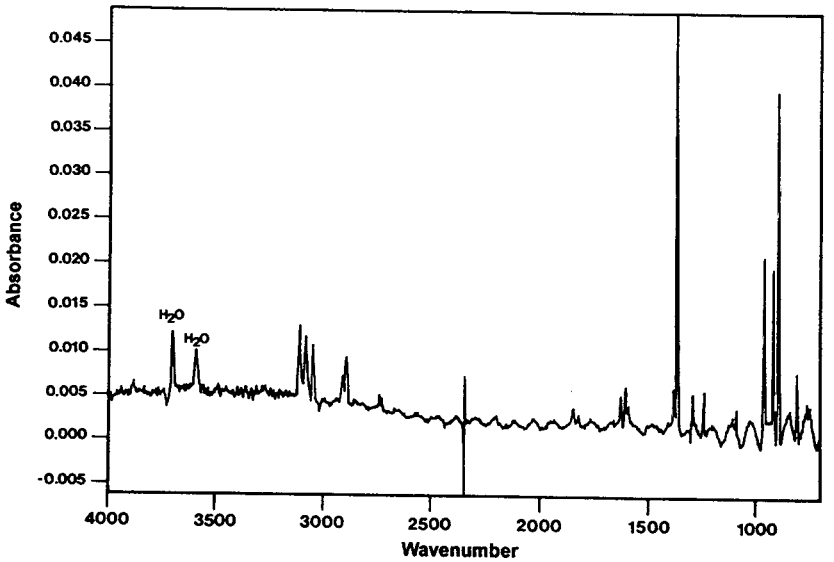

Fig. 9. IR spectrum of peak eluting at 6.53 min (identified as 1,3-cyclopentadiene).

the polyacrylic acid using an inorganic base containing a univalent cation [10,11]. This acceleration of the anhydride-forming reaction apparently arises as a consequence of decarboxylation of the carboxylate salt to form a carbanion which may attack anhydride to form a ketone and regenerate a carboxylate structure [11].

This observation has now been utilized for the development of a method of determination for polyacrylic acid as a partially neutralized salt. In this instance the acid salt was subjected to rapid thermal decomposition at 700°C, a temperature considerably greater than those (120–450°C) used for most previous studies. Under these conditions the partial salt undergoes smooth decomposition to generate a variety of small molecule fragments including most prominently 1,3-cyclopentadiene. As noted above, it is the formation of cyclopentadiene which serves as the basis for the determination method described. As shown in Fig. 10, the presence of even a small amount of neutralization in the starting poly(acid) may greatly accelerate the decarboxylation of the anhydride formed in the initial dehydration step.

As previously noted [10], the carboxylate undergoes decarboxylation to generate a main-chain carbanion. This carbanion is strongly nucleophilic and may attack a neighboring anhydride unit. Nucleophilic addition followed by elimination generates a cyclobutanone unit and at the same time exposes another carboxylate group which is as reactive as the first leading to a

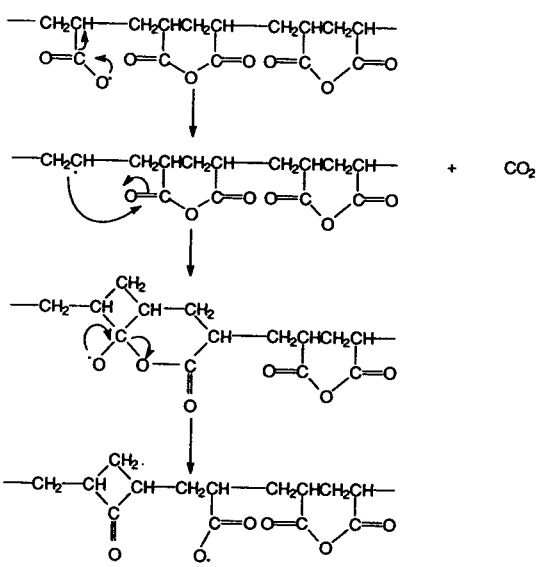

Fig. 10. Decomposition of the anhydride formed from dehydration of partially neutralized polyacrylic acid.

repetition of the sequence: decarboxylation, cyclobutanone formation, generation of another carboxylate unit. This decarboxylation assisted by a neighboring carboxylate group moves rapidly along the polymer chain and accounts for the rapid evolution of carbon dioxide. Since a carboxylate group is regenerated in the ketone-forming step this process should be promoted by even small levels of neutralization. This was demonstrated experimentally in that polyacrylic acid neutralized to the extent of 0.5 to 50% exhibits the same pyrolysis behavior. A possible mode of fragmentation of the keto structure formed from decarboxylation of the anhydride is displayed in Fig. 11.

Of course other less prominent processes are occurring simultaneously with cyclopentadiene formation. A variety of small molecule fragments are formed. It is likely that some of this reflects polyene formation. An alternative mode of formation of cyclopentadiene would be the cyclization/fragmentation of polyene [20].

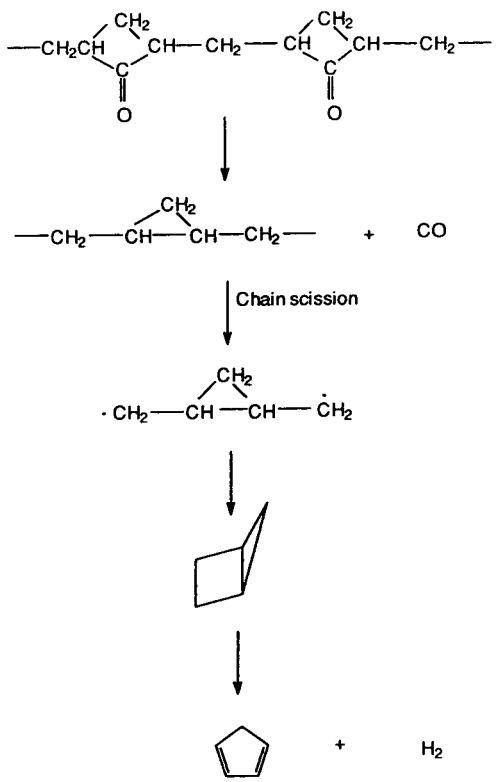

Fig. 11. Potential fragmentation mode leading to the formation of 1,3-cyclopentadiene.

4. Conclusions

Pyrolysis of sodium polyacrylate at 700°C produced 1,3-cyclopentadiene as a unique degradation product and mechanisms were presented for the formation of this compound. The pyrolysis yield of 1,3-cyclopentadiene appeared to be independent of the level of neutralization although yields of other pyrolysis products decreased with increasing levels of neutralization. Although not fully developed in this study, this unique pyrolysis mechanism could be the basis for quantitative procedures to determine sodium polyacrylate in environmental samples. Additional validation is warranted to determine the quantitative limits of this pyrolysis procedure.

References

[1] S.S. Cutié, W.C. Buzanowski and J.A. Berdasco, *J. Chromatogr.*, 513 (1990) 93.
[2] J.C.W. Chien, P.C. Uden and J. Fan, *J. Polym. Sci., Polym. Chem. Ed.*, 20 (1982) 2159.
[3] M.C. McGaugh and S. Kottle, *Polym. Lett.*, 5 (1967) 817.
[4] A. Eisenberg, T. Yokoyama and E. Sambalido, *J. Polym. Sci., Pt. A-l*, 7 (1969) 1717.
[5] F.X. Roux, R. Audebert and C. Quivoron, *Eur. Polym. J.*, 9 (1993) 815.
[6] H. Girard, P. Monjol and R. Audebert, *C.R. Acad. Sci., Ser. C*, 279 (1974) 597.
[7] C.A. Fyfe and M.S. Mckinnon, *Macromolecules*, 19 (1986) 1909.
[8] J.J. Maurer, D.J. Eustace and C.T. Ratcliffe, *Macromolecules*, 20 (1987) 196.
[9] I.C. McNeill and S.M.T. Sadeghi, *Polym. Degrad. Stab.*, 29 (1990) 233.
[10] J.W. Nicholson and A.D. Wilson, *Br. Polym. J.*, 19 (1987) 67.
[11] J.W. Nicholson and A.D. Wilson, *Br. Polym. J.*, 19 (1987) 449.
[12] J.W. Nicholson, E.A. Wasson and A.D. Wilson, *Br. Polym. J.*, 20 (1988) 97.
[13] J.W. Nicholson, R.P. Scott and A.D. Wilson, *J. Oil Colour Chem. Assoc*, 70 (1987) 157.

[14] J.W. Nicholson and A.D. Wilson, *Chem. Ind. (London)*, (1986) 530.
[15] R. Yamada, K. Tamura, S. Harada and T. Yasunaga, *Bull. Chem. Soc. Jpn.*, 55 (1982) 3413.
[16] A. Gronowski and Z. Wojtczak, *J. Thermal Anal.*, 26 (1983) 233.
[17] J. Skupinska, H. Wilczura and H. Boniuk, *J. Thermal Anal.*, 31 (1986) 1017.
[18] E.E. Sileo. P.J. Morando, E.C. Baumgartner and M.A. Blesa, *Thermochim. Acta*, 184 (1991) 295.
[19] B.-C. Ho, Y.-D. Lee and W.-K. Chin, *J. Polym. Sci., Polym. Chem. Ed.*, 30 (1992) 2389.
[20] S.A. Groves, R.S. Lehrle, M. Blazo and T. Szekely, *J. Anal. Appl. Pyrol.*, 19 (1991) 301.

ELSEVIER

Journal of Chromatography A, 677 (1994) 365–376

JOURNAL OF CHROMATOGRAPHY A

Evaluation of the particle beam interface for packed-column supercritical fluid chromatography–mass spectrometry with pure and modified CO_2

Paul T. Jedrzejewski, Larry T. Taylor*

Department of Chemistry, Virginia Polytechnic Institute and State University, Blacksburg, VA 24061, USA

First received 2 February 1994; revised manuscript received 12 April 1994

Abstract

The particle beam interface was evaluated for microbore packed-column supercritical fluid chromatography–mass spectrometry coupling. The experiments were conducted with mobile phase of pure CO_2 and methanol-modified CO_2 under flow injection and chromatographic conditions. The effects of various operational parameters were characterized. The electron impact limits of detection (LODs) of the system for single ion monitoring and scan modes were determined to be 5 and 40 ng for caffeine, respectively. These LODs are 2.5 to 25 times better than previous reported estimates. Sensitivity was found to be highly dependent on the modifier percentage with 4% methanol-modified CO_2 yielding optimal results. Separations of phenylurea pesticides and steroids are shown as demonstrations of system utility. Background subtracted electron impact spectra were artifact-free and comparable with on-line library spectra.

1. Introduction

Mass spectrometric (MS) detection for chromatography is most desirable considering the plethora of detectors. Besides Fourier transform IR and NMR, no other chromatographic detector can provide both quantitative and structural information. Specifically, electron impact (EI) MS is most useful because of the extensive fragmentation resulting in unique compound spectra. These spectra maybe subjected to a comparison with computerized library spectra thereby making analyte identification easier. The specificity of EI spectra is in contrast to other "softer" methods of ionization (thermospray, chemical ionization) which yield spectra characterized by little or no fragmentation. Because of their speed and simplicity, on-line detection (chromatography–MS) is most desirable. Although GC–EI-MS and LC–EI-MS are well established analytical tools, this is not true for other forms of chromatography such as supercritical fluid chromatography (SFC). The goal of a robust and sensitive interface for packed column SFC–EI-MS has been especially elusive. A certain degree of success has been achieved for capillary SFC–EI-MS [1–5]. Even in those experiments, however, some of the resulting spectra were not true EI spectra but were composites of charge-exchange and EI spectra [1,3,4]. The

* Corresponding author.

0021-9673/94/$07.00
SSDI 0021-9673(94)00394-O

sensitivity for these capillary systems was in the pg range for scan data which were comparable to GC–EI-MS. A similar robust and practical solution for packed-column SFC has not been demonstrated. To date two interfaces have been used for packed-column SFC–EI-MS: the moving belt interface and the particle beam (PB) interface. Games and co-workers [6–10] have shown successful coupling via the moving belt interface with applications ranging form steroids and bile acids to antibiotics. The sensitivity for scan EI was reported in the low nanograms. This particular solution is not very desirable because of the inherited non-robustness of the introduction method, the mechanical complexity of the interface, decomposition of thermally labile analytes, and problems with quantitative transfer of non-volatile analytes [11–14]. None of these difficulties hampered the PB interface to the same extent since this interface is mechanically simpler. However, the PB interface does present two important disadvantages: complex optimization and poor mass transfer to the ion source which results in a limited sensitivity.

Two research groups have investigated the PB interface for packed column SFC–EI-MS coupling. The work of Edlund and Henion [15] was performed on a laboratory-made prototype PB interface coupled to a Hewlett-Packard 5985 mass spectrometer. In these experiments no optimization was performed, thus the authors estimated sensitivities in the low micrograms for full scan EI. Separations on analytical-scale (4.6 mm I.D.) and narrow-bore (2.0 mm I.D.) columns with methanol-modified fluids were presented. The utility of the system was demonstrated with applications for the following classes of compounds: pesticides, polymer additives, steroids and xanthines. These separations were accomplished under isobaric conditions at liquid CO_2 mobile phase flow-rates of 0.5 to 1.5 ml/min. Except for the polymer additive separation, the mobile phases were isoconfertic. The mass spectra were artifact-free and comparable to those obtained under GC–EI-MS conditions. In order to facilitate aerosol formation and transmission of analyte through the interface, all data were collected with methanol introduced into the mobile phase post-column and pre-nebulizer.

Browner and co-workers [16,17] demonstrated PB application in SFC–MS with both packed and open tubular columns. This work was performed employing a laboratory-constructed interface coupled to a VG ZAB-E double focusing mass spectrometer. All data were acquired with methanol or acetonitrile introduced prior to nebulization of the mobile phase. Extract of marine sediment was separated on an open tubular column (50 μm I.D.) with pressure programming and a mobile phase flow-rate of 1–5 μl/min of pure liquid CO_2. Packed-column separations of ω3 fatty acids and isomers of pyrrolizidine alkaloids were reported. EI spectra of the compounds were presented with no indication of solvent interference. The detection limit of the system was estimated to be between 100 ng to 1 μg for cholesterol (full scan).

In this paper a performance evaluation of a commercial PB-MS system is presented. The goal of these studies was to evaluate the performance of the PB interface with pure CO_2 and methanol-modified CO_2 as the mobile phase. All experiments were performed without the addition of particle forming solvents prior to nebulization as was done in the referenced studies. Elimination of the particle-forming solvent greatly simplifies the system by eliminating the need for a secondary pump and other hardware. Furthermore, pressure or density programming maybe used without the need for synchronization of CO_2 and particle forming solvent pumps during pressure/density ramps. Parameters that affect the performance of the PB were evaluated. Optimization of the nebulization process was investigated by examining the effects of restrictor position and nebulizing gas pressure on sensitivity. The effect of CO_2 flow-rate and percent of modifier were assessed for their impact on sensitivity. Quantitative EI data are also presented for scan and single ion monitoring. Separations of steroids and phenyl urea pesticides are used to demonstrate the utility of this system for compound identification through artifact-free, library searchable EI spectra.

2. Experimental

2.1. Instrumentation

A Model 5988A MS (Hewlett-Packard, Palo Alto, CA, USA) was coupled via a Model 59980A PB interface (Hewlett-Packard) to the SFC system. For basic studies the SFC system was the Model 200A (Suprex, Pittsburgh, PA, USA) consisting of a syringe pump, oven, injector and dedicated controller. The injection loop was 0.5 μl in volume. For the CO_2 flow-rate study, a Model 100D syringe pump (Isco, Lincoln, NE, USA) was used which consisted of a pump with a controller and an injector (Valco, Houston, TX, USA). The separations of steroids and phenylurea pesticides were generated using a Model 600 Dionex SFC system (Salt Lake City, UT, USA). This system consisted of a syringe pump, oven, 0.5-μl injector and personal computer. All chromatography was performed on a Deltabond CN packed column (100 × 1 mm, 5 μm particle size) (Keystone Scientific, Bellefonte, PA, USA). Pressure in these systems was maintained by a 40 cm linear (25 μm I.D.) capillary restrictor constructed of deactivated fused silica (SGE, Austin, TX, USA). The restrictor was installed in the nebulizer of the PB so that the restrictor tip was even with the orifice of the stainless-steel tube nebulizer (Fig. 1).

2.2. Chemicals

Caffeine and steroids (Sigma, St. Louis, MO, USA) were used as received. Standard solutions of caffeine and steroids were prepared in HPLC-grade methanol (Fisher Scientific, Pittsburgh, PA, USA) and filtered through a 0.2-μm membrane PTFE filter (Supelco, Bellefonte, PA, USA). Solutions of the phenyl urea pesticides (Aldrich, Milwaukee, WI, USA) were prepared in HPLC-grade methylene chloride (Fisher Scientific). SFC-grade CO_2 and methanol-modified CO_2 were obtained from Scott Specialty Gases (Plumsteadville, PA, USA).

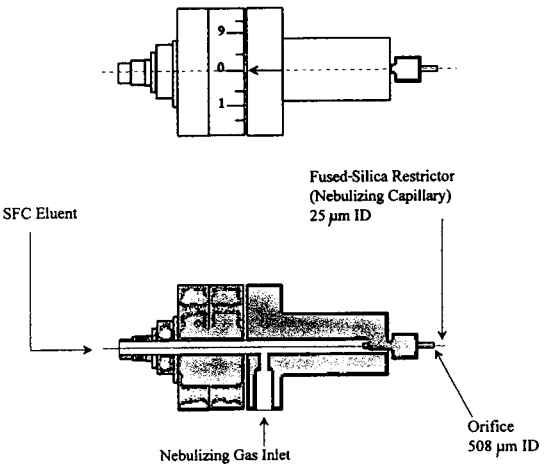

Fig. 1. Schematic of the nebulizer.

3. Results and discussion

3.1. Principle of operation

The PB interface traditionally allows for coupling of the SFC or LC chromatograph to a mass spectrometer by (a) forming an aerosol, (b) separating the analyte from the solvent, (c) concentrating the analyte into a beam and (d) transporting the analyte to the ion source of the mass spectrometer. Following the exit from the column, the effluent is introduced into a pneumatic nebulizer. The nebulizer's function is to generate a fine aerosol of droplets. This aerosol traverses the desolvation chamber, allowing for volatile solvent to evaporate thereby forming optimum size droplets of about 6–15 μm in diameter [18]. This mixture of solvent vapor and analyte droplets encounters the momentum separator. The function of the momentum separator is to separate droplets and vapor based on momentum. Taking advantage of the difference in momenta, the higher-momentum analyte particles are transmitted while the low-momentum vapor is pumped away. From the momentum separator, analyte particles travel through the transfer tube into the ion source where analyte is vaporized, ionized, and focused into the analyzer where detection of ions occurs. For

optimum performance of the interface, a number of parameters must be considered.

Pneumatic nebulization is employed (Fig. 1) to generate an aerosol of droplets. Nebulization occurs due to coaxial flow of helium gas that is introduced before the exit of the nebulizing capillary and that flows concentrically the length of the capillary. Droplets are formed as the nebulizing gas encounters the effluent at the point of exit from the capillary causing shearing of droplets. The effect of the nebulizing gas on sensitivity may be studied by changing the helium gas pressure which in turn affects the size and distribution of the droplets [18–22]. Changing the pressure of the nebulizing gas alters the pressure in the desolvation chamber and consequently alters the efficiency of the desolvation process. Another parameter important in sensitivity optimization is the position of the nebulizing capillary relative to the orifice of the nebulizer. The position of the nebulizing capillary determines the aerosol characteristics of the resulting spray.

The aerosol formed by the nebulizer is sprayed into the desolvation chamber which is a hollow, thermostatically controlled cylinder. The desolvation chamber allows time and effective thermal conduction to occur. Since the desolvation chamber is maintained at a pressure of about 200 Torr (1 Torr = 133.322 Pa), thermal conduction is maintained between the walls of the desolvation chamber and the aerosol droplets. The desolvation chamber temperature influences the size of the droplets and consequently the efficiency of the analyte transport.

At the end of the desolvation chamber the solvent vapor and analyte droplets are separated and concentrated by the momentum separator. The momentum separator consists of a nozzle and a pair of skimmers. The function of the nozzle is to focus the mixture of vapor and droplets formed in the desolvation chamber. Because of the difference (a 40-fold reduction) in pressure, a supersonic jet is created at the exit of the nozzle. As a consequence of the adiabatic cooling by the supersonic jet, the droplets become particles, hence the name particle beam. Some distance from the nozzle orifice a mach

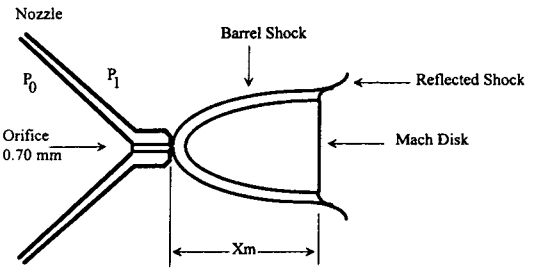

Fig. 2. Diagram of the supersonic jet expansion formed at the nozzle.

disk is formed where the flow makes a transition from supersonic to subsonic velocity. A diagram depicting the supersonic jet is shown in Fig. 2. The distance from the nozzle to the mach disk (X_m) may be predicted by Eq. 1

$$X_m = 0.67 D_n \left(\frac{P_0}{P_1}\right)^{0.5} \quad (1)$$

where D_n is the diameter of the nozzle (0.70 mm), P_0 is the upstream pressure of the gas (200 Torr) and P_1 is the downstream pressure in the expansion region (5 Torr) [23]. The first skimmer is positioned to be just within the distance to the mach disk. At this distance sampling of the particle beam is maximized and the vapor is skimmed off. The volume between the nozzle and the first skimmer is referred to as the first stage of this differentially pumped interface. The second stage of the particle beam exists between the first and second skimmer. At the second stage, there is a reduction in pressure (about 20-fold), resulting in supersonic jet formation. The second skimmer, like the first, samples most of the beam excluding the vapor which gets pumped away by the second-stage mechanical pump. Following the momentum separator, the beam of particles is transported by the transfer tube into the ion source where vaporization and ionization occur. The ions are focused into the quadrupole and detected.

3.2. Optimization under SFC conditions

In the following sections the results of studies of each of the parameters discussed above are

evaluated under SFC conditions. Although the PB interface has been under scientific evaluation for a number of years in different variations (i.e. Thermabeam, MAGIC, Universal interface), the operation of PB at first principles has not been yet achieved. Much of the available data is in qualitative form. However, some areas of the PB have received more attention (i.e. supersonic jet formation and sampling) therefore we hope to use the available principles to give a more concrete description of the operating mechanism(s). Qualitative interpretation of the data is given for the most part. Furthermore, since detection with methanol-modified CO_2 mobile phase was only possible, liquid-like nebulization is assumed. The data were acquired under flow injection conditions (FIA). The mass spectrometer was operated in single-ion monitoring mode; monitoring the 1941 u molecular ion of caffeine. Each data point is the average of at least three replicates. The relative standard deviation (R.S.D.) for these points ranged from 4 to 8%.

Position of the restrictor relative to the end of the nebulizer

At positions far outside of the nebulizer orifice (position >5), a single liquid jet with little divergence was visually observed. The sensitivity decreased in this range due to large droplets formation. Large droplet formation has been shown to be favored by increasing the distance between nebulizer and nebulizing capillary due to a decrease in the interaction between the nebulizing gas and mobile phase flow [18,20–22]. Large droplets are, however, inefficiently transported due to impaction within the interface and gravitational settling. Just outside the nebulizer orifice (position 5), the nebulizing gas and the emerging mobile phase interacted most favorably to yield maximum signal intensity. With the nebulizing capillary within the nebulizer assembly, another optimum setting was found where the flow of the helium gas was least turbulent and formed an efficient aerosol. Beyond this optimum, sensitivity decreased because the analyte was sprayed on the inside of the nebulizer and resulted in inefficient transport of the analyte. This decrease in transport efficiency was observed due to the buildup of caffeine on the inside of the nebulizer. Direct comparison of these data with those obtained under LC conditions is difficult because of the difference in nebulization conditions (nebulizing capillary I.D., mobile phase flow-rate and composition). Nonetheless, under LC conditions the response surface of nebulizing capillary position versus signal exhibits a difference between the peaks and the valleys from 30 to 50% [24,25], whereas these data under SFC indicate less of a range (15 to 20%) between the peaks and the valleys. These results indicate, as might be expected, that the decompressing mobile phase participates in self nebulization. However, this self nebulization alone is not sufficient for efficient transport of analyte through the PB as indicated by the data in the following section.

Pressure of the nebulizer gas

The explanation of the effect of nebulizing gas pressure on signal intensity maybe attributed to changes in the following parameters: size of droplets, desolvation of droplets and sampling efficiency of skimmer 1. It has been shown that with increasing nebulizing gas pressure droplets size decreases [18,20–22]. In this experiment optimum conditions were attained at 45 p.s.i. (1 p.s.i. = 6894.76 Pa) resulting in production of droplets which were effectively transported. Above 45 p.s.i., the produced droplets were too small to be effectively transported through the interface and were pumped away with the vapor.

As the pressure in the desolvation chamber rose due to increasing nebulizing gas pressure, the efficiency of the desolvation process changed. With increasing desolvation chamber pressure, thermal conductivity between chamber walls and the droplets increased. Increases in thermal conductivity resulted in more efficient desolvation of droplets. This relationship was favorable until optimum conditions at a pressure of 45 p.s.i. were reached. Beyond the optimum, signal intensity decreased because of excessive desolvation of droplets. Sampling efficiency of skimmer 1 is dependent on the position of the mach disk. The position of the mach disk (X_m) is determined by Eq. 1. With the rise in desolvation

chamber pressure, the distance from the nozzle to the mach disk increases. An increase in X_m translated into changes in the sampling efficiency of skimmer 1. As the pressure in the desolvation chamber increased, sampling efficiency of skimmer 1 increased and eventually became optimum. Beyond the optimum nebulizing gas pressure, signal intensity decreased due to the influence of an other factor: droplet size reduction as the result of increased desolvation efficiency.

Temperature of the desolvation chamber

The effect of desolvation chamber temperature has been shown to result in decreasing droplet size with increasing temperature [18,21,22]. For our work, the optimum temperature for the desolvation chamber was between 30 to 45°C. In this range the droplets were not excessively desolvated, and droplet distribution was optimum. At temperatures above 45°C, the efficiency of the desolvation process increased resulting in a decrease in the size of the produced droplets. The reduction in droplet size translated into reduction in the efficiency of the momentum separator to transmit smaller and smaller droplets.

Distance of the nebulizer relative to the opening of the nozzle

Since the data on the effect of the desolvation chamber temperature have shown that no extra energy was required to increase the effectiveness of the desolvation process, the effect of the distance of the nebulizer to the nozzle was investigated. The distance between the nebulizer and the opening of the nozzle was changed by increasing the length of the nebulizer. As a consequence of the change in the length of the nebulizer, the time that the droplets spent in the desolvation chamber also was altered. Increasing the length of the nebulizer effectively decreased the time the aerosol was resident in the desolvation chamber. The reduction in time resulted in decreased effectiveness of the desolvation process [21,22]. Large droplets were formed that were too large to be transported to the nozzle orifice. The loss in sensitivity occurred because these droplets impacted in the desolvation chamber in the region in front of the nozzle orifice. Losses occurred also to the preferential loss of these larger droplets to gravitational settling. Also it has been calculated that the Reynolds number (*Re*) at the nebulizer (14 000) exceeds the critical value (2000–3000), thus indicating turbulent flow [22]. Laminar flow is promoted by lengthening the distance for the aerosol to travel. For these reasons, the most effective position of the nebulizer was, therefore, found to be at the maximum distance from the nozzle.

3.3. Mobile phase flow-rate

Since the separation in SFC is achieved (assuming a fixed restrictor) by increasing the pressure (or density) of supercritical fluid while allowing the flow-rate to increase, the effect of mobile phase flow-rate on sensitivity is an important consideration. Furthermore, column selection (I.D.) is dependent on the operating flow-rate of a detector. As the liquid flow-rate of the CO_2 was increased beyond 0.64 ml/min, the efficiency of the interface decreased and so did the sensitivity (Fig. 3). The reasons for the decrease in efficiency and sensitivity were due to inefficient nebulization and increased aerosol impact at high mobile phase flow-rates. As the CO_2 flow-rate increased, the contribution of CO_2

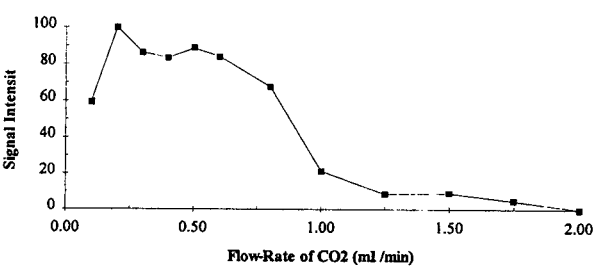

Fig. 3. Effect of liquid CO_2 flow-rate on signal intensity. Conditions: Isco SFC system; 100% CO_2; PB conditions: restrictor position, 5; desolvation chamber temperature, 40°C; nebulizing gas pressure, 45 p.s.i.. FIA of 0.5-μl injection of 100 ng/μl caffeine in methanol. Other conditions given in Experimental section.

to nebulization increased in an adverse manner. With increased flow-rate, a decrease in nebulization efficiency was observed due to the formation of larger droplets. At mobile phase liquid flow-rates greater than 1.0 ml/min, droplets on the underside of the nebulizer and scattering of droplets perpendicular to the nebulizing gas flow were observed. Furthermore, with increasing CO_2 flow-rate, divergence of the spray was observed that resulted in the impact of aerosol on the walls of the desolvation chamber as well as on the nozzle. For these reasons, a reduction in signal intensity was observed as the analyte transport through the PB and into the mass spectrometer decreased. At 0.10 ml/min, the decrease in sensitivity was due to formation of very small droplets. These smaller droplets were inefficiently transported and resulted in a signal decrease. For liquid flow-rates between 0.1 ml/min to 0.64 ml/min, the response was nearly constant. This range is sufficient for optimum operation of 1.0 and 2.0 mm I.D. packed columns.

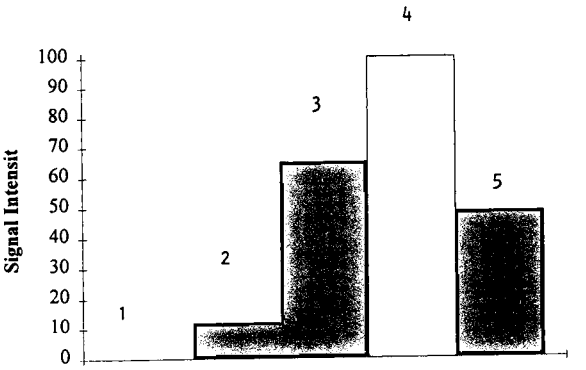

Fig. 4. Effect of percent modified CO_2 on signal intensity. Conditions: Dionex SFC system; PB conditions: restrictor position, −4; desolvation chamber temperature, 40°C; nebulizing gas pressure, 45 p.s.i.. Column: Deltabond CN 100 × 1 mm; isobaric, 75°C; 0.5-μl injection of 400 ng/μl caffeine in methanol. Other conditions given in Experimental section. 1 = Pure CO_2; 2–5 = methanol-modified CO_2: 2 = 1%, 3 = 2%, 4 = 4% and 5 = 8% methanol.

3.4. Mobile phase composition

The effect of percent modified CO_2 was evaluated at four modifier concentrations (mol/mol). Methanol-modified CO_2 was delivered from premixed CO_2 cylinders. The caffeine sample was chromatographed isobarically on a Deltabond CN column with a liquid flow-rate of 0.2 ml/min. As shown in Fig. 4, with increasing modifier percentage (0 to 8%), the signal intensity increased to an optimum at 4% methanol-modified CO_2. At 8% the signal intensity decreased to less than half of the signal intensity at 4%. With pure CO_2 as the mobile phase, no response was observed which is consistent with the available data concerning droplet formation on decompression with pure CO_2. Randall and Wahrhaftig [23] have derived an empirical relationship which allows for estimation of the average number of molecules in a particle (N)

$$N = 6 \cdot 10^{11} P_{0,SF}^{1.44} D_n^{0.86} T_0^{-0.54} \quad (2)$$

where $P_{0,SF}$ is the pressure of the supercritical fluid in Torr, D_n is the diameter of the restrictor orifice in mm and T_0 is the temperature of the supercritical fluid in K [23]. For typical conditions $P_{0,SF} = 304\,117$ Torr (or 395 bar), $D_n = 0.025$ mm and $T_0 = 313$ K, the average cluster size is about $6.6 \cdot 10^4$ molecules which results in a particle size of 0.12 μm in diameter. The typical droplet size distribution under LC conditions was found to range from 6 to 15 μm [18,19]. Therefore, the resulting decrease in the size of the particles (50- to 125-fold reduction) explains the lack of sensitivity when using pure CO_2. The data (Fig. 4) suggest that the introduction of modifier fosters improved aerosol generation and an increase in particle size as indicated by the increase in signal from 1 to 4% modified CO_2. However, at 8% modified CO_2, the decrease in signal may be due to losses of analyte in the nebulization and desolvation processes as a consequence of further increase in particle size as well as dilution of the analyte with the increased amount of modifier. Further studies characterizing the aerosol (particle size and distribution) as a function of modifier concentration are needed to ascertain the exact influence of modifier on sensitivity.

3.5. Sensitivity

Following particle beam optimization, the sensitivity of the SFC–PB-MS system was evaluated. Caffeine was chromatographed isobarically and isoconfertically with 4% methanol-modified CO_2. Data for both single ion monitoring (SIM) and full scan (150 u wide) were acquired with an ion source temperature at 250°C. The mass spectrometer was calibrated with perfluorotributylamine (PFTBA) and tuned to maximize the 219 u peak of PFTBA. The data for SIM are shown in Fig. 5 for the 194 u molecular ion of caffeine. The calibration curve was non-linear ($r = 0.986$) which is consistent with the reported observations by other workers under LC–MS conditions [25–28]. The experimentally evaluated limit of detection (LOD) was 5 ng caffeine injected at S/N 3. The correlation coefficient for scan (150 u wide) acquired data was 0.995 and the LOD was experimentally found to be 40 ng injected at S/N 3. A chromatogram of three replicate injections of 40 ng caffeine is shown in Fig. 6. The reproducibilities for integrated signal ranged from 2 to 10% R.S.D. at the high and low ends of the calibration plots. These obtained detection limits are 2.5 to 25 times lower than the best reported estimates of LOD by other researchers [15,16].

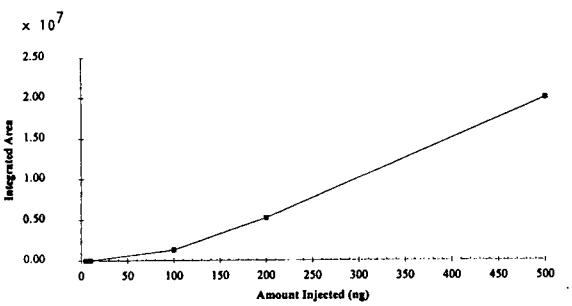

Fig. 5. Calibration curve for caffeine with SIM. Conditions: Dionex SFC system; column 100 × 1 mm I.D. Deltabond CN maintained at 60°C; mobile phase 4% methanol-modified CO_2, 197 bar, and 0.20 ml/min liquid flow; PB conditions: nebulizing gas pressure, 40 p.s.i.; desolvation chamber temperature, 40°C; restrictor position, −3. Other conditions given in Experimental section.

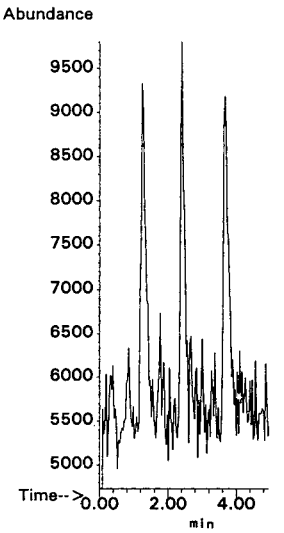

Fig. 6. Chromatogram of three replicate injections of caffeine at 40 ng.

3.6. Applications

The ability to positively identify unknown compounds by virtue of unique EI spectra is the biggest advantage of SFC–PB-MS. An additional advantage of packed-column SFC is that very fast and efficient separations may be generated. Also, due to the mild conditions of SFC, thermally labile compounds maybe separated. Because of their thermal decomposition phenylurea pesticides may not be separated and analyzed by GC–MS directly. Thus, the analysis of these pesticides demonstrates the capabilities of the present system. Fig. 7 shows a separation of six phenylurea pesticides in less than 5 min. The separation was accomplished using a 10 cm × 1.0 mm I.D. microbore column with 4% methanol-modified mobile phase under isobaric conditions. Figs. 8 and 9 show background-subtracted and library spectra of monuron and siduron, respectively. Characteristic of phenylurea pesticides is fragmentation yielding a base peak at 61, 72 or 93 u and a molecular ion peak at less than 50% ion intensity. These base peak fragments are generated by the cleavage of the carbonyl carbon–nitrogen bond. In the case

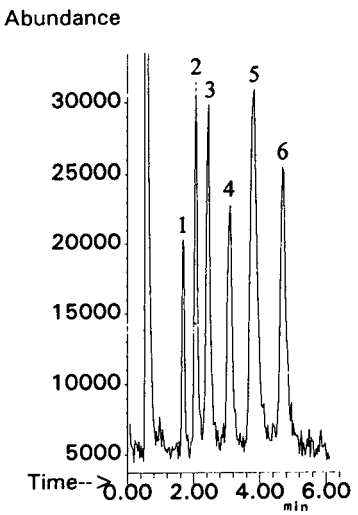

Fig. 7. Separation of phenylurea pesticides. Peaks: 1 = metobromuron; 2 = linuron; 3 = chlorbromuron; 4 = monuron; 5 = siduron; 6 = diuron. Conditions: Dionex SFC system; column 100 × 1 mm I.D. Deltabond CN maintained at 85°C; 4% methanol-modified CO_2; 197 bar; flow-rate, 0.20 ml/min liquid flow; injection 0.5 μl of 1.0 μg/μl per component; PB conditions: restrictor (linear, 25 μm I.D.) position, −4; desolvation chamber temperature, 40°C; nebulizing gas pressure, 45 p.s.i.. Other conditions given in Experimental section.

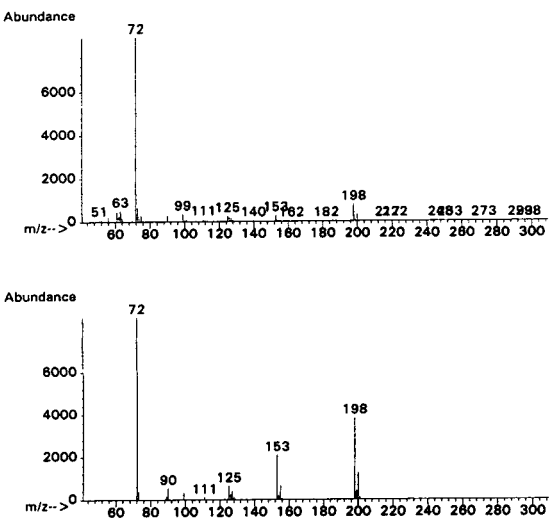

Fig. 8. EI spectrum of monuron (top) and library spectrum (bottom).

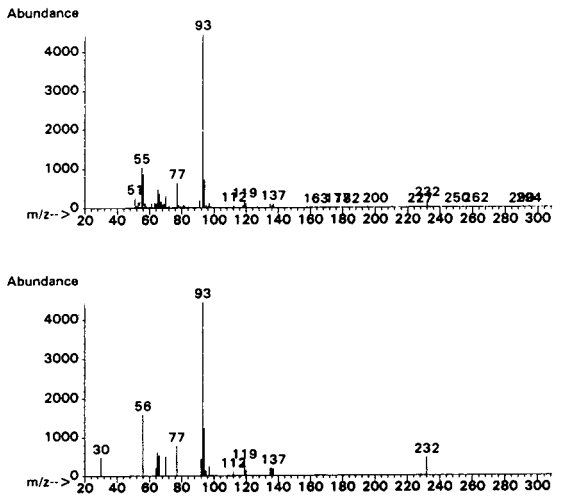

Fig. 9. EI spectrum of siduron (top) and library spectrum (bottom).

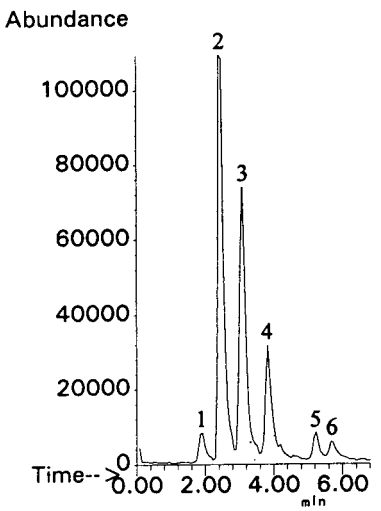

Fig. 10. Separation of steroids. Peaks: 1 = cholesterol; 2 = progesterone; 3 = testosterone; 4 = 17a-hydroxyprogesterone; 5 = 11-deoxycortisol; 6 = corticosterone. Conditions: Dionex SFC system; column 100 × 1 mm I.D. Deltabond CN maintained at 75°C; 4% methanol-modified CO_2; 148 bar; flow-rate, 0.20 ml/min liquid flow; injection 0.5 μl of 2.0 μg/μl per component; PB conditions: restrictor (linear, 25 μm I.D.) position, −2; desolvation chamber temperature, 40°C; nebulizing gas pressure, 40 p.s.i.. Other conditions given in Experimental section.

of siduron, the base peak (93 u) is due to the anilino ion. Whereas for the other five pesticides, the base peak is due to the dimethylisocyanate ion (72 u) or the methylmethoxyisocyanate ion (61 u). The library search results gave search quality results from 70 to 90 which indicate an excellent agreement with the library spectrum. Also, during method development the variation of mobile phase composition (from 0 to 8% methanol-modified CO_2) had no effect on the quality of the spectra. The quality of the spectra is also dependent on the complexity of the chromatogram. Thus, when dealing with real samples where interferences are prevalent, identification of compounds with library searching (or manually) would not be as facile as with these model mixtures.

Another application is the separation of steroids all of which may not be analyzed by GC–MS directly because of their polarity. A fast separation of six steroids under 6 min is shown in Fig. 10. The background-subtracted spectra along with library spectra of progesterone and testosterone are shown in Figs. 11 and 12. Typical of this group of compounds was the extensive fragmentation with the molecular ion present at less than 20% or not at all. In both chromatograms the peaks are symmetrical in-

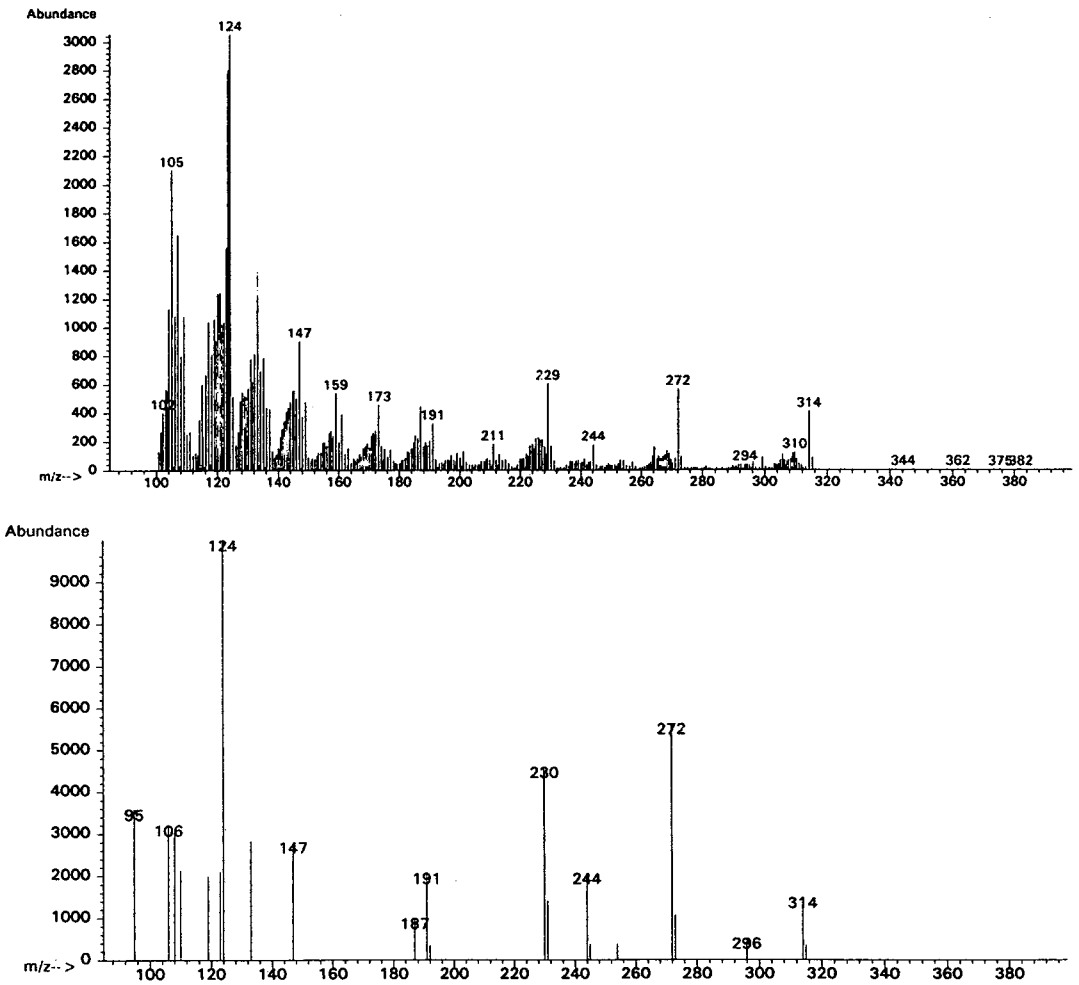

Fig. 11. EI spectrum of progesterone (top) and library spectrum (bottom).

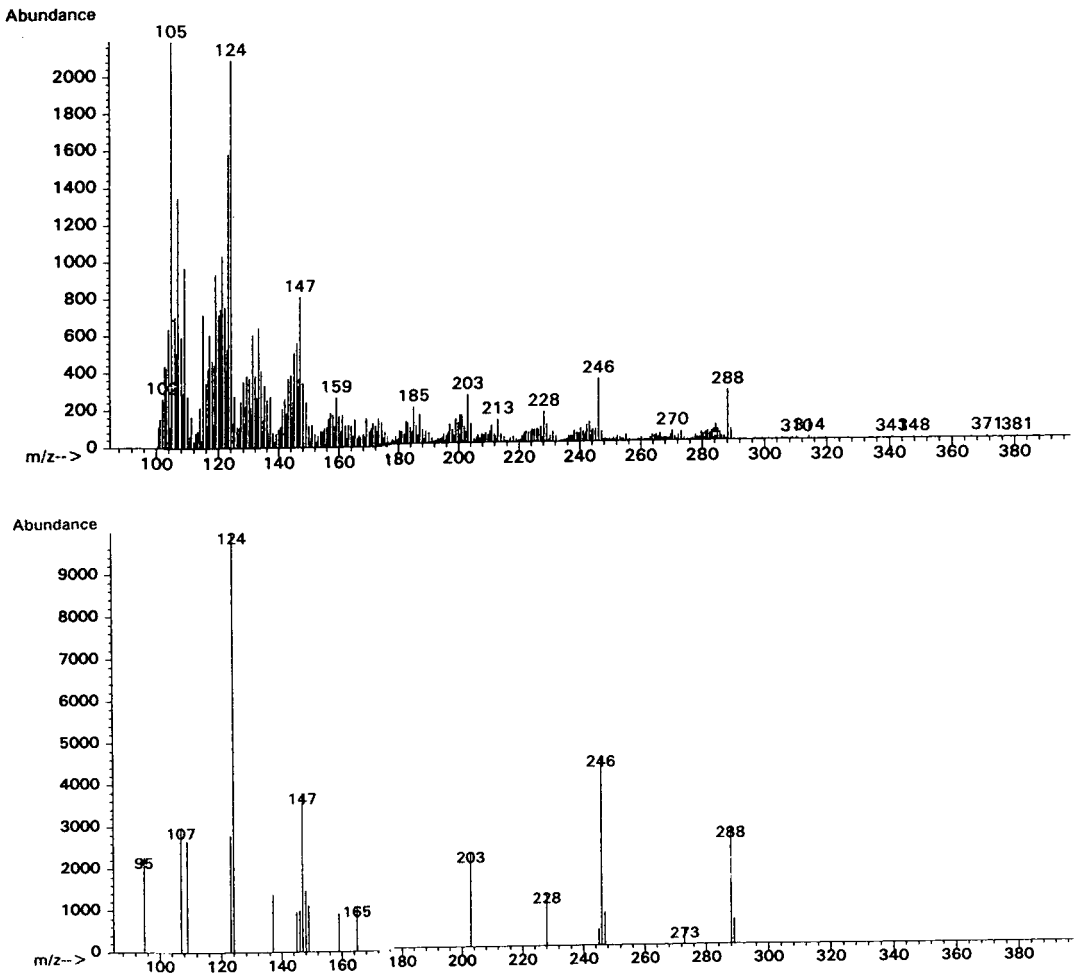

Fig. 12. EI spectrum of testosterone (top) and library spectrum (bottom).

dicating chromatographic fidelity was maintained.

4. Conclusions

Packed-column SFC–PB-MS has been found successful in analyzing phenylurea pesticides and steroids. These compounds because of their thermal lability or polarity may not be easily analyzed by other methods directly (GC–MS). With the current system, the resulting EI spectra were of sufficient quality for identification of these compounds. The effects of various operational parameters were characterized with mobile phase of pure CO_2 and methanol-modified CO_2 under FIA and chromatographic conditions. The position of the restrictor, nebulizing gas pressure, and temperature of the desolvation chamber were found to have a significant effect on the performance of the system. These parameters were optimized separately. However due to an interrelation of these parameters, a sophisticated optimization scheme (i.e. simplex optimization) would have resulted in a better overall sensitivity. For example, such an optimization would have lessened the effect of modifier concentration on sensitivity. Following optimization

of parameters, the EI LODs of the system for SIM and scan were determined to be 5 and 40 ng for caffeine, respectively. These LODs are 2.5 to 25 times better than the previous estimates [15,16]. However, the sensitivity was found to be highly dependent on the modifier percentage with 4% methanol-modified CO_2 yielding optimal sensitivity. Method development in SFC is achieved (in order of most effectiveness) by addition of various amounts of modifier, pressure/density programming and temperature variation [29,30]. Since sensitivity was shown to be highly dependent on modifier concentration, the goals of maximum sensitivity and efficient separations are in direct conflict. Currently studies are underway to address this and other concerns.

Acknowledgement

The authors thank Hewlett-Packard and Dionex for the generous loan of PB-MS and SFC equipment, respectively. Specifically, we wish to acknowledge Dr. Alex Apffel for helpful discussions and invaluable assistance in this research.

References

[1] T.L. Chester, J.D. Pinkston, D.P. Innis and D.J. Bowling, *J. Microcol. Sep.*, 1 (1989) 182.
[2] E.C. Huang, B.J. Jackson, K.E. Markides and M.L. Lee, *Anal. Chem.*, 60 (1988) 2715.
[3] E.R. Baumeister, C.D. West, C.F. Ijames and C.L. Wilkins, *Anal. Chem.*, 63 (1991) 251.
[4] B.W. Wright, H.T. Kalinoski, H.R. Udseth and R.D. Smith, *J. High Resolut. Chromatogr. Chromatogr. Commun.*, 9 (1985) 145.
[5] R.D. Smith, H.T. Kalinoski and H.R. Udseth, *Anal. Chem.*, 56 (1984) 2971.
[6] A.J. Berry, D.E. Games and J.R. Perkins, *J. Chromatogr.*, 363 (1986) 147.
[7] A.J. Berry, D.E. Games and J.R. Perkins, *Anal. Proc. (London)*, 23 (1986) 451.
[8] A.J. Berry, D.E. Games, J.R. Perkins, I.C. Mylchreest and S. Pleasance, *Anal. Proc. (London)*, 24 (1987) 371.
[9] J. Balsevich, L.R. Hogge, A.J. Berry, D.E. Games and I.C. Mylchreest, *J. Nat. Prod.*, 51 (1988) 1173.
[10] E.D. Ramsey, D.E. Games, J.R. Perkins and J.R. Startin, *J. Chromatogr.*, 464 (1989) 353.
[11] R.F. Browner, P.C. Winkler, D.D. Perkins and L.E. Abbey, *Michrochem. J.*, 34 (1986) 15.
[12] A.L. Yergey, C.G. Edmonds, I.A.S. Lewis and M.L. Vestal, *Liquid Chromatography/Mass Spectrometry: Techniques and Applications*, Plenum Press, New York, 1990, Ch. 3, p. 19.
[13] M.L. Lee and K.E. Markides (Editors), *Analytical Supercritical Fluid Chromatography and Extraction*, Chromatography Conferences, Provo, UT, 1990.
[14] L.E. Martin, J. Oxford and R.J.N. Tanner, *J. Chromatogr.*, 251 (1982) 223.
[15] P.O. Edlund and J.D. Henion, *J. Chromatogr. Sci.*, 27 (1989) 274.
[16] G. Holtzer, B. Brudette and F.R. Browner, *Proceedings of the 3rd International Symposium on SFC and Extraction, Park City, UT, January 1991*, p. 35.
[17] A. Burdette, F.R. Browner and G. Holzer, presented at the *1991 Pittsburgh Conference, Chicago, IL, 4–8 March, 1991*, abstract 891.
[18] P.C. Winkler, *Ph.D. Dissertation*, Georgia Institute of Technology, Atlanta, GA, 1986.
[19] R.C. Willoughby and R.F. Browner, *Anal. Chem.*, 56 (1984) 2626.
[20] P.C. Winkler, D.D. Perkins, W.K. Williams and R.F. Browner, *Anal. Chem.*, 60 (1988) 489.
[21] R.F. Browner, *J. Microchem.*, 40 (1989) 4.
[22] R.F. Browner, A.W. Boorn and D.D. Smith, *Anal. Chem.*, 54 (1982) 1411.
[23] L.G. Randall and A.L. Wahrhaftig, *Rev. Sci. Instrum.*, 52 (1981) 1283.
[24] A. Apffel and R.G. Nordman, *Hewlett-Packard J.*, 41 (1990) 69.
[25] T.D. Behymer, T.A. Bellar and W.L. Budde, *Anal. Chem.*, 62 (1990) 1686.
[26] A. Apffel and M.L. Perry, *J. Chromatogr.*, 554 (1991) 103.
[27] L. McLaughlin, T. Wachs, R. Pavelka, G. Maylin and J. Henion, presented at the *6th Montreux Symposium on LC–MS, Cornell, NY 1989.*
[28] I.S. Kim, F.I. Sasinos, R.D. Stephens and M.A. Brown, *J. Agric. Food Chem.*, 38 (1990) 1223.
[29] T.A. Berger, *J. Chromatogr. Sci.*, 32 (1994) 25.
[30] T.A. Berger and J.F. Deye, *Anal. Chem.*, 62 (1990) 1181.

ELSEVIER

Journal of Chromatography A, 677 (1994) 377–384

JOURNAL OF CHROMATOGRAPHY A

Quantitative analysis of quaternary ammonium antiseptics using thin-layer densitometry

J. Paesen, I. Quintens, G. Thoithi, E. Roets, G. Reybrouck, J. Hoogmartens*

Catholic University of Leuven, Laboratory for Pharmaceutical Chemistry, Faculty of Pharmaceutical Sciences, and School of Public Health, Faculty of Medicine, Van Evenstraat 4, B-3000 Leuven, Belgium

First received 14 March 1994; revised manuscript received 5 May 1994

Abstract

A thin-layer chromatography method for quantitative analysis of quaternary ammonium antiseptics is described. Silanized silica gel was used as the stationary phase. The mobile phase consisted of methanol–25% (m/v) sodium acetate solution–acetone (65:35:20). The method is able to separate the chain homologues of benzalkonium chloride, cetylpyridinium chloride and cetrimide. Detection was performed using a colour reaction with potassium triiodide solution. The different homologues were quantified using UV densitometry at 400 nm. A number of commercial samples was analysed using this method. From the results it appears that it is worthwhile to have a limit test for the composition of quaternary ammonium antiseptics in pharmacopoeial monographs, the more so as the antibacterial activity depends on it.

1. Introduction

Quaternary ammonium antiseptics such as benzalkonium chloride (BEC), cetrimide (CTB), cetyltrimethylammonium bromide (C_{16}-CTB) and cetylpyridinium chloride (CPC) are cationic surfactants with bactericidal activity which are frequently used in pharmaceutical preparations. The structures of BEC, CTB, C_{16}-CTB and CPC are shown in Fig. 1. Commercial samples of BEC and CTB are mixtures of homologues with different chain lengths. The antibacterial activity of these homologues is different [1–3]. Homologues of BEC, CTB and CPC have been separated qualitatively using paper chromatography [4]. Quantitative analysis of the chain homologues of BEC has been carried out by gas chromatography (GC), following a modified Hofmann degradation (see [5–7]), or directly [8,9], by GC–mass spectrometry [9], by mass spectrometry [10,11] and by liquid chromatography (LC) [12–19]. Quantitative analysis of CPC by GC has also been reported [20], as well as by LC [21]. The separation of CTB homologues by GC has been described [22], but LC methods were not described, probably due to the lack of a chromophore. Recently, capillary electrophoresis (CE) was described for the separation of homologues of BEC, using direct UV detection, and of homologues of CTB, using indirect UV detection [23]. Quantitative densitometric thin-layer chromatography (TLC) methods have been reported for the determination of cetalkonium chloride, which corresponds to BEC

* Corresponding author.

0021-9673/94/$07.00
SSDI 0021-9673(94)00448-I

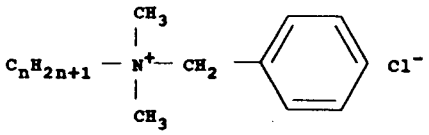

Benzalkonium chloride (BEC) n = 8 to 18

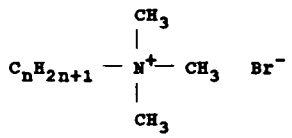

Cetrimide (CTB) n = 12 to 16
Cetyltrimethylammonium bromide (C_{16}-CTB) n = 16
Cetrimonium bromide (C_{16}-CTB) n = 16

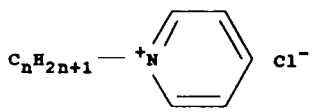

Cetylpyridinium chloride (CPC) n = 16

Fig. 1. Structures for quaternary ammonium antiseptics.

with a C_{16} chain [24] and of BEC [25]. However, no separation of homologues was obtained.

Here a TLC method is described which enables the separation of the chain homologues of BEC, CPC and CTB. Detection is performed using a colour reaction with KI_3. Densitometry (UV 400 nm) is used to quantify the different homologues. The composition of different commercial samples is reported.

2. Experimental

2.1. Chemicals

Methanol and acetone were from Rathburn (Walkerburn, UK). Dichloromethane was from Janssen Chimica (Beerse, Belgium). Water was distilled twice from glass apparatus. Sodium acetate trihydrate and tetrabutylammonium hydrogen sulphate (TBA) of reagent grade were from Janssen Chimica. Potassium iodide and iodine of reagent grade were from Merck (Darmstadt, Germany).

Precoated silanized silica gel layers on glass (20 × 10 cm) (DC Fertigplatten Kieselgel 60 silanisiert) were obtained from Merck.

2.2. Standards and samples

House standards of the C_{12}, C_{14}, C_{16} and C_{18} homologues of BEC, CTB and CPC were prepared in the laboratory. The substances were synthesized by reacting the appropriate alkylbromide with triethylamine, benzyldimethylamine or pyridine [1]. When necessary, the bromides were transformed into the corresponding chlorides. Therefore the tetraphenylborate salts were precipitated [26]. These derivatives were treated with excess potassium chloride. The resulting quaternary chlorides were recovered from the filtrate by extraction with chloroform [27]. The house standards were analysed by Karl Fischer titration of water and by non-aqueous titration of halogenides with perchloric acid, in acetic acid containing mercuric acetate as the solvent.

Commercial samples of BEC, CTB, C_{16}-CTB and CPC were obtained from Aldrich (Milwaukee, MI, USA), BDH (Poole, UK), Federa (Brussels, Belgium), Flandria (Ghent, Belgium), Janssen Chimica, Merck, Pharmachemic (Antwerpen, Belgium) and Schuchardt (Hohenbrunn, Germany).

2.3. Antibacterial activity

The antibacterial activity of the house standards was determined by a quantitative suspension test [28] towards *Staphylococcus aureus* ATCC 6538, *Pseudomonas aeruginosa* ATCC 15442 and *Escherichia coli* ATCC 11229. At time zero 0.1 ml of bacterial suspension was added to 10 ml of disinfectant solution or of water (control). After a medication time of 20 min (for *S. aureus*) or 60 min (for *P. aeruginosa* and *E. coli*), 1 ml was transferred into 9 ml of neutralizing solution containing lecithine (2%), polysor-

bate 80 (2%) and sodium thiosulphate (0.5%) [29]. Aliquots (1 ml) of this mixture and of its tenfold dilutions were brought in subculture and the colony-forming units (cfu) were counted after incubation at 37°C. The germicidal effect was expressed as the logarithm of the ratio of the number of cfu per ml in the medication mixture without disinfectant to the number of cfu per ml after medication with the disinfectant. The concentration of the disinfectant solutions examined was 10^{-4}% (m/v) in water for *S. aureus* and $5 \cdot 10^{-4}$% (m/v) for *P. aeruginosa* and *E. coli*.

2.4. TLC method

The TLC plates were activated by heating at 110°C for 1 h. A narrow band of the layer was removed from both sides of the plate supposed to be in vertical position during development. A dipping solution was prepared by mixing 1 volume of an aqueous solution containing 4% (m/v) potassium iodide and 2% (m/v) iodine (KI_3 solution) and 19 volumes of a mixture methanol–water (1:1). A solution of TBA (1.00 g/l) in methanol–dichloromethane (1:1) was used as an internal standard (I.S.). Commercial samples were dissolved in I.S., in a concentration of 10.0 mg/ml. House standards of the chain homologues were dissolved in I.S. in concentrations chosen to correspond to the amounts present in the commercial samples. Aliquots of 2.0 μl were applied to the TLC plate with a microsyringe (Hamilton, Bonaduz, Switzerland) starting at 20 mm from the edge and at 20 mm from the bottom of the plate. The distance between the lanes was 10 mm, so that 17 spots could be applied per plate. The chromatographic chamber was lined with paper and equilibrated with the mobile phase methanol–25% (m/v) aqueous sodium acetate trihydrate solution–acetone (65:35:20) for at least 1 h prior to use. The plate was developed at room temperature over a distance of 10 cm. After development the plate was dried in the air (5 min) and in an oven at 105–110°C (5 min). Detection of the spots was performed by dipping the plate for 10 s horizontally in a laboratory-made container, containing 200 ml of dipping solution. The TLC plate was allowed to dry on the bench for 15 min and was heated in an oven at 105–110°C for 15 min. Yellowish-brown spots on a colourless background were obtained. The plate was stored at room temperature for 1 h in order to let the colour stabilize. Then the chromatograms were analysed with a CS-990 TLC scanner (Shimadzu, Kyoto, Japan) using the following parameters: zigzag swing width: 10 mm; scan step in the *Y*-direction: 0.1 mm; beam size: 1.2 mm × 1.2 mm; absorption, reflection mode with $\lambda = 400$ nm; linearizer SSX: 3; background correction: off; drift-line integration: 0.3. The ratios of the peak area of each homologue in the commercial samples and the peak area of the I.S. were compared to the ratios obtained for the corresponding spots of the house standards.

3. Results and discussion

For quantitative work, chromatographic methods need reference substances. Laboratory standards for the C_{12}–C_{18} homologues were prepared and analysed. The results for titration and for antibacterial activity of the laboratory standards are reported in Table 1. The result of the titration of the halogenides is expressed as the percentage of the corresponding homologue. For all the samples the total mass explained by this titration and the water content is between 97 and 101% except for C_{12}-CTB where the high titration value is probably due to the presence of some inorganic halogenide. The chromatographic purity of the homologues was checked by the TLC method described in this paper; no impurities were observed. In all further experiments using solutions of the laboratory standards the titration value was taken into account to calculate the concentration of those standards for which the titration value was below 100. The results in Table 1 show that the longer-chain homologues show a stronger germicidal activity. This confirms earlier observations [1,2]. It means that the germicidal activity of a quaternary ammonium compound depends upon the composition of the sample and therefore this composition should be limited by official compendia. The

Table 1
Chemical analysis and antibacterial activity of the laboratory standards

Laboratory standard	Content (non-aqueous titration)[a]	Water (Karl Fischer titration)	Germicidal effect		
			S. aureus	*P. aeruginosa*	*E. coli*
C_{12}-BEC	88.3 (0.3)	9.3	0.12	0.13	0.41
C_{14}-BEC	89.4 (0.3)	8.6	0.80	1.93	2.28
C_{16}-BEC	90.3 (0.1)	8.0	1.73	>4	>4
C_{18}-BEC	93.8 (0.3)	6.5	1.98	>4	>4
C_{12}-CTB	104.0 (0.1)	0.4	0.07	0	0.08
C_{14}-CTB	100.0 (0.1)	0.0	0.14	0.11	0.69
C_{16}-CTB	99.8 (0.3)	0.1	1.99	2.72	1.97
C_{18}-CTB	99.4 (0.2)	0.5	2.27	2.03	4.00
C_{12}-CPC	94.0 (0.3)	6.0	0.15	0	0.11
C_{14}-CPC	92.8 (0.4)	5.4	0.23	1.18	1.54
C_{16}-CPC	92.0 (0.4)	4.9	2.12	3.33	3.42
C_{18}-CPC	96.4[b]	4.7	2.14	4.22	>4

[a] Relative standard deviations (%) in parentheses.
[b] This sample was titrated only once.

European Pharmacopoeia (Ph. Eur.) does not prescribe such limits for the composition of BEC, CTB or CPC [30]. The United States Pharmacopoeia (USP) prescribes a limit test for the composition of BEC, using LC [31].

This paper describes an easy to perform TLC test which does not need a chromophore for detection. Originally the TLC method was developed in this laboratory for identification of CTB and the method was adopted by the Ph. Eur. for this purpose [30]. The composition of the mobile phase described here is slightly adapted by increasing the amount of methanol so that the method is able to separate the homologues of BEC, CTB and CPC. R_F values are reported in Table 2. TBA, used as I.S., is well separated ($R_F = 0.65$). Much effort was put in the development of a detection method suitable for quantitative analysis.

Table 2
R_F values for the different homologues

	C_{12}	C_{14}	C_{16}	C_{18}
BEC	0.40	0.31	0.22	0.15
CTB	0.45	0.36	0.26	0.12
CPC	0.43	0.33	0.24	0.17

R_F TBA = 0.65

3.1. Detection method

First, the plates were sprayed with a solution consisting of a methanol–KI_3 (1:1) solution. The major drawback of spraying was the background colour not being uniform. Unstable baselines were obtained and integration was difficult to standardize. Another disadvantage of the spraying method was the long time needed for stabilization of the colour before a plate could be scanned. A dipping method was then developed using a solution consisting of 1 volume of KI_3 solution and 19 volumes of methanol–water (1:1). The TLC plate was dipped horizontally in the solution for 10 s, which was determined to be the optimal time. When after dipping the plate was allowed to dry on the bench for 15 min and was heated in an oven at 105–110°C for 15 min, the background colour had disappeared completely. The time required for stabilization of the colour of the spots was checked by scanning a plate with 17 chromatograms of the same sample after 0.5, 1, 2 and 4 h. The ratio between the

Table 3
R.S.D.s on the area of BEC homologues in a commercial sample using two detection techniques

Homologue	R.S.D. (%)	
	Spraying	Dipping
C_{12}	7.0	4.3
C_{14}	9.5	5.8
C_{16}	10.0	9.0
C_{18}	31.0	9.3

The sample contains 74% (m/m) C_{12}-BEC, 19% C_{14}-BEC, 4% C_{16}-BEC and 3% C_{18}-BEC. The plate was scanned 3 h after spraying or dipping. Number of analyses: 17.

area of the homologues and the area of the I.S. was constant after 1 h of stabilization. The results obtained by the dipping method were compared to those obtained with the spraying method. The relative standard deviations (R.S.D.s) on the ratio area homologue/area I.S. for the different homologues of a commercial BEC sample using both detection methods are compared in Table 3. The R.S.D. for the dipping method was much lower than that of the spraying method.

Cetylpyridinium chloride is the only compound absorbing sufficiently in UV at 254 nm, so that the spots can be detected without previous dipping of the plate. Two commercial CPC samples containing only C_{16}-CPC were assayed using scanning before ($\lambda = 254$ nm) and after ($\lambda = 400$ nm) dipping. Here a solution of C_{12}-CPC laboratory standard (5.0 mg/ml) in methanol–dichloromethane (1:1) was used as internal standard solution, since TBA is not absorbing at 254 nm. The content (in %, m/m) obtained by scanning at 254 nm was 90.8% for both samples, showing a R.S.D. of 1.6% (sample 1) and 1.4% (sample 2) for a number of 6 analyses. After dipping and scanning at 400 nm, the content was 91.1% for sample 1 (R.S.D. = 3.3%) and 90.5% for sample 2 (R.S.D. = 2.1%). These results were similar, but the variation was higher after dipping, which is normal since an additional colour reaction had to be performed. Scanning of BEC in UV at 254 nm was found to be unsuitable, due to lack of sensitivity. Scanning of BEC or CTB at lower wavelengths (205–210 nm) was possible but the results were not as good as with the dipping method, due to the higher noise and baseline drift.

3.2. Linearity and detection limits

The linearity of the method was examined for the homologues most frequently present in commercial samples of BEC, CTB and CPC. Results are shown in Table 4, where y = area homologue/area I.S.; x = amount (μg) of sample applied to the plate; r = coefficient of correlation; $S_{y,x}$ = standard error of estimate; MR = range of mass (μg) examined; number of analyses = 18; number of concentrations = 6.

Table 4
Regression lines

Compound	Slope	Intercept	r	$S_{y,x}$	MR (μg)
C_{12}-BEC	0.89	−1.24	0.996	0.060	4–20
C_{14}-BEC	0.60	−0.40	0.960	0.020	4–16
C_{16}-BEC	0.44	−0.04	0.985	0.003	1–3
C_{18}-BEC	0.43	−0.08	0.937	0.001	1–3
C_{12}-CTB	0.60	−0.21	0.980	0.005	1–4
C_{14}-CTB	0.61	0.01	0.994	0.030	8–20
C_{16}-CTB	0.45	1.02	0.935	0.161	12–24
C_{16}-CPC	0.56	0.95	0.954	0.189	12–24

See text.

The mass ranges were chosen with respect to the amounts usually present in commercial samples. In the assay of commercial samples the calibration curves are not used, but standard solutions, applied on the same plate, are used in a single-point calibration.

For an application of 20 μg of the sample to the plate, the limit of detection for all homologues was about 1% (m/m) (0.2 μg).

3.3. Assay of commercial samples

Several commercial samples of BEC, CTB and CPC were assayed using the described method. In each chromatogram the areas of the spots were divided by the area of the I.S. (TBA). This ratio was calculated for the commercial samples and for the standard solutions. To calculate the percentage of each homologue in a commercial sample, the nearest chromatogram of a standard solution, containing the desired homologue, was used. The concentration of the standard solutions was adapted to the percentage of the homologues present in the samples. Results for different commercial samples of BEC, CTB and CPC are shown in Table 5.

BEC sample 1 was a mixture of four homologues (Fig. 2), with C_{12}-BEC as the principal component. BEC sample 2 contained only C_{14}-BEC, while BEC sample 3 was a mixture of C_{12}- and C_{14}-BEC. The total content in quaternary ammonium homologues varied for BEC samples from 93.5 to 99.9% (m/m), calculated on anhydrous. The residual mass may be explained by the presence of inorganic salts that are not detected by this TLC method. Following the USP and the Ph. Eur. BEC should be a mixture of alkylbenzyldimethylammonium chlorides. BEC sample 2 does not comply with this description. Moreover the USP prescribes that C_{12}-BEC > 40%, C_{14}-BEC > 20% and C_{12}-BEC + C_{14}-BEC > 70%, determined by LC, using peak

Table 5
Composition of commercial samples

Sample	Origin	Homologue compositions (%) on anhydrous[a]				Total homologues (%) on anhydrous	Water (%), Karl Fischer titration
		C_{12}	C_{14}	C_{16}	C_{18}		
(1) BEC	a	61.8 (1.0)	18.5 (5)	6.0 (11)	7.2 (23)	93.5	13.0
(2) BEC	b	ND	99.9 (5)	ND	ND	99.9	1.2
(3) BEC	d	58.6 (4)	31.3 (3)	ND	ND	98.9	9.0
(4) Cetrimide	e	14.0 (5)	71.6 (0.8)	7.9 (7)	ND	93.5	1.1
(5) C_{16}-CTB	a	ND	99.2 (2.6)	ND	ND	99.2	0.0
(6) C_{16}-CTB	f	ND	98.8 (4)	ND	ND	98.8	0.03
(7) C_{16}-CTB	g	ND	97.4 (2.2)	ND	ND	97.4	0.04
(8) C_{16}-CTB	a	ND	ND	96.2 (3)	ND	96.2	0.03
(9) C_{16}-CTB	h	ND	ND	97.4 (2.5)	ND	97.4	0.15
(10) C_{16}-CTB	i	ND	ND	96.6 (5)	ND	96.6	0.6
(11) C_{16}-CTB	j	ND	ND	91.7 (4)	ND	91.7	0.6
(12) C_{16}-CTB	k	ND	ND	83.6 (3)	ND	83.6	0.9
(13) C_{16}-CTB[b]	c	15.0 (5)	59.3 (4)	3.9 (10)	ND	78.2	NA
(14) CPC	h	ND	ND	95.6 (3)	ND	95.6	4.9
(15) CPC	a	ND	ND	95.1 (2.1)	ND	95.1	4.8

ND = Not detected; NA = not applicable.
[a] R.S.D.s (%) are mentioned in parentheses. Number of analyses per sample = 4.
[b] This sample is a 40% (m/v) solution.

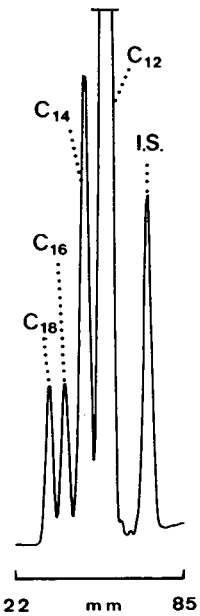

Fig. 2. Typical densitogram of a commercial sample of benzalkonium chloride containing four homologues.

normalisation. BEC samples 1 and 3 comply with these limits. The Ph. Eur. does not prescribe a limit test for the composition.

According to the Ph. Eur. CTB should be a mixture of the bromides of three homologues: mainly C_{14}-CTB with as minor components C_{12}-CTB and C_{16}-CTB. The USP stipulates that cetrimide (CTB) is cetyltrimethylammonium bromide (C_{16}-CTB) [31]. C_{16}-CTB is also called cetrimonium bromide. In fact, the latter two names should be used only for the pure C_{16}-CTB, while cetrimide should be used to indicate a mixture with C_{14}-CTB as the main component. This is clearly stated in the Merck Index [32] and Martindale [33]. As can be seen in Table 5, so-called C_{16}-CTB samples 5 to 7 contain only the C_{14} homologue. C_{16}-CTB samples 8 to 12 contain the correct C_{16} homologue. C_{16}-CTB sample 13 is a mixture and should be called cetrimide (CTB). Most of the cetyltrimethylammonium bromide (C_{16}-CTB) samples are quite pure, except for samples 11 and 12. The low content of sample 13 is probably due to a faulty preparation procedure. CPC samples 14 and 15 contain cetylpyridinium chloride monohydrate. Only the C_{16} homologue is present. R.S.D. values on the results for the main compound were not higher than 5%. For secondary components the R.S.D. values were even higher. Compared to LC methods, the results obtained using this TLC method showed more variation, also because the method uses a colour reaction for detection.

4. Conclusions

The different chain homologues of quaternary ammonium antiseptics can be separated using TLC. The method can be used to determine the composition of commercial samples. The R.S.D. of the assay of the main component is about 5% or better, which is fairly good for a TLC method that uses a colour reaction for detection. Comparison of commercial samples showed that the qualitative composition of benzalkonium chloride samples can differ a lot. Samples of cetylpyridinium chloride mostly contain only the C_{16} homologue. Cetyltrimethylammonium bromide samples mostly contain only one homologue, but the name cetyltrimethylammonium bromide is sometimes erroneously used for samples that contain only the C_{14} homologue instead of the required C_{16} homologue and also for samples which should be called cetrimide. The results indicate the need for limit tests for composition in official texts such as pharmacopoeias. Apart from a recent CE method, no other method has been described that is able to determine the relative amounts of the different chain homologues in CTB.

References

[1] T.L. Welsh, G.C. Hoss, B.T. Palermo and A.I. Dines, *J. Pharm. Sci.*, 56 (1967) 1464.
[2] R.M.E. Richards and L.M. Mizrahi, *J. Pharm. Sci.*, 67 (1978) 380.
[3] K. Jono, T. Takayama, M. Kuno and E. Higashide, *Chem. Pharm. Bull.*, 34 (1986) 4215.
[4] H. Holness and W.R. Stone, *Analyst*, 83 (1958) 71.

[5] E. Jennings and H. Mitchner, *J. Pharm. Sci.*, 56 (1967) 1590.
[6] H. Mitchner and E. Jennings, *J. Pharm. Sci.*, 56 (1967) 1595.
[7] S. Suzuki, Y. Nakamura, M. Kaneko, K. Mori and Y. Watanabe, *J. Chromatogr.*, 463 (1989) 188.
[8] Z.R. Cybulski, *J. Pharm. Sci.*, 73 (1984) 1700.
[9] N. Lay-Keow, M. Hupé and A.G. Harris, *J. Chromatogr.*, 351 (1986) 554.
[10] N.N. Daoud, P.A. Crooks, R. Speak and P. Gilbert, *J. Pharm. Sci.*, 72 (1983) 290.
[11] M. Bambagiotti-Alberti, S. Pinzauti, G. Moneti, G. Agati, V. Giannellini, S.A. Coran and E.F. Vincieri, *J. Pharm. Biomed. Anal.*, 2 (1984) 409.
[12] R.C. Meyer, *J. Pharm. Sci.*, 69 (1980) 1148.
[13] D.F. Marsh and L.T. Takahashi, *J. Pharm. Sci.*, 72 (1983) 521.
[14] M. Euerby, *J. Clin. Hosp. Pharm.*, 10 (1985) 73.
[15] G. Ambrus, L.T. Takahashi and P.A. Marig, *J. Pharm. Sci.*, 76 (1987) 174.
[16] R. Herrmann, *Arch. Pharm.*, 320 (1987) 589.
[17] A. Gomez-Gomar, M.M. Gonzales-Aubert, J. Garces-Torrents and J. Costa-Segarra, *J. Pharm. Biomed. Anal.*, 8 (1990) 871.
[18] L. Elrod, T.G. Golich and J.A. Morley, *J. Chromatogr.*, 625 (1992) 362.
[19] J.E. Parkin, *J. Chromatogr.*, 635 (1993) 75.
[20] H. Binder, W. Krainer and W. Lindner, *Arch. Pharm.*, 319 (1986) 642.
[21] B. Nyhowski de Bukanski, *Int. J. Cosm. Sci.*, 9 (1987) 193.
[22] H.H. Laycock and B.A. Mulley, *J. Pharm. Pharmacol.*, 18 (1966) Suppl. 9 S.
[23] C.S. Weiss, J.S. Hazlett, M.H. Datta and M.H. Danzer, *J. Chromatogr.*, 608 (1992) 325.
[24] K. Wenz and B. Renger, *J. Planar Chromatogr.*, 2 (1989) 476.
[25] R. El-Agamy, H. Hofmann and G. Seifert, *Pharm. Z.*, 133 (1988) 87.
[26] J.T. Cross, *Analyst*, 90 (1965) 315.
[27] E.D. Schall, *Anal. Chem.*, 29 (1957) 1044.
[28] G. Reybrouck, J. Borneff, H. van de Voorde and H.-P. Werner, *Zbl. Bakt. Hyg., I. Abt. Orig. B*, 168 (1979) 463.
[29] G. Reybrouck, *Zbl. Bakt. Hyg., I. Abt. Orig. B*, 168 (1979) 480.
[30] *European Pharmacopoeia*, Maisonneuve, Sainte-Ruffine, France, 2nd ed., 1980.
[31] *United States Pharmacopeia XXII*, United States Pharmacopeial Convention, Rockville, MD, 1990.
[32] S. Budavari (Editor), *The Merck Index*, Merck & Co., Rahway, NJ, 11th ed., 1989.
[33] J.E.F. Reynolds (Editor), *Martindale, The Extra Pharmacopeia*, The Pharmaceutical Press, London, 29th ed., 1989.

ELSEVIER

Journal of Chromatography A, 677 (1994) 385–389

JOURNAL OF CHROMATOGRAPHY A

Short Communication

Use of liquid chromatography–nuclear magnetic resonance spectroscopy for the identification of impurities in drug substances

John K. Roberts*, Richard J. Smith

Department of Analytical Sciences, SmithKline Beecham Pharmaceuticals, Coldharbour Road, The Pinnacles, Harlow, Essex CM19 5AD, UK

First received 18 March 1994; revised manuscript received 3 June 1994

Abstract

There are many complex analytical problems in the pharmaceutical industry which require the use of more than one instrumental technique for their solution. Hyphenated techniques such as GC–MS, LC–MS and LC–NMR have been developed to help solve such problems in a time-efficient manner. The on-line combination of HPLC and NMR offers the potential for rapid collection of detailed structural information from samples in a way no other hyphenated technique can. LC–NMR, however, is an inherently insensitive technique but this paper shows that worthwhile data can be obtained on a medium-field (400 MHz) instrument.

1. Introduction

Direct coupling of liquid chromatography (LC) to ^{1}H NMR using stopped-flow methods was reported in 1978 [1] and flowing LC–NMR was reported the year after [2]. Since then, great improvements have been made in spectrometer design and field strength, in flow-cell design and in pulse sequences for solvent suppression [3,4] which have enabled wider exploitation of the technique [5]. LC–NMR combines a powerful separation technique with a detector that offers a wealth of structural and stereochemical information. It would thus be expected to have wide application in the pharmaceutical industry in, for example, investigating impurities in drug compounds at both the research and development stage [6]. Unpublished work from this laboratory has shown that the technique is particularly powerful for the analysis of compounds which cannot be isolated. LC–NMR is an inherently insensitive technique and consequently some recent publications have exploited the increased sensitivity of high- and ultra-high-field NMR spectrometers [5,7,8]. For the identification of impurities in drug substances, however, this paper shows that spectra on impurities at around the 3% level can be obtained in a respectable time frame using a medium-field spectrometer.

2. Experimental

2.1. HPLC

All HPLC was performed using a Unicam

* Corresponding author.

0021-9673/94/$07.00
SSDI 0021-9673(94)00523-C

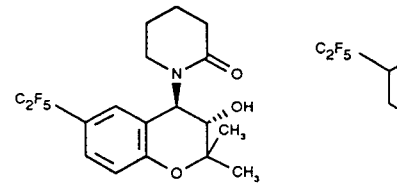

1

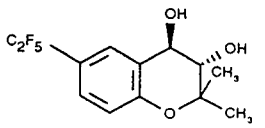

2

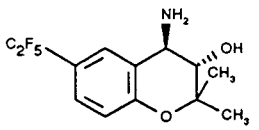

3

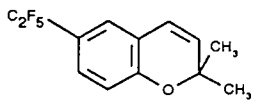

4

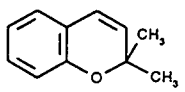

5

Crystal 200 pump and 250 photodiode array detector. The spiked sample of **1** was dissolved at a concentration of approximately 10 mg/ml in eluent and injections of 100 or 200 μl made using a Rheodyne 7125 manual injector, equipped with a 200-μl loop. The outlet of the detector was connected to the inlet of the LC–NMR probe by 3 m of polyether ether ketone (PEEK) tubing (0.010 in. internal diameter; 1 in. = 2.54 cm). The transfer time from the UV detector to the flow cell of the probe was approximately 30 s at 1 ml/min. Analysis of **4** was performed by injecting on to the column 100 or 200 μl from an approximately 10 mg/ml solution.

2.2. NMR

All spectra were recorded on a Bruker AMX 400 NMR spectrometer fitted with an inverse-geometry LC–NMR probe with a 240-μl flow cell. Flowing data were accumulated using a pseudo-two-dimensional version of the "noesyprtp" pulse programme. A number of 8192 data points was used in f2, with each increment in "f1" corresponding to 16 scans and taking approximately 27 s. The acetonitrile peak was suppressed by presaturation; the residual water peak was also suppressed if its height was significantly greater than that of the acetonitrile ^{13}C satellites. Spectra were referenced to the position of the water peak, taken to be 4.41 ppm at 40% MeCN and 4.16 ppm at 60% MeCN. Stopped-flow spectra were also accumulated into 8192 data points and zero-filled once before transformation. Presaturation of acetonitrile and water resonances and referencing was performed as for the flowing experiments.

3. Results and discussion

To investigate to what extent sensitivity is a limiting factor in LC–NMR, a sample of a research drug substance **1** was spiked with the related compounds **2** and **3**, at levels of 9 and 4%

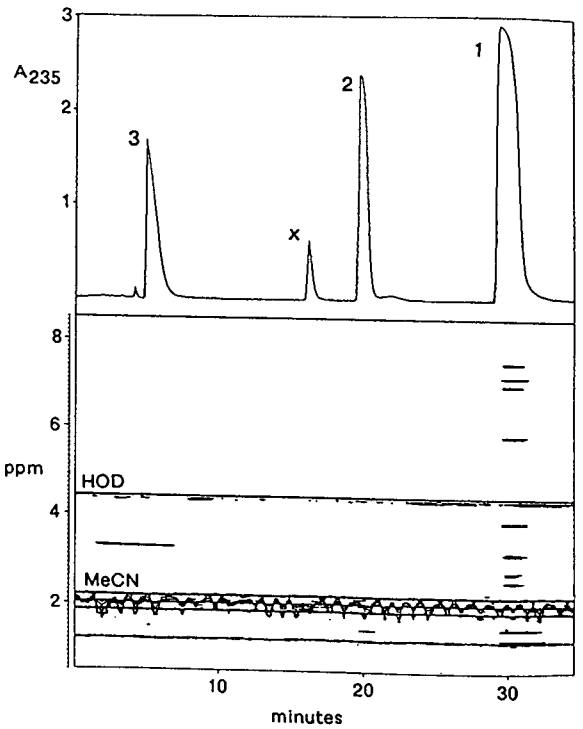

Fig. 1. Typical UV (absorption at 235nm) and ^1H NMR data for sample of **1**, spiked with **2** and **3** at levels of 9 and 4% (w/w), respectively. Approximately 100 μl of sample were injected on to a Spherisorb S5 ODS2 column, 250 × 4.6 mm, and eluted with acetonitrile–0.05 *M* potassium dihydrogen-orthophosphate in ^2H_2O (40:60), adjusted to pH 3.5 with orthophosphoric acid, at a flow-rate of 1.0 ml/min. The signals from the solvent are indicated by HOD (water) and MeCN (acetonitrile). The peak labels correspond to the structures in the text. The peak labelled x is a 1% impurity not investigated in this study. D = Deuterium.

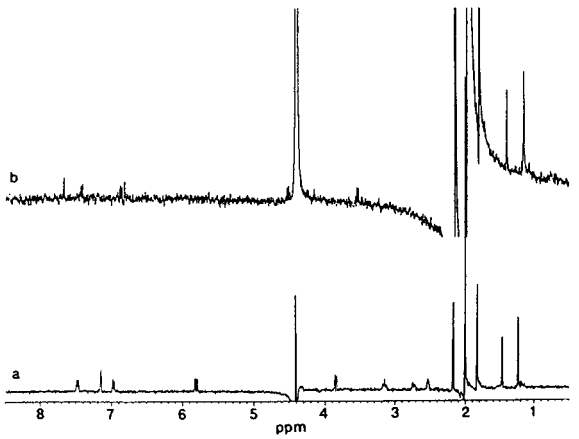

Fig. 2. Rows abstracted from the data matrix in Fig. 1, corresponding to **1** (trace a) and **2** (trace b). The former is a single row (16 scans), the latter is a summation of four rows.

(w/w), respectively and then examined by LC–NMR, using a 400 MHz spectrometer. Typical UV and ^{1}H NMR data for such an experiment are shown in Fig. 1. The two-dimensional plot of chemical shift versus retention time represents the spectrum observed at approximately 27-s time intervals. Two species are observed in the ^{1}H plot and they correspond to the main component, **1**, and the 9% component, **2**. For the latter, only the methyl resonances at approximately 1.54 and 1.79 ppm are clearly visible in the two-dimensional plot, indicating that the limit of detection for this compound under the flowing conditions used here is approximately 50 μg injected on column. Rows from the data matrix were abstracted for compounds **1** and **2** and the corresponding spectra are shown in Fig. 2. Considerable improvements in spectral quality are obtainable by performing stopped-flow LC–NMR. Stopped-flow ^{1}H spectra for all three components are shown in Fig. 3. The LC–NMR data on **3** clearly show that useful structural information can be obtained on relatively minor components of mixtures. At present on our equipment it appears that sample amounts in the range 25–50 μg injected on column are needed to obtain good quality ^{1}H data in reasonable accumulation times (30 min). Minor components of mixtures (say 1%) would therefore be investi-

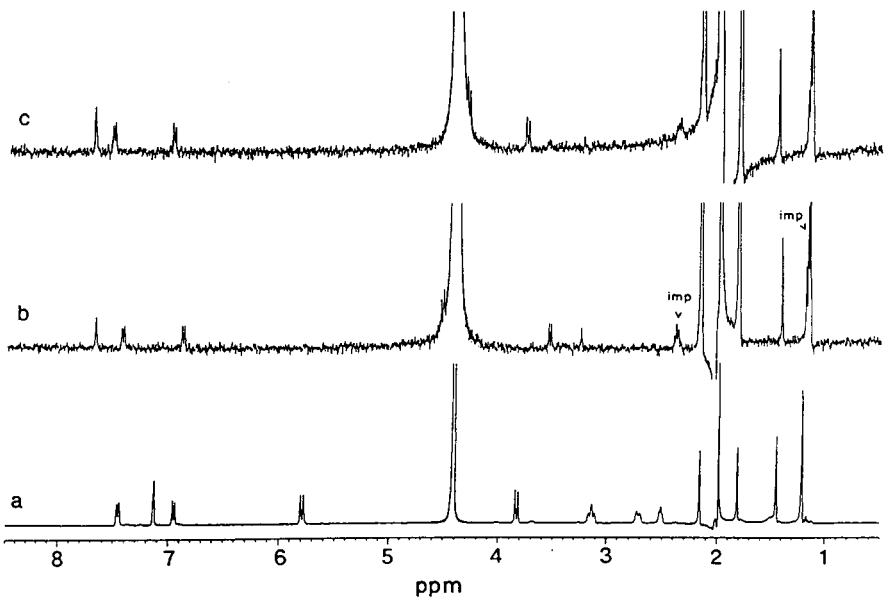

Fig. 3. Stopped-flow ^{1}H spectra for **1** (trace a), **2** (trace b) and **3** (trace c). Chromatographic conditions as in Fig. 1, except that a separate injection of 200 μl of the mixture was used to obtain the data on **3**. A number of 512 scans was acquired for **1**, 1024 for **2** and 1255 for **3**. The multiplets indicated by "imp" at 1.17 and 2.39 ppm are due to an impurity/impurities in the acetonitrile. Note the impurity resonance at 1.17 ppm obscures one of the methyl resonances of **2** (trace b) and **3** (trace c).

gated by injecting more of the mixture on to the column and/or by allowing longer accumulation times.

Having demonstrated the use of LC–NMR in a model system, a "real" sample was examined. This sample was presented as consisting mainly of compound **4** but containing an unknown, early-eluting impurity at a level estimated to be 3%. The chromatogram is shown in Fig. 4, together with the ^{1}H spectra obtained for the main peak, **4**, and the unknown. The ^{1}H spectrum of the latter is very similar to that of **4** with a singlet for the two methyl groups (1.35 ppm) and two doublets for the olefinic protons (5.65 and 6.35 ppm) indicating that these groups are common in both the unknown impurity and **4**. The fact that both methyl groups appear as a singlet resonance in the ^{1}H NMR spectra of **4** and **5** implies that an olefinic bond is present in both molecules. If this bond were saturated, individual resonances would be observed for the methyl groups as in structures **3**, **2** and **1** (Fig. 3). Compound **4** has three aromatic resonances (6.86, 7.33 and 7.37 ppm) with chemical shifts and coupling patterns as expected for a trisubstituted ring. The four aromatic resonances of the unknown impurity (7.08, 7.00, 6.83 and 6.69 ppm) are typical of a 1,2 disubstituted aromatic ring and indicate that the unknown impurity has the structure **5**. J values for **4** and **5** are not quoted because of the low digital resolution of the data. On-flow data will necessarily have low digital resolution in order to obtain sufficient increments in "f1". Stopped-flow data could have been acquired with sufficient digital resolution to measure J coupling constants, but in this work, lower digital resolution was used to maximize the S/N ratio of the spectrum. It is obviously useful to obtain UV spectra on each peak at the same time as the ^{1}H NMR spectra, using a photodiode array detector in-line (as was the case in this work). In this case the UV spectrum confirmed that **5** was structurally distinct from other known possible impurities. LC–MS and LC–NMR would normally be combined to identify unknown impurities, but here using

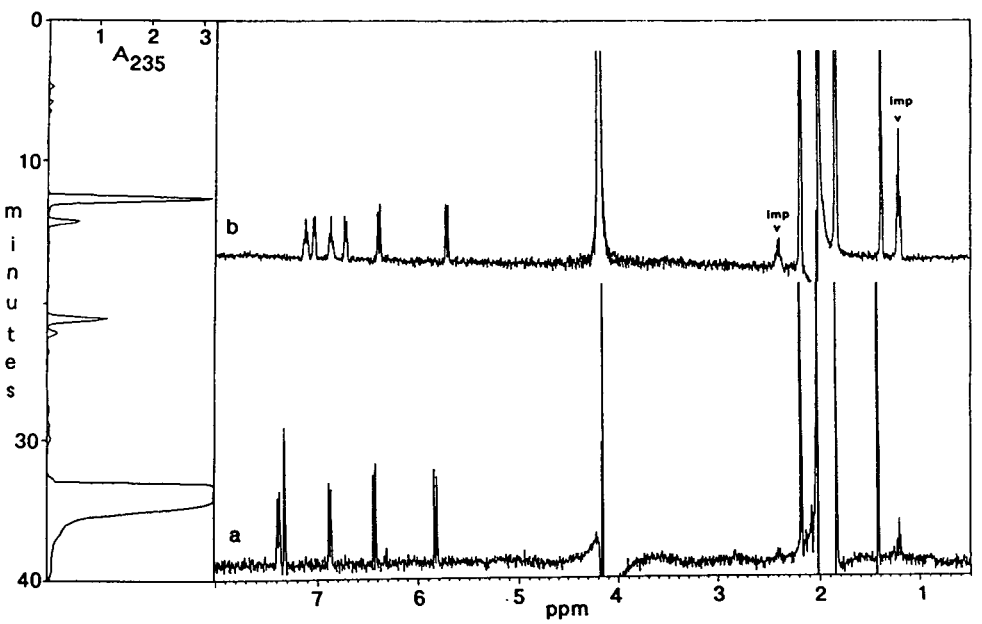

Fig. 4. Chromatogram for sample consisting mainly of **4**, with ^{1}H spectra of **4** (flowing, trace a) and the impurity **5** (stopped-flow, 1024 scans, trace b). Conditions as in Fig. 1 except that acetonitrile–buffer ratio was 60:40. Approximately 100 μl sample injected on to the column for the flowing data and 200 μl for the stopped-flow data. The multiplets indicated by "imp" at 1.20 and 2.40 ppm are due to an impurity/impurities in the acetonitrile.

both frit fast atom bombardment and thermospray, LC–MS failed to identify **5**. It is also advantageous that typical reversed-phase eluents pose no problem of compatibility with LC–NMR. For example, LC–NMR has been performed in this laboratory using ammonium formate buffers and tetrahydrofuran–aqueous trifluoroacetic acid mixtures as eluents in addition to the phosphate buffers used in this study.

4. Conclusions

LC–NMR can provide very useful structural information on relatively minor components of mixtures, even using a 400 MHz spectrometer. Relatively high loadings may be needed to obtain data on low-level impurities (depending on flow cell size and spectrometer field strength) but this is not usually a problem with the robust separation methods used to examine pharmaceuticals.

Acknowledgements

Thanks are due to our Synthetic Chemistry Department for the preparation of all compounds studied, to Gregory Jonas and Barbara O'Reilly for developing the original chromatographic conditions, and to Unicam, Cambridge, UK for the loan of the HPLC system used for this work.

References

[1] N. Watanabe and E. Niki, *Proc. Jpn. Acad.*, 54 (1978) 194.
[2] E. Bayer, K. Albert, M. Nieder, E. Grom and T. Keller, *Adv. Chromatogr.*, 14 (1979) 525.
[3] K. Albert, M. Kunst, E. Bayer, M. Spraul and W. Bermel, *J. Chromatogr.*, 463 (1989) 355.
[4] M. Spraul, M. Hofmann, H. Glauner, J. Gans and K. Albert, *Bruker Report*, 90(2) (1990) 12.
[5] M. Spraul, M. Hofmann, P. Dvortsak, J.K. Nicholson and I.D. Wilson, *J. Pharm. Biomed. Anal.*, 10 (1992) 601.
[6] K. Albert, M. Kunst, E. Bayer, H. Jan de Jong, P. Genissel, M. Spraul and W. Bermel, *Anal. Chem.*, 61 (1989) 772.
[7] M. Spraul, M. Hofmann, P. Dvortsak, J.K. Nicholson and I.D. Wilson, *Anal. Chem.*, 65 (1993) 327.
[8] M. Spraul, M. Hofmann, I.D. Wilson, E. Lenz, J.K. Nicholson and J.C. Lindon, *J. Pharm. Biomed. Anal.*, 11 (1993) 1009.

Author Index

ANALYTICAL BIOTECHNOLOGY

Proceedings of the 4th International Symposium on Analytical Methods, Systems and Strategies in Biotechnology (ANABIOTEC '92), Noordwijkerhout, The Netherlands, 21-23 September 1992

Edited by **C. van Dijk**

Previously published as part of the 1993 subscription to the journals *Analytica Chimica Acta* and *Journal of Biotechnology*

ANABIOTEC '92 focused on the further integration of biotechnology and analytical chemistry. The results of this symposium clearly demonstrated that a substantial progress could be reported in the application of both conventional and new analytical techniques, the latter essentially based on natural analytical tools such as biomolecules. The main themes covered during this meeting are fermentation monitoring, chromatography, instrumental analysis, biosensors and bioanalysis.

A selection of the contents.
Preface.
Process Control. Monitoring and control of recombinant protein production (K. Schügerl *et al.*). Rapid and quantitative analysis of bioprocesses using pyrolysis mass spectrometry and neural networks: application to indole production (R. Goodacre, D.B. Kell). Characterization of a sampling unit based on tangential flow filtration for on-line bioprocess monitoring (T. Buttler, L. Gorton, G. Marko-Varga). Automated monitoring of biotechnological processes using on-line ultrafiltration and column liquid chromatography (N.C. Van de Merbel *et al.*). On-line monitoring of penicillin V during penicillin fermentations: a comparison of two different methods based on flow-injection analysis (M. Carlsen *et al.*). Development of an on-line method for the monitoring of vicinal diketones and their precursors in beer fermentation (C. Mathis *et al.*). Monitoring of fermentation by infrared spectrometry. Alcoholic and lactic fermentations (D. Picque *et al.*).
Chromatography and other Separation Techniques. Chromatographic analysis of biopolymers distribution in "poly-hemoglobin", an intermolecularly crosslinked hemoglobin solution (J. Simoni, G. Simoni, M. Feola). Application of multivariate mathematical-statistical methods for the comparison of the retention behaviour of porous graphitized carbon and octadecylsilica columns (E. Forgács, T. Cserháti, B. Bordás).
Antibodies. Catalytic antibodies: new developments (R. Hilhorst).
Biosensors. Measurements of nitric oxide in biological materials using a porphyrinic microsensor (T. Malinski *et al.*). Reusable fiber-optic-based immunosensor for rapid detection of imazethapyr herbicide (R.B. Wong, N. Anis, M.E. Eldefrawi). Biosensor monitoring of blood lactate during open-heart surgery (M. Kyröläinen *et al.*).
Instrumental Techniques. Introduction to the dielectric estimation of cellular biomass in real time, with special emphasis on measurements at high volume fractions (C.L. Davey *et al.*). Spectral analysis of interactions between proteins and dye ligands (J. Hubble, A.G. Mayes, R. Eisenthal).
Enzymatic Analysis. Preservation of shelf life of enzyme based analytical systems using a combination of sugars, sugar alcohols and cationic polymers or zinc ions (T.D. Gibson, J.N. Hulbert, J.R. Woodward).
Colloidal Carbon Particles. Colloidal carbon particles as a new label for rapid immunochemical test methods: Quantitative computer image analysis of results (A. van Amerongen *et al.*). Author Index.

© 1993 208 pages Hardbound
Price: Dfl. 265.00 (US $ 151.50)
ISBN 0-444-81640-2

ORDER INFORMATION
For USA and Canada
ELSEVIER SCIENCE INC.
P.O. Box 945
Madison Square Station
New York, NY 10160-0757
Fax: (212) 633 3880
In all other countries
ELSEVIER SCIENCE B.V.
P.O. Box 330
1000 AH Amsterdam
The Netherlands
Fax: (+31-20) 5862 845
US$ prices are valid only for the USA & Canada and are subject to exchange rate fluctuations; in all other countries the Dutch guilder price (Dfl.) is definitive. Customers in the European Union should add the appropriate VAT rate applicable in their country to the price(s). Books are sent postfree if prepaid.

ELSEVIER SCIENCE B.V.

0021-9673(19940819)677:2;1-E

PUBLICATION SCHEDULE FOR THE 1994 SUBSCRIPTION

Journal of Chromatography A and *Journal of Chromatography B: Biomedical Applications*

MONTH	1993	J–M	J	J	A	
Journal of Chromatography A	652–657	658–669	670/1 + 2 671/1 + 2 672/1 + 2	673/1 673/2 674/1 + 2 675/1 + 2 676/1	676/2 677/1 677/2 678/1	The publication schedule for further issues will be published later.
Bibliography Section		681/1	681/2			
Journal of Chromatography B: Biomedical Applications		652–655	656/1 656/2	657/1 657/2	658/1 658/2	

INFORMATION FOR AUTHORS

(Detailed *Instructions to Authors* were published in *J. Chromatogr. A*, Vol. 657, pp. 463–469. A free reprint can be obtained by application to the publisher, Elsevier Science B.V., P.O. Box 330, 1000 AH Amsterdam, Netherlands.)

Types of Contributions. The following types of papers are published: Regular research papers (full-length papers), Review articles, Short Communications and Discussions. Short Communications are usually descriptions of short investigations, or they can report minor technical improvements of previously published procedures; they reflect the same quality of research as full-length papers, but should preferably not exceed five printed pages. Discussions (one or two pages) should explain, amplify, correct or otherwise comment substantively upon an article recently published in the journal. For Review articles, see inside front cover under Submission of Papers.

Submission. Every paper must be accompanied by a letter from the senior author, stating that he/she is submitting the paper for publication in the *Journal of Chromatography A* or *B*.

Manuscripts. Manuscripts should be typed in **double spacing** on consecutively numbered pages of uniform size. The manuscript should be preceded by a sheet of manuscript paper carrying the title of the paper and the name and full postal address of the person to whom the proofs are to be sent. As a rule, papers should be divided into sections, headed by a caption (*e.g.*, Abstract, Introduction, Experimental, Results, Discussion, etc.). All illustrations, photographs, tables, etc., should be on separate sheets.

Abstract. All articles should have an abstract of 50–100 words which clearly and briefly indicates what is new, different and significant. No references should be given.

Introduction. Every paper must have a concise introduction mentioning what has been done before on the topic described, and stating clearly what is new in the paper now submitted.

Experimental conditions should preferably be given on a *separate* sheet, headed "Conditions". These conditions will, if appropriate, be printed in a block, directly following the heading "Experimental".

Illustrations. The figures should be submitted in a form suitable for reproduction, drawn in Indian ink on drawing or tracing paper. Each illustration should have a caption, all the *captions* being typed (with double spacing) together on a *separate sheet*. If structures are given in the text, the original drawings should be provided. Coloured illustrations are reproduced at the author's expense, the cost being determined by the number of pages and by the number of colours needed. The written permission of the author and publisher must be obtained for the use of any figure already published. Its source must be indicated in the legend.

References. References should be numbered in the order in which they are cited in the text, and listed in numerical sequence on a separate sheet at the end of the article. Please check a recent issue for the layout of the reference list. Abbreviations for the titles of journals should follow the system used by *Chemical Abstracts*. Articles not yet published should be given as "in press" (journal should be specified), "submitted for publication" (journal should be specified), "in preparation" or "personal communication".

Vols. 1–651 of the *Journal of Chromatography*; *Journal of Chromatography, Biomedical Applications* and *Journal of Chromatography, Symposium Volumes* should be cited as *J. Chromatogr.* From Vol. 652 on, *Journal of Chromatography A* (incl. Symposium Volumes) should be cited as *J. Chromatogr. A* and *Journal of Chromatography B: Biomedical Applications* as *J. Chromatogr. B.*

Dispatch. Before sending the manuscript to the Editor please check that the envelope contains four copies of the paper complete with references, captions and figures. One of the sets of figures must be the originals suitable for direct reproduction. Please also ensure that permission to publish has been obtained from your institute.

Proofs. One set of proofs will be sent to the author to be carefully checked for printer's errors. Corrections must be restricted to instances in which the proof is at variance with the manuscript.

Reprints. Fifty reprints will be supplied free of charge. Additional reprints can be ordered by the authors. An order form containing price quotations will be sent to the authors together with the proofs of their article.

Advertisements. The Editors of the journal accept no responsibility for the contents of the advertisements. Advertisement rates are available on request. Advertising orders and enquiries can be sent to the Advertising Manager, Elsevier Science B.V., Advertising Department, P.O. Box 211, 1000 AE Amsterdam, Netherlands; courier shipments to: Van de Sande Bakhuyzenstraat 4, 1061 AG Amsterdam, Netherlands; Tel. (+31-20) 515 3220/515 3222, Telefax (+31-20) 6833 041, Telex 16479 els vi nl. *UK*: T.G. Scott & Son Ltd., Tim Blake, Portland House, 21 Narborough Road, Cosby, Leics. LE9 5TA, UK; Tel. (+44-533) 753 333, Telefax (+44-533) 750 522. *USA and Canada*: Weston Media Associates, Daniel S. Lipner, P.O. Box 1110, Greens Farms, CT 06436-1110, USA; Tel. (+1-203) 261 2500, Telefax (+1-203) 261 0101.